Clinical Value of Massive Parallel HIV-1 Sequencing in Antiretroviral Treatment Experienced Subjects

CHRISTIAN POU GONZÀLEZ
irsiCaixa Institute for AIDS Research
Molecular Epidemiology Group

Department of Biochemistry and Molecular Biology
Universitat Autònoma de Barcelona
Director // Roger Paredes i Deiros

Doctoral thesis 2013

Thesis to obtain the PhD degree in Biochemistry, Molecular Biology and Biomedicine

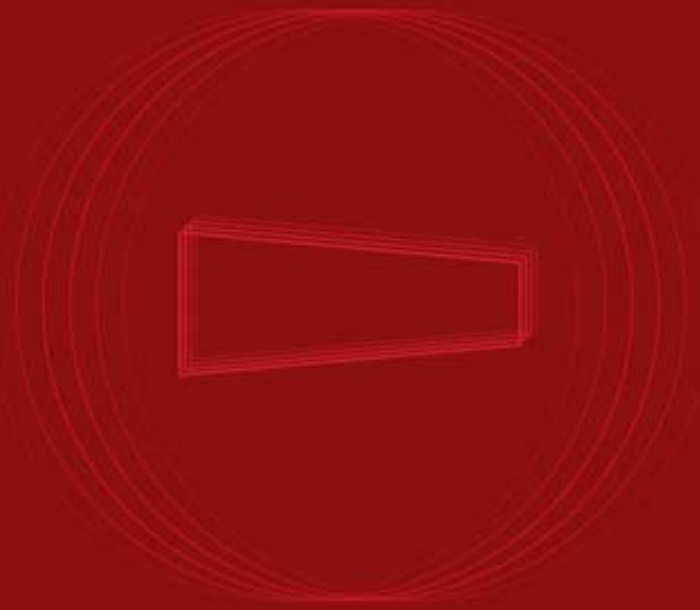

DEPARTMENT OF BIOCHEMISTRY AND MOLECULAR BIOLOGY
UNIVERSITAT AUTÒNOMA DE BARCELONA

DOCTORAL THESIS, 2013

Clinical Value of Massive Parallel HIV-1 Sequencing in Antiretroviral Treatment-Experienced Subjects

CHRISTIAN POU GONZÀLEZ
irsiCaixa Institute for AIDS Research
Molecular Epidemiology Group

Thesis to obtain the PhD degree in Biochemistry, Molecular Biology and Biomedicine of the Universitat Autònoma de Barcelona

Director: Roger Paredes i Deiros, MD, PhD
IrsiCaixa Institute for AIDS Research
Senior Investigator of Molecular Epidemiology Group

Tutor: Jaume Farrés Vicén, PhD
Catedràtic d'Universitat
Departament de Bioquímica i Biologia Molecular UAB

En Dr. Roger Paredes i Deiros, investigador principal del Grup d'Epidemilogia Molecular a l'Institut de Recerca de la SIDA – irsiCaixa,

Certifica:

Que el treball experimental i la redacció de la memòria de la Tesi Doctoral titulada "*Clinical Value of Massive Parallel HIV-1 Sequencing in Antiretroviral Treatment-Experienced Subjects*" han estat realitzats per en Christian Pou Gonzàlez sota la seva direcció i considera que és apta per ésser presentada per optar al grau de Doctor en Bioquímica, Biologia Molecular i Biomedicina per la Universitat Autònoma de Barcelona.

I per tal que quedi constància, signa aquest document.

Badalona, 17 de setembre de 2013.

Dr. Roger Paredes i Deiros

En Dr. Jaume Farrés Vicén, Catedràtic d'Universitat del Departament de Bioquímica i Biologia Molecular UAB,

Certifica:

Que el treball experimental i la redacció de la memòria de la Tesi Doctoral titulada "*Clinical Value of Massive Parallel HIV-1 Sequencing in Antiretroviral Treatment-Experienced Subjects*" han estat realitzats per en Christian Pou Gonzàlez sota la seva tutoria i considera que és apta per ésser presentada per optar al grau de Doctor en Bioquímica, Biologia Molecular i Biomedicina per la Universitat Autònoma de Barcelona.

I per tal que quedi constància, signa aquest document.

Badalona, 17 de setembre de 2013.

Dr. Jaume Farrés Vicén

Agraïments

Aquesta és la part que en principi sembla la fàcil d'escriure, però alhora m'és molt difícil resumir el que sento per vosaltres en poques paraules. M'heu ajudat a créixer com a científic i com a persona. Ha estat un plaer compartir experiències amb tots vosaltres.

Voldria començant agraint als membres del meu grup que són qui veritablement han fet possible tota aquesta feina. BIT, VM, GEM? Tant se val, sou collonuts. Roger, saps que sense la teva ajuda i dedicació això no hagués estat possible. M'has fet créixer professionalment, però el més important és que m'emporto un amic increïble. Ets un científic superbrillant, amb mil idees i projectes que fan que la gent del teu voltant s'enganxi a aquesta feina i se senti valorada. Rocío, gracias por enseñarme y ayudarme en todo durante estos años, has sido mi apoyo en todo momento. Comenzamos los dos solitos y mira ahora, eso serà que tampoco lo hemos hecho tan mal no?? A la Maria Casadellà, qui m'ha sofert en el seu temps de pràctiques, espero que no hagi estat molt dur. Et deixo les claus del 454, no sé si dir-te que el cuidis o el cremis. Espero que t'ho passis tant bé com jo fent la tesi. Gràcies per tots els bons moments, sobren les paraules no? Marc ets artista de la bioinformàtica, que fas anar l'ordinador a una velocitat imperceptible per l'ull humà (els de la cara eh, segur que t'ha vingut al cap l'altre, ja et conec). Ets capaç de fer preguntes interessants sobre qualsevol tema. A més, m'encanta les bombes que deixes anar durant les converses, i com després et retires veien com la gent s'encén. Tere, sempre transmetent alegria i bon humor, espero que et vagi molt bé en aquesta nova aventura. Per cert, reserva'm data pel safari. Susana, gràcies per fer l'estadística més entenedora, tot i que saps que no ho és per la resta de terrenals. Molta sort amb la tesi! A la Cristina Rodríguez, por estar siempre de buen humor y transmitir tranquilidad. I a la nova incorporació, la Muntsa, a qui desitjo que vagi molt bé la tesi i aprengui molt de la gent que té al voltant. No vull oblidar-me dels que han passat per aquest grup, com el Paco, un amic que no para mai, molt difícil aguantar el teu ritme. T'agraeixo la teva feina en tot això. I el Mattia, un tio genial i un apassionat que es coneixia Barcelona com ningú i fa un tiramisú espectacular. Espero que siguis molt feliç en els projectes en els que estiguis immers.

Als del grup GREC, començant pel Javier, un científic genial i el culpable que jo aparegués un dia d'estiu a irsi. Gràcies per donar-me la oportunitat començar a

treballar en això que m'ha enganxat des del primer dia i explicar la ciència d'una manera tan didàctica. Mª José, todavía tengo las cicatrices de los grilletes de las prácticas... Qué verano más largo se me hizo! Gracias por tu paciencia ;) Gerard, tu m'has fet riure moltíssim, gràcies per tots els bons moments malparit. Segur que ens tornarem a veure aviat, no s'ha acabat el bròquil entre nosaltres!! A la Mª Carmen, vaya mano a mano de chistes nos echamos en Sevilla! Se te va a echar muchísimo de menos, sobretodo en los desayunos, siempre nos quedara el whatsapp... Gracias también por estar siempre dispuesta a ayudar en cualquier cosa. A la Judith, una persona molt especial en la qual gairebé tothom s'ha recolzat en algun moment difícil. Hauries de cobrar suplement per fer de psicòloga de tota aquesta colla de bojos. A la Itziar, quien recuerdo que un día me dijo que tenia un caràcter parecido al de su hermano. Hay hermanos que se llevan a matar, no es nuestro caso no?? Gracias por transmitir alegria al módulo. A la Mª Teresa, quien definió mi humor como "inclassificable". Ahora se ve que ya lo han clasificado, lo han puesto dentro de "humor inteligente". Por cierto, gracias por los consejos para la tesis. Mª Salgado, lo nuestro ha sido corto pero intenso. Me has puesto fàcil ser amigo tuyo, más fàcil que mis amigas de la Jonquera ;) Ahora es cuando me dices que no eres amiga mía!! Nuria, gracias a tus espectaculares charlas he aprendido a no hacer el pulpo en la discoteca, ahora hago la dendrítica! Pero el resultado es el mismo, un par de ostias y nunca colocalizamos en la misma cama. Maria Pino, encara recordo el viatge a NY, i aquella dutxa que no sabíem com collons funcionava... va ser molt divertit! Per cert, vagi on vagi faré el *Couch Surfing*, així podràs venir a veure'm sempre que vulguis. Dan, debe ser duro lidiar con todas las mujeres de tu grupo… la *p* más importante en tu vida ya no es la del test estadístico si no la p de paciencia.

Als del grup VIC, encapçalats pel Julià, un científic increïble que sempre està disponible per explicar i ajudar en el que faci falta. I més ara que va ser escollit com a responsable dels EPIs per majoria absoluta. Per fi he entès que són els discordants, són becaris que es treballen molt i cobren molt poc oi? I como no, su dúo Pimpinela, la Ceci, compañera de inglés y psicóloga. Supongo que te acuerdas de aquella conversación el bar, desde ese dia no me he vuelto a sentar en esa mesa. Suerte que no se puede salir a la terraza porque sinó nos hubiéramos tirado los dos. Gracias por todos tus consejos. Se me olvidaba, los controles de recombinación ya casi están. A la Sílvia, encara que no em treguis a patinar he rigut moltíssim amb tu, hem tingut bones converses als esmorzars, inclús algun dia vaig tenir la sort d'esmorzar amb les veteranes, i això no és fàcil! Al Jorge, vaya crack, qué manera de contar chistes. A parte de esto, tendría que patrocinarte Wikipedia tío, te sabes hasta las comas cabrón! Lo siento pero tengo que decírtelo, por Skype estàs más guapo. Eli García, dales caña

a todos éstos. Cuando me vaya esta responsabilidad quedará en tus manos... Todavía recuerdo cuando decías que no querías un niño, y ahora se te cae la baba con el peque. El segundo para cuándo? A la Marisa, gràcies per estar sempre de bon humor i alegrar-me el dia durant l'esmorzar, haurem d'esmorzar per Skype. Al Luis, mi Juaquín Cortés. Te pillé y lo sabes. Cada mañana te imprimes el mismo paper 4 veces para secarte la melena debajo del aire acondicionado. Y que sepas que tienes una deuda conmigo, me tienes que llevar al Cangrejo! A la Eli Gómez, qui m'ha patit com a responsable de pràctiques. Espero no haver estat molt dur i que t'hagi pogut ensenyar una mica del poc que sé. Encara recordo aquella conversa a Toledo sobre la parella eh, no pensis que ho he oblidat. Em volíeu matar entre totes... I als que ja no hi són com la Marta Massanella, la meva colega del "*toasted beagle with cream cheese*". Se't troba a faltar a irsi, quina enveja em fan els teus companys de San Diego! A la Marta Curriu, la meva altra companya d'anglès. Tens un salero per explicar les coses que si no fos per l'accent diria que ets sevillana. Moltes gràcies per posar-me al dia amb el teu Facebook! Isa tu em vas fer situar Viladecavalls al mapa, i això és un gran què, suposo que jo devia fer el mateix amb Sant Celoni. Et vas emportar el glamour de Badalona... Francesc, o estàs fart de *reggaeton* o ja "*te gusta la gasolina*"! Et desitjo que et vagin molt bé les coses per Miami. Encara recordo la Cursa de la Sanitat Catalana, quin fart de patir.

Continuem per les molones, dirigides pel Miguel Ángel, con quien han sido entretenidas las charlas sobre fútbol y las previas Barça-Madrid. Sandra, trobaré a faltar els teus catxetes a l'aire dient: Trixxx! I sí, una vegada em vas salvar la vida amb un antihistamínic (m'ho hauré de sentir tota la vida això). Mariona, qui juntament amb la Sílvia organitza el laboratori i ens fa netejar una vegada al mes :(Que sàpigues que et tinc com a spam perquè només envies correus d'ofertes i de dies de neteja. Gràcies per posar-me al dia dels concerts de la Troba Kung-Fú, per cert m'has de deixar el nou CD perquè me'l copïi. Elena, aún estoy esperando la paella... Vendré a verte a París, que no sé si lo sabes pero dicen que es la ciudad del amor... (ahí lo dejo) Glòria, activa com ningú, fas carregar les piles a tothom. Encara recordo el dia que vam sortir a córrer, com et poses vermella com un tomàquet. Em tens saturat de fotos a l'Instagram! A la Maria Nevot, per transmetre aquesta tranquilitat i forma racional de veure les coses. Sense oblidar-me de la Cristina Andrés, a qui desitjo molta sort en el que faci, i l'Ester Aparicio, gran viatge a San Francisco en el que ens vas fer de reportera, em vaig divertir moltíssim sobretot baixant per Lombard Street i creuant el Golden Gate en bici, no canviïs!

Als jaecitos, dirigits pel José Esté, un apasionado del tenis con quien es un placer mantener charlas sobre cualquier tema. Ester Ballana, gràcies per estar sempre de

bon humor i ajudar-me en els temes universitaris, i per deixar-me la cabina encara que no estigués apuntat, “és un moment només!”. Marc, si en algun moment et falla la ciència pots dedicar-te a la interpretació. Per cert, encara em ve al cap el pastís de xocolata Godiva que ens cascar a Boston i el teu efímer dubte en demanar amanida o patates fregides (“sssss... fries fries!!!”). A l’Alba Ruíz, qui també veu la llum al final del túnel per ser doctora. Ànims que això ja va de baixada! Edu, tu ets de les persones que més feina m’ha donat a irsi, segur que no ho recordes però em vas passar el manteniment del descalcificador i no pares de demanar-e cubetes de l’espectro, passa’t ja al Nanodrop tiu!! Et tinc a la llista negra. A l’Eva i el Roger Badia, dues noves incorporacions de bona pasta que sempre estan de bon rotllo i amb qui és un plaer compartir el cafè i anècdotes després de dinar. Sin dejarme a Emmanuel, quien intentó violarme en San Francisco. Desde aquel día no he vuelto a pisar esa ciudad. Espero que te vaya superbién por DF. Tampoco me olvido de ti Encarna, acabaste con el stock de Converse en NY! Buena suerte con el nuevo trabajo!

Julia, de momento amigos, despues de la tesis ya veremos. Por cierto, me han dicho que el jamón està en reparto. Sabes un montón y seguro que te irá muy bien con tu nuevo grupo (no es peloteo, bueno sí). Esther Jiménez, cuantas veces habré escuchado la palabra “abuelaaaa!!” en el módulo. Gracias por estar siempre alegre y sacarme una sonrisa. Oye, no seràs piscis verdad?? Es que me caes muy bien... A la Ruth, per estar sempre de bon humor i riure dels meus acudits, saps que t’ho poso fàcil perquè són molt bons.

Al grup serveis, sota la direcció de la Lídia, qué difícil debe ser coordinar este laboratorio de locos! Gracias por hacerme reir mientras trabajaba en la poyata de delante de tu despacho (ha llovido desde aquel entonces en el que trabajaba eh…). A la Teresa, per riure no cal mirar el Club de la Comedia, només cal treure’t un tema de conversa. Les teves punyalades són úniques! Eulàlia, mira que he fet màsters, però un de tan ben coordinat com el d’irsi enlloc. Sempre és divertit parar davant del teu immens despatx i xerrar una estona. A la Samandhy, la chica más chévere de irsiCaixa, siempre cariñosa y con ganas de montar cenitas. Cristina Ramírez, gracias por esas conversaciones en Pre-PCR explicándome tus batallitas de cuando trabajabas con animales... bueno como ahora casi ;) A la Rafi, todavía recuerdo del día del incendio... No sin mis células!! Lucía, desde que estás en P3 ya no se te ve el pelo, has tenido suerte porque ha coincidido con las derrotas del Madrid... A la Tània, que allà on sigui explicarà les seves peripècies als companys, sempre contagiant bon rotllo. A la Susana Esteban, por esas charlas entre bambalinas y por mostrarme el mercado negro de Can Ruti! Que la verdad no sé si es mercado negro o està montado por el propio hospital, porque entre el bar y las compras casi no llega dinero a casa.

Al Christian Brander, mi tocayo. Sé que cuando aprendes un idioma nuevo te hace gracia aprender las palabrotas, però tu te las sabes todas cabrón! Gracias por tus charlas majistrales sobre CTLs! Anuska, gracias por estar siempre de buen humor, todavía me acuerdo del día que llegaste con la pulsera PowerBalance y hacías la prueba empujando a la gente… Bea, no sé perquè experimentar amb micos fora quan irsi n'està ple! Per cert, et deixo la xurrera a preu d'amic, la vols? A l'Àlex, gràcies per explicar-nos les batalletes viscudes amb els teus col·legues. De gent boja n'hi ha per tot arreu, però per la teva zona més! A veure si un dia em portes a l'estabulari… Vanessa, gràcies pels teus gelats en gel sec, se m'oblidava, em deus dues factures de dentista. Marta Ruíz, seguro que ahora te està cambiando radicalmente la vida, gracias por comentar chismorreos en voz baja en el módulo ;)

Al Pep Coll, únic en els journals, cada vegada que menjo coliflors hi penso... Gràcies per posar-nos la malaltia en el context social, el qual moltes vegades oblidem quan estem tancats al laboratori. I para de fer esport perquè em fas sentir gran! A la Mireia Manent, a qui li costen molt els matins però que es va animant mica en mica. Gràcies per fer-me riure tant!

A la Cristina Mesa, quien en tiempos de sequía (o sea casi siempre) eres la primera persona que me da los buenos días con una sonrisa. Y sé que no te debe resultar fàcil, porque aguantar al Jordi... la procesión va por dentro no?? Penélope, gràcies pel teu optimisme i per fer-me feliç cada vegada que em truques i em dius... "Christian tens un paquet!!". Ara ja no és el mateix quan m'ho diu l'Alejandro... por cierto bienvenido! Julián, te van a hacer mártir de irsicaixa, como te presiona la gente, espero que la fibra óptica te devuelva los años de vida perdidos.

Gràcies també als membres de l'equip de comunicació, Rosina, Matilde i Josep, per vendre tan bé la nostra feina de portes en fora. Es creuen que ho fem bé i tot!!

Al Ventura, un crack. Encara que tu jugues en una altra divisió sempre estàs disposat a donar un cop de mà. Gràcies pel teu suport durant tots aquests anys, veritablement ha estat un plaer treballar a irsi. Lourdes, gracias por tu ayuda durante estos años. Tienes razón, estos científicos de irsicaixa viven muy bien y se quejan mucho, contrólales los gastos que me los conozco....

No vull oblidar-me de la Margarita, capaç de sorprendre a tothom amb un ball de cabaret després d'un sopar o amb una cançó sobre l'HIVACAT. Tampoco de ti Ferdinand, que sepas que estoy en primero de *iniciación*. Tu cuándo comenzaste a notar los resultados?? Seguro que eso viene de serie al nacer… Al Raul Ruíz, echo de menos tus anécdotas por el Raval, espero que te vaya todo muy bien.

També volia fer una reflexió general i agrair a tot el gènere femení d'irsiCaixa, per posar-me al dia sobre la seva vida sentimental. És com si ja fos de la família, si el dia

de Nadal algú truca a la porta no us estranyeu si sóc jo. A més, crec que amb tot el que he après durant aquests anys sobre canalla ja estic a punt per ser pare, però el que no em queda tan clar és això de tenir marit... Pobres homes! Els deixeu verds sempre que podeu, ja estic patint per veure el que direu de mi quan marxi...

No voldria oblidar-me dels companys de Lluita contra la Sida, uns cracks amb els que és un plaer col·laborar i aprendre la part clínica. Agrair a tres persones en espacial, tres que semblen adolescents. Jordi, estàs muy loco. Gracias por los chistes que me cuentas por el pasillo. A ver, tengo que reconocer que algunos son muy malos pero me río para subirte la moral! José Ramón, cuánta razón tienes de que "*todo esto es una vaina!*". Ésta es una de esas palabra que se puede utilitzar en cualquier situación. También me acuerdo de algun momento surrealista en las clases de inglés eh... I per últim en Jose Muñoz, a qui sempre que em trobo pel passadís li dic *mindfulness* encara que sé que ell no hi té res a veure.

Gràcies al Martin Däumer per obrir-me les portes del seu laboratori i donar-me la oportunitat d'aprendre d'un dels grups de recerca més importants del món en seqüenciació ultrasensible.

Vull també agrair el suport rebut des de Roche Diagnostics i la seva valentia per apostar pel nostre grup. Gracias por estar siempre ahí Miguel Álvarez y darnos soporte en todo momento, es muy fácil dedicarse a la ciencia de este modo. Este agradecimiento es también extensible a Artur Palet, Ana Zamora y Álex Pérez.

Jaume Farrés, gràcies per estar sempre disponible i donar-me suport des de la Universitat Autònoma de Barcelona.

I per descomptat moltíssimes gràcies als meus amics i a la meva família, la part més important de la meva vida. Gràcies per confiar sempre en mi. Sentiu-vos artífexs d'això perquè sense el vostre suport incondicional res hagués estat possible.

“I am among those who think that science has great beauty. A scientist in his laboratory is not only a technician: he is also a child placed before natural phenomena which impress him like a fairy tale“

Marie Curie

Abbreviations code

/r	Ritonavir-boosted
3TC	Lamivudine
ABC	Abacavir
AIDS	Acquired immunodeficiency syndrome
AMOVA	Analysis of molecular variance
ANRS	Agence Nationale de Recherche sur le Sida et les hépatites
APV	Amprenavir
ART	Antiretroviral therapy
ARV	Antiretroviral
ASPCR	Allele-specific polymerase chain reaction
ATP	Adenosine triphosphate
ATV	Atazanavir sulfate
AVA	Amplicon Variant Analyzer
AZT	Azidothymidine, Zidovudine
BAF	Barrier-to-autointegration factor
BID	*Bis in die* (twice a day)
Bp	Basepair
c/mL	Copies per millilitre
CA	Capside, p24
CCR5	C-C chemokine receptor type 5
CDC	Centers for Disease Control and Prevention
cDNA	Complementary desoxy ribonucleic acid
CLIA	US Congress Clinical Laboratory Improvement Act
COBI	Cobicistat
CPE	Cytopathic effect
CRF	Circulating recombinant form
CRS	Cis-acting repressive sequences
CTL	Cytotoxic T lymphocytes
CVC	Cenicriviroc
CXCR4	C-X-C chemokine receptor type 4
d4T	Stavudine
ddC	Zalcitabine, Dideoxycytidine
ddI	Didanosine
ddIEC	Enteric coated didanosine
ddNTP	Dideoxynucleotide triphosphates
DHHS	Department of Health and Human Services
dL	Deciliter
DLG	Dolutegravir
DLV	Delavirdine
DNA	Deoxyribonucleic acid
DRM	Drug resistance mutation
DRT	Drug resistance testing
DRV	Darunavir
dsDNA	Double strand deoxyribonucleic acid
EACS	European AIDS Clinical Society
EFV	Efavirenz
EI	Entry inhibitor
ELV	Elvitegravir

emPCR	Emulsion polymerase chain reaction
ENF	Enfuvirtide
Env	Envelope
ERCC1	Excision repair cross-complementation group 1 gene
ESTA	Enhanced Sensitivity Trofile^{TM} Assay
ETV	Etravirine
FAPV	Fosamprenavir
FDA	US Food and Drug Administration
FPR	False Positive Rate
FTC	Emtricitabine
G2P	Geno2Pheno algorithm
GALT	Gut associated lymphoid tissues
Gp160	Glicoprotein 160
Gp120	Glicoprotein 120
Gp41	Glicoprotein 41
GSS	Genotypic susceptibility score
HBV	Hepatitis B virus
HCV	Hepatitis C virus
HDL	High-density lipoprotein
HIV	Human immunodeficiency virus
HIV-1	Human immunodeficiency virus type 1
HIV-2	Human immunodeficiency virus type 2
HIVdb	Stanford HIV drug resistance database
HR1	Heptad repeat-region 1
HR2	Heptad repeat-region 2
HTLV	Human T-lymphotropic viruses
HYPHY	Hypothesis testing using phylogenies
IAS-USA	International AIDS Society-USA
IC	Inhibitory concentration
ID	Identification
IDV	Indinavir
IDVU	Intravenous drug user
IER3	Immediate early response 3 gene
IN	Integrase, p32
INS	Inhibitory/Instability RNA sequences
InSTI	Integrase strand-transfer inhibitor
IQR	25^{th}-75^{th} interquartile range
Kbp	Kilobase pair
LAV	Lymphadenopathy-associated virus
LDL	Low-density lipoprotein
LEDGF/p75	Lens-epithelium-derived growth factor
Log	Logarithm
LPV	Lopinavir
LTNP	Long-term nonprogressors
LTR	Long terminal repeat
MA	Matrix, p17
MCCP	Multi-class combination products
mg	Milligram
Mg^{2+}	Magnesium
MHC	Major histocompatibility complex
MID	Multiple identifiers
mL	Millilitre
MLV	Murine leukemia virus

mm^3	Cubic millimeter
mmol	Millimol
MPI	Maximum percentage of inhibition
mRNA	Messenger RNA
MSA	Multiple sequence alignement
MTT	-3(4,5-dimethylthiazol-2-yl)-2,5-dyphenyltetrazolium bromide
MVC	Maraviroc
N	Number
N/A	Not applicable
NC	Nucleocapside, p7
NCEP	National Cholesterol Education Program
Nef	Negative regulatory factor, p27-p25
NFV	Nelfinavir
NGS	Next generation sequencing
NK	Natural killer cells
Nm	Nanometre
NNGS	Next-next generation sequencing
NNRTI	Non-nucleoside analogue reverse transcriptase inhibitor
NPV	Negative predictive value
NRTI	Nucleoside analogue reverse transcriptase inhibitor
NVP	Nevirapine
ORF	Open reading frame
OTA	Original Trofile™ Assay
PBMC	Peripheral blood mononuclear cell
PCR	Polymerase chain reaction
PE	Psi elements
PGM	Personal genome machine
PHA	Phytohemagglutinin
PI	Protease inhibitor
PIC	Preintegration complex
PNGS	Potential N-linked glycosylation site
PPi	Pyrophosphate
PPV	Positive predictive value
PR	Protease, p10
PS	Population sequencing
PSSM	Position-specific scoring matrices
PTP	PicoTiterPlate™
QD	*Quaque die* (one a day)
qRTPCR	Quantitavive Real-time polymerase chain reaction
R5	CCR5-using viruses
RAL	Raltegravir
Rev	Regulator of expression of virion proteins, p19
RNA	Ribonucleic Acid
RPV	Rilpivirine
RRE	Rev responsive element
RT	Reverse transcriptase, p66, p51
RT-PCR	Reverse transcription polymerase chain reaction
RTV	Ritonavir
SD	Standard deviation
SDF-1	Stromal cell-derived factor 1
SGS	Single genome sequencing
SIV	Simian Immunodeficienty Virus
SMRT	Single-molecule real-time sequencing
SNV	Single nucleotide variant

SOLID	Sequencing by Oligo Ligation Detection
SP1	Spacer Peptide 1, p1
SP2	Spacer Peptide 2, p2
SQV	Saquinavir mesylate
ssRNA	Single-stranded RNA copies
STARD	Standards for reporting of diagnostic accuracy
SVM	Support vector machine
T20	Enfuvirtide
TAM	Thymidine analogues mutations
TAR	Target sequence for viral Transactivation
Tat	Trans-activator of transcription, p16/p14
TCR	T cell receptor
TDF	Tenofovir disoproxil fumarate
TDRM	Transmitted Drug Resistance Mutation
Tev	Tat/Rev activities, p28
TGS	Third generation sequencing
TM	Transmembrane
TPV	Tipranavir
UDS	Ultra-deep sequencing
VF	Virological Failure
Vif	Viral infectivity factor, p23
Vpr	Viral protein R, p10-p15
Vpu	Viral protein U, p16
Vpx	Viral protein X, p12-p16
X4	CXCR4-using viruses
ZDV	Azidothymidine, Zidovudine
ZMW	Zero-mode waveguides

Contents

Summary

Drug resistance testing is utilized in the clinical routine to personalize ART of HIV-1 infected people. Population sequencing is employed for HIV-1 genotyping obtaining good correlations with clinical outcomes. However, its lack of sensitivity to detect minority DRM mutations or minor CXCR4-using viruses can compromise the efficacy of antiretroviral therapy (ART). The use of next generation sequencing technologies for ultrasensitive HIV-1 genotyping might allow deep characterization of the viral population optimizing the ART.

The objective of this work was to evaluate the clinical value of ultrasensitive HIV-1 genotyping obtained by 454 sequencing for the management of ART-experienced HIV-1 subjects in different treatment situations.

During the utilization of 454 sequencing for viral tropism determinations, this technology achieved the closest diagnostic accuracy to ESTA^{TM} in plasma ARN. Although population sequencing had lower sensitivity than 454 sequencing, its highest specificity led to obtain closest accuracy to ESTA. Even though tropism determinations were equivalent between plasma and cellular compartments, phylogenetic analyses from data generated by 454 sequencing revealed sequence compartmentalization in some subjects.

We also validated triplicate population HIV-1 genotyping from PBMC-associated DNA for viral tropism determinations in a prospective and randomized clinical trial. Here, genotypic tropism testing in proviral DNA demonstrated to become a suitable tool to guide treatment switches to CCR5 antagonists in aviremic individuals. In this study, 454 sequencing was capable to detect non-R5 viral strains in two subjects previously classified as harboring R5 HIV-1 strains by population sequencing. This compartmentalization might compromise viral tropism determinations depending on the compartment analyzed. Furthermore, the absence of evolution observed during prolonged periods of aviremia suggested that testing of stored plasma sample would be generally safe and informative.

Regarding the detection of minority DRM in *pol* gene, 454 sequencing for ultrasensitive HIV-1 genotyping was technically non-inferior than population HIV-1 genotyping during the assessment of antiretroviral drug susceptibility. However, although this technology provided additional genotypic information beyond population sequencing in most of

heavily pre-treated individuals tested, only few antiretroviral susceptibility predictions were modified.

This technology was also useful to explore the origin of DRM in integrase gene, revealing that mutants detected at the time of virological failure can be originated from pre-existing minority drug resistance variants.

In summary, this thesis has shown the clinical utility of ultrasensitive HIV-1 genotyping in ART-experienced HIV-1 infected individuals. However, further studies should extend our findings.

454 sequencing allowed a deep characterization of the HIV-1 diversity within a host helping to understand viral evolution and HIV-1 pathogenesis. Moreover, the standardization and automation of 454 sequencing protocols for HIV-1 sequencing would allow the implementation of this technology for HIV-1 diagnosis.

Resum

Els test de resistència al antiretrovirals són utilitzats en la pràctica clínica per la personalització del tractament antiretroviral (TARV) de les persones infectades pel VIH-1. La seqüenciació poblacional (SP) és la tècnica més emprada pel genotipat del VIH-1 obtenint una bona correlació amb la resposta clínica dels pacients. No obstant, la baixa sensibilitat de la SP pel que fa a la detecció de mutacions de resistència als antiretrovirals (DRM) o soques X4-tròpiques presents en baixes prevalences pot comprometre l'eficàcia del TARV. L'aplicació de noves tècniques de seqüenciació massiva pel genotipat del VIH-1 (genotipat ultrasensible) permetria una caracterització de la població viral amb major resolució optimitzant el TARV.

L'objectiu d'aquesta tesi era avaluar el valor clínic del genotipat ultrasensible pel maneig clínic de pacients infectats pel VIH-1 que han estat exposats a TARV.

Durant la utilització de 454 sequencing per la determinació del tropisme viral, 454 sequencing va obtenir una major concordança amb ESTA (Enhanced Sensitivity TrofileTM Assay) en l'anàlisi de l'ARN viral. Tot i que la SP tenia una menor sensibilitat respecte 454 sequencing, la seva elevada especificitat li va permetre obtenir una millor precisió. Anàlisis filogenètics a partir de dades obtingudes per 454 sequencing van revelar que, encara que les determinacions eren equivalents entre amdós compartiments, en alguns pacients es va observar compartimentalització de seqüències pel que fa als haplotips i a la seva prevalença. Aquesta compartimentalització podria comprometre la determinació del tropisme viral en funció del compartiment que s'analitzi.

Durant aquest treball també es va fer la validació de la SP per determinacions del tropisme a partir d'ADN proviral en un assaig clínic prospectiu i aleatoritzat. Aquest assaig va demostrar ser útil per guiar canvis de tractament antiretroviral que incloguin antagonistes de CCR5. De tota manera, 454 sequencing va ser capaç de detectar variants X4 tròpiques en dos pacients prèviament classificats com a R5 tròpics per SP.

Pel que fa a la detecció de DRM en el gen pol, 454 sequencing va demostrar ser no-inferior a la SP durant l'avaluació de la susceptibilitat al tractament antiretroviral. Cal destacar que 454 sequencing va aportar informació genotípica addicional en la majoria dels pacients, encara que aquesta modifiqués poques prediccions de susceptibilitat. A més, aquesta tecnologia va ser utilitzada per explorar l'origen de les DRM en el gen de la integrasa del VIH-1, demostrant que virus mutants detectats

durant el fracàs virològic poden ésser originats a partir de virus mutants minoritaris pre-existents.

En resum, aquesta tesi ha mostrat la utilitat clínica del genotipat ultrasensible del VIH-1 en pacients experimentats al TARV. 454 sequencing ha permès una profunda caracterització de la diversitat viral dins l'hoste, facilitant l'estudi l'evolució viral i la seva patogènesi del VIH-1. A més, l'estandardització i automatització dels protocols de 454 sequencing permetria la implementació d'aquesta tecnologia pel diagnòstic del VIH-1.

Resumen

Los ensayos de resistencia a los antiretrovirales son utilizados en la práctica clínica para la personalización del tratamiento antirretroviral (TARV) de las personas infectadas por el VIH-1. La secuenciación poblacional (SP) es la técnica más utilizada para el genotipado del VIH-1 obteniendo una buena correlación con la respuesta clínica de los pacientes. Asimismo, la baja sensibilidad de la SP para la detección de mutaciones de resistencia a los antiretrovirales o variantes X4-trópicas presentes en baja prevalencia puede comprometer la eficacia de la TARV.

El objetivo de esta tesis era evaluar el valor clínico del genotipado ultrasensible para el manejo clínico de pacientes infectados por el VIH-1 que han estado expuestos a TARV.

Durante la utilización de *454 sequencing* para la determinación del tropismo viral, 454 sequencing obtuvo una mayor concordancia con ESTA (*Enhanced Sensitivity Trofile^{TM} Assay*) en el análisis del ARN viral. Aunque la SP mostró una menor sensibilidad que 454 sequencing, su elevada especificidad le permitió obtener una mayor precisión. La información genotípica generada por *454 sequencing* fue utilizada para evaluar la compartimentalización. Aunque las determinaciones del tropismo viral eran equivalentes entre los compartimentos, en algunos pacientes se observó compartimentalización de secuencias, lo que puede comprometer la determinación del tropismo viral en función del compartimento que analizado.

Durante este trabajo también se hizo la validación de la SP para determinaciones del tropismo a partir de ADN proviral en un ensayo clínico prospectivo y aleatorizado. Este ensayo demostró ser útil para guiar cambios de tratamiento antirretroviral que incluyan antagonistas de CCR5. De todos modos, *454 sequencing* fue capaz de detectar variantes X4 trópicas en dos pacientes previamente clasificados como R5 trópicos por SP.

En cuanto a la detección de DRM en el gen *pol*, *454 sequencing* demostró ser no inferior a la SP durante la evaluación de la susceptibilidad al tratamiento antirretroviral. Cabe mencionar que 454 sequencing aportó información genotípica adicional en la mayoría de los pacientes, aunque esta modificara pocas predicciones de susceptibilidad. Además, esta tecnología fue útil para explorar el origen de las DRM en el gen de la integrasa del VIH-1, mostrando que los mutantes detectados durante el fracaso virológico pueden ser originados a partir de mutantes pre-existentes.

En resumen, esta tesis ha mostrado la utilidad clínica del genotipado ultrasensible del VIH-1 en pacientes experimentados al TARV. *454 sequencing* ha permitido una profunda caracterización de la diversidad viral dentro del huésped, facilitando el estudio de la evolución viral i la patogénesis del VIH-1. Además, la estandarización i automatización de los protocolos de *454 sequencing* permitiría la implementación de esta tecnología para el diagnóstico clínico del VIH-1.

Introduction

The human immunodeficiency virus (HIV) is the etiologic agent of the acquired immunodeficiency syndrome (AIDS). The AIDS pandemic affects more than 34 million people, with more than 2.5 million of people becoming infected and causing 1.7 million AIDS-related deaths every year. Fortunately, the efficacy of antiretroviral therapy has reduced the morbidity and mortality of subjects and has reduced the possibility of the transmission of HIV infection. Nonetheless, morbidity and mortality rates for AIDS remain higher in poor countries areas because of limited access to antiretroviral treatment.

1. Classification

HIV-1 is a member of the genus *Lentivirus*, in the *Retroviridae* family. Outstanding features of the infection caused by genus *Lentivirus* are the long incubation period, the high host specificity and the association with the accumulation of unintegrated linear and circular viral complementary deoxyribonucleic acid (cDNA) in infected cells achieving latent or persistent cell infection. The main characteristics of the viruses are the cone-shaped core protecting the ribonucleic acid (RNA) genome, the need for the ARN genome to be translated to the DNA before integration into the host cell genome, the highly polymorphic long genomes with truncated genes translating for several proteins, the use of different open reading frames and the highly glycosylated envelope.

2. Origin

There are two types of HIV, HIV-1 and HIV-2. Both strains are originated in non-human primates from different zoonotic processes in the 20th century in West-Central Africa. Phylogenetic analysis performed from cryopreserved samples revealed that HIV-1 and HIV-2 originated from the evolution of a simian immunodeficiency virus (SIV) that infected wild chimpanzees (*Pan troglodytes troglodytes*)[1] and from different SIV responsible for the infection in the sooty mangabey (*Cercocebus atys atys*)[2, 3], respectively (Figure 1). Although both viruses cause AIDS, HIV-1 is more virulent and easily transmitted whereas HIV-2 is characterized by a longer period between initial infection and illness. HIV-1 causes a global pandemic and is the etiologic agent of the vast majority of HIV infections, whereas HIV-2 is largely restricted to West Africa.

Three groups of HIV-1 have been identified representing an interspecific transference from simian, M (main), N (new), and O (outlier). The group M is divided into eight subtypes or clades (A, B, C, D, F, G, H, J and K), where subtype B is the most prevalent in North America and Europe. Coinfection with distinct subtypes gives rise to circulating recombinant forms (CRFs).

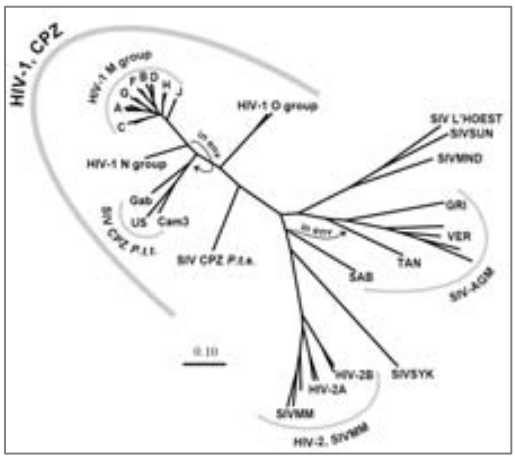

FIGURE 1. PHYLOGENETIC TREE OF THE SIV AND HIV VIRUSES. Source: *Theoretical Biology and Biophysics Group, Los Alamos National Laboratory.*

3. Structure and genome organization

HIV-1 has a spherical shape with a diameter of around 120 nanometers (nm). It has a diploid genome composed by 2 positive single-stranded RNA copies (ssRNA). The viral genome has a length of about 10 kilobase pair (Kbp) and codifies for 9 genes encoding 19 proteins. The viral ARN is tightly bound to nucleocapsid proteins (p7) and is associated with different proteins such as reverse transcriptase, protease, ribonuclease and integrase. A matrix (p17) surrounds the capsid and ensures the integrity of the virion particle. On the outer face is the viral membrane, composed of phospholipids taken from the cellular membrane and viral glycoproteins (gp160) (Figure 2).

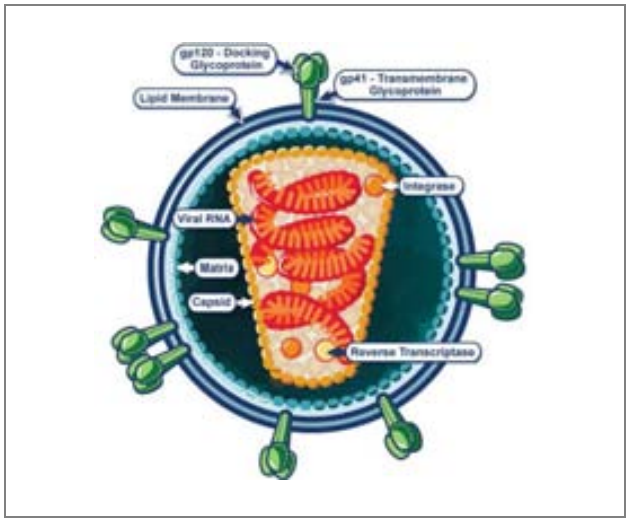

FIGURE 2. SCHEMATIC REPRESENTATION OF THE HIV-1 STRUCTURE. Source: *National Institute of Allergy and Infectious Diseases (http://www.niaid.nih.gov/topics/hivaids/understanding/biology/Pages/structure.aspx).*

The viral genes have structural, regulatory and structural landmarks (Figure 3). They are involved in the making of new viral particles or in the control of the ability of HIV-1 to infect cells, to replicate or to cause disease.

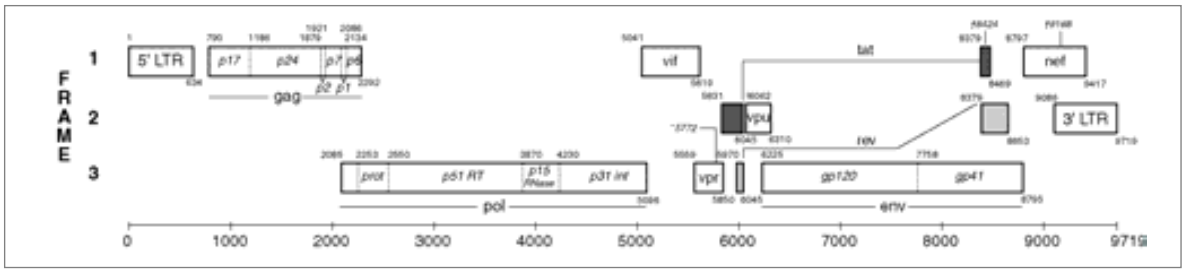

FIGURE 3. LANDMARKS OF THE HIV-1 GENOME, HXB2 STRAIN. Numbering Positions in HIV in relation to HXB2CG, in the database compendium. Source: *Theoretical Biology and Biophysics Group, Los Alamos National Laboratory (http://www.hiv.lanl.gov/content/sequence/HIV/IMAGES/hxb2genome.gif).*

The known activities of the genomic structural landmarks, accessory proteins and structural and enzymatic proteins are listed below:

Structural and enzymatic proteins:

- Gag (p55): it is a myristylated protein which is processed by the viral protease in matrix (MA, p17), capsid (CA, p24), Spacer Peptide 1 (SP1, p1), nucleocapsid (NC, p7), Spacer Peptide 2 (SP2, p2), and p6. It is associated with the plasma membrane and plays a structural role in the viral assembly.
- Pol: it encodes the viral enzymes protease, reverse transcriptase, and integrase. The precursor Gag-Pol polyprotein, produced by ribosome frameshifting near the 3' end of *gag*, is also processed by the viral protease.

- Reverse transcriptase (RT, p66, p51): it is a dimer of p66 and p51 subunits which mediates RNA-dependent DNA synthesis, the excision of HIV-1 RNA from RNA (RNAse H, p15) and DNA-directed DNA synthesis.
- Protease (PR, p10): it is an aspartyl-protease responsible for the proteolytic processing of the viral polyproteins (maturation) required for the assembly of the virions.
- Integrase (IN, p32): it is involved in the integration of the viral cDNA into the host chromosomal DNA. Integrase is a part of the preintegration complex in association with the viral DNA.

- Envelope: viral glycoproteins are produced as a precursor (gp160) composed of the noncovalent interaction between the external gp120 and the glycoprotein gp41. The formation of trimers of gp160 complexes is required to penetrate into the cells[4]. Gp160 complexes are the product of the interaction between gp41 and gp120.
  - Gp120: it is exposed on the surface of the HIV-1 envelope and is involved in the viral tropism containing the binding site for the CD4 receptor and for the coreceptors. It is composed of 5 conserved and 5 variable domains, with the third variable domain (V3-loop) being the main determinant of the viral tropism. Gp120 contains potential N-linked glycosylation sites (PNGSs) and many neutralizing antibodies binding sites[5].
  - Gp41: it is the envelope transmembrane (TM) protein. It facilitates the approach of the viral and cellular membranes and their subsequent fusion[6].

Accessory proteins:

- Trans-activator of transcription (Tat, p16/p14): it binds to the target sequence for viral transactivation (TAR) RNA element and acts as a transcriptional transactivator of gene expression for Long Terminal Repeat (LTR) promoter acting. The TAR may also be processed into microRNAs that regulate the apoptosis genes ERCC1 and IER3. Tat is localized primarily in the nucleolus/nucleus, although extracellular Tat can be found and can be taken up by cells in culture.
- Regulator of expression of virion proteins (Rev, p19): it is involved in shuttling RNAs from the nucleus to the cytoplasm by binding to the RRE RNA element. It regulates the expression of the viral mRNA promoting the

nuclear export, the stabilization and the utilization of the unspliced viral mRNAs containing Rev Responsive Element (RRE). It is localized in the nucleolus/nucleus.

- Viral infectivity factor (Vif, p23): it helps in proviral DNA synthesis and the virion assembly promoting infectivity. It is also involved in shuttling RNAs from the nucleus and the cytoplasm by binding to the RRE RNA element. Moreover, it prevents the action of APOBEC3G/F, a cell protein that deaminates DNA:RNA hybrids and/or interferes with the Pol protein[7, 8]. It is primarily located in the cytoplasm, in a soluble or membrane-associated form.
- Negative regulatory factor (Nef, p27-p25): it is the most immunogenic of the accessory proteins. It increases viral infectivity and down-regulates the CD4 receptor and the major histocompatibility complex class I molecules (MHC-I)[9]. Nef also interacts with SH3 domains. Nef has been located in the cytoplasm, associated with the nucleus, with the cytoskeleton and with the plasma membrane via the myristyl residue linked to the conserved second amino acid.
- Viral protein R (Vpr, p10-p15): it is involved in the virus replication and transactivation and is incorporated into the virion. It interacts with the p55 precursor and also with the p6. It is primarily located in the nucleus with postulated functions such as targeting the nuclear import of preintegration complexes[10], cell growth arrest at G2/M[11], transactivation of cellular genes[12] and induction of cellular differentiation.
- Viral protein U (Vpu, p16): it is an integral membrane protein that influences the release of new virus particles from infected cells inducing the depletion of tetherin (cellular restriction factor). Furthermore, it promotes the degradation of CD4 in the endoplasmic reticulum. The Vpu gene is found exclusively in HIV-1 and some HIV-1-related SIV isolates, but not in HIV-2 or the majority of SIV isolates.
- Viral Protein X (Vpx, p12-p16): it plays a role in the entry and infectivity. It is a homolog protein of HIV-1 Vpr (Viral Protein R)[13, 14], and although the virus presents Vpx it also carries Vpr. The Vpx function is not fully elucidated, but some studies have suggested a redundancy in the function of Vpr and Vpx. It has been found in HIV-2 but not in HIV-1 or other SIVs.
- Tev (p28): tripartite tat-env-rev protein. It is primarily localized in nucleus.

Structural landmarks:

- Long terminal repeat (LTR): it is a DNA sequence flanking the genome of the integrated provirus. It acts by controlling the production of new viruses and can be triggered by proteins from either HIV-1 or from the host cell.
- Psi elements (PE): they are involved in the viral genome packaging and recognized by Gag and Rev proteins.
- SLIP element (TTTTTT): it is involved in the regulation of the -1 ribosomal frameshift in the Gag-Pol polyprotein reading frame required to make functional Pol.
- Target sequence for viral Transactivation (TAR): the first 45 nucleotides of the viral mRNAs in HIV-1 where Tat and cellular proteins bind. It forms a hairpin stem-loop structure with a side bulge required for binding.
- Rev responsive element (RRE): it is encoded within the env gene and is necessary for Rev function.
- Cis-acting Repressive Sequences (CRS): it inhibits structural protein expression in the absence of Rev.
- Inhibitory/Instability RNA sequences (INS): they are found within the structural genes. They transcriptionally inhibit the expression of the structural proteins.

4. HIV-1 REPLICATION CYCLE

The replication cycle of the HIV-1 involves viral entry, transcription of the viral genome, integration into the chromatin, transcription of the proviral DNA, RNA processing, protein synthesis, viral budding and maturation (Figure 4).

Viral entry

The virus penetrates the host cells after an interaction between gp120 exterior viral glycoprotein and the CD4 cellular receptor[15] and subsequent contact with the cellular coreceptors, CCR5 or CXCR4 (chemokine coreceptors)[16-20]. The binding between gp120 and the cellular coreceptor facilitates the interaction between the heptad repeat 1 and 2 (HR1 and HR2) domains of gp41. These domains are rearranged in an antiparallel orientation to form a six-helix bundle which leads to the approximation of the two membranes and the eventual membrane fusion. The process ends with the penetration of the viral capsid into the host cell.

Cellular receptors have different functions; the CD4 receptor assists the T cell receptor (TCR) in communicating with an antigen-presenting cell; the CCR5 receptor is involved in the regulation of leukocyte migration and tumor growth, having MIP-1α, MIP-1β and RANTES as natural ligands; the CXCR4 receptor is involved in maintaining

stem cell homeostasis and has SDF-1 as a natural ligand. Cellular receptor expression is heterogeneous, being expressed by different subsets of cells; the CD4 receptor is found in different cell subsets as T helper cells, regulatory T cells, monocytes, macrophages, and dendritic cells; the CCR5 is restricted to T-cells (memory and activated CD4+ T lymphocytes), gut-associated lymphoid tissues (GALT), macrophages, dendritic cells, and microglia; and the CXCR4 is restricted to T cells (naïve and resting CD4+ T lymphocytes, as well as CD8+ T cells), B cells, neutrophils, and eosinophils.

Viral tropism refers to the cell type that HIV-1 infects and replicates in. Viruses can be classified depending on the viral tropism; viruses that exclusively use the CCR5 coreceptor are defined as R5 viruses or M-tropic due to their ability to infect macrophages; viruses that exclusively use the CXCR4 coreceptor are defined as X4 viruses or T-tropic due to their ability to infect T-cells; finally viruses that can use both coreceptors are defined as Dual-Tropic viruses[16, 21-23]. It should be noted that subjects can be infected by a mixture of CCR5 and CXCR4-using the viruses at once, with the viral tropism being defined as Mixed-tropic.

The utilization of these coreceptors has been associated with the disease. CXCR4-using viruses are related to higher and faster CD4+ T cell count decay, higher cytopathocity and faster progression to AIDS[24]. Primary HIV-1 infections are caused almost exclusively by the CCR5-tropic HIV-1 strains, whereas nearly 50% of HIV-1 infected people present CXCR4 using viruses at advanced stages of the disease[25]. The use of the CCR5 coreceptor during the early stages of the infection seems to be governed by the expression of CCR5 in macrophages and dendritic cells on the mucous membranes of the genital and gastrointestinal tract. The depletion of CCR5 target cells, the loss of HIV-1 specific immune inhibition or the low expression of RANTES have been postulated as possible factors of viral tropism switch. Two possible scenarios have been described to explain the change in viral tropism; the evolution of CCR5 using viruses toward the use of CXCR4 coreceptor, or the pre-existence of minor X4 viruses from the initial stages of the infection[24, 26]. These minor CXCR4-using viruses could be missed by conventional tropism assays because of their low sensitivity and would emerge in an advantageous environment.

Transcription of the viral genome

Two copies of positive ssRNA molecules are present inside the viral capsid. Together with the genetic material, enzymes such as reverse transcriptase (RT), integrase and protease are also present. Once the capsid penetrates into the cytoplasm, the RT starts to transcribe the ssRNA molecules into a cDNA. The RT

shows ribonuclease activity degrading the viral RNA during the synthesis of cDNA (RNAse H)[27], as well as DNA-dependent DNA polymerase activity, which is involved in the polymerization of the sense DNA from the antisense cDNA. The absence of proofreading activity 5'-3' in the HIV-1 polymerase is responsible for the extraordinary variability of ARN viruses. The formation of a nucleoprotein reverse transcription complex, which includes MA, CA, Vpr, RT and IN, is required to carry out this step. The synthesis of full-length DNA produces the preintegration complex (PIC) promoting the integration of the DNA molecules into the cellular chromosomes.

Integration

The double strand DNA (dsDNA) is transported to the nucleus by the PIC for its integration into the cellular genome. Apart from viral proteins, Lens-epithelium-derived growth factor (LEDGF/p75) and Barrier-to-autointegration factor (BAF) cytoplasmatic cellular proteins[28] are also incorporated into the PIC. LEDGF/p75 seems to be involved in several functions such as favoring the nuclear-like accumulation of IN and its stable tethering to chromatin, to enhance the integration-site selection of the viral DNA, and to anchor the PICs[27] to the chromatin together with BAF. Once the viral DNA penetrates into the nucleus, the integrase cleaves a few bases from each 3' end, providing the 3'-OH groups required for the attachment to the host DNA. Afterwards, the processed 3' ends of the viral DNA are covalently ligated to the host chromosomal DNA during the strand transfer reaction.

Transcription of the proviral DNA

Integrated dsDNA (proviral DNA)[29] can remain at a latent[30] stage or it can be activated by AP-1 and NF-*κ*B transcription factors[31-33] to initiate the viral transcription via cellular type-II polymerases. Proviral DNA is transcribed into messenger RNA (mRNA) and later spliced into small pieces that are transported to the cytoplasm and are translated into the regulatory proteins Tat and Rev.

RNA processing

Tat and Rev intensify virus production and permit the transport of unspliced mRNAs out of the nucleus, respectively. Unspliced mRNAs are transported to the cytoplasm for transcription comprising two phases; an early phase where Tat, Rev, and Nef are synthesized; and a later phase with the expression of the remaining genes.

Protein synthesis

The production of structural proteins as Gag and Env starts from the full-length mRNAs. The full-length mRNAs bind to the Gag protein and are packaged into new viral particles. Viral assembly is placed at the plasma membrane of the host cell. Once the full Env polyproteins are processed on the membrane-bound polyribosomes of the endoplasmic reticulum, they are transported toward the Golgi apparatus. There, they are glycosylated and cleaved by a cellular enzyme into the gp41 and gp120. Both proteins are transported to the host cell plasmatic membrane where the gp41 anchors the gp120 to the membrane of the infected cell. The budding of the new particles occurs after the association of the Gag and Gag-Pol polyproteins along the HIV-1 genomic RNA on the inner surface of the plasma membrane, while part of the cellular membrane is incorporated into the viral membrane.

In parallel, the *gag*, *pro*, and *in* genes are processed from the same initiation codon. They maintain a balance of expression; Gag proteins are required in a ratio of 20:1 to protease and *pol*[34].

Viral budding and maturation

Portions of the Gag proteins are needed for the assembly of new virions. Interactions between MA and the cytoplasmic tail gp120 take place on the surface of the budding particle. Cellular proteins such as MHC are also incorporated into the viral membrane[27]. Various viral proteins participate actively during the budding; Vpu removes synthesized CD4 from the endoplasmic reticulum, Nef removes and degrades cell-surface CD4 and Env binds to itself and sequesters CD4.

In the maturation step, the HIV-1 protease enzyme cleaves the Gag-Pro-Pol precursors into individual functional HIV-1 proteins. Moreover, a condensation of the core into its characteristic cone shape leads to the development of fully-infective viruses[27].

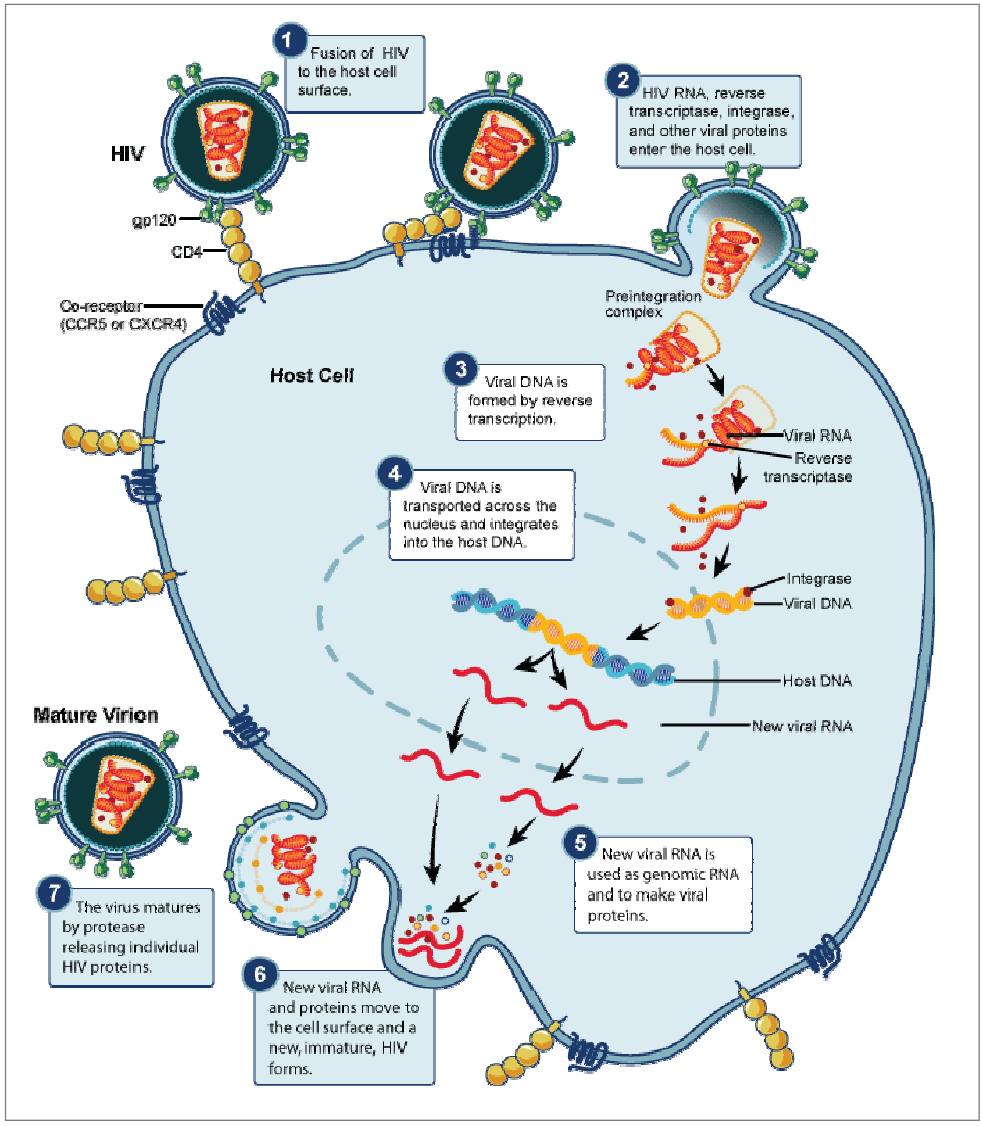

FIGURE 4. SCHEMATIC REPRESENTATION OF THE HIV-1 REPLICATION CELL CYCLE. Source: *National Institute of Allergy and Infectious Diseases, (http://www.niaid.nih.gov/SiteCollectionImages/topics/hivaids/hivReplicationCycle.gif).*

5. HIV-1 INFECTION

HIV-1 can be transmitted through the blood, semen, vaginal fluids and breast milk[35, 36]. HIV-1 infection has three clinical stages: primoinfection or acute infection, chronic or asymptomatic infection and advanced or symptomatic infection (Figure 5).

In acute infection (2-6 weeks) the CD4+ T cells are infected. This generates an important production of viral particles in the lymphatic system and the establishment of the infection in the lymphatic system of the intestine. The viruses produced are disseminated throughout the body and reflected as high levels of viremia. An important depletion of target CD4+T lymphocytes in peripheral blood and digestive tract takes place. During this phase, more than 40% of subjects develop symptoms such as a sore throat, fever, large, tender lymph nodes, a rash, nausea, diarrhea, vomiting, neurological syndromes and they may also develop opportunistic infections. At this stage humoral and cellular immunological responses occur. The humoral and cellular responses are based on the activity of the antibodies against HIV-1 and the activity of cytotoxic T lymphocytes (CTLs) and natural killer cells (NK), respectively[37]. They charge to eliminate the infected cells presenting viral antigens on their cellular surface. The virus may present first-escape mutations due to the selective pressure exercised by the immune system.

The chronic or asymptomatic phase lasts on average 10 years in the absence of antiretroviral treatment. Here, a reduction of viremia accompanied by gradual CD4+ T cells reduction is observed. Despite the potency of the humoral and cellular immune responses, the virus is not cleared from the body. Viral replication is not completely blocked and the viruses can escape from immunological responses through the accumulation of changes in their genomes. In the absence of ART, HIV-1 infected individuals typically have a detectable viral load (VL) and progress to AIDS. However, subpopulations of HIV-1 infected subjects defined as controllers or long-term nonprogressors (LTNP) are capable of maintaining low or undetectable viral loads and high levels of CD4+ T cells for more than 5 years.

The symptomatic phase of AIDS is characterized by an accelerated viral replication and massive destruction of the immune system. Neutralizing antibodies and cytotoxic cells are unable to suppress the viral replication. Consequently, this phase is characterized by high VL accompanied by the depletion of CD4+ T cells and the occurrence of opportunistic infections and HIV-1-related disease, such as Kaposi's sarcoma, human papillomavirus, *Pneumocystis carinii*, esophageal candidiasis, Burkitt's lymphoma, primary central nervous system lymphoma, and cervical cancer.

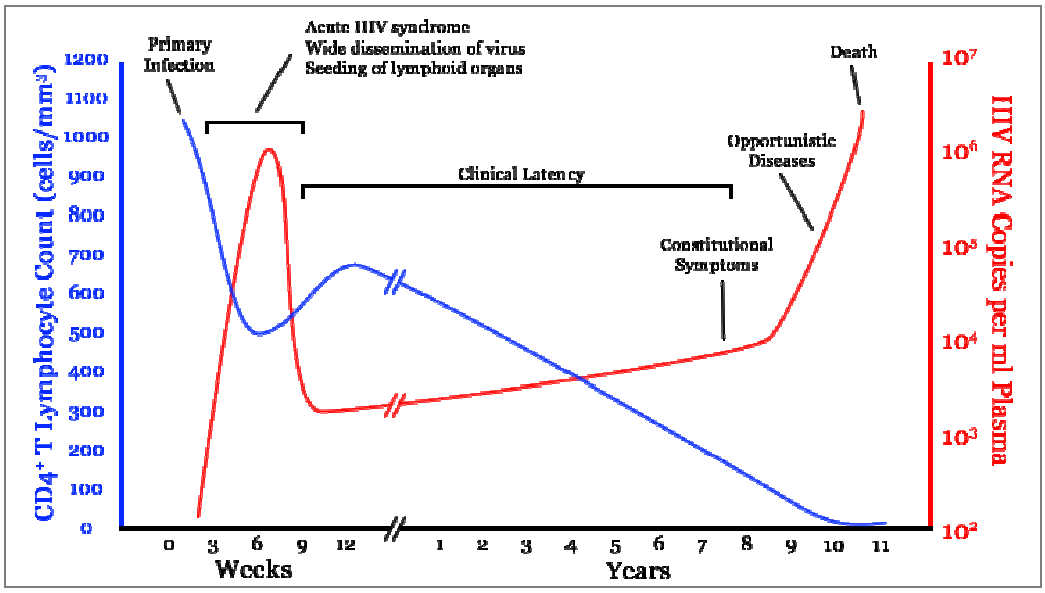

FIGURE 5. SCHEMATIC REPRESENTATION OF A TYPICAL COURSE OF PATHOGENIC HIV/SIV INFECTION. Source: *Wikipedia Commons (http://en.m.wikipedia.org/wiki/File:Hiv-timecourse_copy.svg).*

6. HETEROGENEITY OF HIV-1

Although subjects are probably exposed to hundreds of HIV virions, only one or, less frequently, two or three initial or "founder" virus variants are able to establish primary HIV infection. This oligoclonal population of founder viruses rapidly replicates and is disseminated throughout the body. The massive HIV-1 turnover and the lack of proof-reading activity of the reverse transcriptase lead to the production of $10^{9\text{-}12}$ virions per day in an untreated subject[38]. Moreover, the recombination events and the activity of cellular restriction factors also participate in this extraordinary source of variability. This genetic plasticity of HIV-1 becomes an important obstacle in developing an immunological response and defining an efficient therapy.

The estimated *in vivo* mutation rate of the reverse transcriptase in HIV-1 is 3.4×10^{-5} per base pair (bp) per replication cycle[39-41]. It multiplies with the size of the HIV-1 genome (about 10 Kbp) meaning that the new cDNA from its ARN precursor contains a nucleotide change or even a dual mutant.

Recombination events occur when a) more than one viral cDNA coinfect and integrate into the cellular genome[42], b) they produce ARN from different proviral DNA, c) they are incorporated into the same virion during the viral assembling and d) reverse transcriptase generates a recombinant cDNA from two ssRNA molecules. The ssRNA molecules form a dimer thanks to palindromic sequences located in the 5' end of the RNA molecule[43], facilitating the jump between ARN strands during the generation of cDNA products[44, 45].

The activity of cellular restriction factors also prevents viral replication in the host cells. For instance, APOBEC3G/F is a cytidine deaminase cellular enzyme that participates in innate immunity, producing hypermutation of guanine to adenine during the cDNA polymerization[46, 47]. However, HIV-1 has developed mechanisms with the purpose of blocking their activity. The viral accessory protein Vif triggers the ubiquitination and subsequent proteasomic degradation of APOBEC3G/F[7].

The combination of these factors drives a population of genetically-related viral strains competing within a highly mutagenic environment. This distribution of mutants is defined as quasiespecies[48].

7. ANTIRETROVIRAL THERAPY AND ANTIRETROVIRAL DRUG RESISTANCE

7.1. General principles of ART

The aim of ART is the reduction of mortality and morbidity of HIV-1-infected people and the prevention of HIV1 transmission. It blocks the principal stages of the virus replication cycle leading to a reconstruction of the immune system[21, 49, 50].

Panels of experts make a distinction between the clinical parameters for first-line ART initiation (Table 1). It should be noted that ART is recommended and offered to all HIV-1-infected persons during the acute phase of primary HIV-1 infection or persons with tuberculosis, opportunistic infections, coinfection by Hepatitis B or C virus (HBV or HCV). Table 1 shows the recommendations for first-line ART by the three main panels of experts: the Department of Health and Human Services (HHS) Panel on Antiretroviral Guidelines for Adults and Adolescents (DHHS)[21]; the International AIDS Society (IAS-USA)[51] and the European AIDS Clinical Society (EACS)[52].

Generally, first-line ART includes 2 nucleoside reverse transcriptase inhibitors (tenofovir/emtricitabine or abacavir/lamivudine) plus a non-nucleoside reverse transcriptase inhibitor (efavirenz), a ritonavir-boosted protease inhibitor (atazanavir or darunavir) or an integrase strand transfer inhibitor (dolutegravir). CD4+ T cell count and HIV-1 RNA levels should be monitored, as should engagement in care, ART adherence, HIV-1 ARV drug resistance, and quality-of-care indicators.

Table 1. Antiretroviral treatment guidelines for first-line therapy in adult patients.

EACS[1]	**DHHS**[2]	**IAS-USA**[3]
Recommendations are graded while taking into account both the degree of progression of HIV disease and the presence of or high risk for developing various types of (co-morbid) conditions Asymptomatic HIV infection: CD4 count 300-500 cells/mm^3: C; CD4 count 500 cells/ mm^3: D Symptomatic HIV disease (CDC[4] B or C conditions) incl. tuberculosis: CD4 count 300-500 cells/mm3: R; CD4 count 500 cells/ mm^3: R Primary HIV infection: CD4 count 300-500 cells/mm^3: C; CD4 count 500 cells/ mm^3: C	Antiretroviral therapy (ART) is recommended for all HIV-infected individuals to reduce the risk of disease progression. The strength and evidence for this recommendation vary by pretreatment CD4 cell count: CD4 count <350 cells/mm^3 (AI) CD4 count 350–500 cells/ mm^3 (AII) CD4 count >500 cells/ mm^3 (BIII) ART also is recommended for HIV-infected individuals for the prevention of transmission of HIV. The strength and evidence for this recommendation vary by transmission risks: Perinatal transmission (AI) Heterosexual transmission (AI) Other transmission risk groups (AIII)	ART is recommended and should be offered regardless of CD4 cell count. The strength of the recommendation increases as CD4 cell count decreases: CD4 count ≤500 cells/ mm^3: AIa CD4 count >500 cells/ mm^3: BIII
C= use of ART should be considered; for patients under these circumstances; some experts would recommend starting ART whereas others would recommend deferral of ART; this clinical equipoise reflects that whereas certain evidence supports starting ART, this needs to be balanced against the risk of known or undiscovered adverse drug reactions from use of ART, and hence the risk/benefit ratio for use of ART under these circumstances has not yet been well defined. D= defer initiation of ART. R= use of ART is recommended.	Rating of Recommendations: A= Strong; B= Moderate; C= Optional Rating of Evidence: I= Data from randomized controlled trials; II= Data from well-designed nonrandomized trials or observational cohort studies with long-term clinical outcomes; III= Expert opinion	AIa= Strong support for the recommendation. Evidence from 1 or more randomized controlled clinical trials published in peer-reviewed literature BIII= Moderate support for the recommendation. Recommendation based on the panel's analysis of the accumulated available evidence

[1]EACS: European AIDS Clinical Society; [2]Department of Health and Human Services (DHHS); [3]IAS-USA: International AIDS Society; [4]CDC: Centers for Disease Control and Prevention.

7.2. General principles of ARV resistance

The efficacy of the ART can be compromised by the development of ARV resistance. Antiretroviral drug resistance is the ability of one virus to replicate in the presence of ARV drug concentrations that suppress the replication of the susceptible virus.

Antiviral drug resistance is conferred by changes in the HIV-1 genome. It involves changes in one nucleotide (point mutations), insertions/deletions of various nucleotides or genetic recombination. Phenotypically, these genetic changes can be classified according to their effect on the replicative capacity; neutral (they have no impact on viral fitness), deleterious (they reduce the replicative capacity with respect to wild-type virus) and advantageous (they improve the replicative capacity respect to wild-type under selective pressure)[48, 53]. Clinically, the appearance of DRM forces clinicians to administrate more complex, toxic and expensive treatments.

Several factors are involved in the development and evolution of ARV resistance; the viral turnover, the *in vivo* mutation rate of the reverse transcriptase, the recombination events, the incomplete viral suppression in subjects under therapy, the magnitude of resistance conferred by each mutation, the impact of these mutations on viral fitness, the interaction between resistance mutations and resistance pathways, the genetic drug barrier (the number of critical drug-resistance mutations to overcome the anti-HIV activity) and treatment adherence[40, 48, 54-59]. Each antiretroviral therapeutic class has a unique adherence profile.

With regard to their effect on *in vitro* drug susceptibility, DRMs can be classified as primary or accessory. Primary DRMs (major) reduce susceptibility to one or more drugs and are early selected in the process of resistance development to one drug[22, 60]. They impair the viral fitness in a different range, but viral fitness is often rescued by the presence of accessory (or minor) DRMs. Accessory DRMs have little or no effect on drug susceptibility but often restore viral fitness.

Antiviral drug resistance can also be classified as primary resistance or secondary resistance[39]. Primary resistance is observed in treatment-naïve subjects and can be conferred by transmitted DRM (TDRM) or spontaneously-generated (*de novo*)[35, 36].

TDRM occurs when one subject becomes infected by a virus harboring mutations associated with drug resistance, whereas in the second case, the subject becomes infected by a wild type virus that develops drug resistance mutations before treatment administration[35, 36]. TDRM is a major public health concern because it could lead to a situation in which no effective drugs are available for the treatment of HIV-1 infected people. In well-resourced countries, the prevalence of TDRMs for first-line drugs ranges from 8% to 19% for any drug, 5% to 12 % for NRTIs, 2% to 8% for NNRTIs and

3 to 7 % for PIs[61-64]. The prevalence of TDRMs for InSTIs is almost non-existent because of recent administration. On the other hand, spontaneous generation of drug resistance occurs because the high genetic variability of the HIV-1 allows the generation of all possible mutants in an untreated subject in one day. Based on the hypothesis that all single mutants can pre-exist in treatment-naïve subjects, some double mutants may pre-exist and triple mutants do not pre-exist, triple therapy is recommended to ensure the effectiveness of first-line ART[40].

Secondary resistance (acquired) is observed in treatment-experienced subjects under ART. Here, DRMs are spontaneously generated in a background of a transmitted drug-susceptible virus evolving from ongoing selective pressure during ART exposure.

Due to the similarity of antiretroviral compounds in terms of their chemical structure and mechanism of inhibition, the presence of DRMs that affect the capacity of viral suppression exerted by one compound can alter the antiretroviral activity of another compound. Cross-resistance or hypersusceptibility occurs when the viral suppression capacity of the new drug is reduced or enhanced by the presence of DRM to a previous drug, respectively. For instance, T215Y is a DRM to zidovudine that confers cross-resistance to stavudine and hypersusceptibility to etravirine.

7.3. Specific ARV drug resistance profiles

Twenty-nine Food and Drug Administration (FDA)-approved drugs from six different classes are available for treatment of HIV-1 infections[21, 49]: entry inhibitors (including fusion inhibitors and coreceptor antagonists)[6], nucleoside-analogue reverse transcriptase inhibitors[65], non–nucleoside reverse transcriptase inhibitors[66], integrase strand-transfer inhibitor[67] and protease inhibitors[68, 69] (Table 2).

7.3.1. Protease inhibitors

Protease inhibitors (PIs) bind directly to the catalytic core of viral protease blocking the maturation of new viral particles[39, 56]. Due to the high genetic barrier of the PIs, monotherapy with boosted PI has attracted interest in recent years as a simplification strategy in HIV-1 infected subjects with sustained viral suppression. This strategy could reduce adverse effects related to the use of NRTIs such as damage to the mitochondria and may be useful in improving the treatment adherence and reducing the ART cost.

Drug resistance pathway to PIs is governed by the accumulation of primary resistance near the substrate/inhibitor binding site[56, 60, 70]. The presence of drug

resistance mutations (DRM) decreases viral fitness, although compensatory mutations in other parts of the enzyme restore the enzyme activity. Moreover, mutations in the cleavage sites of the Gag and Gag-Pol polyproteins are selected, improving the activity of the enzyme[22]. D30N, V32I, G48H, I50V, V82A, I84V, N88S or L90M are examples of DRMs present in patients receiving PI, often showing M46I/L and L63P compensatory mutations.

7.2.2. Nucleoside/Nucleotide Reverse transcriptase inhibitors

Nucleoside/Nucleotide Reverse transcriptase inhibitors (NRTIs) are artificial nucleotides lacking in 3'-OH that stop the polymerization once they are incorporated into the growing DNA strand. They compete against natural dideoxynucleotide triphosphates, preventing the completion of the synthesis of the viral dsDNA. NRTIs are prodrugs which require phosphorylation via cellular kinases. There are two mechanisms of resistance:

- Nucleoside pyrophospholysis via ATP eliminates artificial nucleosides from the 3' end of the growing DNA[71, 72]. DRM generated are called thymidine analogue mutations (TAMs), and two distinct mutation pathways are observed in nature, TAM1 (M41L, L210W, T215Y and D67N) and TAM2 (D67N, K70R, T215F and 219E/Q).
- A steric inhibition of the enzyme due to structural changes enables the differentiation between natural and artificial nucleosides[73]. It increases the affinity for natural nucleosides and promotes polymerization. M184V/I or K65R are examples of NRTIs mutations developed after the administration of lamuvidine or tenofovir, respectively.

7.2.3. Non-Nucleoside/Nucleotide Reverse transcriptase inhibitors

Non-nucleoside reverse transcriptase inhibitors (NNRTIs) are small molecules that block the enzyme activity by allosteric inhibition, inducing the formation of a proximal hydrophobic pocket[74-80]. Drug resistance mutations affect residues that are directly involved in inhibitor binding. However, few DRM have been found to act indirectly, by changing the position or the orientation of the amino acids involved in direct contact with the inhibitor. L100, K101, K103, E138, V179, Y181 and Y188 are the most common substitutions in the NNRTI-binding pocket.

Unlike the impairment in the viral fitness observed in other drug classes by the accumulation of several DRM, the presence of single nucleotide changes can

be interpreted as a high level of drug resistance without reducing the replicative fitness.

7.2.4. Integrase strand transfer inhibitors (InSTIs)

Integrase strand transfer inhibitors (InSTIs) prevent the strand transfer between retrotranscribed cDNA and the host cell genome. Their mechanism of action is based on binding to the pre-integration complex and the sequestration of the Mg^{2+} cations essential for the integration step[81]. Resistance to InSTIs is observed by the presence of DRMs in the catalytic core of the enzyme. Drug resistance shows three mutually exclusive patterns of resistance defined by primary mutations at Y143, Q148 and N155. An accumulation of secondary mutations is often observed, where E92Q, V151L, T97A, G163R and L74M or G140S/A and E138K are detected for N155H and Q148K/R/H, respectively[82, 83].

There is extensive cross-resistance between raltegravir and elvitegravir, while dolutegravir remains active in many RAL and EVG-resistant clones. Nonetheless, if the viruses continuously replicate in the presence of raltegravir or elvitegravir, those viruses might become resistant to dolutegravir[83, 84].

7.2.5. Entry inhibitors

Entry inhibitors prevent the entry of HIV-1 into the CD4+ T cells by attaching themselves to viral proteins or proteins in the host cell membrane.

- Fusion Inhibitors. Fusion inhibitors block the approximation of viral and cellular membranes. Enfuvirtide (T20) is a peptide of 36 amino acids in length derived from the HR2 sequence. It blocks the interaction between HR1-HR2 by binding to HR1. G36D, I37T, V38A/M, N42T/D and N43K are DRM present in HR1 in patients failing in monotherapy with enfurvitide[85, 86]. Apart from the impairment in viral fitness, these drug resistance mutations also sensitize viruses to neutralization by monoclonal antibodies that target the gp41 domain. Some limitations of this drug are its low genetic barrier and the requirement of subcutaneous administration which produces toxicities in terms of local reactions in 96% of the subjects[85].
- CCR5 antagonists. Maraviroc (MVC) is an allosteric inhibitors of the CCR5 cellular coreceptor[23]. It imitates the natural protection against HIV-1 infection presented in subjects harboring a 32-basepair deletion in the CCR5 gene (Δ-32). MVC binds to the hydrophobic pocket within the transmembrane helices of CCR5, altering the conformation of

CCR5 at the cell surface and disrupting its interaction with HIV-1 gp120.The inhibition only prevents the viral entry of CCR5 using strains without compromising the binding of chemokines and their subsequent signal transduction. Although ARV resistance can be conferred by a virus that acquires the ability to recognize receptor conformations stabilized by CCR5 antagonists[18, 19], the major cause of virologic failure to CCR5-antagonist based therapy is the emergence of pre-existing CXCR4-using viruses[26].

Table 2. Currently-available antiretroviral agents

Generic Name	Abbreviation	Brand Name	Manufacturer Name	Family
Atazanavir sulfate	ATV	Reyataz	Bristol-Myers Squibb	PI
Darunavir	DRV	Prezista	Tibotec, Inc.	PI
Fosamprenavir Calcium	FOS-APV	Lexiva	GlaxoSmithKline	PI
Lopinavir and Ritonavir	LPV/RTV	Kaletra	Abbott Laboratories	PI
Ritonavir	RTV	Norvir	Abbott Laboratories	PI
Saquinavir mesylate	SQV	Invirase	Hoffmann-La Roche	PI
Tipranavir	TPV	Aptivus	Boehringer Ingelheim	PI
Abacavir sulfate	ABC	Ziagen	GlaxoSmithKline	NRTI
Emtricitabine	FTC	Emtriva	Gilead Sciences	NRTI
Enteric coated didanosine	ddIEC	Videx EC	Bristol Myers-Squibb	NRTI
Lamivudine	3TC	Epivir	GlaxoSmithKline	NRTI
Tenofovir disoproxyl fumarate	TDF	Viread	Gilead	NRTI
Zidovudine, Azidothymidine	AZT or ZDV	Retrovir	GlaxoSmithKline	NRTI
Efavirenz	EFV	Sustiva	Bristol Myers-Squibb	NNRTI
Etravirine	ETV	Intelence	Tibotec Therapeutics	NNRTI
Nevirapine	NVP	Viramune XR	Boehringer Ingelheim	NNRTI
Rilpivirine	RPV	Edurant	Tibotec Therapeutics	NNRTI
Dolutegravir	DLG	GSK572	ViiV Healthcare	InSTI
Elvitegravir	ELV	GS-9137	Gilead Sciences	InSTI
Raltegravir	RAL	Isentress	Merck & Co	InSTI
Enfuvirtide	ENF	Fuzeon	Hoffmann-La Roche & Trimeris	EI (fusion inhibitor)
Maraviroc	MVC	Selzentry or Celsentri	Pfizer	EI (CCR5 antagonist)
Abacavir and Lamivudine	ABC+3TC	Epzicom	GlaxoSmithKline	MCCP*
Abacavir, Zidovudine, and Lamivudine	ABC+ZDV+3TC	Trizivir	GlaxoSmithKline	MCCP
Efavirenz, Emtricitabine and Tenofovir disoproxyl fumarate	EFV+FTC+TDF	Atripla	Bristol-Myers Squibb and Gilead Sciences	MCCP
Elvitegravir, Cobicistat, Emtricitabine, Tenofovir disoproxyl fumarate	ELV+COBI+TDF+FTC	Stribild/Quad	Gilead Sciences	MCCP
Emtricitabine, Rilpivirine, and Tenofovir disoproxyl fumarate	FTC+RPV+TDF	Complera	Janssen Therapeutics and Gilead Sciences	MCCP
Lamivudine and Zidovudine	AZT+3TC	Combivir	GlaxoSmithKline	MCCP
Tenofovir disoproxyl fumarate and Emtricitabine	TDF+FTC	Truvada	Gilead Sciences, Inc.	MCCP

PI, protease inhibitors; NRTI, nucleoside/nucleotide reverse transcriptase inhibitors, NNRTI, non-nucleoside/nucleotide reverse transcriptase inhibitors; InsTI, integrase strand transfer inhibitors; EI, entry inhibitors; MCCP, Multi-class Combination Products.

*Drug combinations in order to obtain better treatment adherence and effectiveness.

Adapted from (http://www.aidsmeds.com).

Figure 6. International AIDS society-USA (IAS-USA) drug resistance mutations list.

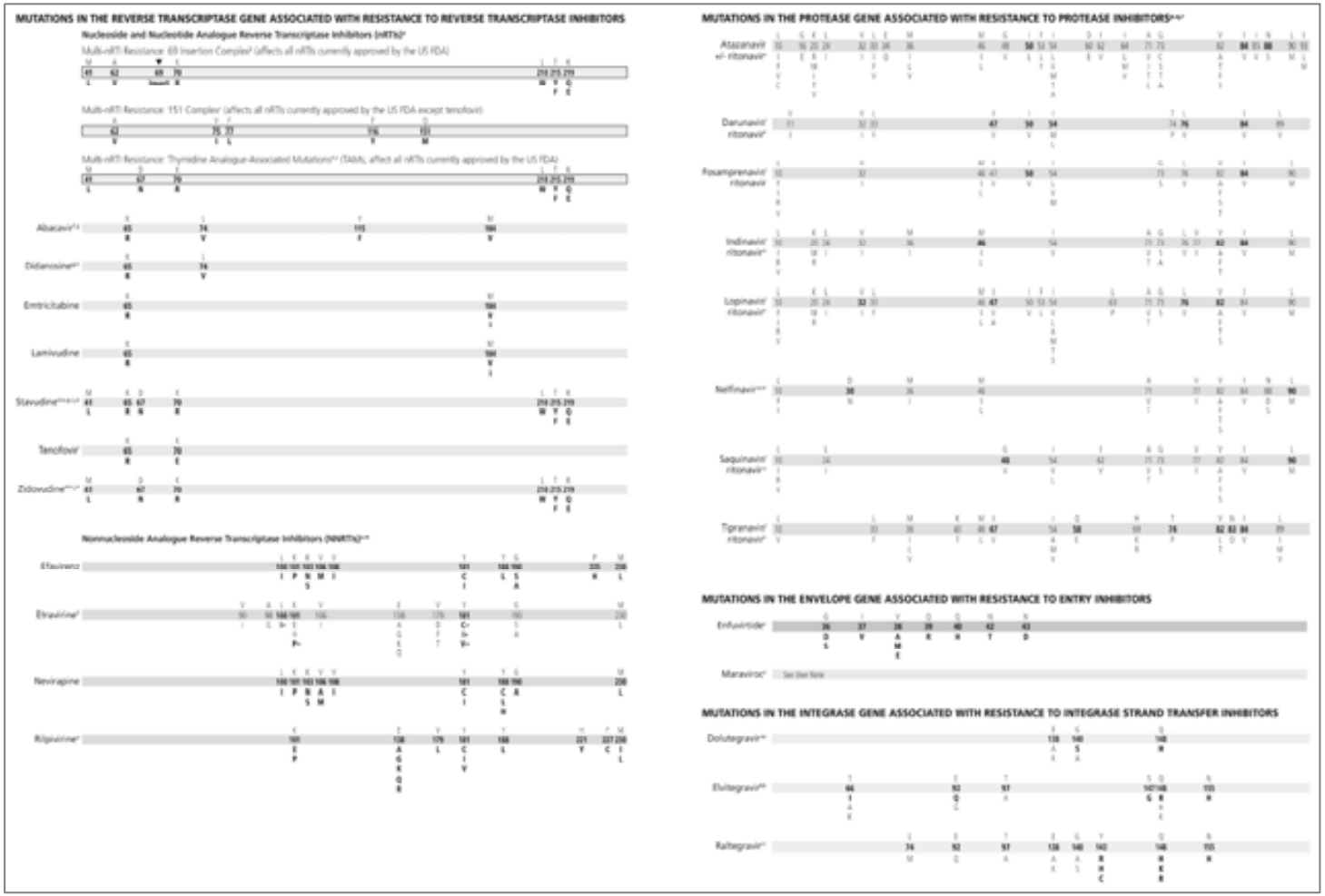

FIGURE 6. MUTATIONS IN HIV-1 THAT AFFECT SUSCEPTIBILITY TO ANTIRETROVIRAL DRUGS, BY HIV-1 GENE TARGET. The letter above each position is the wild-type amino acid and the letter(s) below each position indicate the substitution(s) that are associated with drug resistance. Source: *adapted from Johnson VA et al. Update of the Drug Resistance Mutations in HIV-1. Topics in Antiviral Medicine, 2013.*

8. METHODS OF TESTING FOR HIV-1 DRUG RESISTANCE

Drug resistance testing (DRT) is an essential tool for HIV-1 clinical care. DRT provides information about antiretroviral drug susceptibility helping to define the most optimal ART. International antiretroviral treatment guidelines recommend its performance before ART initiation, after virologic failure, in pregnancy, with suboptimal suppression of viral load after therapy initiation, when the appearance of toxicities or side effects suggests a change of ART or before the administration of CCR5 antagonist-based therapy[21, 22].

Several factors can compromised the reliability of DRT, such as the prevalence of viral strains harboring DRM (mutational load) and the number of inspected genomes. As occurs with the spontaneous variability of the HIV-1, the pre-test ability to detect DRM follows a Poisson distribution. Thus, to detect a strain present in 10%, 1% and 0.1% of the viral population with a 99% probability one should inspect at least 50, 500 and 5,000 genomes, respectively.

ARV resistance can be measured using either genotypic or phenotypic assays. The main characteristics of phenotypic and genotypic assays are shown in Table 3.

Table 3. Characteristics of phenotypic and genotypic assays.

Assay	Advantages	Disadvantages
Phenotypic	Direct and quantitative measure Any new ARV agents can be assessed Net effect of mutations measured (including cross-resistance mutations) Non-B subtypes can be evaluated	Cost Less sensitive than genotypes for wild-type and mutant mixtures Labor-intensive Cut-offs not defined for all drugs Inter-assay standardization not defined
Genotypic	Widely available Relatively simple to perform Less expensive Short turn-around time Detection of mutation may precede phenotypic resistance Sensitivity to detecting mixtures Indirect measure of drug susceptibility	Indirect measure Algorithms based on subtype B Interpretation complex, when many mutations present Discordance with phenotypic assay Interactions between mutations not predicted

8.1. Phenotypic assays

In general, phenotypic assays assess drug susceptibility by determining the effect of different anti-HIV-1 agents on the replication of viral isolates or recombinant vectors carrying patient-derived viral domains.

Most ARV agents are competitive inhibitors that inhibit a viral enzyme by competing with the natural substrate for attachment to the enzyme's catalytic site. Drug resistance to competitive inhibitors is a function of viral susceptibility and the level of drug levels achieved in the target cells. Drug resistance in phenotypic assays is often expressed

as the fold increase in IC50, IC90 or IC95, which reflect the drug concentration that inhibits 50%, 90% and 95% of viral replication relative to a wild type reference virus, respectively[22]. In the case of allosteric inhibitors, such as MVC, the decrease in viral susceptibility is reflected by the progressive decrease in the maximum percent inhibition (MPI). In this type of inhibitors, the increase in drug concentration does not achieve further virologic suppression once drug resistance is established.

Technically, the phenotypic assay procedure is based on the construction of recombinant viruses by polymerase chain reaction (PCR) amplification of the HIV-1 genomic region and its subsequent insertion into the backbone of a clone of HIV-1 from which the region of interest has been removed by cloning/in vitro recombination[87]. Afterwards, the constructs are transfected into susceptible cells for the production of large quantities of replication-competent recombinant viruses in the presence of different drug concentrations. The viral production is monitored by the expression of reporter genes carried in the vector. The most used commercial phenotypic assays are summarized below:

- **Antivirogram® (Virco BVBA):** viral constructs from PR-RT are transfected into an MT4 cell line. Infectivity is monitored by the cytopathic effect (CPE) using a 50% endpoint method (50% cell culture infectious dose). HIV-1 drug susceptibility is determined by -3(4,5-dimethylthiazol-2-yl)-2,5-dyphenyltetrazolium bromide (MTT) (MT4-MTT)-based CPE protection assay. Fold-resistance values are calculated by dividing the mean IC_{50} of the patient-derived recombinant virus by the mean IC_{50} of the wild-type control.
- **PhenoSense™ (Monogram Biosciences):** resistance test vector (RTV) is generated by the insertion of amplified region of HIV-1 into an indicator gene viral vector using ApaI and PinAI restriction sites. Then the cells are cotransfected with RTV DNA and a plasmid that expresses the envelope protein of amphotropic murine leukemia virus. The viruses produced are used to infect fresh target cells. Infectivity is monitored by the production of luciferase in the presence and absence of different drugs. PIs and RT inhibitors are added at the transfection and infection steps, respectively, to ensure a single cycle of viral replication, avoiding the evolution of viruses during multiple infection cycles[88]. To test the susceptibility of constructs to entry inhibitors, serial dilutions of drugs are incorporated into the cultures. Drug susceptibility is measured by the luciferase activity.
- **PhenoScript™ (Viralliance):** this assay is also based on a single cycle of in vitro replication. The viral capacity of replication of gag-protease, RT and

env constructs is measured in the presence of drugs. Each gene is independently amplified and co-transfected into producer cells along with the corresponding PhenoScript™ plasmid. The single cycle of in vitro replication is ensured for the prot and rt genes by the deletion of the env gene. The infection is carried out by the G protein of the Vesicular Stomitis Virus. In addition, PIs and RT inhibitors are added at the transfection step and at the infection step, respectively. To test the susceptibility of constructs to entry inhibitors, serial dilutions of drugs are incorporated into the cultures. The reporter cells contain a LacZ gene under control of the HIV-1 LTR, which produce b-galacosidase once they become infected. The b-galacosidase is measured using a CPRG based colorimetric assay by optical density.

8.2. Genotypic assays

Genotypic assays involve the nucleic acid analysis of the desired genome region of the HIV-1, the identification of a pattern of mutations associated with resistance to specific antiretroviral agents and the phenotype interpretation by algorithms or rules.

HIV-1 genotyping has attracted interest in clinical practice as an alternative to HIV-1 phenotyping because it is widely available, has lower cost and faster turnaround time to results. Despite their clinical utility, the lack of standardization among specialized laboratories leads to variations in the results obtained from genotypic and phenotypic assays. Moreover, the interpretation of the genotype is complex, requiring a continuous update due to the release of new drug approvals and the appearance of new resistance patterns (Table 4).

8.2.1. Point mutations assays

Point mutation assays interrogate specific genomic positions by specific primers or probes. They show a high sensitivity for detecting minor populations of resistance viruses[89].

- **Hybridization methods.** These methods detect the entire sequence of the PCR-amplified product or specific DRMs of HIV-1. They are based on chips that contain numerous probes for multiplexing, allowing the analysis of several DRM at once. The biotin labeled probes targeting specific codons in the PR and RT coding regions are attached to a nitrocellulose strip for subsequent recognition of specific codons. The revealed result is based on color production in the presence of the avidin-enzyme complex and substrate. Their utilization for clinical

purposes is restricted by their complexity, low sensitivity, cost, presence of insertions and deletions that affect the binding of probes, the variability depending on the HIV-1 subtype, the limited set of mutations detected and the non-interpretation of 10% of the results.

- **Allele Specific PCR (ASPCR).** This assay detects selected DRMs through separate real-time PCR amplifications of mutant and wild-type alleles of a codon[90-92]. Distinct oligonucleotides are used to amplify mutant and wild-type strains. Modifications in the 3' end of the mutant-specific oligonucleotide increase the discrimination of the method. The amplification of standards in parallel to the samples allows the monitoring of the number of amplified copies. Validation of the assay using combinations of wild type and mutant alleles is required for reliable determinations. The development of Multiplex-ASPCR allows the simultaneous analysis of genetic variants in a single reaction by the use of several pairs of oligonucleotides annealing to different target sequences. This assay is able to detect DRMs present at 0.003% of the viral population in optimal settings[92], although the presence of polymorphisms next to the target DRM inspected can compromise their detection, generating different cut-offs for the sensitivity and specificity of each mutation. The assay is widely employed for surveillance of HIV-1 drug resistance studies carried out in low- and middle-income countries.

8.2.2. Sequencing assays

Sequencing assays interrogate broad genomic regions by inspecting different genomic positions at once.

- **Population sequencing (PS).** This assay is based on PCR-amplification of the desired genomic region and its subsequent sequencing using the Sanger enzymatic dideoxy technique[93]. Here, dideoxynucleotide triphosphates (ddNTPs) are introduced for DNA synthesis in the presence of specific oligonucleotides. The incorporation of ddNTPs leads to chain termination, generating numerous DNA molecules of varying lengths, separated by polyacrylamide gel electrophoresis. Nucleotide incorporation is detected by fluorometric labeling in an automated sequencer. The sequence generated is called a population sequence because it is a summary of the entire viral population.

Despite the clinical value of population sequencing, in the population sequences generated only DRM present in more than 20% of the viral population are represented[22, 94]. The low sensitivity of the assay rules out its utilization to explore the presence of minority DRM.

Three commercial sequencing systems reporting DRM in protease and the first two thirds of reverse transcriptase of the HIV-1 have been validated in clinical trials; HIV-1 TruGene™ Genotyping Kit (Siemens), ViroSeq™ HIV-1 Genotyping System (Abbott Molecular) and GeneSeq™ HIV (Monogram Biosciences). As an alternative to commercial sequencing systems, “in house” sequencing methods have been developed, allowing reductions in cost and the customizing of protocols in order to sequence any genomic region and subtype. Nonetheless, the lack of standardization of “in house” sequencing methods might compromise drug resistance determinations.

- **Standard cloning and sequencing of multiple clones.** This assay is based on PCR-amplification and cloning of the HIV-1 desired genomic region. The constructs are transformed into bacterial cells and are then plated into solid selection media. Individual colonies are picked up for independent subcultures and the constructs are sequenced by Sanger sequencing after plasmid extraction. This technique is employed for the study of single viral strains allowing the linkage between genetic positions. The main limitations of the assay are its labor-consuming and its low sensitivity, which requires the analysis of a huge number of clones to ensure moderate values of sensitivity. Moreover, standard cloning is also affected by PCR-derived recombination.
- **Single Genome Sequencing (SGS).** Single genome sequencing assay is an alternative to standard cloning and sequencing, and is also suitable for studies focused on genetic linkage[95]. The assay is based on PCR-amplification of the desired HIV-1 genomic region from the limiting dilution of the template[96-100]. The limiting dilution prevents the generation of PCR-mediated recombinant DNA molecules. However, it is not useful for routine resistance testing due to its labor-intensiveness and low sensitivity.
- **Next generation sequencing (NGS).** Massive parallel sequencing generates hundreds or thousands of sequences from a single sample with a similar base accuracy to Sanger sequencing. The increased

sensitivity and the clonal amplification of unique viruses permit the study of the viral populations with a higher resolution[101-103]. Nonetheless, some pitfalls associated with the technology must be solved for its implementation in laboratory practice such as the investment in sequencing platforms, the cost of the reagents, the length of the readouts or the need for sophisticated computational analysis.

Table 4. Characteristics of genotypic assays.

Method	**Advantages**	**Disadvantages**	**Sensitivity**	**Field**
Mutation Point Assays (eg ASPCR)	High sensitivity/specificity Moderately labor-intensive Easy interpretation Cost	False positive results at lower limits Polymorphisms affect sensitivity/specificity Single-allele analysis No genetic linkage PCR artefacts	0.003-0.4%	DRM, surveillance
Population sequencing	Length of sequencing reads Moderate labor-intensive Cost	No genetic linkage PCR artifacts	15-25%	DRM, tropism, surveillance
Single Genome Sequencing	Extended sequence analyzed Genetic linkage No PCR artifacts	Turnaround-time Cost	Depends on the number of sequenced genomes (2%)	Linkage, founder viruses
Standard cloning and sequencing	Extended sequence analyzed Genetic linkage	Turn-around time PCR artifacts	Depends on the number of sequenced clones (>10%)	Linkage
Next generation sequencing	Throughput Genetic linkage Multiplexing	Strong bioinformatics support Accuracy Length of sequencing readouts Turn-around time Cost PCR artifacts	>0.5%	DRM, tropism, linkage, founder viruses

8.3. Genotypic assay interpretation

The interpretation of antiviral drug susceptibility from genotyping provides valuable tools to support decision-making in clinical practice. It is carried out through bioinformatics algorithms or rules.

The interpretation rules are based on correlations between genotypic data with treatments of patients from whom sequenced HIV-1 isolates have been obtained, in vitro drug susceptibility assays and virological response[104-107]. They are developed by panels of experts and statistical procedures and are continuously updated with information about new compounds and DRMs.

Since ART is administrated as a combination of drugs, the level of ARV drug resistance should be assessed overall. The individual level of resistance for each drug is inferred by the rules, and then the scores are later combined to give an interpretation of the global susceptibility to the combined treatment. Essentially, it involves the sum of scores assessing the activity of the different drugs, defined as Genotypic Susceptibility Score (GSS). GSS refers to the potency of the treatment combination where a total regimen score of 0 implies that none of the drugs in the regimen has antiretroviral activity against the virus.

Rules-based algorithms measure the level of resistance in a specific way, but the level of resistance can be classified into susceptible, intermediate resistance or resistant. Although different genotypic scoring systems are available, their overall performance is equivalent. The most common genotypic scoring systems are listed in the Table 5:

Table 5. Genotypic scoring systems

Interpretation system	Reported levels of resistance	Access
HIVdb v6.2.0; Stanford, USA	Susceptible (0-9), Potential low-level resistance (10-14), low-level resistance (15-29), intermediate resistance (30-59), High-level resistance (≥60)	http://hivdb.stanford.edu
Rega v8.0.2, (HIV-1&HIV-2) Leuven, Belgium	Susceptible (1.5-1), intermediate resistance (0.75-0.25), resistant (0) with drug-GSS weighting factors	www.kuleuven.ac.be/rega/cev/links
ResRis Spanish AIDS Network	Susceptible, intermediate resistance, resistant	www.retic-ris.net
AntiRetroScan v2.2; ARCA, Italy	Maximal (100), good (75), partial (50), modest (25), minimal(0) in % activity with drug-GSS weighting factors	http://www.hivarca.net/includeGenPub/AntiRetroScan_2x
Virco®TYPE HIV-1 report vpt-LM 4.3.01; Virco	Lower clinical cut-off at 20% loss of response, upper at 80% Quantitative	http://www.janssendiagnostics.com/hiv-resistance/vircotype-hiv-1
MGRM GeneSeq; Monogram Bioscience	Susceptible, resistant	www.monogramhiv.com
HIV-GRADE 12/2008; Germany	Susceptible, intermediate resistance, low susceptible, resistant	www.hiv-grade.de
Geno2Pheno$_{[resistance]}$, v3.3; Arevir, Germany	Quantitative Susceptible, intermediate resistance, resistant	www.geno2pheno.org
EuResist 1.0; EuResist Network GEIE	Quantitative Probability for short-term response with specific drug combinations	www.euresist.org
ANRS v22 (HIV-1&HIV-2); France	Quantitative Susceptible (1), possible resistance (0.5), resistant (0)	www.hivfrenchresistance.org/index
ViroSeq™ v2.8; Abbott/Celera	Susceptible, intermediate resistance, resistant	No access or information on line available
TRUGENE® Guidelines™ Ruler 14.0 ; Siemens (Bayer)	Susceptible, intermediate resistance, resistant	No access or information on line available

The version listed here is the one available in March 2013. Adapted from European HIV Drug Resistance Guidelines (www.europeanaidsclinicalsociety.org).

8.4. Viral tropism assays

The main source of virologic failure to CCR5 antagonist-based therapy is the emergence of pre-existing low-frequency CXCR4-using viruses, often missed by tropism assays[26, 108-111]. Thus, the sensitivity of the viral tropism assays is essential to ensure the virologic response.

European guidelines on the clinical management of HIV-1 tropism testing recommend HIV-tropism testing before treatment with a CCR5 antagonist is initiated, in all patients who have virologic failure for whom a CCR5 antagonist is being considered as part of the subsequent regimen and in all patients for whom treatment has failed to provide insight into future treatment options. It should be noted that in subjects failing in CCR5 antagonist-based therapy, the information obtained by tropism test only can be used to detect a switch from coreceptor CCR5 to coreceptor CXCR4[26].

Several phenotypic and genotypic assays have been developed to determine viral tropism[112] No coreceptor tropism test has been validated in prospective, randomized, double-blind clinical trials. However, phenotypic Enhanced Sensitivity Trofile™ Assay (ESTA)[113] or HIV-1 V3-loop genotypic sequencing (population sequencing and 454 sequencing) were able to discriminate the virologic response to CCR5 antagonist ART in retrospective analyses of prospective clinical trials and in retrospective cohort studies. The choice of co-receptor tropism test depends on the plasma HIV-1 RNA levels. If the plasma HIV-1 RNA load is greater than 1,000 c/mL, tropism testing can be performed with ESTA or population genotypic analysis. On the contrary, if the plasma HIV-1 RNA is between <1,000 c/mL, population genotypic analysis of PBMCs is the only tropism test recommended.

8.4.1. Phenotypic tropism assays

Phenotypic assays consist of detecting viral infection of non-lymphoid cell lines that stably express the CD4 receptor and CCR5 or CXCR4 coreceptors or detect the syncytium formation by HIV-1 on MT-2 cells.

Similar to other phenotypic assays, ESTA is based on the construction of recombinant or pseudo-typed viruses generated from patient-derived envelope sequences amplified through reverse transcription PCR (RT-PCR) from plasma RNA or, more recently, through the amplification of PBMC-associated DNA[114-116]. The amplification products are cloned into expression vectors and co-transfected with Δenv vectors in the presence of the luciferase gene to generate pseudovirions. Replicatively incompetent pseudovirions are exposed to U87 cell line expressing the CD4 receptor and either the CCR5 or the CXCR4 coreceptors. Antiretroviral drug targeting cellular coreceptors are added to the culture in order to determine the coreceptor used by the viruses to penetrate into the cell. Once the luciferase substrate is added to the culture, the luminescence is monitored to determine the infection. In cases where both R5 and X4 expressing cells have luminescence, the patient may have dual- and/or mixed-tropic viruses.

ESTA tests the entire envelope with high sensitivity, and is able to detect CXCR4-using or dual-mixed viral strains present in a prevalence of 0.3% of the viral population with 100% sensitivity[113]. The assay was retrospectively validated during the reanalysis of samples from MERIT, MOTIVATE 1 and 2 and ACTG 5211 clinical trials. In these studies, the use of the new Trofile™ (ESTA) version detected CXCR4-using or dual-mixed viruses in 10%, 8% and 15% subjects

previously classified as R5 by the old version of Trofile™ assay (OTA), respectively.

The main drawbacks associated with the assay are the cost (approximately $1,000 per sample), the long turn-around time (3 weeks), the need for centralized testing and the requirement of plasma samples with a viral load ≥1,000 copies/mL.

An alternative "in-house" phenotypic assay to ESTA for viral tropism determination is the MT-2 assay[117, 118]. It is based on a co-culture of IL-2 and phytohemagglutinin-stimulated patient PBMC cells with MT-2 cells. MT-2 cells only express the CXCR4 coreceptor becoming exclusively infected by CXCR4 or dual-tropic using viruses. Phenotypically, the infection produces the formation of syncytia which can be detected by flow-cytrometry or optical microscopy visualization. Infection can be confirmed by the production of viral antigen in the culture supernatant. The ability of HIV-1 isolates to replicate in MT-2 cells has been used as a prognostic marker for disease progression and CD4+ lymphocyte depletion. Furthermore, the assay obtained very good agreement with OTA and/or with ESTA in previous studies. This assay can be performed in subjects with undetectable HIV-1 RNA levels, however it is ruled out for diagnostic purposes because it is labor-intensive and has low sensitivity.

8.4.2. Genotypic tropism assays

In recent years, genotypic tropism assays are becoming an alternative to phenotypic assays because of their low cost, decentralization and the time required to conduct them[112, 119]. They consist of the sequencing and sequence interpreting of the HIV-1 V3-loop. Although the V3-loop is postulated as the main determinant of the viral tropism[5, 112, 120-130], changes in other regions such as V1, V2[131-135], C4[124, 133, 134, 136, 137], gp41[138] as well as differences in env glycosilation patterns[139] can modulate coreceptor usage.

Genotypic population sequencing was retrospectively validated in MERIT, MOTIVATE 1 and 2 and A4001029 clinical trials[140, 141], including subjects harboring R5 and dual or mixed tropic strains by OTA[116], respectively. Triplicate population sequencing of the V3-loop with G2P FPR≤5.75 to classify X4 viruses was strongly associated with very little or no response to treatment with maraviroc. Moreover, G2P FPR>5.75 was associated with being a good predictor of sustained response in a retrospective analysis with data from treatment-naïve subjects from the MERIT trial.

Based on cohort studies, European guidelines on the clinical management of HIV-1 tropism testing recommend a more conservative G2P FPR for genotypic population sequencing in routine clinical practice. Thus, in triplicate genotypic population sequencing from either plasma RNA or PBMC-associated DNA, the panel advises the use of G2P FPR≤10% to classify X4 viruses, and the use of G2P FPR≤20% if only one sequence is generated. It is worth noting that if any one of the three generated sequences from a sample is inferred to be non-R5, the patient is unlikely to respond to a CCR5-antagonist.

Despite the suitability of genotypic population sequencing for diagnostic purposes, the heterogeneity of HIV-1 env in virus populations makes it difficult to obtain coherent population sequences. Although a few studies have shown significant concordance and predictive values[142-144], it has low specificity, sensitivity and complex genotypic interpretation[98, 112, 145-149].

The use of next generation sequencing for HIV-1 genotyping, in particular 454 sequencing, was highly predictive of clinical outcome during retrospective analyses in MERIT, MOTIVATE 1 and 2 and A4001029 clinical trials[144, 150]. The assay obtained good correlation with OTA using a G2P≤3.5% and discarded minority strains present below 2% in classifying X4 viruses. Nevertheless, the assay is not currently recommended by European guidelines because of its cost, its availability and the need for complex analyses.

Concerning the phenotypic interpretation, the most used algorithm to predict HIV-1 coreceptor usage for HIV-1 V3-loop sequence interpretation is the Geno2Pheno[coreceptor][151] algorithm (G2P). The algorithm is based on a statistical learning method called a support vector machine (SVM) and it has been trained with sequences with previously-known coreceptor usage by OTA. It reports a False Positive Rate (FPR) for each imputed HIV-1 V3-loop sequence. The FPR is the probability of classifying an R5-virus falsely as X4. Nevertheless, the algorithm generates a significant overlap between the two distributions for the CXCR4-using viruses and CCR5-using viruses making it difficult to choose the appropriate cut-off for tropism prediction. Apart from G2P, other bioinformatics tools are available for inferring coreceptor usage; web-PSSM (position-specific scoring matrices)[152], 11/25 rule, and 11/24/25 rule[153, 154].

9. Next Generation Sequencing

DNA sequencing based on the Sanger enzymatic dideoxy technique[93] has been employed in the vast majority of sequencing projects, such as the Human Genome

Project. However, an upgrade in the scale of data generation in a cost-effective manner was essential to cope with the sequencing of complete genomes. In order to solve that problem, manufacturers triggered the enhancing of Sanger sequencing with automation of the sample preparation, the development of new enzymes and biochemicals or the increase of capillaries. Nonetheless, the revolution in the sequencing field was not achieved until the arrival of next generation sequencing (NGS).

NGS generates hundreds or thousands or millions of sequences per sample decreasing the cost per megabase in several orders of magnitude. Currently, several NGS platforms are available in the market, characterized by the high-quality base calls obtained (>Phred20 or >Q20). This technology is based on ligation or DNA sequencing by synthesis, including pyrosequencing, and reversible chain termination.

The avalanche of data generated by NGS has also been accompanied by the development of infrastructures focused on the data analysis, encompassing data transfer, storage and computational analysis. Several available software applications manage and analyze data, thereby bringing the technology closer to clinical practice.

Although the main objective of the development of NGS was the sequencing of complete genomes, NGS is applied in other disciplines, such as the variant discovery by the resequencing of targeted regions of interest, genome-wide profiling of epigenetic marks, the analysis of gene expression by RNA sequencing, the replacement of microarray mapping and microbial genomics. With respect to HIV-1, NGS is an alternative to the tedious and time-consuming bacterial cloning method. It helps to characterize the viral population with unprecedented resolution. Antiretroviral drug resistance, viral tropism, viral evolution and viral diversity are some areas in which NGS can be appropriate.

Despite the high sensitivity and specificity of NGS, some pitfalls are associated with this technology. They include the need to invest in costly equipment, the length of the sequences generated (shorter than that obtained by Sanger sequencing) and the requirement of sophisticated bioinformatics-based analytical approaches to interpret large data sets.

Next Generation Sequencing Platforms

Competition between manufacturers leads to continuous improvements in the technology, involving an increase in the amount and length of the readouts, the base-calling accuracy, the decrease in costs and the automation of protocols.

In general, all NGS platforms share some common principles, such as the ligation of adaptors containing universal priming sites to the target ends (DNA randomly fragmented or amplified), the spatial clonal amplification isolated on a solid surface[155]

or liquid mediumREF, and the direct stepwise detection of each nucleotide base incorporated during the sequencing reaction (sequencing-by-synthesis). The particularities of each platform are explained below:

9.1.454 sequencing (454 Life Sciences/Roche Diagnostics)

In 2005, 454 sequencing was launched by 454 Life Sciences becoming the first next-generation platform available on the market. It generated readouts of 100-150 bp in length with an accuracy of 99.9%. The platform was upgraded to GS FLX Titanium in 2008, allowing the sequencing of the 400 bp length while maintaining the accuracy of the base calling. Currently, there is a promising improvement to GS FLX Titanium Plus, which would reach sequencing readout lengths of up to 1,000 bp without compromising accuracy. A more scalable system called GS Junior was launched in 2009 with the objective of bringing the sequencing method closer to laboratory practice.

454 sequencing is based on sequencing-by-synthesis[102] with pyrophosphate chemistry. It detects the pyrophosphates released during nucleotide incorporation following a real-time sequencing strategy. It requires DNA produced from a previous PCR amplification or gene fragmentation as a template for emulsion-based parallel pyrosequencing (Figure 7). Fusion adapters are bound to the 5' end to allow the attachment between the DNA and the capture beads in the emulsion PCR (emPCR)[156]. Inside the water-in-oil mixture, each DNA molecule is immobilized onto a 28 µm DNA capture bead with PCR reagents. Here, each unique DNA molecule is amplified in a unique microreactor (clonal amplification). The DNA molecules to be amplified and the beads must be combined in a 1:1 ratio allowing the hybridization of only one molecule to one bead. This ratio avoids the presence of beads containing more than one DNA molecule (mixed beads) or beads without DNA (empty beads). Then, DNA-beads are captured and cleaned during the emulsion breaking reaction. The DNA-beads are purified thanks to magnetic streptavidin labeled beads, which bind to the biotin-labeled primer added to the emPCR. These enriched beads are loaded onto a PicoTiterPlateTM (PTP)[101]. The PTP contains up to two million wells with a diameter of 44µM, which allows for only one bead per well. Moreover, the enzyme and packing beads are loaded into the wells. Instead of the labeled dideoxynucleotide triphosphates utilized in Sanger's chain-terminator chemistry, cycles of individual nucleotides flow in a fixed order across the wells (T-A-C-G). The nucleotides carry phosphate groups bound to them, which are released during the incorporation of one (or more) complementary nucleotide(s) in the

template strand. The concentration of the PPi in the system is monitored using an enzymatic reaction. ATP sulfurylase converts PPi to ATP, which leads to the conversion of luciferin into oxyluciferin by firefly luciferase with the ensuing emission of light. The sequential base flows and the intensity of the chemiluminescent signal recorded by a CCD camera are used by the software to reconstruct the nucleotide sequence for each well of the PTP. It should be noted that the chemiluminescent signal is proportional to the number of bases incorporated into the growing DNA molecule.

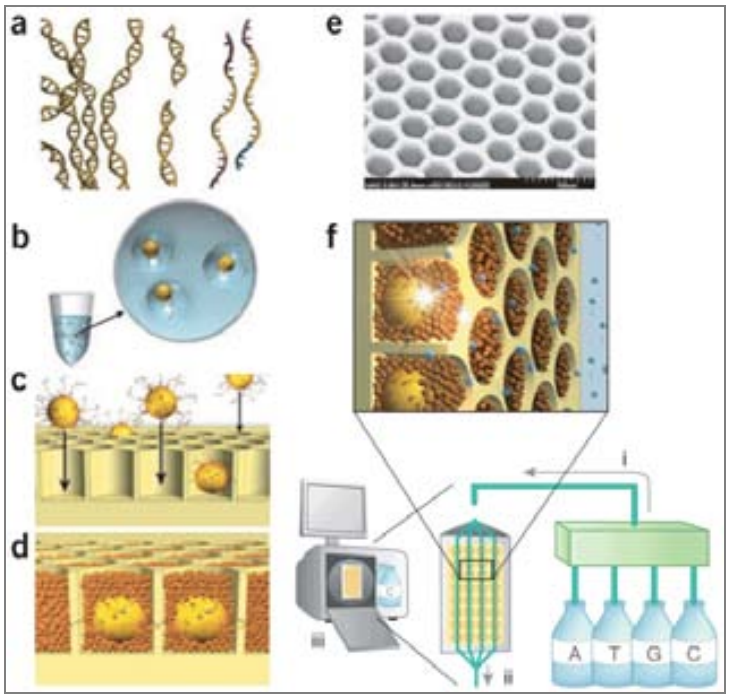

FIGURE 7. SCHEMATIC PROCEDURE FOR 454 SEQUENCING. a) Binding of fusion adapters to the DNA, b) EmPCR and microreactors, c) Loading of enriched-beads into the PTP™, d) Loading of enzyme-beads and packing-beads into the PTP, e) Image of PTP from electron microscopy, f) Detection of chemiluminescent signals by the CCD camera. Source: *adapted from Rothberg JM and Leamon JH, The development and impact of 454 sequencing, Nat Biotechnol. 2008.*

The downstream analysis provided with the 454 Sequencing Systems includes three different bioinformatics tools depending on the experimental design;

- GS De Novo Assembler: it produces high-quality assemblies for microbial genomes.
- GS Reference Mapper: it maps reads to any reference genome and generate a consensus sequence.
- GS Amplicon Variant Analyzer: it aligns amplicon reads, with a reference sequence and identifies variants reporting frequencies.

Furthermore, other commercialized software is available. The DeepChek™ HIV System is fully integrated and simplified HIV-1 clinical genotyping solution for antiviral drug resistance. It has been developed through a consortium formed by ABL and Roche Diagnostics in collaboration with irsiCaixa AIDS Research

Institute, Hospital Universitario San Cecilio, Hospital 12 de Octubre and Mútua de Terrassa.

With respect to viral tropism, Geno2Pheno[454] is an open-source tool that assists in pre-processing the ultra-deep sequencing data, makes the coreceptor predictions based on the Geno2Pheno[coreceptor] approach and displays the results in easily understandable tables and plots.

The main advantages of 454 sequencing versus other platforms are the long readout-length[157] and improved Q20 readout length of 400 bases, being suitable for phylogenetic analysis, de novo assembly or metagenomics. However, some weakness are associated with 454 sequencing. For instance, the lack of resolution showed in homopolymeric regions due to the pyrosequencing chemistry leads to a higher error rate of incorporation versus nonincorporation[158]. In addition, the per-base cost of sequencing is higher than with other next-generation sequencing platforms[158].

9.2. Illumina Genome Analyzer

In 2007 Illumina purchased the Genome Analyzer released by Solexa in 2006. Although several sequencers are available, MiSeq is the more scalable version for diagnostic laboratories. During sample preparation, two different adapters are covalently bound to each end of the DNA (Figure 8). Then a “bridge amplification” is carried out on a glass surface using several rounds of PCR[159], generating dense clusters of the amplified DNA templates. Sequencing consists of cyclic reversible termination through a proprietary reversible terminator and detection of the incorporation of terminators in the growing DNA strands[160]. A fluorescently labeled terminator is imaged as each dNTP is added. Then the terminator is removed in a cleavage step and termination is reversed by regenerating the 3’-OH group. The four nucleotides are added together during the sequencing reaction producing a natural competition that minimizes incorporation bias. The non-incorporated reagents are subsequently washed away. The base calling is made directly from the measurement of fluorescent signal intensities during each cycle by the CCD camera.

Despite of readouts length is up to 250 bp, this technology generates an accurate and robust base-by-base sequencing that eliminates sequence context-specific errors, solving possible problems during the sequencing of homopolymeric regions.

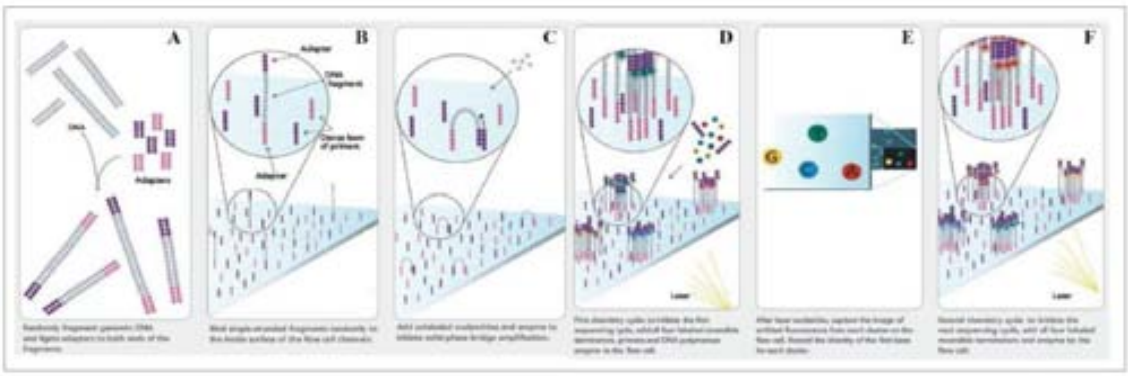

FIGURE 8. SCHEMATIC PROCEDURE FOR ILLUMINA. a) Binding of fusion adapters to the library, b) library binding to a gel surface, c) bridge amplification, d) amplification (clusters), e) addition of labeled nucleotides, f) detection of the incorporation of labeled nucleotides.

9.3. The Life Technologies SOLID™ System (5500 W Series Genetic Analysis Systems)

The Applied Biosystems SOLID System (Sequencing by Oligo Ligation Detection)[161] was released in 2006. The library preparation is similar to other platforms and barcoding is required if several samples are sequenced at once for the binding of the adapter sequence for binding to the beads in the emPCR and the subsequent bead deposition. This parallel sequencing chemistry is different due to the use of four fluorescently labeled di-base probes which compete to ligate to the sequencing primer. The specificity of the di-base probe is achieved by interrogating every 1st and 2nd base in each ligation reaction[162]. An 8 base-probe ligation containing the ligation site (the first base), the cleavage site (the fifth base) and 4 different fluorescent dyes (linked to the last base) are used to sequence the libraries (Figure 9). Multiple cycles of ligation, detection and cleavage are performed with the number of cycles determining the eventual readout length. Following a series of ligation cycles, the extension product is removed and the template is reset with a primer complementary to the n-1 position for a second round of ligation cycles. The short-read sequencing generated limits its applications in clinical routine[157].

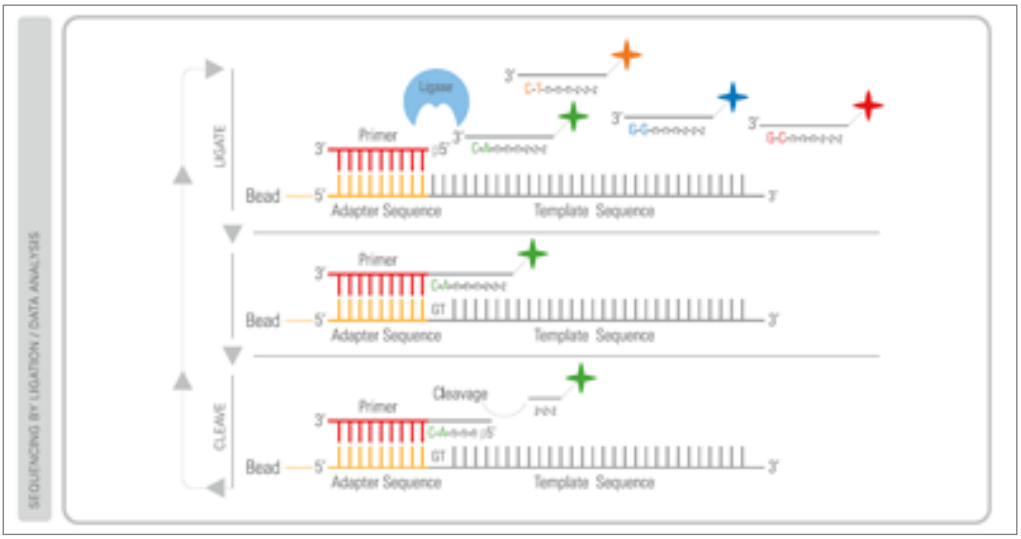

FIGURE 9. SCHEMATIC PROCEDURE FOR THE SOLID™ SYSTEM. Multiple cycles of ligation, detection and cleavage of the 8 base-probes.

9.4. Ion Torrent PGM (Ion PGM)

Ion Torrent released its Ion PGM (Personal Genome Machine) in 2010. The library preparation consists of emPCR, similar to the 454 sequencing, but the sequencing chemistry is different from the pyrosequencing. Here, the sequencing is based on the release of protons when a nucleotide is incorporated into the growing DNA strain[163] (Figure 10). The bases sequentially flood the chip and a semiconductor sequencing technology detects a change in pH produced by the releasing of protons. The change in pH is proportional to the number of nucleotides incorporated. The sequencer platform is characterized by its small size, speed and lower cost since it does not require fluorescence and camera scanning. This technology also shows low resolution in homopolymeric regions.

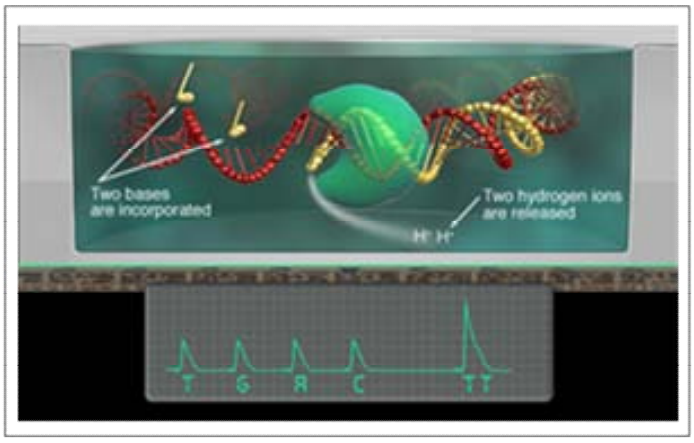

FIGURE 10. SCHEMATIC PROCEDURE FOR ION PGM. Source: *www.iontorrent.com*.

10. Future next-generation sequencing technologies ("Next-next generation technologies" or "Third generation sequencing" technologies)

Next-next generation sequencing technologies (NNGS) are currently being developed. The capture of the sequencing signal by NNGS differs from NGS. It does not require chemical labeling, and it is done in real time during the DNA polymerization or depolymerization steps. Although the throughputs are limited in comparison to the NGS, this promising technology permits the sequencing of longer readouts (up to 5 kb) and does not need PCR for sample preparation.

Next Generation Sequencing Platforms

10.1. Pacific Bioscience RS System (Pacific Biosciences)

PacBio has been developed by Pacific Biosciences. It consists of Single-molecule real-time sequencing (SMRT)[164] in millions of zero-mode waveguides (ZMWs)[165] (Figure 11). A set of enzymes is required for DNA polymerization, which binds to the DNA template. It should be noted that the sequencing of mRNA is allowed due to the substitution of DNA polymerase by a ribosome.

The nucleotides are labeled on the "γ-phosphate," the part of the nucleotide which is naturally cleaved off when it is incorporated into the strand of DNA being synthesized by a polymerase. Unlike NGS, SMRT does not require the cycling of different chemicals. The fluorescent dye is monitored and filmed by a camera.

PacBio produces readouts with average lengths of 3,000 to 5,000 bp, with the longest readouts being over 20,000 base pairs with extremely high accuracy (>99.999%). It would allow the detection of minor HIV-1 variants present at a frequency of less than 0.1%.

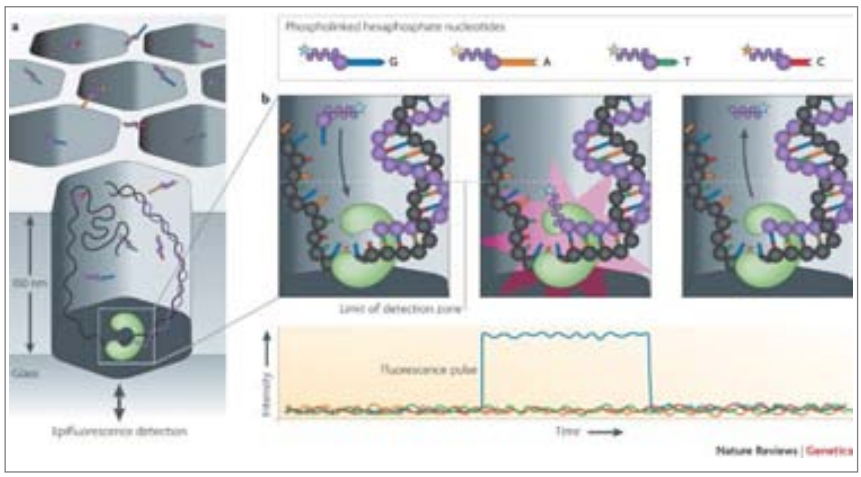

FIGURE 11. SCHEMATIC PROCEDURE FOR *PacBio*. a) zero-mode waveguides (ZMWs), b) fluorescently labeled nucleotide incorporation and cleavage of the fluorescent dye. Source: *Metzker ML, Sequencing technologies - the next generation sequencing. Nat Reviews, 2010.*

10.2. Oxford Nanopore GridION™ (Oxford Nanopore Technologies™)

Oxford Nanopore Technologies® has developed the GridION™. Nanopore sequencing technology is based on DNA strand depolymerization[166]. The system is based on a biopore of 1 nanometer in internal diameter inserted into a protein channel embedded on a lipid bilayer. The machinery is immersed in a conduction fluid across which a potential voltage is applied. The nucleotides are excised when they pass through the nanopore disrupting the voltage across the channel (Figure 12). Different nucleotides exert different variation patterns in the voltage and such disruption is monitored to reconstruct the DNA sequence.

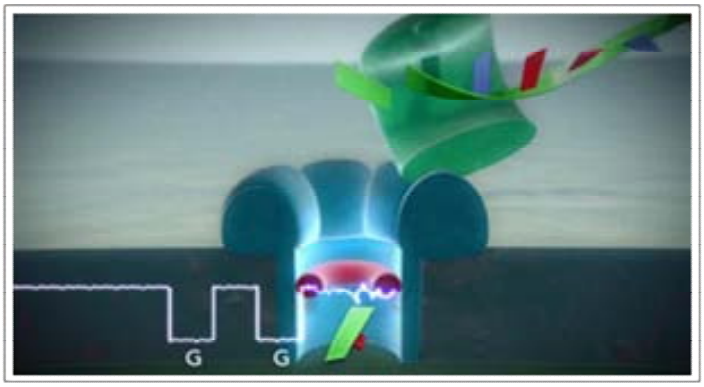

FIGURE 12. SCHEMATIC PROCEDURE FOR GridION™. Nucleotides excised by a biopore inserted into a protein channel embedded on a lipid bilayer. Differences in voltage exercised by the distinct nucleotides are used to construct the sequences. Source: *https://www.nanoporetech.com.*

Table 6. Characteristics of next and next-next generation sequencing technologies

Manufacturer	**Roche/454 sequencing GS FLX Titanium**	**Life Technologies 5,500 series SOLiD**	**Illumina MiSeq**	**Ion PGM "314 chip" (Ion Torrent)**	**Pacific Biosciences RS (SMRT)**	**Oxford Nanopore GridION 8,000 (Oxford Nanopore TechnologiesTM)**
Library preparation	emPCR on bead surface from fragmented DNA or PCR product	emPCR on bead surface from fragmented DNA or PCR product	Enzymatic amplification on glass surface from fragmented DNA or PCR product	Fragmented DNA or PCR product	Fragmented DNA or RNA. PCR product is required for HIV	Amplification not required (single molecule detection)
Sequencing	Polymerase-mediated incorporation of sequentially added unlabelled nucleotides	Ligase-mediated addition of 2-base encoded fluorescent oligonucleotides	Polymerase- mediated incorporation of endblocked fluorescent nucleotides	Release of protons when a nucleotide is incorporated into the growing DNA strain	Polymerase-mediated incorporation of terminal phosphate labelled fluorescent Nucleotides	DNA stand depolymerisation
Detection	Light emitted from secondary reactions initiated by release of PPi	Fluorescent emission from ligated dye-labelled oligonucleotides	Fluorescent emission from incorporated dye-labelled nucleotides	Change in pH	Real time detection of fluorescent dye in polymerase active site during incorporation	Change in the voltage magnitude
Post incorporation	Unlabelled nucleotides are added in base-specific fashion, followed by detection	Chemical cleavage removes fluorescent dye and 39 end of oligonucleotide	Chemical cleavage of fluorescent dye and 39 blocking group	Non-available	Non-available (fluorescent dyes are removed as part of PPi release on nucleotide incorporation)	Non-available
Error model	Insertion/deletion at homopolymers	A-T bias	Substitutions	Insertion/deletion at homopolymers	GC deletion	Deletions
Read length	400 bp/variable length mate pairs (1,000 bp upgrade FLX+)	75+35 bp	150+150 bp	200-250 bp	6-10 kb (median 3 kb)	10,000
Millions of reads/run	1	>1,410	4	0.25	0.01	10
Yield Mb/run	400	155,100	1,200	50	5-10	100,000
Run time	10 h	8 days	26 h	2.5 h	2 h	5h
Reagent cost/run	6,200	10,503	1,160	350	300-1,700	Not available
Reagent cost/Mb	12	<0.07	1	7	7-38	Not available
Cost/equipment	500,000$	595,000$	125,000$	49,500$ (sequencer); 16,500$ (Torrent Server)/~2,500$ (18MΩ water and argon gas)	Not available	Not available
Advantages	Long read-length	High accuracy, throughput	Library preparation (Nextera DNA Sample Prep Kits), instrument&reagent cost, cost/Mb	Instrument&reagent cost, simple machinery,	Long read-length, single molecule real-time sequencing (in HIV-1 requires PCR)	Long read-length, Cost per instrument, Cost/Gb
Disadvantages	Library preparation, cost/Mb	Short read-length, Long run time, instrument cost	Few reads and higher cost/Mb compared to other Illumina platforms	High error rate	High error rate, instrument&reagent cost	Not available

Adapted from "A decade's perspective on DNA sequencing technology"[167].

References

1. Gao, F., et al., Origin of HIV-1 in the chimpanzee Pan troglodytes troglodytes. Nature, 1999. 397(6718): p. 436-41.
2. Damond, F., et al., Identification of a highly divergent HIV type 2 and proposal for a change in HIV type 2 classification. AIDS Res Hum Retroviruses, 2004. 20(6): p. 666-72.
3. Hirsch, V.M., et al., An African primate lentivirus (SIVsm) closely related to HIV-2. Nature, 1989. 339(6223): p. 389-92.
4. Zhu, P., et al., Distribution and three-dimensional structure of AIDS virus envelope spikes. Nature, 2006. 441(7095): p. 847-52.
5. Carrillo, A. and L. Ratner, Cooperative effects of the human immunodeficiency virus type 1 envelope variable loops V1 and V3 in mediating infectivity for T cells. J Virol, 1996. 70(2): p. 1310-6.
6. Chan, D.C. and P.S. Kim, HIV entry and its inhibition. Cell, 1998. 93(5): p. 681-4.
7. Sheehy, A.M., et al., Isolation of a human gene that inhibits HIV-1 infection and is suppressed by the viral Vif protein. Nature, 2002. 418(6898): p. 646-50.
8. Kobayashi, M., et al., Ubiquitination of APOBEC3G by an HIV-1 Vif-Cullin5-Elongin B-Elongin C complex is essential for Vif function. J Biol Chem, 2005. 280(19): p. 18573-8.
9. Laguette, N., et al., Human immunodeficiency virus (HIV) type-1, HIV-2 and simian immunodeficiency virus Nef proteins. Mol Aspects Med, 2010. 31(5): p. 418-33.
10. Agostini, I., et al., Phosphorylation of Vpr regulates HIV type 1 nuclear import and macrophage infection. AIDS Res Hum Retroviruses, 2002. 18(4): p. 283-8.
11. Mueller, S.M. and S.M. Lang, The first HxRxG motif in simian immunodeficiency virus mac239 Vpr is crucial for G(2)/M cell cycle arrest. J Virol, 2002. 76(22): p. 11704-9.
12. Cui, J., et al., The role of Vpr in the regulation of HIV-1 gene expression. Cell Cycle, 2006. 5(22): p. 2626-38.
13. Singhal, P.K., et al., Nuclear export of simian immunodeficiency virus Vpx protein. J Virol, 2006. 80(24): p. 12271-82.
14. Ueno, F., et al., Vpx and Vpr proteins of HIV-2 up-regulate the viral infectivity by a distinct mechanism in lymphocytic cells. Microbes Infect, 2003. 5(5): p. 387-95.
15. Dumonceaux, J., et al., Spontaneous mutations in the env gene of the human immunodeficiency virus type 1 NDK isolate are associated with a CD4-independent entry phenotype. J Virol, 1998. 72(1): p. 512-9.
16. Alkhatib, G., et al., CC CKR5: a RANTES, MIP-1alpha, MIP-1beta receptor as a fusion cofactor for macrophage-tropic HIV-1. Science, 1996. 272(5270): p. 1955-8.
17. Berger, E.A., P.M. Murphy, and J.M. Farber, Chemokine receptors as HIV-1 coreceptors: roles in viral entry, tropism, and disease. Annu Rev Immunol, 1999. 17: p. 657-700.
18. Briz, V., E. Poveda, and V. Soriano, HIV entry inhibitors: mechanisms of action and resistance pathways. J Antimicrob Chemother, 2006. 57(4): p. 619-27.
19. Este, J.A. and A. Telenti, HIV entry inhibitors. Lancet, 2007. 370(9581): p. 81-8.
20. Soriano, V., et al., Optimal use of maraviroc in clinical practice. AIDS, 2008. 22(17): p. 2231-40.
21. DHHS Panel on Antiretroviral Guidelines for Adults and Adolescents: Guidelines for the use of antiretroviral agents in HIV-1-infected adults and adolescents. 2013.
22. Hirsch, M.S., et al., Antiretroviral drug resistance testing in adult HIV-1 infection: 2008 recommendations of an International AIDS Society-USA panel. Clin Infect Dis, 2008. 47(2): p. 266-85.
23. Tsibris, A.M. and D.R. Kuritzkes, Chemokine antagonists as therapeutics: focus on HIV-1. Annu Rev Med, 2007. 58: p. 445-59.
24. Koot, M., et al., Prognostic value of HIV-1 syncytium-inducing phenotype for rate of CD4+ cell depletion and progression to AIDS. Ann Intern Med, 1993. 118(9): p. 681-8.
25. Glushakova, S., et al., Evidence for the HIV-1 phenotype switch as a causal factor in acquired immunodeficiency. Nat Med, 1998. 4(3): p. 346-9.
26. Westby, M., et al., Emergence of CXCR4-using human immunodeficiency virus type 1 (HIV-1) variants in a minority of HIV-1-infected patients following treatment with the CCR5 antagonist maraviroc is from a pretreatment CXCR4-using virus reservoir. J Virol, 2006. 80(10): p. 4909-20.

27. Coffin, Molecular Biology of HIV In: Crandall KA, ed. The evolution of HIV. Baltimore, Maryland: Johns Hopkins University Press, 1999.
28. Liu, S., et al., Slide into action: dynamic shuttling of HIV reverse transcriptase on nucleic acid substrates. Science, 2008. 322(5904): p. 1092-7.
29. Greene, W.C. and B.M. Peterlin, Charting HIV's remarkable voyage through the cell: Basic science as a passport to future therapy. Nat Med, 2002. 8(7): p. 673-80.
30. Lassen, K., et al., The multifactorial nature of HIV-1 latency. Trends Mol Med, 2004. 10(11): p. 525-31.
31. Duh, E.J., et al., Tumor necrosis factor alpha activates human immunodeficiency virus type 1 through induction of nuclear factor binding to the NF-kappa B sites in the long terminal repeat. Proc Natl Acad Sci U S A, 1989. 86(15): p. 5974-8.
32. Margolis, D.M., et al., Transactivation of the HIV-1 LTR by HSV-1 immediate-early genes. Virology, 1992. 186(2): p. 788-91.
33. Ross, E.K., et al., Contribution of NF-kappa B and Sp1 binding motifs to the replicative capacity of human immunodeficiency virus type 1: distinct patterns of viral growth are determined by T-cell types. J Virol, 1991. 65(8): p. 4350-8.
34. Swanstrom, R. and J.W. Wills, Synthesis, Assembly, and Processing of Viral Proteins. 1997.
35. Little, S.J., Transmission and prevalence of HIV resistance among treatment-naive subjects. Antivir Ther, 2000. 5(1): p. 33-40.
36. Little, S.J., et al., Reduced antiretroviral drug susceptibility among patients with primary HIV infection. JAMA, 1999. 282(12): p. 1142-9.
37. McMichael, A.J. and S.L. Rowland-Jones, Cellular immune responses to HIV. Nature, 2001. 410(6831): p. 980-7.
38. Perelson, A.S., et al., HIV-1 dynamics in vivo: virion clearance rate, infected cell life-span, and viral generation time. Science, 1996. 271(5255): p. 1582-6.
39. Clavel, F. and A.J. Hance, HIV drug resistance. N Engl J Med, 2004. 350(10): p. 1023-35.
40. Coffin, J.M., HIV population dynamics in vivo: implications for genetic variation, pathogenesis, and therapy. Science, 1995. 267(5197): p. 483-9.
41. Preston, B.D., B.J. Poiesz, and L.A. Loeb, Fidelity of HIV-1 reverse transcriptase. Science, 1988. 242(4882): p. 1168-71.
42. Hu, W.S., et al., Retroviral recombination: review of genetic analyses. Front Biosci, 2003. 8: p. d143-55.
43. Lever, A.M., HIV-1 RNA packaging. Adv Pharmacol, 2007. 55: p. 1-32.
44. Coffin, J.M., Structure, replication, and recombination of retrovirus genomes: some unifying hypotheses. J Gen Virol, 1979. 42(1): p. 1-26.
45. Temin, H.M., Retrovirus variation and reverse transcription: abnormal strand transfers result in retrovirus genetic variation. Proc Natl Acad Sci U S A, 1993. 90(15): p. 6900-3.
46. Holmes, R.K., M.H. Malim, and K.N. Bishop, APOBEC-mediated viral restriction: not simply editing? Trends Biochem Sci, 2007. 32(3): p. 118-28.
47. Ott, D.E., Cellular proteins detected in HIV-1. Rev Med Virol, 2008. 18(3): p. 159-75.
48. Domingo, E. and J.J. Holland, RNA virus mutations and fitness for survival. Annu Rev Microbiol, 1997. 51: p. 151-78.
49. Hammer, S.M., et al., Antiretroviral treatment of adult HIV infection: 2008 recommendations of the International AIDS Society-USA panel. JAMA, 2008. 300(5): p. 555-70.
50. Wilson, D.P., et al., Relation between HIV viral load and infectiousness: a model-based analysis. Lancet, 2008. 372(9635): p. 314-20.
51. Thompson, M.A., et al., Antiretroviral treatment of adult HIV infection: 2012 recommendations of the International Antiviral Society-USA panel. JAMA, 2012. 308(4): p. 387-402.
52. EACS, E.A.C.S., European Guidelines for treatment of HIV infected adults in Europe. 2012.
53. Quinones-Mateu, M.E. and E.J. Arts, Fitness of drug resistant HIV-1: methodology and clinical implications. Drug Resist Updat, 2002. 5(6): p. 224-33.
54. Bangsberg, D.R., A.R. Moss, and S.G. Deeks, Paradoxes of adherence and drug resistance to HIV antiretroviral therapy. J Antimicrob Chemother, 2004. 53(5): p. 696-9.
55. Condra, J.H., et al., In vivo emergence of HIV-1 variants resistant to multiple protease inhibitors. Nature, 1995. 374(6522): p. 569-71.
56. Flexner, C., HIV-protease inhibitors. N Engl J Med, 1998. 338(18): p. 1281-92.

57. Kuritzkes, D.R., et al., Drug resistance and virologic response in NUCA 3001, a randomized trial of lamivudine (3TC) versus zidovudine (ZDV) versus ZDV plus 3TC in previously untreated patients. AIDS, 1996. 10(9): p. 975-81.
58. Molla, A., et al., Ordered accumulation of mutations in HIV protease confers resistance to ritonavir. Nat Med, 1996. 2(7): p. 760-6.
59. Tisdale, M., et al., Cross-resistance analysis of human immunodeficiency virus type 1 variants individually selected for resistance to five different protease inhibitors. Antimicrob Agents Chemother, 1995. 39(8): p. 1704-10.
60. Johnson, V.A., et al., Update of the drug resistance mutations in HIV-1: Spring 2008. Top HIV Med, 2008. 16(1): p. 62-8.
61. Shet, A., et al., Tracking the prevalence of transmitted antiretroviral drug-resistant HIV-1: a decade of experience. J Acquir Immune Defic Syndr, 2006. 41(4): p. 439-46.
62. Truong, H.M., et al., Routine surveillance for the detection of acute and recent HIV infections and transmission of antiretroviral resistance. AIDS, 2006. 20(17): p. 2193-7.
63. Wensing, A.M., et al., Prevalence of drug-resistant HIV-1 variants in untreated individuals in Europe: implications for clinical management. J Infect Dis, 2005. 192(6): p. 958-66.
64. Yerly, S., et al., Transmission of HIV-1 drug resistance in Switzerland: a 10-year molecular epidemiology survey. AIDS, 2007. 21(16): p. 2223-9.
65. Das, K. and E. Arnold, HIV-1 reverse transcriptase and antiviral drug resistance. Part 1. Curr Opin Virol, 2013. 3(2): p. 111-8.
66. Schinazi, R.F., et al., Characterization of human immunodeficiency viruses resistant to oxathiolane-cytosine nucleosides. Antimicrob Agents Chemother, 1993. 37(4): p. 875-81.
67. Steigbigel, R.T., et al., Raltegravir with optimized background therapy for resistant HIV-1 infection. N Engl J Med, 2008. 359(4): p. 339-54.
68. Molina, J.M., et al., Once-daily atazanavir/ritonavir versus twice-daily lopinavir/ritonavir, each in combination with tenofovir and emtricitabine, for management of antiretroviral-naive HIV-1-infected patients: 48 week efficacy and safety results of the CASTLE study. Lancet, 2008. 372(9639): p. 646-55.
69. Ortiz, R., et al., Efficacy and safety of once-daily darunavir/ritonavir versus lopinavir/ritonavir in treatment-naive HIV-1-infected patients at week 48. AIDS, 2008. 22(12): p. 1389-97.
70. Karacostas, V., et al., Human immunodeficiency virus-like particles produced by a vaccinia virus expression vector. Proc Natl Acad Sci U S A, 1989. 86(22): p. 8964-7.
71. Arion, D., et al., Phenotypic mechanism of HIV-1 resistance to 3'-azido-3'-deoxythymidine (AZT): increased polymerization processivity and enhanced sensitivity to pyrophosphate of the mutant viral reverse transcriptase. Biochemistry, 1998. 37(45): p. 15908-17.
72. Meyer, P.R., et al., A mechanism of AZT resistance: an increase in nucleotide-dependent primer unblocking by mutant HIV-1 reverse transcriptase. Mol Cell, 1999. 4(1): p. 35-43.
73. Huang, H., et al., Structure of a covalently trapped catalytic complex of HIV-1 reverse transcriptase: implications for drug resistance. Science, 1998. 282(5394): p. 1669-75.
74. Bacheler, L.T., et al., Human immunodeficiency virus type 1 mutations selected in patients failing efavirenz combination therapy. Antimicrob Agents Chemother, 2000. 44(9): p. 2475-84.
75. Boyer, P.L., et al., Analysis of nonnucleoside drug-resistant variants of human immunodeficiency virus type 1 reverse transcriptase. J Virol, 1993. 67(4): p. 2412-20.
76. Esnouf, R.M., et al., Unique features in the structure of the complex between HIV-1 reverse transcriptase and the bis(heteroaryl)piperazine (BHAP) U-90152 explain resistance mutations for this nonnucleoside inhibitor. Proc Natl Acad Sci U S A, 1997. 94(8): p. 3984-9.
77. Hsiou, Y., et al., The Lys103Asn mutation of HIV-1 RT: a novel mechanism of drug resistance. J Mol Biol, 2001. 309(2): p. 437-45.
78. Ren, J., et al., Structural mechanisms of drug resistance for mutations at codons 181 and 188 in HIV-1 reverse transcriptase and the improved resilience of second generation non-nucleoside inhibitors. J Mol Biol, 2001. 312(4): p. 795-805.
79. Ren, J., et al., Structural insights into mechanisms of non-nucleoside drug resistance for HIV-1 reverse transcriptases mutated at codons 101 or 138. FEBS J, 2006. 273(16): p. 3850-60.
80. Richman, D.D., et al., Nevirapine resistance mutations of human immunodeficiency virus type 1 selected during therapy. J Virol, 1994. 68(3): p. 1660-6.
81. Grobler, J.A., et al., Diketo acid inhibitor mechanism and HIV-1 integrase: implications for metal binding in the active site of phosphotransferase enzymes. Proc Natl Acad Sci U S A, 2002. 99(10): p. 6661-6.

82. Blanco, J.L., et al., HIV-1 integrase inhibitor resistance and its clinical implications. J Infect Dis, 2011. 203(9): p. 1204-14.
83. Mesplede, T., P.K. Quashie, and M.A. Wainberg, Resistance to HIV integrase inhibitors. Curr Opin HIV AIDS, 2012. 7(5): p. 401-8.
84. Katlama, C. and R. Murphy, Dolutegravir for the treatment of HIV. Expert Opin Investig Drugs, 2012. 21(4): p. 523-30.
85. Rimsky, L.T., D.C. Shugars, and T.J. Matthews, Determinants of human immunodeficiency virus type 1 resistance to gp41-derived inhibitory peptides. J Virol, 1998. 72(2): p. 986-93.
86. Wei, X., et al., Emergence of resistant human immunodeficiency virus type 1 in patients receiving fusion inhibitor (T-20) monotherapy. Antimicrob Agents Chemother, 2002. 46(6): p. 1896-905.
87. Kellam, P. and B.A. Larder, Recombinant virus assay: a rapid, phenotypic assay for assessment of drug susceptibility of human immunodeficiency virus type 1 isolates. Antimicrob Agents Chemother, 1994. 38(1): p. 23-30.
88. Japour, A.J., et al., Standardized peripheral blood mononuclear cell culture assay for determination of drug susceptibilities of clinical human immunodeficiency virus type 1 isolates. The RV-43 Study Group, the AIDS Clinical Trials Group Virology Committee Resistance Working Group. Antimicrob Agents Chemother, 1993. 37(5): p. 1095-101.
89. Nissley, D.V., et al., Sensitive phenotypic detection of minor drug-resistant human immunodeficiency virus type 1 reverse transcriptase variants. J Clin Microbiol, 2005. 43(11): p. 5696-704.
90. Boltz, V.F., et al., Optimization of allele-specific PCR using patient-specific HIV consensus sequences for primer design. J Virol Methods, 2010. 164(1-2): p. 122-6.
91. Johnson, J.A., et al., Simple PCR assays improve the sensitivity of HIV-1 subtype B drug resistance testing and allow linking of resistance mutations. PLoS One, 2007. 2(7): p. e638.
92. Paredes, R., et al., Systematic evaluation of allele-specific real-time PCR for the detection of minor HIV-1 variants with pol and env resistance mutations. J Virol Methods, 2007. 146(1-2): p. 136-46.
93. Sanger, F. and A.R. Coulson, A rapid method for determining sequences in DNA by primed synthesis with DNA polymerase. J Mol Biol, 1975. 94(3): p. 441-8.
94. Brun-Vezinet, F., et al., Clinically validated genotype analysis: guiding principles and statistical concerns. Antivir Ther, 2004. 9(4): p. 465-78.
95. Metzner, K.J., et al., Detection of minor populations of drug-resistant HIV-1 in acute seroconverters. AIDS, 2005. 19(16): p. 1819-25.
96. Brown, A.J. and A. Cleland, Independent evolution of the env and pol genes of HIV-1 during zidovudine therapy. AIDS, 1996. 10(10): p. 1067-73.
97. Holmes, E.C., et al., Convergent and divergent sequence evolution in the surface envelope glycoprotein of human immunodeficiency virus type 1 within a single infected patient. Proc Natl Acad Sci U S A, 1992. 89(11): p. 4835-9.
98. Palmer, S., et al., Multiple, linked human immunodeficiency virus type 1 drug resistance mutations in treatment-experienced patients are missed by standard genotype analysis. J Clin Microbiol, 2005. 43(1): p. 406-13.
99. Simmonds, P., et al., Analysis of sequence diversity in hypervariable regions of the external glycoprotein of human immunodeficiency virus type 1. J Virol, 1990. 64(12): p. 5840-50.
100. Zhang, L.Q., et al., Detection, quantification and sequencing of HIV-1 from the plasma of seropositive individuals and from factor VIII concentrates. AIDS, 1991. 5(6): p. 675-81.
101. Leamon, J.H., et al., A massively parallel PicoTiterPlate based platform for discrete picoliter-scale polymerase chain reactions. Electrophoresis, 2003. 24(21): p. 3769-77.
102. Margulies, M., et al., Genome sequencing in microfabricated high-density picolitre reactors. Nature, 2005. 437(7057): p. 376-80.
103. Simen, B.B., et al., Low-abundance drug-resistant viral variants in chronically HIV-infected, antiretroviral treatment-naive patients significantly impact treatment outcomes. J Infect Dis, 2009. 199(5): p. 693-701.
104. Bacheler, L., et al., Genotypic correlates of phenotypic resistance to efavirenz in virus isolates from patients failing nonnucleoside reverse transcriptase inhibitor therapy. J Virol, 2001. 75(11): p. 4999-5008.
105. Beerenwinkel, N., et al., Geno2pheno: Estimating phenotypic drug resistance from HIV-1 genotypes. Nucleic Acids Res, 2003. 31(13): p. 3850-5.

106. Mazzotta, F., et al., Real versus virtual phenotype to guide treatment in heavily pretreated patients: 48-week follow-up of the Genotipo-Fenotipo di Resistenza (GenPheRex) trial. J Acquir Immune Defic Syndr, 2003. 32(3): p. 268-80.

107. Perez-Elias, M.J., et al., Phenotype or virtual phenotype for choosing antiretroviral therapy after failure: a prospective, randomized study. Antivir Ther, 2003. 8(6): p. 577-84.

108. Fatkenheuer, G., et al., Subgroup analyses of maraviroc in previously treated R5 HIV-1 infection. N Engl J Med, 2008. 359(14): p. 1442-55.

109. Gulick, R.M., et al., Maraviroc for previously treated patients with R5 HIV-1 infection. N Engl J Med, 2008. 359(14): p. 1429-41.

110. Gulick, R.M., et al., Phase 2 study of the safety and efficacy of vicriviroc, a CCR5 inhibitor, in HIV-1-Infected, treatment-experienced patients: AIDS clinical trials group 5211. J Infect Dis, 2007. 196(2): p. 304-12.

111. Tsibris, A.M., et al., In vivo emergence of vicriviroc resistance in a human immunodeficiency virus type 1 subtype C-infected subject. J Virol, 2008. 82(16): p. 8210-4.

112. Rose, J.D., et al., Current tests to evaluate HIV-1 coreceptor tropism. Curr Opin HIV AIDS, 2009. 4(2): p. 136-42.

113. Reeves JD, C.E., Petropoulos CJ, Whitcomb JM, An Enhanced-Sensitivity Trofile™ HIV Coreceptor Tropism Assay for Selecting Patients for Therapy with Entry Inhibitors Targeting CCR5: A Review of Analytical and Clinical Studies. Journal of Viral Entry 3, 2009: p. 94–102.

114. Raymond, S., et al., Frequency of CXCR4-using viruses in primary HIV-1 infections using ultra-deep pyrosequencing. AIDS, 2011. 25(13): p. 1668-70.

115. Trouplin, V., et al., Determination of coreceptor usage of human immunodeficiency virus type 1 from patient plasma samples by using a recombinant phenotypic assay. J Virol, 2001. 75(1): p. 251-9.

116. Whitcomb, J.M., et al., Development and characterization of a novel single-cycle recombinant-virus assay to determine human immunodeficiency virus type 1 coreceptor tropism. Antimicrob Agents Chemother, 2007. 51(2): p. 566-75.

117. Schuitemaker, H. and N.A. Kootstra, Determination of co-receptor usage of HIV-1. Methods Mol Biol, 2005. 304: p. 327-32.

118. Koot, M., et al., HIV-1 biological phenotype in long-term infected individuals evaluated with an MT-2 cocultivation assay. AIDS, 1992. 6(1): p. 49-54.

119. Poveda, E., et al., Genotypic determination of HIV tropism - clinical and methodological recommendations to guide the therapeutic use of CCR5 antagonists. AIDS Rev, 2010. 12(3): p. 135-48.

120. Chesebro, B., et al., Macrophage-tropic human immunodeficiency virus isolates from different patients exhibit unusual V3 envelope sequence homogeneity in comparison with T-cell-tropic isolates: definition of critical amino acids involved in cell tropism. J Virol, 1992. 66(11): p. 6547-54.

121. Choe, H., et al., The beta-chemokine receptors CCR3 and CCR5 facilitate infection by primary HIV-1 isolates. Cell, 1996. 85(7): p. 1135-48.

122. Huang, H.L., et al., [Sequence analysis of the full-length glycoprotein 120 gene of HIV-1 CRF01_AE in Fujian, China]. Zhonghua Yi Xue Za Zhi, 2006. 86(44): p. 3104-8.

123. Kwong, P.D., et al., Structure of an HIV gp120 envelope glycoprotein in complex with the CD4 receptor and a neutralizing human antibody. Nature, 1998. 393(6686): p. 648-59.

124. O'Brien, W.A., et al., HIV-1 tropism for mononuclear phagocytes can be determined by regions of gp120 outside the CD4-binding domain. Nature, 1990. 348(6296): p. 69-73.

125. Rizzuto, C.D., et al., A conserved HIV gp120 glycoprotein structure involved in chemokine receptor binding. Science, 1998. 280(5371): p. 1949-53.

126. Shioda, T., J.A. Levy, and C. Cheng-Mayer, Macrophage and T cell-line tropisms of HIV-1 are determined by specific regions of the envelope gp120 gene. Nature, 1991. 349(6305): p. 167-9.

127. Poveda, E., et al., HIV tropism: diagnostic tools and implications for disease progression and treatment with entry inhibitors. AIDS, 2006. 20(10): p. 1359-67.

128. Weber, J., H. Piontkivska, and M.E. Quinones-Mateu, HIV type 1 tropism and inhibitors of viral entry: clinical implications. AIDS Rev, 2006. 8(2): p. 60-77.

129. De Jong, J.J., et al., Minimal requirements for the human immunodeficiency virus type 1 V3 domain to support the syncytium-inducing phenotype: analysis by single amino acid substitution. J Virol, 1992. 66(11): p. 6777-80.

130. Fouchier, R.A., et al., Simple determination of human immunodeficiency virus type 1 syncytium-inducing V3 genotype by PCR. J Clin Microbiol, 1995. 33(4): p. 906-11.

131. Boyd, M.T., et al., A single amino acid substitution in the V1 loop of human immunodeficiency virus type 1 gp120 alters cellular tropism. J Virol, 1993. 67(6): p. 3649-52.

132. Cho, M.W., et al., Identification of determinants on a dualtropic human immunodeficiency virus type 1 envelope glycoprotein that confer usage of CXCR4. J Virol, 1998. 72(3): p. 2509-15.

133. Koito, A., et al., Functional role of the V1/V2 region of human immunodeficiency virus type 1 envelope glycoprotein gp120 in infection of primary macrophages and soluble CD4 neutralization. J Virol, 1994. 68(4): p. 2253-9.

134. Koito, A., L. Stamatatos, and C. Cheng-Mayer, Small amino acid sequence changes within the V2 domain can affect the function of a T-cell line-tropic human immunodeficiency virus type 1 envelope gp120. Virology, 1995. 206(2): p. 878-84.

135. Ross, T.M. and B.R. Cullen, The ability of HIV type 1 to use CCR-3 as a coreceptor is controlled by envelope V1/V2 sequences acting in conjunction with a CCR-5 tropic V3 loop. Proc Natl Acad Sci U S A, 1998. 95(13): p. 7682-6.

136. Carrillo, A. and L. Ratner, Human immunodeficiency virus type 1 tropism for T-lymphoid cell lines: role of the V3 loop and C4 envelope determinants. J Virol, 1996. 70(2): p. 1301-9.

137. Groenink, M., et al., Phenotype-associated env gene variation among eight related human immunodeficiency virus type 1 clones: evidence for in vivo recombination and determinants of cytotropism outside the V3 domain. J Virol, 1992. 66(10): p. 6175-80.

138. Huang, W., et al., Coreceptor tropism can be influenced by amino acid substitutions in the gp41 transmembrane subunit of human immunodeficiency virus type 1 envelope protein. J Virol, 2008. 82(11): p. 5584-93.

139. Ogert, R.A., et al., N-linked glycosylation sites adjacent to and within the V1/V2 and the V3 loops of dualtropic human immunodeficiency virus type 1 isolate DH12 gp120 affect coreceptor usage and cellular tropism. J Virol, 2001. 75(13): p. 5998-6006.

140. McGovern, R.A., et al., Population-based sequencing of the V3-loop can predict the virological response to maraviroc in treatment-naive patients of the MERIT trial. J Acquir Immune Defic Syndr, 2012. 61(3): p. 279-86.

141. McGovern, R.A., et al., Population-based V3 genotypic tropism assay: a retrospective analysis using screening samples from the A4001029 and MOTIVATE studies. AIDS, 2010. 24(16): p. 2517-25.

142. Recordon-Pinson, P., et al., Evaluation of the genotypic prediction of HIV-1 coreceptor use versus a phenotypic assay and correlation with the virological response to maraviroc: the ANRS GenoTropism study. Antimicrob Agents Chemother, 2010. 54(8): p. 3335-40.

143. Seclen, E., et al., High concordance between the position-specific scoring matrix and geno2pheno algorithms for genotypic interpretation of HIV-1 tropism: V3 length as the major cause of disagreement. J Clin Microbiol, 2011. 49(9): p. 3380-2.

144. Swenson, L.C., et al., Deep V3 sequencing for HIV type 1 tropism in treatment-naive patients: a reanalysis of the MERIT trial of maraviroc. Clin Infect Dis, 2011. 53(7): p. 732-42.

145. Delobel, P., et al., Population-based sequencing of the V3 region of env for predicting the coreceptor usage of human immunodeficiency virus type 1 quasispecies. J Clin Microbiol, 2007. 45(5): p. 1572-80.

146. Low, A.J., et al., Current V3 genotyping algorithms are inadequate for predicting X4 co-receptor usage in clinical isolates. AIDS, 2007. 21(14): p. F17-24.

147. Poveda, E., et al., Design and validation of new genotypic tools for easy and reliable estimation of HIV tropism before using CCR5 antagonists. J Antimicrob Chemother, 2009. 63(5): p. 1006-10.

148. Lin, N.H. and D.R. Kuritzkes, Tropism testing in the clinical management of HIV-1 infection. Curr Opin HIV AIDS, 2009. 4(6): p. 481-7.

149. Schuurman, R., et al., Worldwide evaluation of DNA sequencing approaches for identification of drug resistance mutations in the human immunodeficiency virus type 1 reverse transcriptase. J Clin Microbiol, 1999. 37(7): p. 2291-6.

150. Swenson, L.C., et al., Deep sequencing to infer HIV-1 co-receptor usage: application to three clinical trials of maraviroc in treatment-experienced patients. J Infect Dis, 2011. 203(2): p. 237-45.

151. Sing, T., et al., Predicting HIV coreceptor usage on the basis of genetic and clinical covariates. Antivir Ther, 2007. 12(7): p. 1097-106.

152. Jensen, M.A., et al., Improved coreceptor usage prediction and genotypic monitoring of R5-to-X4 transition by motif analysis of human immunodeficiency virus type 1 env V3 loop sequences. J Virol, 2003. 77(24): p. 13376-88.

153. Hoffman, N.G., et al., Variability in the human immunodeficiency virus type 1 gp120 Env protein linked to phenotype-associated changes in the V3 loop. J Virol, 2002. 76(8): p. 3852-64.

154. Xiao, L., et al., CCR5 coreceptor usage of non-syncytium-inducing primary HIV-1 is independent of phylogenetically distinct global HIV-1 isolates: delineation of consensus motif in the V3 domain that predicts CCR-5 usage. Virology, 1998. 240(1): p. 83-92.

155. Harris, T.D., et al., Single-molecule DNA sequencing of a viral genome. Science, 2008. 320(5872): p. 106-9.

156. Dressman, D., et al., Transforming single DNA molecules into fluorescent magnetic particles for detection and enumeration of genetic variations. Proc Natl Acad Sci U S A, 2003. 100(15): p. 8817-22.

157. Metzker, M.L., Sequencing technologies - the next generation. Nat Rev Genet, 2010. 11(1): p. 31-46.

158. Rothberg, J.M. and J.H. Leamon, The development and impact of 454 sequencing. Nat Biotechnol, 2008. 26(10): p. 1117-24.

159. Adessi, C., et al., Solid phase DNA amplification: characterisation of primer attachment and amplification mechanisms. Nucleic Acids Res, 2000. 28(20): p. E87.

160. Bentley, D.R., et al., Accurate whole human genome sequencing using reversible terminator chemistry. Nature, 2008. 456(7218): p. 53-9.

161. Housby, J.N. and E.M. Southern, Fidelity of DNA ligation: a novel experimental approach based on the polymerisation of libraries of oligonucleotides. Nucleic Acids Res, 1998. 26(18): p. 4259-66.

162. Mckernan, K., Blanchard, A., Kotler, L., and Costa, G, Reagents, methods, and libraries for bead-based sequencing. 2006.

163. Rothberg, J.M., et al., An integrated semiconductor device enabling non-optical genome sequencing. Nature, 2011. 475(7356): p. 348-52.

164. Eid, J., et al., Real-time DNA sequencing from single polymerase molecules. Science, 2009. 323(5910): p. 133-8.

165. Levene, M.J., et al., Zero-mode waveguides for single-molecule analysis at high concentrations. Science, 2003. 299(5607): p. 682-6.

166. Kasianowicz, J.J., et al., Characterization of individual polynucleotide molecules using a membrane channel. Proc Natl Acad Sci U S A, 1996. 93(24): p. 13770-3.

167. Mardis, E.R., A decade's perspective on DNA sequencing technology. Nature, 2011. 470(7333): p. 198-203.

Objectives

1. To investigate the ability of different state-of-the-art genotypic and phenotypic tropism tests in PBMC-associated HIV-1 DNA and plasma RNA in order to detect CXCR4-using viruses relative to ESTA in subjects before they initiated first-line ART without CCR5 antagonists.
2. To investigate whether pre-treatment PBMC V3-loop form populations are different from those simultaneously observed in plasma and those observed in PBMCs after at least 2 years of continuous HIV-1 RNA suppression.
3. To investigate viral evolution in PBMCs during viremia suppression under ART without CCR5 antagonists.
4. To test the safety and efficacy of switching from a PI/r or an NNRTI to maraviroc in subjects with persistent virologic suppression and with R5 viruses by proviral HIV-1 V3-loop population sequencing.
5. To explore the potential of 454 sequencing for adding clinically-relevant information relative to population sequencing in deep salvage therapy at various adherence levels.
6. To explore the origin of antiviral drug resistance mutations present in subjects developing virological failure.

Hypotheses

1. The structure of viral populations and the diagnostic performance of tropism assays vary between the plasma and PBMC compartments. This is important in order to understand the biological and clinical correlates of tropism testing in proviral DNA.
2. Proviral DNA tropism testing allows subjects with sustained undetectable HIV-1 RNA levels experiencing antiretroviral-related toxicity to safely switch their current PI/r or NNRTI drug to maraviroc.
3. 454 sequencing is technically non-inferior to population sequencing and provides additional resistance and/or tropism information.
4. 454 sequencing may provide essential information for improving the efficacy of HIV-1 treatment in treatment-experienced subjects, and increase our understanding of HIV-1 pathogenesis.

Chapter 1

HIV-1 Tropism Testing in Subjects Achieving Undetectable HIV-1 RNA: Diagnostic Accuracy, Viral Evolution and Compartmentalization

Christian Pou[1*], Francisco M. Codoñer[1], Alexander Thielen[3], Rocío Bellido[1], Susana Pérez-Álvarez[1], Cecilia Cabrera[1], Judith Dalmau[1], Marta Curriu[1], Yolanda Lie[5], Marc Noguera-Julian[1], Jordi Puig[2], Javier Martínez-Picado[1,4], Julià Blanco[1], Eoin Coakley[5], Martin Däumer[6], Bonaventura Clotet[1,2], Roger Paredes[1,2*]

[1]Institut de Recerca de la SIDA irsiCaixa - HIVACAT & [2]HIV Unit-Fundació Lluita contra la SIDA, Hospital Universitari Germans Trias i Pujol, Universitat Autònoma de Barcelona, Catalonia, Spain; [3]Max-Planck-Institut für Informatik, Saarbücken, Germany; [4]Institució Catalana de Recerca i Estudis Avançats (ICREA), Barcelona, Spain; [5]Monogram Biosciences Inc., South San Francisco, California, USA, [6]Institut für Immunologie und Genetik, Kaiserlautern, Germany

PLoS One. 2013 Aug 1;8(8):e67085.

Abstract

Background. Technically, HIV-1 tropism can be evaluated in plasma or peripheral blood mononuclear cells (PBMCs). However, only tropism testing of plasma HIV-1 has been validated as a tool to predict virological response to CCR5 antagonists in clinical trials. The preferable tropism testing strategy in subjects with undetectable HIV-1 viraemia, in whom plasma tropism testing is not feasible, remains uncertain.

Methods&Results. We designed a proof-of-concept study including 30 chronically HIV-1-infected individuals who achieved HIV-1 RNA < 50 copies/mL during at least 2 years after first-line ART initiation. First, we determined the diagnostic accuracy of 454 and population sequencing of gp120 V3-loops in plasma and PBMCs, as well as of MT-2 assays before ART initiation. The Enhanced Sensitivity Trofile^{TM} Assay (ESTA) was used as the technical reference standard. 454 sequencing of plasma viruses provided the highest agreement with ESTA. The accuracy of 454 sequencing decreased in PBMCs due to reduced specificity. Population sequencing in plasma and PBMCs was slightly less accurate than plasma 454 sequencing, being less sensitive but more specific. MT-2 assays had low sensitivity but 100% specificity. Then, we used optimized 454 sequence data to investigate viral evolution in PBMCs during viraemia suppression and only found evolution of R5 viruses in one subject. No *de novo* CXCR4-using HIV-1 production was observed over time. Finally, Slatkin-Maddison tests suggested that plasma and cell-associated V3 forms were sometimes compartmentalized.

Conclusions. The absence of tropism shifts during viraemia suppression suggests that, when available, testing of stored plasma samples is generally safe and informative, provided that HIV-1 suppression is maintained. Tropism testing in PBMCs may not necessarily produce equivalent biological results to plasma, because the structure of viral populations and the diagnostic performance of tropism assays may sometimes vary between compartments. Thereby, proviral DNA tropism testing should be specifically validated in clinical trials before it can be applied to routine clinical decision-making.

Keywords: HIV-1 tropism; Evolution; Sensitivity; Specificity; 454 Sequencing; CCR5 antagonist.

Introduction

The efficacy of CCR5 antagonist therapy depends on the accurate characterization of HIV-1 tropism. A major cause of virological failure to CCR5-antagonist therapy is the emergence of pre-existing CXCR4-using viruses, often missed by tropism assays[1,2]. Retrospective reanalyses of pre-treatment plasma samples from maraviroc trials in treatment-naïve[3] and -experienced[4,5,6] individuals found that population and 454 sequencing (454 Life Sciences/Roche) of the V3-loop of gp120 were able to predict virological response to maraviroc as accurately as Trofile™ and the enhanced sensitivity version of Trofile™ (ESTA), respectively[7,8]. In the MERIT trial, first-line therapy with maraviroc in treatment naïve individuals only achieved non-inferiority to efavirenz when the ESTA[3] or 454 sequencing [9] and not the former, less sensitive version of Trofile™ were used to assess presence of CXCR4-using virus at screening. Moreover, the risk of virological failure to maraviroc-including therapy was directly proportional to the amount of CXCR4-using viruses in the viral population in other studies[10]. Presence of as little as 2% CXCR4-using viruses in the population conferred an increased risk of virological failure to maraviroc-including therapy. As with other regimens, lower CD4+ counts, resistance to other drugs or inclusion of less than 3 active drugs in the regimen further increased the risk of virological failure to maraviroc regimens.

Tropism assays validated in clinical trials to date characterize plasma viruses from subjects with detectable HIV-1 RNA. Maraviroc clinical trials enrolled individuals with HIV-1 RNA ≥ 2,000 copies/mL (MERIT Study in ART-naïve individuals) and ≥ 5,000 copies/mL (MOTIVATE 1&2 studies in treatment –experienced subjects). However, most HIV-1-infected individuals who could potentially benefit from the favorable toxicity and drug-drug-interaction profile of CCR5 antagonists have undetectable HIV-1 RNA levels under antiretroviral therapy (ART). The optimal strategy to evaluate HIV tropism in aviraemic subjects, in whom plasma tropism testing is not feasible, remains uncertain. Testing of stored pre-therapy plasma samples, when available, may not capture potential virus evolution towards CXCR4-use during ART. Conversely, proviral DNA testing might assess different virus populations than those circulating simultaneously in plasma, implying that both tests may not necessarily provide equivalent genotypic or phenotypic information for clinical decision-making and may need to be validated independently in clinical trials.

We designed this study to gain further insight into the aforementioned questions. First, we investigated the ability of different state-of-the-art genotypic and phenotypic tropism tests in proviral DNA and plasma RNA to detect CXCR4-using viruses relative to the ESTA in 30 subjects before they initiated first-line ART without CCR5

antagonists. Then, we examined if virus evolution occurred after at least 2 years of persistent HIV-1 RNA suppression under ART in these same individuals. Finally, we used population differentiation tests to investigate if pre-treatment PBMC V3 form populations were different from a) those simultaneously observed in plasma and b) those observed in PBMCs after at least 2 years of continuous HIV-1 RNA suppression.

Materials and methods

Study design and participants

This was a retrospective proof-of-concept study that included chronically HIV-1-infected adults who achieved persistent HIV-1 RNA levels <50 copies/mL during at least 2 years after starting first-line ART without CCR5 antagonists. Subjects had to have cryopreserved samples available for testing within 6 months before ART initiation (baseline, T1) and after at least 2 years of undetectable viraemia (persistent viraemia suppression, T2) (Figure 1). The Institutional Review Board of the Hospital Universitari Germans Trias i Pujol, Badalona, Spain, approved the study; participants provided written informed consent for retrospective sample testing. Tropism tests performed at T1 included the *Enhanced-Sensitivity Trofile™ Assay* (ESTA), direct cocultivation of patient-derived PBMCs with MT-2 cells (MT-2 assay), and population and 454 sequencing of the V3-loop in plasma RNA and proviral DNA. Tropism tests performed at T2 included population and 454 sequencing in PBMCs and the MT-2 assay. HIV-1 RNA levels (NucliSens EasyQ HIV-1, Biomerieux, Marcy l'Etoile, France), CD4+ and CD8+ cells counts were determined at regular 3 to 4-month intervals as part of the routine clinical follow-up of subjects.

Tropism testing

The ESTA was performed in Monogram Biosciences, South San Francisco, USA, blinded for clinical characteristics or other tropism testing results. ESTA was considered the technical reference standard for comparison with the remaining tropism assays because a) it has been used in most CCR5 antagonist clinical trials, b) is widely recognized as a sensitive, accurate and robust tropism test. c) is the only FDA-approved and CLIA-certified HIV tropism test and d) is readily available to HIV clinics worldwide. For the MT-2 assay, HIV-1 was isolated by direct cocultivation with 1-5x10^6 patient-derived cryopreserved PBMCs with 1x10^6 MT-2 cell line, in duplicate, as in[11]. Functional CXCR4-using viruses were defined by their ability to grow in MT-2 cocultures, as confirmed by p24 production. Virus growth ability was evaluated with cocultures of 1x10^6 patient-derived PHA-stimulated PBMCs and PHA-stimulated PBMC

from healthy seronegative donors. For population and 454 V3 loop sequencing, HIV-1 RNA was extracted from 1 mL of plasma after ultracentrifugation at 30,000 rpm during 1.5 hours; HIV-1 DNA was extracted from 10 million PBMCs. Reverse transcription and DNA amplification were performed in triplicate parallel reactions followed by pooling of PCR products to avoid founder effects. First-round PCR products were used for both population and 454 V3-loop sequencing. The V3-loop of functional viruses extracted from the supernatant of positive MT-2 assays was also sequenced for comparison with 454 sequencing. The combined error threshold for PCR amplification and 454 sequencing was established identifying the percentage of different V3-loop unique sequences (haplotypes) obtained after amplifying a commercial pNL4.3 DNA clone under the same PCR conditions used to generate patient samples and using the same filtering steps. A total of 2,702 V3-loop pNL4.3 clonal sequences and 154 different haplotypes were obtained by 454 sequencing, which followed a Poisson-like distribution. The 99th percentile of such distribution established the threshold for detecting "valid" V3-loop haplotypes at ≥0.6% of the viral population. The percentage of valid V3-loop haplotypes with predicted CXCR4-using tropism was then calculated.

Statistical analyses

Mean and 95% confidence intervals of the sensitivity, specificity, positive and negative predictive value and accuracy of each assay were calculated assuming a binomial distribution of the data. “Accuracy” (also known as “Fraction Correct”) was defined as: (True positives + True negatives) / Total. V3 loop genotypes derived from population and 454 sequencing were interpreted using Geno2Pheno$_{[coreceptor]}$ [12] at false positive rates (FPR) ranging from 3.5% to 20%. The FPR cut-off providing better diagnostic performance relative to the ESTA was used to define viral tropism in subsequent analyses. HIV subtype was determined with the Geno2Pheno$_{[coreceptor]}$ tool. The prevalence of subjects with CXCR4-using viruses was determined with each assay and setting; differences relative to ESTA were tested for significance using a two-sided exact binomial test. Statistical analyses were performed with *R*$_{[13]}$.

Phylogenetic analyses

The phylogenetic relatedness between viruses present in plasma and PBMCs at T1 and in PBMCs at T2 was determined using valid 454 sequencing V3-loop haplotypes. Sequences were codon-aligned with HIValign; the optimal nucleotide evolution model was determined with FindModel (http://www.hiv.lanl.gov). Maximum likelihood trees were constructed with PhyML$_{[14]}$ and were edited with Mega v4.0$_{[15,16]}$; node reliability was evaluated with 1,000 bootstraps. Tree labels were manually edited

to make their size proportional to the sequence representation in the virus population. Trees were rooted at the most prevalent plasma V3-loop haplotype present before antiretroviral treatment initiation. Patterns of temporal and CXCR4-using clustering were investigated in subjects with 454 sequencing data available from the three compartments (plasma at T1 and PBMC at T1 and T2). The presence or absence of CXCR4-using clustering was only evaluated in subjects with at least two CXCR4-using viruses in any compartment. CXCR4-using clustering was defined as the presence of at least one cluster of at least two CXCR4-using haplotypes, supported by a bootstrap value or 70% or higher. Temporal clustering was defined as the grouping of all V3-loop haplotypes from one timepoint into a single cluster, supported by a bootstrap value or 70% or higher.

Population differentiation

Population differentiation was assessed using the tree topology-based Slatkin-Maddison test[17] implemented in HYPHY[18]. The Slatkin-Maddison test compares tree topologies without taking into account haplotype frequency in the population. In previous controls, no compartmentalization was observed between duplicate measurements of 6 different PBMC samples by the Slatkin-Maddison test. However, an analysis of molecular variance (AMOVA)[19] provided statistically significant differences between duplicate samples, indicating that AMOVA can provide false positive results when deep sequencing data is used to estimate frequencies of closely related viral variants and, therefore, is not suitable for this analysis.

Sequence Data Sets

V3-loop population and 454 sequences were deposited in GenBank (http://www.ncbi.nlm.nih.gov/ genbank/index.html) and the Sequence Read Archive (http://www.ncbi.nlm.nih.gov/sra/), respectively, accession numbers: JF297475-JF297561 and SRP018530. Descriptions of biological source materials used in experimental assays are available in the Biosample database (http://www.ncbi.nlm.nih.gov/biosample) under consecutive accession numbers SAMN01914993 to SAMN01915082. The BioProject (http://www.ncbi.nlm.nih.gov/bioproject) code for this work is PRJNA188778.

Results

Subjects' characteristics

Thirty-five chronically HIV-1-infected adults were recruited for this study in Badalona, Spain, between June and October 2008. Subjects had to have stored samples available for tropism testing within 6 months before ART initiation (baseline, T1) and after at least 2 years of undetectable viraemia (T2) (Figure 1). Five individuals were excluded from the analysis due to non-interpretable ESTA results (n=1), treatment interruption during follow-up (n=1), lack of amplification by any genotypic method (n=1) and absence of sufficient sample material for testing (n=2). The median age of the 30 individuals providing data was 44 years; they were mostly men and had acquired HIV through sexual practices (Table 1). The median time between T1 and T2 were 45 months. The median T1 viraemia and CD4+ counts were 58,500 copies/mL and 224 cells/mm^3, respectively; median nadir CD4+ counts were 215 cells/mm^3. Median CD4+ counts increased to 560 cells/mm^3 at T2 while HIV-1 RNA levels remained <50 copies/mL. Five individuals developed one HIV-1 RNA blip each during follow-up (HIV-1 RNA range: 125-275 copies/mL, incidence rate 1.7 blips/1,000 person-years). 454 sequencing produced a median (interquartile range, IQR) number of total, valid and unique V3-loop sequences of 5,366 (3,228 ; 6,553), 4,591 (2,751 ; 5,371) and 7 (4 ; 15) in plasma at T1; 3,983 (3,042 ; 5,256), 3,315 (2,238 ; 3,963) and 8 (6 ; 14) in PBMCs at T1; and 3,498 (2,444 ; 4,512), 2,562 (1,718 ; 3,509) and 8 (6 ; 15) in PBMCs at T2, respectively. All subjects were infected with subtype B HIV.

Accuracy of tropism assays relative to ESTA

The accuracy of tropism tests in plasma and PBMCs was only evaluated before ART initiation, when all assays could be simultaneously compared to the technical reference standard in the same clinical conditions (Table 2).

454 sequencing of plasma viruses provided the best agreement with ESTA, particularly at a $Geno2Pheno_{[coreceptor]}$ False Positive Rate (FPR) of 10% (73% sensitivity, 95% specificity, 87% accuracy). Increasing the FPR to 15% did not improve the sensitivity but worsened the specificity; decreasing the FPR improved the specificity to 100%, but decreased the sensitivity to levels overlapping those of population sequencing (Figure 1, Table 2). Interestingly, 454 sequencing was less accurate in proviral DNA than in plasma HIV-1 RNA, being similarly sensitive but less specific. Increases in specificity could be achieved by decreasing the FPR cut-off, but this also decreased the assay's sensitivity considerably. Moreover, the PBMC X4 load in subjects with detectable CXCR4-using HIV in PBMCs by 454 but R5 HIV-1 by ESTA (Table 3, subjects 13, 14, 19, 21 and 23) was usually high enough to suggest a

different HIV population structure in plasma and PBMCs, rather than fluctuations around the sensitivity threshold of each technology amenable to fine-tuning.

Population sequencing was invariably less sensitive than 454 sequencing although it retained high specificity. No differences in accuracy were observed using either 10% or 5.75% FPR cut-offs. However, increasing the FPR threshold to 20% improved the sensitivity of the assay without compromising its specificity. Of note, population sequencing achieved similar accuracy in proviral DNA than in plasma HIV-1 RNA. All subjects with CXCR4-using viruses by population sequencing except one had CXCR4-using virus levels above 15% by 454 sequencing in proviral DNA, further supporting the idea that clinically relevant CXCR4-using cut-off levels might be different for plasma and PBMCs.

The MT-2 assays had low sensitivity but high specificity. As observed elsewhere[20], internal controls of direct cocultivation of patient and healthy donor PBMCs indicated that we were only capable of obtaining productive HIV infection from about 50% of subjects overall (not shown).

The prevalence of subjects with a CXCR4-using virus varied among tropism tests and settings (Figure 1). ESTA detected CXCR4-using viruses in 36.7% of subjects. The prevalence of CXCR4-using HIV was significantly underestimated by plasma 454 sequencing using a FPR of 3.5%, population sequencing of plasma and PBMC V3 forms using FPRs of 10% or 5.75%, and by the MT-2 assay ($p<0.05$ for all comparisons with ESTA, two-sided exact binomial test). No statistically significant differences in CXCR4-using prevalence were observed between plasma and PBMCs.

Viral evolution during viraemia suppression and population differentiation

Overall, there was good individual agreement in the longitudinal detection of CXCR4-using HIV (Table 3), but slightly more CXCR4-using viruses were detected in PBMCs after at least two years of viraemia suppression (Table 3, Figure 1). To evaluate if viruses evolved in PBMCs during suppressive ART, we used V3 forms generated by 454 sequencing present in ≥ 0.6% in the virus population. Based on the previous accuracy assessments, a FPR ≤ 10% was chosen to define CXCR4 use. Twenty-eight subjects had 454 sequencing data available from plasma at T1, PBMCs at T1 and PBMCs at T2 (Figure 2, Supplementary material 1).

We only observed evolution of CCR5 viruses in one individual (Subject 7), who showed bootstrap-supported temporal clustering of new CCR5 viruses at T2. Apparently, another subject seemed to have developed CXCR4-using HIV-1 *de novo* during viraemia suppression (subject 26). The emerging CXCR4-using V3-loop form (sequence ID 2; Figure 2B), however, was present before therapy in 0.04% of PBMC-

associated viruses, suggesting that detection of such CXCR4-using virus was more likely due to fluctuations around the sensitivity threshold of 454 sequencing than to a true emergence of a CXCR4-using virus *de novo*. Subject 30 (Table 3) also had low-frequency CXCR4-using HIV detected only at T2. Phylogenetic analysis (supplementary material 1) confirmed that such variant clustered with pre-treatment viruses. This indicates that this was a pre-existing which was detected at T2 due to fluctuations around the sensitivity threshold of 454 sequencing, rather than to true virus evolution. Of the remaining individuals, 9 (32.1%) showed bootstrap-supported CXCR4-using HIV-1 clustering across timepoints and compartments, 3 (10.7%) had non-significant CXCR4-using virus clustering and 15 (53.6%) had only R5 viruses detected in all timepoints and compartments. Interestingly, the V3-loop sequence of syncytium-inducing viruses grown in all positive MT-2 assays was identical to one of the predominant V3-loop haplotypes simultaneously detected by 454 sequencing in proviral DNA and/or plasma RNA (Figure 3), suggesting that 454 sequencing can detect V3 forms that are also present in functional CXCR4-using viruses.

There were no differences in nucleotide variability (π) among compartments in any subject (Table 4). The Slatkin-Maddison test indicated the presence of sequence compartmentalization between plasma and PBMCs at T1 in 2/28 (7%) individuals, and between PBMCs at T1 and T2 in 6/28 (21%) individuals.

Discussion

Only assays assessing tropism of plasma HIV-1 have been validated in clinical trials. Given that tropism cannot be routinely assessed in plasma of subjects with HIV-1 RNA levels <500-1,000 copies/mL, the optimal tropism testing strategy for clinical decision-making in these individuals remains unclear. To better understand the advantages and limitations of different tropism testing strategies in aviraemic subjects, we first evaluated the diagnostic performance of various state-of-the-art tropism tests relative to the ESTA. The latter was chosen as the technical reference standard for this study because it is widely recognized as a sensitive and robust assay, it is CLIA-validated, and has been used in most previous clinical trials of CCR5 antagonists[3,4,5,6,21], including those leading to the approval of maraviroc[3,4,5].

In our hands, the tropism assay providing closest diagnostic accuracy to ESTA was 454 sequencing of plasma RNA. The highest accuracy of this assay was obtained after applying strict PCR and 454 sequencing error controls, considering only V3 forms present in at least 0.6% of the virus population and using a Geno2Pheno[coreceptor] FPR cut-off of 10% to define CXCR4-using viruses. Such settings provided 73% sensitivity,

95% specificity and 87% accuracy. Using a 2% level of minor CXCR4-using variants and a 3.5% Geno2Pheno[coreceptor] FPR to define non-R5 use, other authors found that 454 sequencing of plasma HIV-1 was able to accurately predict virological response to maraviroc-including regimens in retrospective reanalyses of maraviroc trials[4,5,6,7]. However, applying such settings to our own dataset (including the assessment of tropism by Geno2Pheno[454] starting from raw sequence data) resulted in decreased sensitivity and accuracy of the assay (50% sensitivity, 95% specificity and 79% accuracy). Consequently, the settings chosen for 454 sequencing in our study might potentially provide a more accurate assessment of phenotypic tropism; proper validation of our 454 settings in larger datasets including clinical endpoints is however warranted before they can be routinely used to predict virological outcomes to CCR5 antagonists.

454 sequencing was remarkably less accurate in proviral DNA than in plasma, mainly due to reduced specificity. In fact, population sequencing in proviral DNA was slightly less sensitive but more specific and, overall, more accurate than 454 sequencing in PBMCs. The reasons for such discrepancy are not fully understood. On one hand, tropism prediction engines have been trained and validated using data from plasma viruses, and might require different settings in other compartments. Peripheral blood mononuclear cells contain a historical repository of current and past HIV, some of which might be defective or unable to replicate. Also, identical V3 forms are often present at different frequency in plasma and PBMCs; whether this has an impact on treatment outcomes remains unclear. Even if identical V3 forms can be identified simultaneously in plasma RNA, proviral DNA and in syncytium-inducing viruses growing in MT-2 cells, as observed in this study, such V3 loops may be present in viruses with different genetic backgrounds and, thus, have different phenotypic tropism. Mutations in gp120 outside V3 loop and in gp41[22], as well as differences in env glycosylation patterns[23] can modulate the viral tropism in a minority of subjects. This is a limitation of most genotypic techniques based on V3 loop sequencing. However, although mutations in gp41 are correlated with coreceptor tropism, they do not improve tropism prediction methods substantially[24].

The accuracy of population sequencing of plasma or PBMC-associated HIV in our study was similar to that of other studies that also used the ESTA as the reference standard[25,26]. Interestingly, although population sequencing was less sensitive than plasma 454, it was more specific and, overall, just slightly less accurate, particularly when a 20% FPR was used. This suggests that population sequencing might be an acceptable alternative to 454 sequencing in settings without access to next-generation sequencing provided that high FPR cutoffs are used.

One particular interest of our study was to evaluate to which extent tropism tests in plasma and PBMCs provide equivalent biological results. The observation of sequence compartmentalization in some subjects suggests that, although plasma and PBMCs often provide similar tropism reports[27], their biological or clinical meaning might not be necessarily equivalent. Indeed, in a retrospective reanalysis of pretreatment samples of the MOTIVATE and A4001029 studies, HIV DNA-based methods were generally good predictors of virological response to maraviroc regimens, but virologic response was better predicted by plasma compared to PBMC 454 sequencing[28]. Contrasting with our dataset, the PBMC compartment harbored more variable V3 forms than plasma. Concordance between plasma and PBMC tropism by 454 sequencing ranged from 74% amongst samples with CD4+ counts <50 cells/mm^3 to 100% concordance at CD4+ counts >350 cells/mm^3, suggesting that, in addition to the sequence compartmentalization observed in our study, a CD4+ count-dependant bias in DNA input might also affect PBMC results. Moreover, the existence of V3 compartmentalization between PBMCs at T1 and T2 in the absence of overt viral evolution during prolonged viraemia suppression suggests the presence of drifts in PBMC composition that may further affect DNA sampling for tropism testing.

We also sought to explore if HIV-1 tropism shifts were frequently observed during persistent viraemia suppression, which would be informative of the clinical feasibility of using stored plasma samples collected before ART initiation for tropism testing. The absence of CXCR4 virus evolution during prolonged periods of viraemia suppression suggests that, when available, testing of stored plasma samples is generally safe and informative, provided that HIV-1 RNA levels remain continuously suppressed. Our findings are in agreement with previous publications using population sequencing of proviral DNA[29,30]. Importantly, subjects in this study did not receive CCR5 antagonists; it remains largely unexplored if HIV-1 tropism may still evolve under the selective pressure of CCR5 antagonists if continuous viraemia suppression is achieved.

This study represents a comprehensive comparison of the main state-of-the-art tropism tests with potential application to HIV clinical management and fulfills the Standards for Reporting of Diagnostic Accuracy (STARD)[31]. The study design allowed investigating population differentiation and longitudinal CXCR4-using evolution in different compartments, which is informative of the optimal timing and source for tropism testing in subjects with undetectable HIV-1 RNA levels. The main weaknesses of the study are its small sample size, its retrospective nature, the lack of association of tropism data with outcomes to CCR5 antagonist therapy, and the use of cryopreserved PBMCs for MT-2 assays. This last factor, and the fact that subjects had had HIV RNA <50 copies/mL during more than 2 years of ART at T2, likely reduced our ability to

recover infectious viruses, leading to a decreased performance of MT-2 assays relative to previous publications[32]. We only used Geno2Pheno[coreceptor] to interpret genotypic data because previous comparisons demonstrated equivalence with other interpretation systems[33,34] and it is extensively used in our setting. Differences in FPR settings observed in this study were sometimes due to a small number of patients, which is reflected in the wide confidence intervals of our diagnostic accuracy estimations.

Conclusions

Although plasma and PBMCs may often provide similar tropism reports[27], tropism testing in PBMCs may not necessarily produce equivalent biological results to plasma, because the structure of viral populations and the diagnostic performance of tropism assays vary between compartments. Thereby, proviral DNA tropism testing should be specifically validated in clinical trials before it can be applied to routine clinical decision-making. Clinically relevant cut-offs and settings should be identified for clonal and population genotypic tropism testing in proviral DNA. The absence of tropism shifts during viraemia suppression suggests that, when available, testing of stored plasma samples is generally safe and informative, provided that HIV suppression is maintained. Next-generation sequencing technologies have the potential to be a cost-effective alternative to assess viral tropism and provide essential information to increase the efficacy of HIV therapeutics and advance our understanding of HIV pathogenesis.

Competing Interests

We have read the journal's policy and have the following conflicts: JMP has received research funding, consultancy fees, or lecture sponsorships from GlaxoSmithKline, Merck. JB has received research funding from Merck and consultancy fees from GlaxoSmithKline. YL and EC are employees of Monogram Biosciences, South San Francisco CA, USA. BC has been a consultant on advisory boards or participated in speakers' bureaus or conducted clinical trials with Boehringer-Ingelheim, Abbott, GlaxoSmithKline, Gilead, Janssen, Merck, Shionogi and ViiV. RP has received consulting fees from Pfizer and grant support from Pfizer, Roche Diagnostics, Siemens, Merck and Boehringer-Ingelheim. CP, FMC, AT, RB, SPA, CC, JD, MC, JP, MN and MD report no competing interests. This does not alter our adherence to all the PLOS ONE policies on sharing data and materials.

Author's contributions

The study was conceived by RP, JMP, JB and BC. JP, CP, RP and BC selected the study participants and collected clinical, HIV-1 RNA and CD4+ data. CP and MD performed 454 sequencing. CP and MC performed population sequencing. RB, JD and CC performed the MT-2 assays. YL and EC performed the ESTA. FMC and AT performed the bioinformatic analyses of 454 sequences. SPA and MN performed the statistical analysis. CP and RP drafted the article, which was reviewed, edited and approved by all authors.

Acknowledgements

This study was supported through an unrestricted research grant from Pfizer, 'CHAIN, Collaborative HIV and Anti-HIV Drug Resistance Network', Integrated Project no. 223131, funded by the European Commission Framework 7 Program, the Spanish AIDS network 'Red Temática Cooperativa de Investigación en SIDA' (RD06/0006), and the 'Gala contra la sida – Barcelona 2011'. FMC was supported by the Marie Curie European Reintegration Grant number 238885, 'HIV Coevolution', European Commission Framework 7 Program. None of the funding bodies had any role in the design, collection, analysis, or interpretation of data; in the writing of the manuscript or in the decision to submit the manuscript for publication. This study was presented in part at the 17th Conference on Retroviruses and Opportunistic Infections, San Francisco, USA, February 16-19, 2010, Abstract# 544; and 18th Conference on Retroviruses and Opportunistic Infections, Boston, USA, February 27-March 2, 2011, Abstract# 669.

References

1. Tsibris AM, Sagar M, Gulick RM, Su Z, Hughes M, et al. (2008) In vivo emergence of vicriviroc resistance in a human immunodeficiency virus type 1 subtype C-infected subject. J Virol 82: 8210-8214.
2. Westby M, Lewis M, Whitcomb J, Youle M, Pozniak AL, et al. (2006) Emergence of CXCR4-using human immunodeficiency virus type 1 (HIV-1) variants in a minority of HIV-1-infected patients following treatment with the CCR5 antagonist maraviroc is from a pretreatment CXCR4-using virus reservoir. J Virol 80: 4909-4920.
3. Cooper DA, Heera J, Goodrich J, Tawadrous M, Saag M, et al. (2010) Maraviroc versus efavirenz, both in combination with zidovudine-lamivudine, for the treatment of antiretroviral-naive subjects with CCR5-tropic HIV-1 infection. J Infect Dis 201: 803-813.
4. Gulick RM, Lalezari J, Goodrich J, Clumeck N, DeJesus E, et al. (2008) Maraviroc for previously treated patients with R5 HIV-1 infection. N Engl J Med 359: 1429-1441.
5. Fatkenheuer G, Nelson M, Lazzarin A, Konourina I, Hoepelman AI, et al. (2008) Subgroup analyses of maraviroc in previously treated R5 HIV-1 infection. N Engl J Med 359: 1442-1455.
6. Saag M, Goodrich J, Fatkenheuer G, Clotet B, Clumeck N, et al. (2009) A double-blind, placebo-controlled trial of maraviroc in treatment-experienced patients infected with non-R5 HIV-1. J Infect Dis 199: 1638-1647.
7. Swenson L, Dong W, Mo T, Thielen A, Jensen M, et al. (2010) Large-scale Application of Deep Sequencing Using 454 Technology to HIV Tropism Screening. 17th Conference on Retroviruses and Opportunistic Infections. San Francisco, USA.

8. McGovern RA, Thielen A, Mo T, Dong W, Woods CK, et al. (2010) Population-based V3 genotypic tropism assay: a retrospective analysis using screening samples from the A4001029 and MOTIVATE studies. AIDS 24: 2517-2525.

9. Swenson LC, Mo T, Dong WW, Zhong X, Woods CK, et al. (2011) Deep Third Variable Sequencing for HIV Type 1 Tropism in Treatment-Naive Patients: A Reanalysis of the MERIT Trial of Maraviroc. Clin Infect Dis 53: 732-742.

10. Heera J, Harrigan PR, Lewis M, Chapman D, Biswas P, et al. (February 27-March 2, 2011) Predicting MVC Responses According to Absolute Number vs. Proportion of CXCR4-Using Virus Among Treatment-experienced Patients. 18th Conference on Retroviruses and Opportunistic Infections. Boston.

11. Koot M, Vos AH, Keet RP, de Goede RE, Dercksen MW, et al. (1992) HIV-1 biological phenotype in long-term infected individuals evaluated with an MT-2 cocultivation assay. AIDS 6: 49-54.

12. Sing T, Low AJ, Beerenwinkel N, Sander O, Cheung PK, et al. (2007) Predicting HIV coreceptor usage on the basis of genetic and clinical covariates. Antivir Ther 12: 1097-1106.

13. R_Development_Core_Team (2009) R: A language and environment for statistical computing. In: Computing RFfS, editor. Austria, Vienna: R Foundation for Statistical Computing.

14. Guindon S, Gascuel O (2003) A simple, fast, and accurate algorithm to estimate large phylogenies by maximum likelihood. Syst Biol 52: 696-704.

15. Tamura K, Dudley J, Nei M, Kumar S (2007) MEGA4: Molecular Evolutionary Genetics Analysis (MEGA) software version 4.0. Mol Biol Evol 24: 1596-1599.

16. Kumar S, Nei M, Dudley J, Tamura K (2008) MEGA: a biologist-centric software for evolutionary analysis of DNA and protein sequences. Brief Bioinform 9: 299-306.

17. Slatkin M, Maddison WP (1989) A cladistic measure of gene flow inferred from the phylogenies of alleles. Genetics 123: 603-613.

18. Kosakovsky Pond SL, Frost SD (2005) Not so different after all: a comparison of methods for detecting amino acid sites under selection. Mol Biol Evol 22: 1208-1222.

19. Excoffier L, Laval G, Schneider S (2005) Arlequin (version 3.0): an integrated software package for population genetics data analysis. Evol Bioinform Online 1: 47-50.

20. Hosoya N, Su Z, Wilkin T, Gulick RM, Flexner C, et al. (2009) Assessing human immunodeficiency virus type 1 tropism: Comparison of assays using replication-competent virus versus plasma-derived pseudotyped virions. J Clin Microbiol 47: 2604-2606.

21. Gulick RM, Su Z, Flexner C, Hughes MD, Skolnik PR, et al. (2007) Phase 2 study of the safety and efficacy of vicriviroc, a CCR5 inhibitor, in HIV-1-Infected, treatment-experienced patients: AIDS clinical trials group 5211. J Infect Dis 196: 304-312.

22. Huang W, Toma J, Fransen S, Stawiski E, Reeves JD, et al. (2008) Coreceptor tropism can be influenced by amino acid substitutions in the gp41 transmembrane subunit of human immunodeficiency virus type 1 envelope protein. J Virol 82: 5584-5593.

23. Ogert RA, Lee MK, Ross W, Buckler-White A, Martin MA, et al. (2001) N-linked glycosylation sites adjacent to and within the V1/V2 and the V3 loops of dualtropic human immunodeficiency virus type 1 isolate DH12 gp120 affect coreceptor usage and cellular tropism. J Virol 75: 5998-6006.

24. Thielen A, Lengauer T, Swenson LC, Dong WW, McGovern RA, et al. (2011) Mutations in gp41 are correlated with coreceptor tropism but do not improve prediction methods substantially. Antivir Ther 16: 319-328.

25. Prosperi MC, Bracciale L, Fabbiani M, Di Giambenedetto S, Razzolini F, et al. (2010) Comparative determination of HIV-1 co-receptor tropism by Enhanced Sensitivity Trofile, gp120 V3-loop RNA and DNA genotyping. Retrovirology 7: 56.

26. Svicher V, D'Arrigo R, Alteri C, Andreoni M, Angarano G, et al. (2010) Performance of genotypic tropism testing in clinical practice using the enhanced sensitivity version of Trofile as reference assay: results from the OSCAR Study Group. New Microbiol 33: 195-206.

27. Raymond S, Delobel P, Mavigner M, Cazabat M, Encinas S, et al. (2010) CXCR4-using viruses in plasma and peripheral blood mononuclear cells during primary HIV-1 infection and impact on disease progression. AIDS 24: 2305-2312.

28. Swenson LC, McGovern RA, James I, Demarest J, Chapman D, et al. (February 27-March 2, 2011) Analysis of Cellular HIV V3 DNA to Predict Virologic Response to Maraviroc: Performance of Population-based and 454 Deep V3 Sequencing. 18th Conference on Retroviruses and Opportunistic Infections. Boston.

29. Soulie C, Lambert-Niclot S, Wirden M, Simon A, Valantin MA, et al. (2011) Low frequency of HIV-1 tropism evolution in patients successfully treated for at least 2 years. AIDS 25: 537-539.

30. Seclen E, Del Mar Gonzalez M, De Mendoza C, Soriano V, Poveda E (2010) Dynamics of HIV tropism under suppressive antiretroviral therapy: implications for tropism testing in subjects with undetectable viraemia. J Antimicrob Chemother 65: 1493-1496.

31. Bossuyt PM, Reitsma JB, Bruns DE, Gatsonis CA, Glasziou PP, et al. (2003) Towards complete and accurate reporting of studies of diagnostic accuracy: the STARD initiative. BMJ 326: 41-44.

32. Coakley E, Reeves JD, Huang W, Mangas-Ruiz M, Maurer I, et al. (2009) Comparison of human immunodeficiency virus type 1 tropism profiles in clinical samples by the Trofile and MT-2 assays. Antimicrob Agents Chemother 53: 4686-4693.

33. Abbate I, Rozera G, Tommasi C, Bruselles A, Bartolini B, et al. (2010) Analysis of co-receptor usage of circulating viral and proviral HIV genome quasispecies by ultra-deep pyrosequencing in patients who are candidates for CCR5 antagonist treatment. Clin Microbiol Infect.

34. Recordon-Pinson P, Soulie C, Flandre P, Descamps D, Lazrek M, et al. (2010) Evaluation of the genotypic prediction of HIV-1 coreceptor use versus a phenotypic assay and correlation with the virological response to maraviroc: the ANRS GenoTropism study. Antimicrob Agents Chemother 54: 3335-3340.

TABLE 1. SUBJECTS' CHARACTERISTICS [A]

Age, median (IQR)	44 (39; 49)
Gender, n (%)	
Male	20 (67.7)
Female	10 (33.3)
Transmission route, n (%)	
Heterosexual	11 (36.7)
Homosexual	11 (36.7)
IVDU	2 (6.7)
IVDU + Homosexual	1 (3.3)
Transfusion of blood derivatives	1 (3.3)
Unknown	4 (13.3)
Pre-treatment HIV-1 RNA copies/mL, median (IQR)	58,500 (7,925; 107,500)
Pre-treatment CD4+ T cells/mm^3	
Absolute, median (IQR)	224 (120; 326)
Percentage, median (IQR)	15 (10; 19)
Nadir, median (IQR)	216 (86; 267)
CD4+ T cells/mm^3 after >2 years of viraemia suppression	
Absolute, median (IQR)	560 (416; 788)
Percentage, median (IQR)	29 (25; 37)
Pre-treatment CD8+ T cells count (cells/mm^3)	
Absolute, median (IQR)	886 (657; 1,196)
Percentage, median (IQR)	41 (38; 51)
CD8+ T cells/mm^3 >2 years of viraemia suppression	
Absolute, median (IQR)	959 (665; 1,120)
Percentage, median (IQR)	62 (56; 71)
Antiretroviral treatment initiated, n (%)	
2 NRTIs + PIr	14 (46.7)
2 NRTIs + NNRTI	12 (40.0)
2 NRTIs + NNRTI + Pir	3 (10.0)
2 NRTIs	1 (3.3)
Time in months between events	
HIV diagnosis and T1, median (IQR)	2 (1;8)
T1 and T2, median (IQR)	45 (32;72)
ART initiation and T2, median (IQR)	33 (25; 51)

[a] IQR, 25^{th}-75^{th} interquartile range; ART, Antiretroviral treatment; IVDU, Intravenous Drug User; NRTI, Nucleoside reverse transcriptase inhibitor; NNRTI, Non-nucleoside reverse transcriptase inhibitor; PIr, Ritonavir-boosted Protease Inhibitor; T1, first timepoint when tropism was measured (i.e. before ART initiation); T2, second timepoint when tropism was measured (i.e., after > 2 years of HIV-1 RNA suppression).

TABLE 2. ACCURACY OF TROPISM ASSAYS RELATIVE TO THE ENHANCED-SENSITIVITY TROFILE™ ASSAY [A]

	Tests performed in pre-treatment Plasma RNA							Tests performed in pre-treatment Proviral DNA							
	Population V3-loop sequencing [b]			454 V3-loop sequencing				Population V3-loop sequencing [b]			454 V3-loop sequencing				MT-2 [c]
G2P FPR [b]	20	10	5.75	15	10	5.75	3.5	20	10	5.75	15	10	5.75	3.5	
Sensitivity	60.0 (26.2-87.4)	40.0 (12.1-73.8)	40.0 (12.1-73.8)	72.7 (39.0-94.0)	72.7 (39.0-94.0)	63.6 (30.8-89.1)	45.5 (16.7-76.6)	63.6 (30.8-89.1)	36.4 (10.9-69.2)	36.4 (10.9-69.2)	72.7 (39.0-94.0)	72.7 (39.0-94.0)	54.5 (23.4-83.3)	45.5 (16.7-76.6)	45.5 (16.7-76.6)
Specificity	100 (74.0-100)	100 (74.0-100)	94.4 (74.0-100)	84.2 (60.4-96.6)	94.7 (74.0-99.9)	100 (75.1-100)	100 (75.1-100)	100 (75.1-100)	100 (75.1-100)	100 (75.1-100)	73.7 (48.8-90.9)	73.7 (48.8-90.9)	84.2 (60.4-96.6)	89.5 (66.9-98.7)	100 (75.1-100)
PPV [d]	100 (42.1-100)	100 (28.4-100)	100 (28.4-100)	72.7 (30.0-94.0)	88.9 (51.8-99.7)	100 (47.3-100)	100 (35.9-100)	100 (47.3-100)	100 (28.4-100)	100 (28.4-100)	61.5 (31.6-86.1)	61.5 (31.6-86.1)	66.7 (29.9-92.5)	71.4 (29.0-96.3)	100 (35.9-100)
NPV [d]	81.8 (59.7-94.8)	75.0 (53.3-90.2)	75.0 (53.3-90.2)	84.2 (60.4 -96.6)	85.7 (63.7-97.0)	82.6 (61.2-95.0)	76.0 (54.9-90.6)	82.6 (61.2-95.0)	73.1 (52.2-88.4)	73.1 (52.2-88.4)	82.4 (56.6-96.2)	82.4 (56.6-96.2)	76.2 (52.8-91.8)	73.9 (51.6-89.8)	76 (54.9-90.6)
Accuracy [d]	85.7 (67.3-96.0)	78.6 (59.0-91.7)	78.6 (59.0-91.7)	80.0 (61.4-92.3)	86.7 (69.3-96.2)	86.7 (69.3-96.2)	80.0 (61.4-92.3)	86.7 (69.3-96.2)	76.7 (57.7-90.1)	76.7 (57.7-90.1)	73.3 (54.1-87.7)	73.3 (54.1-87.7)	73.3 (54.1-87.7)	73.3 (54.1-87.7)	80 (61.4-92.3)

[a] Values are mean percentages (95% confidence interval of the mean), calculated assuming a binomial distribution of the data

[b] *G2P FPR*, Geno2Pheno$_{[coreceptor]}$ false positive rate used for population and 454 sequencing to assign CXCR4 use . The Geno2Pheno$_{[coreceptor]}$ clonal model was always used.

[c] *MT-2*, Direct cocultivation of patient-derived peripheral blood mononuclear cells with MT-2 cells

[d] *PPV*, Positive Predictive Value

[e] *NPV*, Negative Predictive Value

[f] "Accuracy" is defined as: (True positives + True negatives)/Total

TABLE 3. LONGITUDINAL TROPISM TESTING RESULTS PER SUBJECT [A,B,C]

Subject ID	Before ART initiation (T1)								≥ 2 years of HIV-1 RNA suppression (T2)			
	HIV-1 RNA (c/mL)	CD4+ counts (c/mm^3)	Tropism in Plasma RNA			Tropism in Proviral DNA			CD4+ counts (c/mm^3)	Tropism tests in Proviral DNA		
			ESTA	Pop Seq	454 (% X4)	Pop Seq	454 (% X4)	MT-2		Pop Seq	454 (% X4)	MT-2
1	300,000	191	DM	X4	100	X4	100	SI	326	X4	29.0	SI
2	60,000	88	DM	X4	100	X4	98.1	SI	272	X4	30.4	-
3	29,000	55	DM	X4	100	X4	90.1	SI	904	X4	79.4	SI
4	130,000	345	DM	X4	67.7	X4	93.9	SI	655	X4	100	SI
5	1,300,000	82	DM	-	12.2	-	15.7	SI	368	X4	16.0	-
6	40,000	231	DM	-	1.8	X4	68.9	-	950	X4	61.5	-
7	6,800	262	DM	-	2.8	-	-	-	528	X4	19.3	-
8	52,000	259	DM	X4	7.6	X4	15.4	-	872	X4	22.6	-
9	65,000	214	DM	X4	-	X4	1.8	-	471	X4	-	-
10	80,000	35	DM	NA	NA	-	-	-	488	-	-	-
11	89,000	379	DM	-	-	-	-	-	684	-	18.1	-
12	65,000	213	-	-	16.3	-	-	-	502	-	-	-
13	88,000	614	-	NA	-	-	99.0	-	1,384	NA	NA	-
14	2,300	265	-	-	-	-	36.0	-	665	-	3.3	-
15	1,220	418	-	-	-	-	-	-	760	-	-	-
16	1,290	281	-	-	-	-	-	-	298	-	-	-
17	57,000	539	-	-	-	-	-	-	1,232	-	-	-
18	860,000	52	-	-	-	-	-	-	608	-	-	-
19	180,000	131	-	-	-	-	11.4	-	1,056	-	-	-
20	226,195	182	-	-	-	-	-	-	490	-	-	-
21	1,600	64	-	-	-	-	7.3	-	283	-	1.2	-
22	1,000	331	-	-	-	-	-	-	1,001	NA	-	-
23	1,400	335	-	-	-	-	1.1	-	590	-	-	-
24	100,000	325	-	-	-	-	-	-	420	-	-	-
25	8,300	217	-	-	-	-	-	-	529	-	-	-
26	200,000	284	-	-	-	-	-	-	614	-	1.3	-
27	87,000	269	-	-	-	-	-	-	673	-	-	-
28	43,000	184	-	-	-	-	-	-	524	-	-	-
29	16,000	158	-	-	-	-	-	-	403	-	-	-
30	32,000	39	-	-	-	-	-	-	382	-	1.9	-

[a] *ESTA*, *Enhanced-Sensitivity Trofile™ Assay*; *Pop Seq,* population sequencing of the V3-loop; *454*, 454 sequencing of the V3-loop; *MT-2*, direct co-cultivation of patient-derived peripheral blood mononuclear cells with MT-2 cells. HIV-1 RNA levels are in copies/mL; CD4+ cell counts are in cells/mm^3.

[b] Population and 454 sequencing data shown here used the $Geno2Pheno_{[coreceptor]}$ false positive rate cut-off providing highest accuracy when assigning HIV-1 tropism, i.e.: 20% and 10%, respectively. Based on internal error controls, only V3 forms present in ≥ 0.6% of viruses were considered for tropism prediction with 454 sequencing.

[c] Tests detecting CXCR4-using HIV are reported as "*dual-mixed, DM*" for ESTA, *"X4"* for population sequencing, "*percent of X4 viruses"* for 454, and "*syncytium-inducing, SI*" for MT-2 assays; for clarity, viruses only using CCR5 are shown as dashes; NA, tropism test result not available due to lack of amplification.

TABLE 4. POPULATION STRUCTURE ANALYSIS OF PLASMA AND PBMC V3 FORMS DETECTED BY 454 SEQUENCING[A]

	Intracompartment Variability (Π)			Slatkin-Madison Test	
Subject ID	Plasma T1	PBMC T1	PBMC T2	Plasma T1 vs PBMC T1	PBMC T1 vs PBMC T2
1	0.0156	0.0097	0.1469	2	2
2	NC	0.1190	0.1052	1	4
3	0.0351	0.0476	0.0457	18	7**
4	0.0645	0.0591	0.0276	13	13
5	0.0476	0.0606	0.0622	14	16
6	0.0271	0.0277	0.0307	4	4
7	0.0362	0.0293	0.0923	6	3*
8	0.0329	0.0286	0.0349	20	16
9	0.0130	0.0171	0.0779	3	1**
11	0.0116	0.0096	0.0274	4	3
12	0.1184	0.0170	0.0000	4*	2
14	0.0176	0.1509	0.0728	2**	6**
15	0.0156	0.0187	0.0163	4	4
16	0.1598	0.0169	0.0157	3	4
17	0.0167	0.0244	0.0230	3	8
18	0.0214	0.0208	0.0162	5	3
19	NC	0.0317	0.0605	1	2
20	0.0379	0.0286	0.0360	9	8
21	0.0264	0.0560	0.0472	4	10
22	0.0337	0.0342	0.0483	5	5
23	0.0425	0.0539	0.0424	12	2**
24	0.0130	0.0177	0.0163	3	4
25	0.1163	0.0225	0.0271	7	2**
26	0.0108	0.0306	0.1447	4	2
27	0.0129	0.0262	0.0262	2	6
28	0.0502	0.0552	0.0184	10	4
29	0.0222	0.0145	0.0182	4	4
30	0.0347	0.0321	0.0346	8	11

[a] The intracompartment variability (*Π*) of each sample is measured with the best evolutionary model found with *Findmodel* (www.hiv.lanl.gov); it corresponds to the average number of nucleotide differences per site between sequences. Migration events with *p-value,* and F_{ST} with *p-value* are indicated for Slatkin-Madison population structure tests. *NA* indicates comparisons where the tests were not applicable. *NC* indicates that variability cannot be calculated because there is only one haplotype. * *p*-value between 0.05 and 0.01; ** p-value < 0.01 and 10^{-6}. Statistically significant p-values are colored; the color intensity is proportional to the p-value. Note that a complete dataset was not available for subjects 10 and 13, which were, therefore, not included in this analysis.

FIGURE 1. PREVALENCE OF CXCR4-USING VIRUSES USING DIFFERENT TROPISM ASSAYS AND SETTINGS

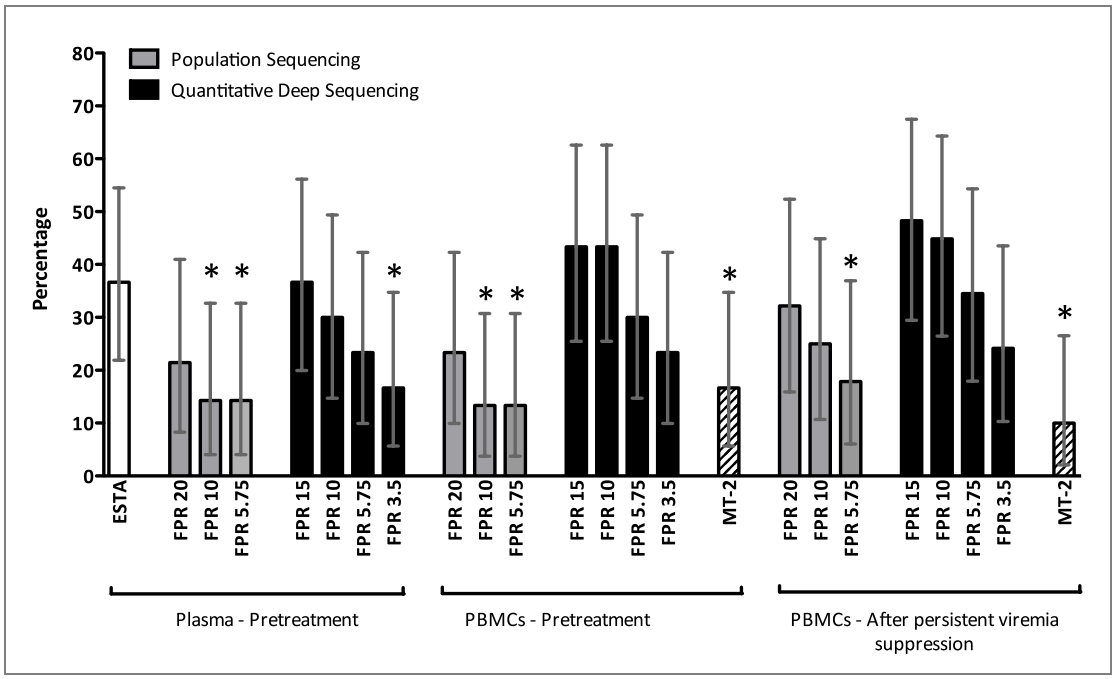

Bar plot showing the mean and 95% confidence intervals of the prevalence of subjects with CXCR4-using viruses using different tropism assays and settings. The Geno2Pheno$_{[coreceptor]}$ clinical model was only used in pre-treatment bulk sequences derived from plasma RNA; otherwise, the clonal model was used. ESTA, Enhanced-Sensitivity Trofile^{TM} Assay; FPR, Geno2Pheno$_{[coreceptor]}$ false positive rate used to assign tropism; MT-2, Direct cocultivation of patient-derived peripheral blood mononuclear cells with MT-2 cells. * p-value <0.05, two-sided exact binomial tst.

FIGURE 2. SELECTION OF A CXCR4-USING VARIANT ABOVE THE 454 SEQUENCING ERROR THRESHOLD DURING PERSISTENT VIRAEMIA SUPPRESSION IN SUBJECT 26

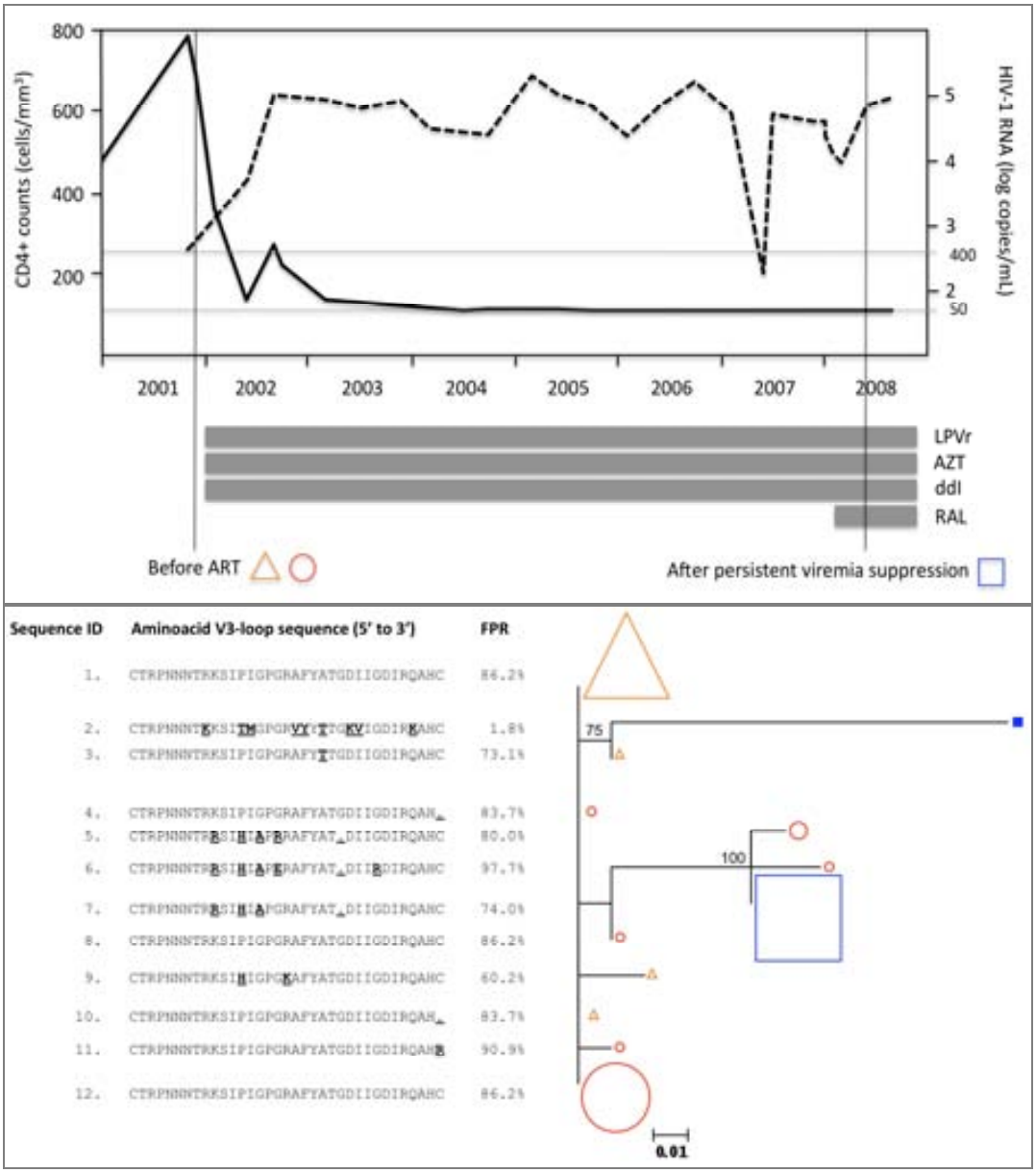

Panel A, antiretroviral treatment history, virological and immunological evolution. Continuous line, HIV-1 RNA levels; dashed line, CD4+ counts; horizontal bars, time period during which a given antiretroviral drug was prescribed. Vertical lines indicate the timepoints when 454 sequencing was performed. LPVr, lopinavir/ritonavir; AZT, zidovudine; ddI, didanosine; RAL, raltegravir. Panel B, maximum likelihood nucleotide-based phylogenetic tree including V3-loop haplotypes present at a frequency ≥0.6% in the virus population in plasma (triangles), PBMCs before therapy initiation (circles) and PBMCs after persistent viraemia suppression (squares). The tree is rooted at the most frequent plasma sequence before antiretroviral treatment initiation. Filled symbols show predicted CXCR4-using viruses; open symbols show predicted CCR5-using viruses. Symbol size increases proportionally to the V3-loop haplotype frequency in the virus population in 10% intervals. Node reliability was tested using 1,000 bootstraps; bootstrap values ≥ 50% are shown. The V3-loop aminoacid sequence translation is shown next to each taxon. Aminoacid changes relative to the predominant sequence in plasma are highlighted in bold and underlined. Gaps correspond to aminoacid indeterminations. A Geno2Pheno$_{[coreceptor]}$ false positive rate (FPR) equal or lower than 10% was used to define CXCR4 use. The actual false positive rate of each sequence is shown. *Sequence #2 was identical to one detected in 0.04% of PBMC-associated viruses, below the error threshold, before treatment initiation.

FIGURE 3. PANELS A-D. V3-LOOP HAPLOTYPES DETECTED BY QUANTITATIVE DEEP SEQUENCING ARE ALSO FOUND IN CXCR4-USING VIRUSES GROWING IN MT-2 ASSAYS

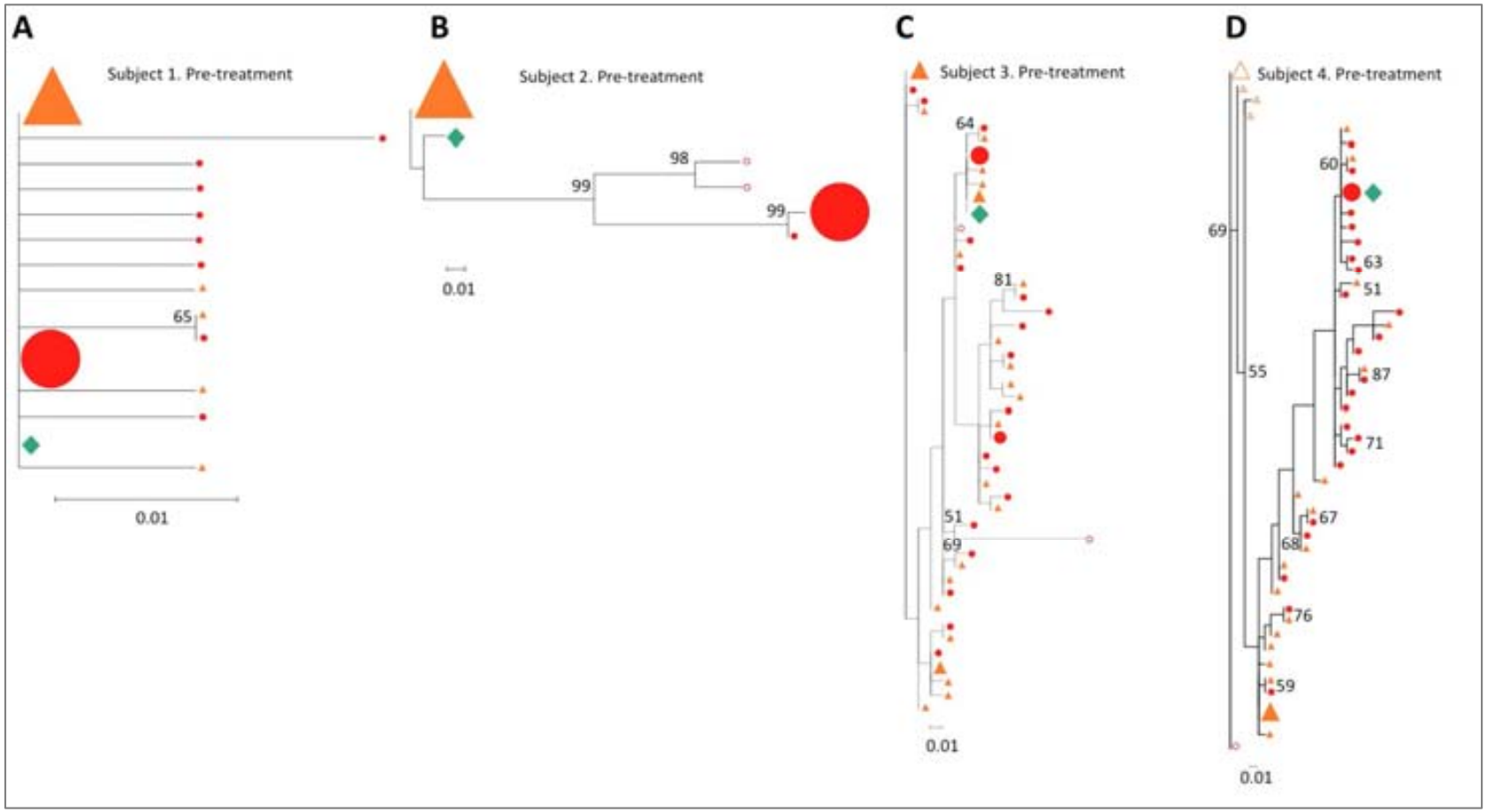

Maximum likelihood phylogenetic trees showing that the V3-loop sequence of syncytium-inducing viruses grown in MT-2 assays (diamond) is identical to one of the predominant V3-loop haplotypes detected with quantitative deep sequencing in proviral DNA and/or plasma RNA before antiretroviral therapy initiation (Trees A to D). Trees include V3-loop haplotypes present at a frequency ≥ 0.6% in the virus population in plasma (triangles), PBMCs before therapy initiation (circles) and PBMCs after persistent viraemia suppression (squares); trees are rooted at the predominant plasma (trees A to E) or PBMC (trees G to H) V3-loop haplotype. Filled symbols represent CXCR4-using viruses; open symbols show R5 viruses. Symbol size increases proportionally to the V3-loop haplotype frequency in the virus population in 10% intervals. Node reliability was tested using 1,000 bootstraps; bootstrap values ≥ 50% are shown. CXCR4 use was defined by a $Geno2Pheno_{[coreceptor]}$ false positive rate ≤10%.

FIGURE 3. PANELS E-H. V3-LOOP HAPLOTYPES DETECTED BY QUANTITATIVE DEEP SEQUENCING ARE ALSO FOUND IN CXCR4-USING VIRUSES GROWING IN MT-2 ASSAYS

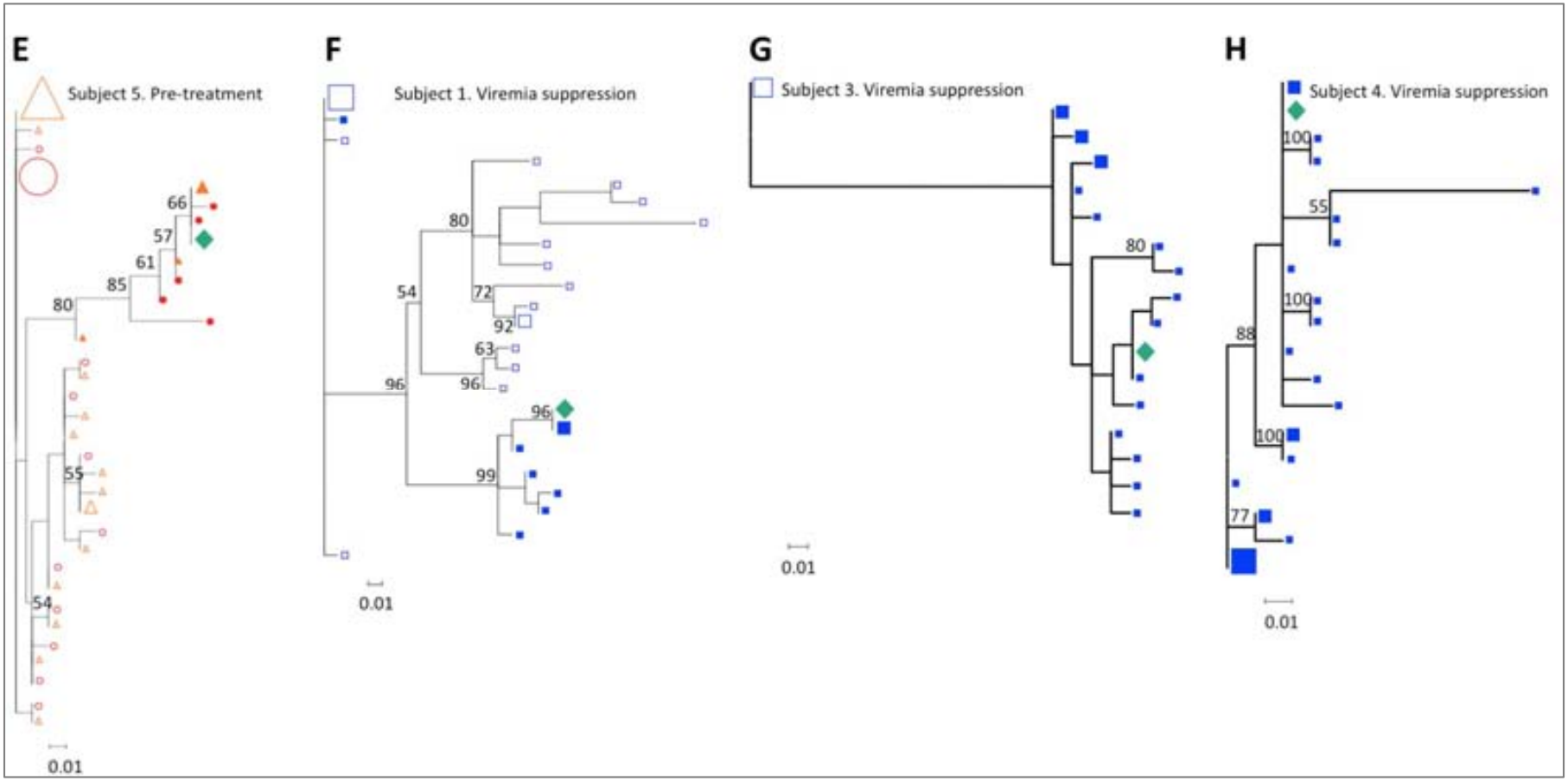

Maximum likelihood phylogenetic trees showing that the V3-loop sequence of syncytium-inducing viruses grown in MT-2 assays (diamond) is identical to one of the predominant V3-loop haplotypes detected with quantitative deep sequencing in proviral DNA and/or plasma RNA before antiretroviral therapy initiation (Tree E) or after at least 2 years of persistent viraemia suppression (trees F to H). Trees include V3-loop haplotypes present at a frequency ≥ 0.6% in the virus population in plasma (triangles), PBMCs before therapy initiation (circles) and PBMCs after persistent viraemia suppression (squares); trees are rooted at the predominant plasma (trees A to E) or PBMC (trees G to H) V3-loop haplotype. Filled symbols represent CXCR4-using viruses; open symbols show R5 viruses. Symbol size increases proportionally to the V3-loop haplotype frequency in the virus population in 10% intervals. Node reliability was tested using 1,000 bootstraps; bootstrap values ≥ 50% are shown. CXCR4 use was defined by a Geno2Pheno $_{[coreceptor]}$ false positive rate ≤10%.

SUPPLEMENTARY FILE S1. PHYLOGENETIC RELATEDNESS OF V3 FORMS BEFORE TREATMENT INITIATION AND AFTER 2 YEARS IN EACH SUBJECT

Maximum-likelihood phylogenetic trees including V3-loop haplotypes present at a frequency ≥0.6% in the virus population in plasma (triangles), PBMCs before therapy initiation (circles) and PBMCs after persistent viraemia suppression (squares). One tree is shown per each subject. Trees are rooted at the most frequent plasma sequence before antiretroviral treatment initiation. Filled symbols show predicted CXCR4-using viruses; open symbols show predicted CCR5-using viruses. Symbol size increases proportionally to the V3-loop haplotype frequency in the virus population in 10% intervals. Node reliability was tested using 1000 bootstraps; bootstrap values ≥ 50% are shown. A Geno2Pheno$_{[coreceptor]}$ false positive rate (FPR) equal or lower than 10% was used to define CXCR4 use.

[illegible]

[illegible]

[illegible]

[

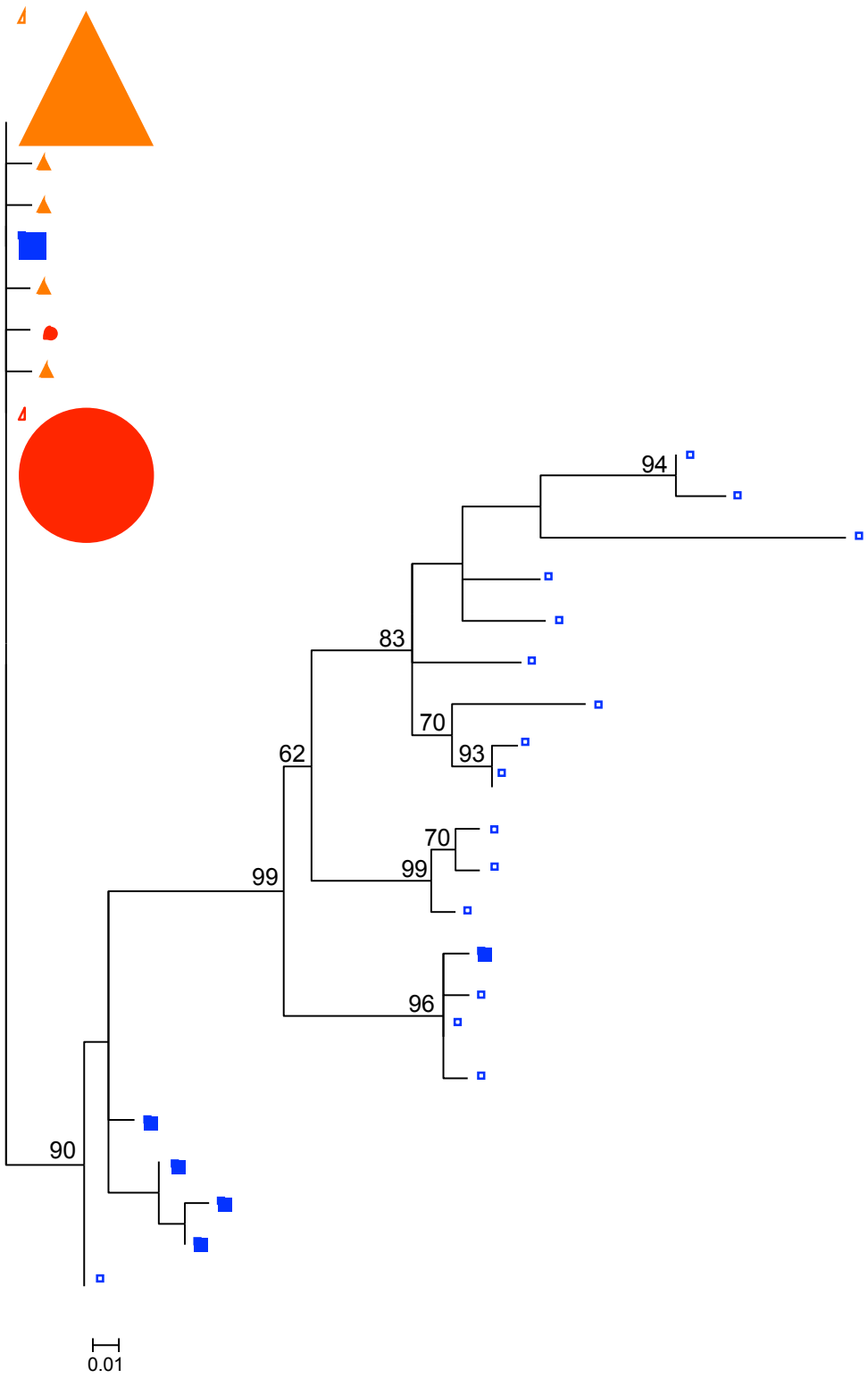

Subject 1

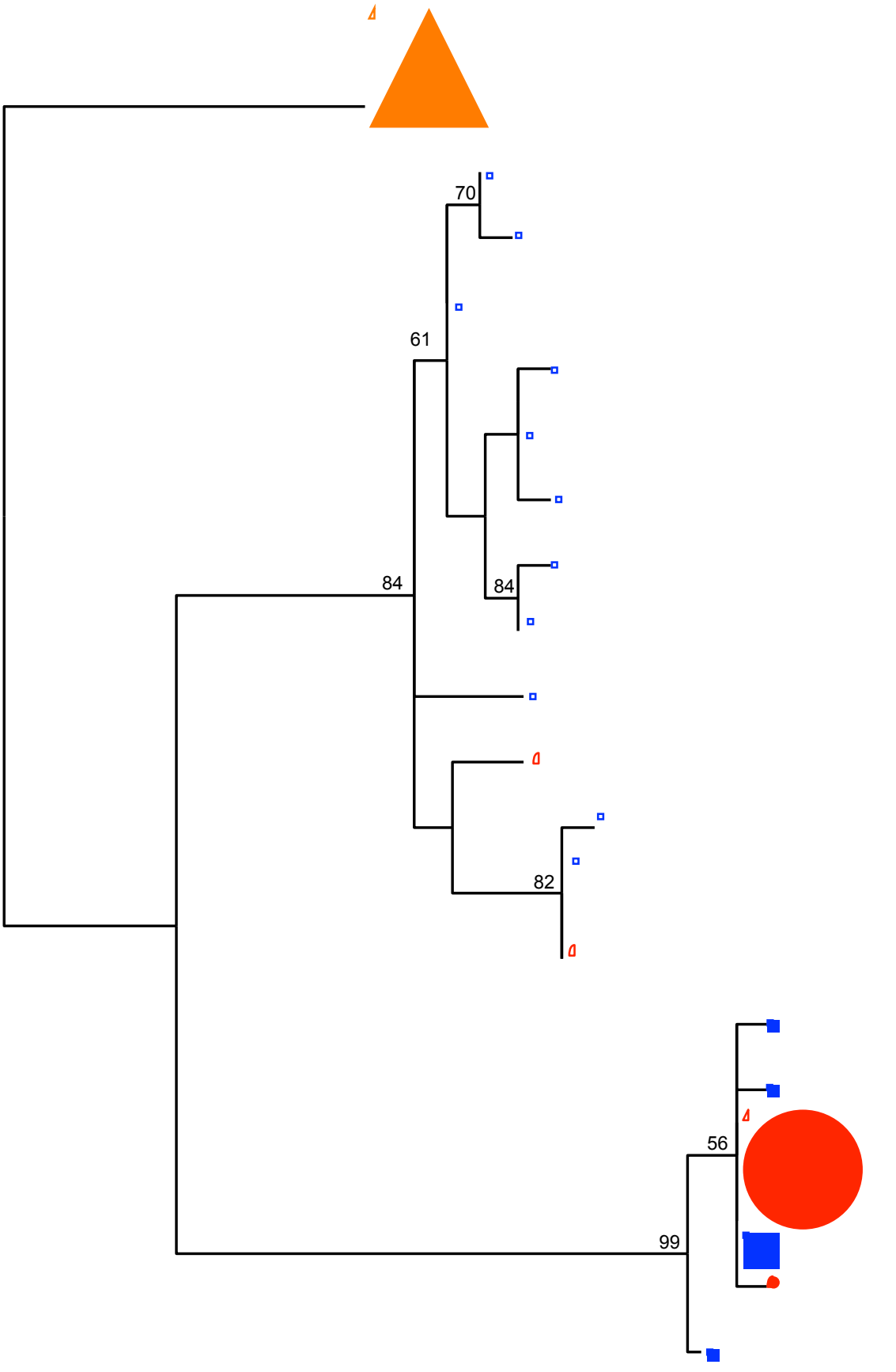
70
61
84
84
82
56
99
0.01
Subject 2

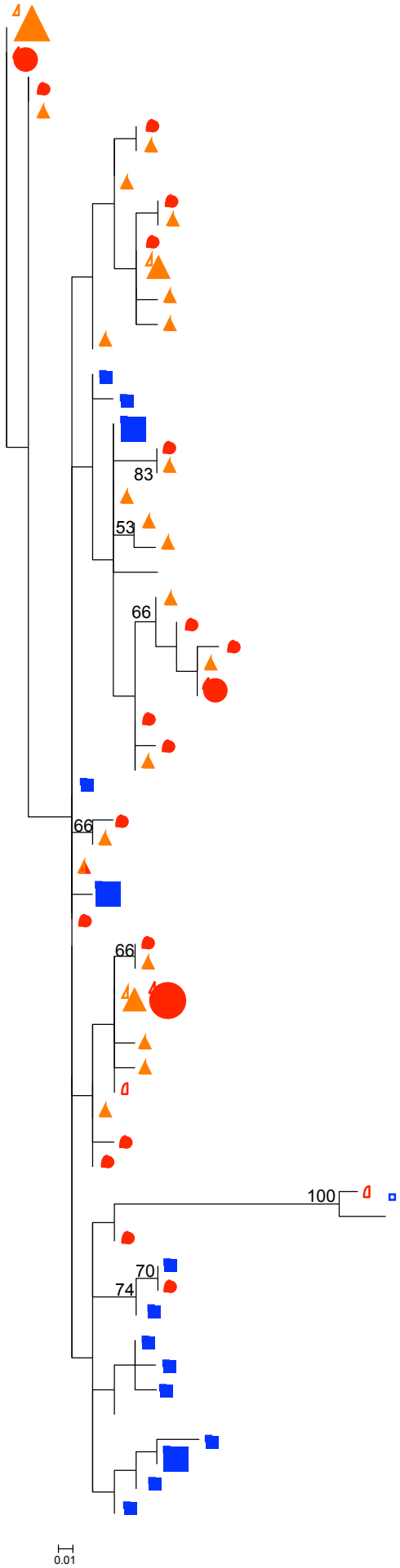

Subject 3

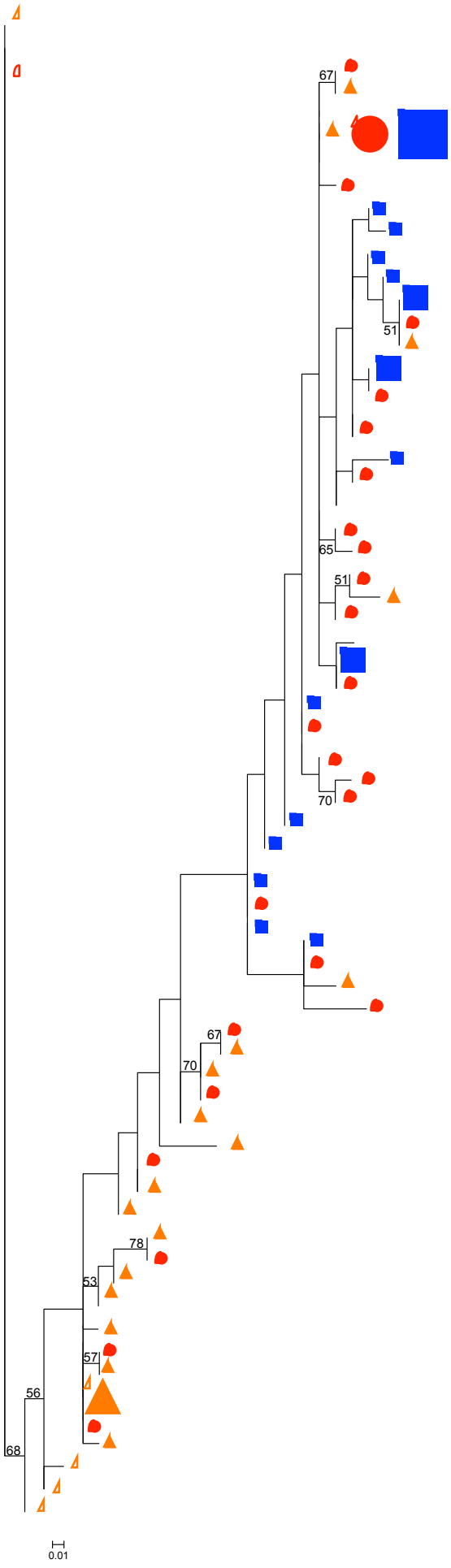

Subject 4

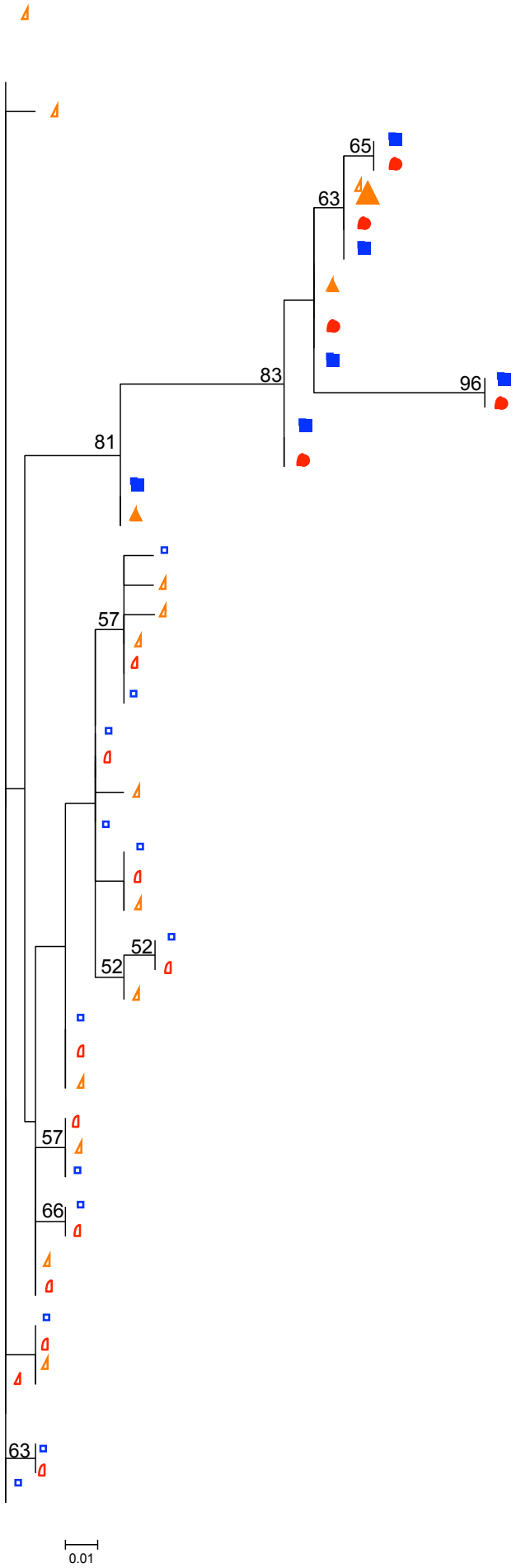

Subject 5

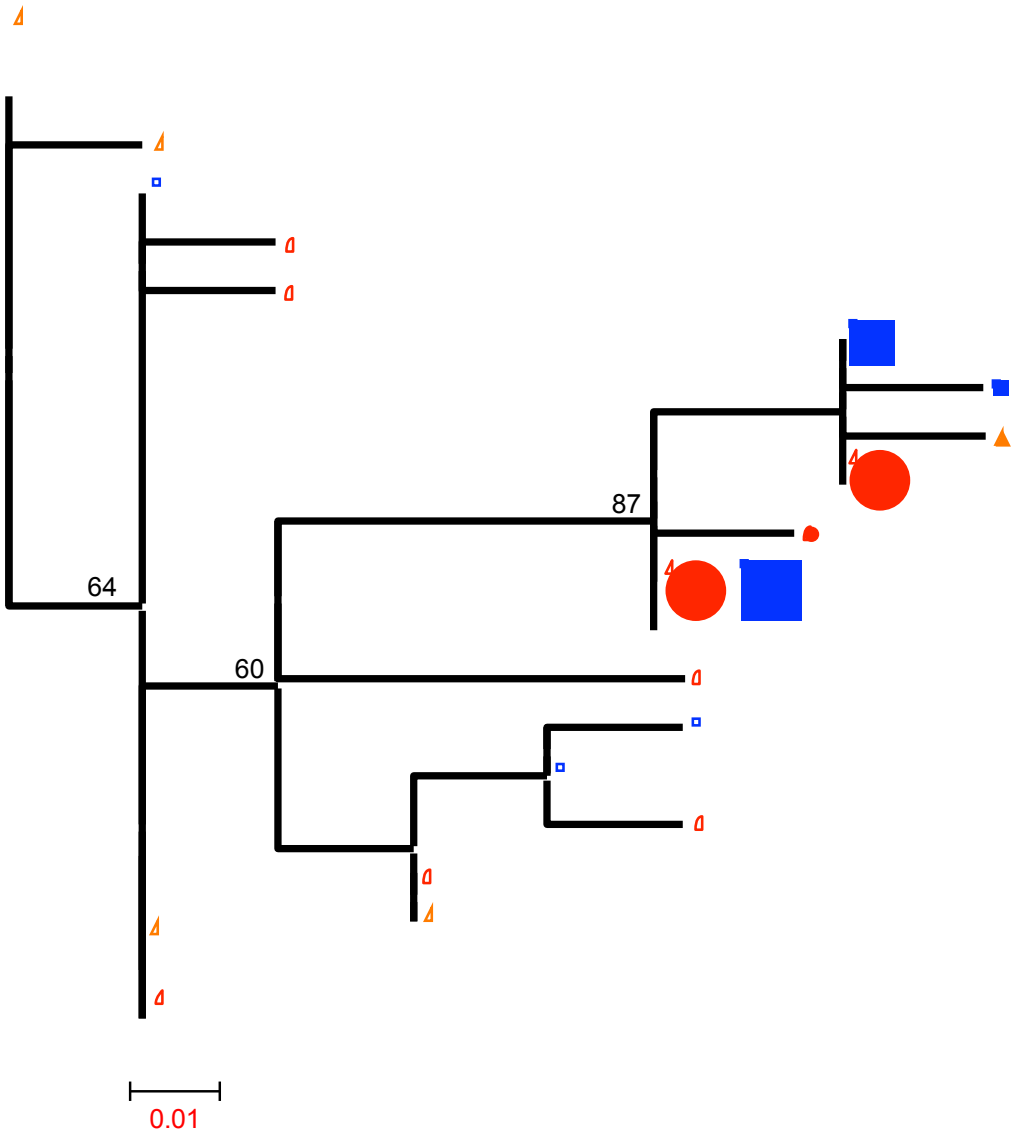

Subject 6

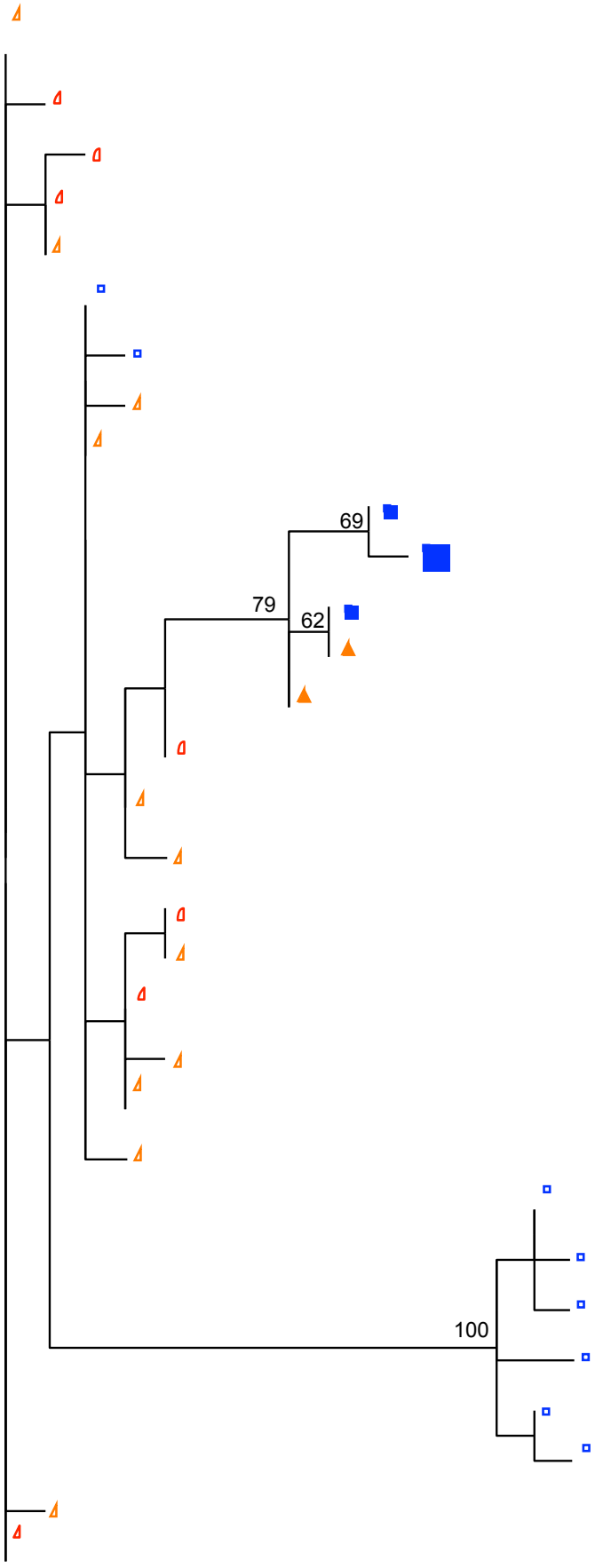

Subject 7

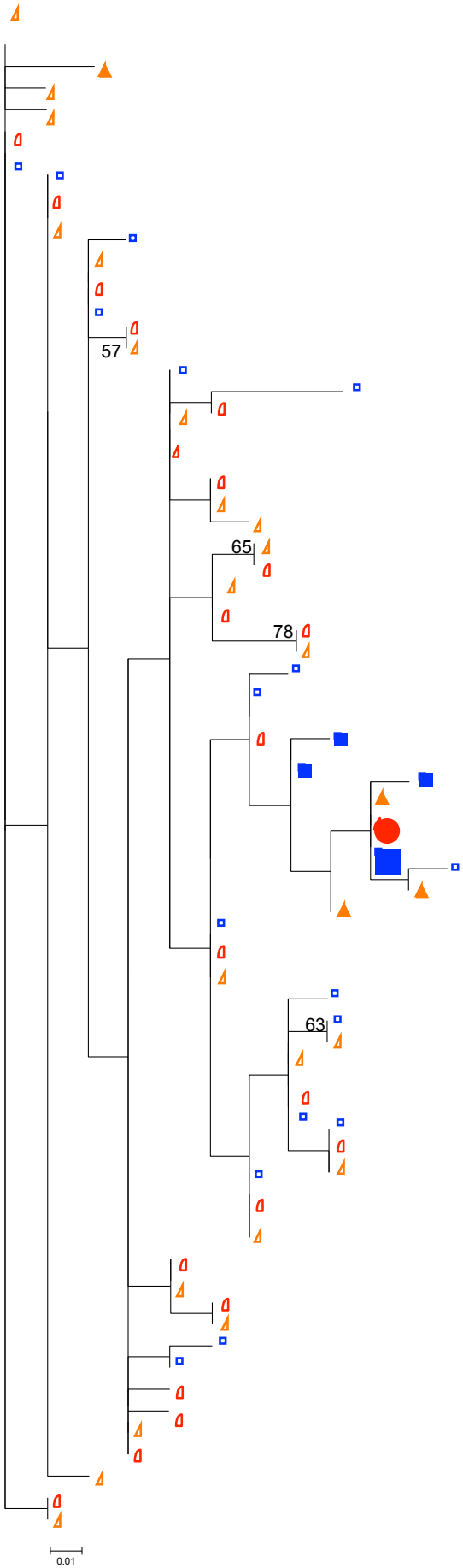

Subject 8

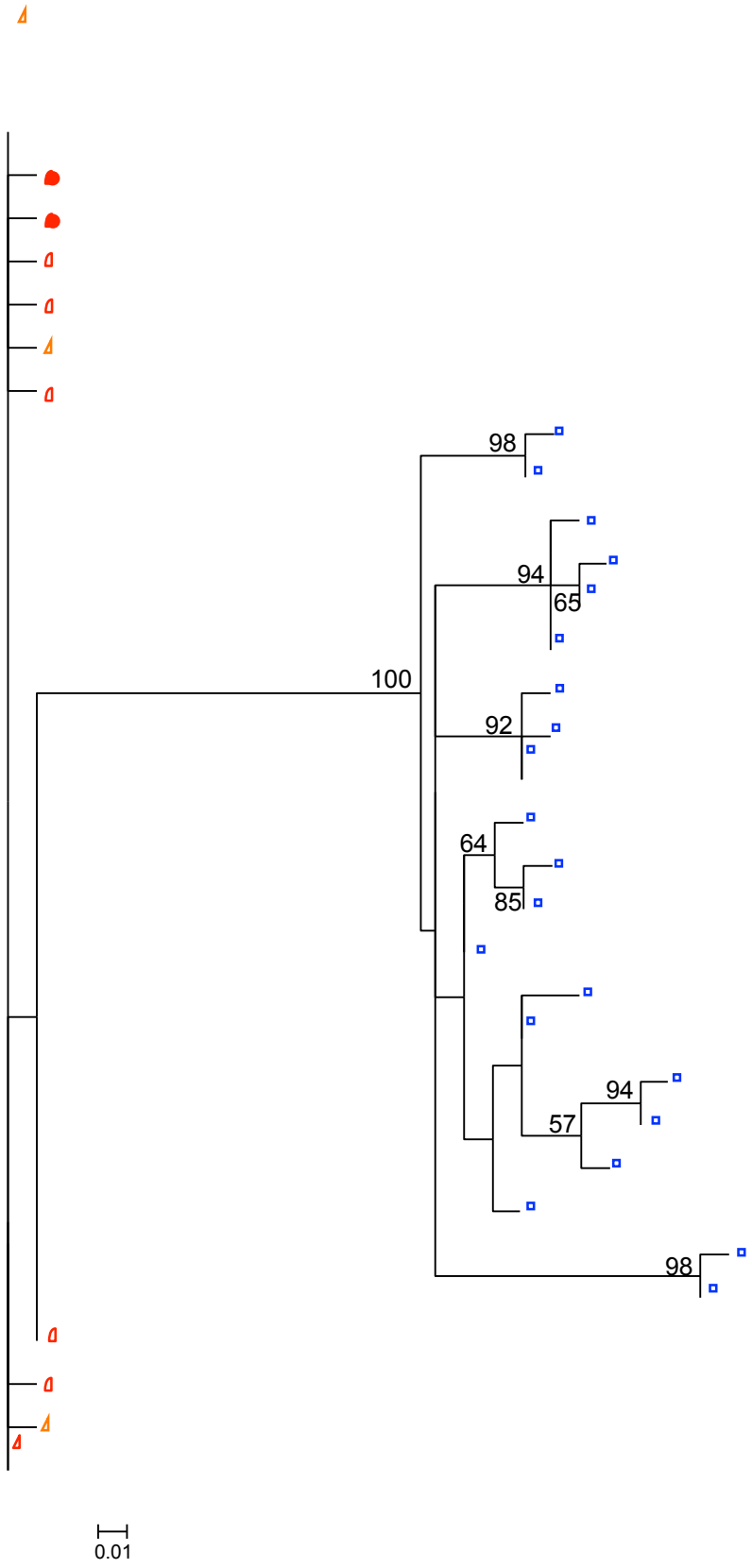

Subject 9

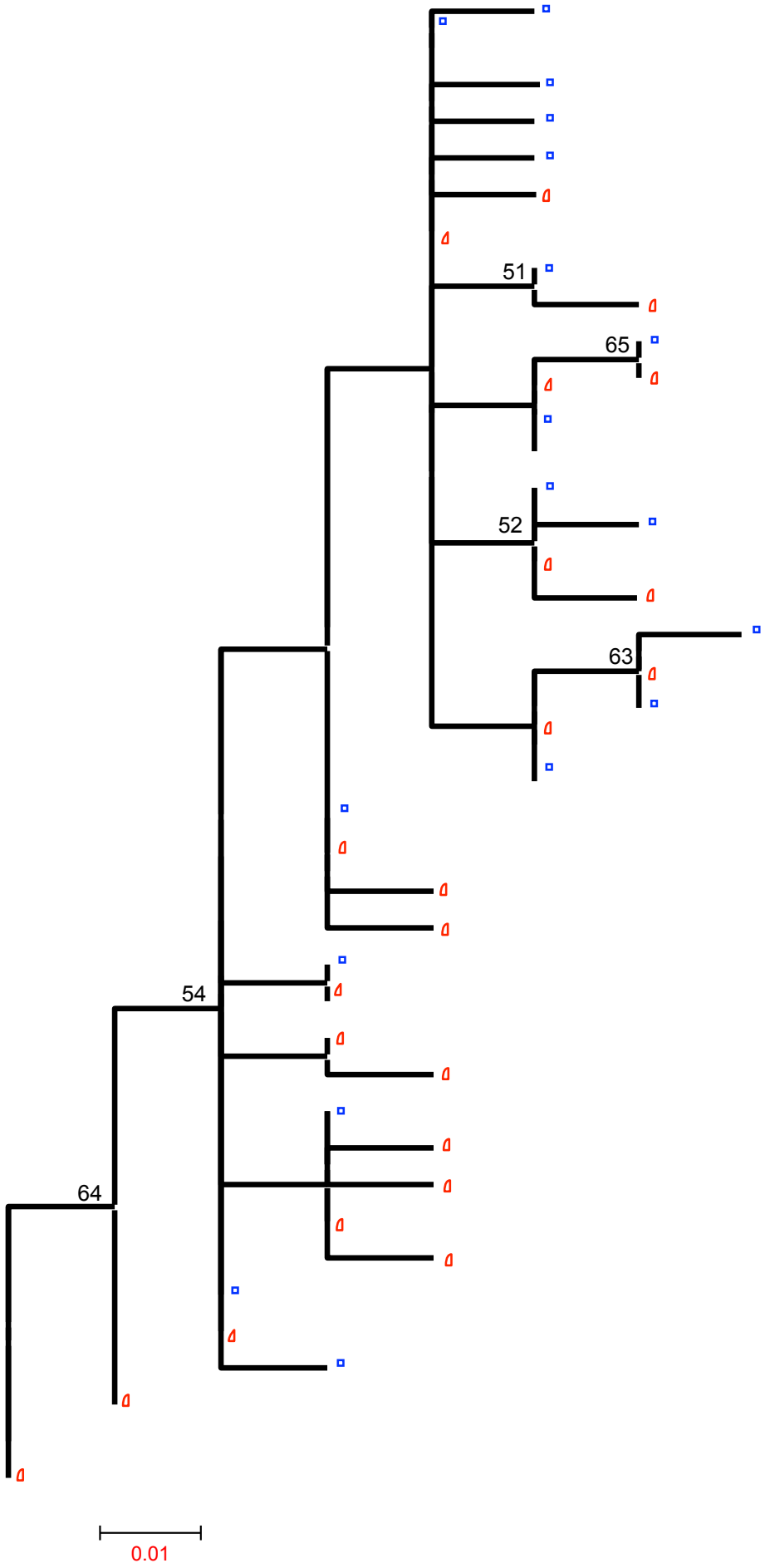

Subject 10

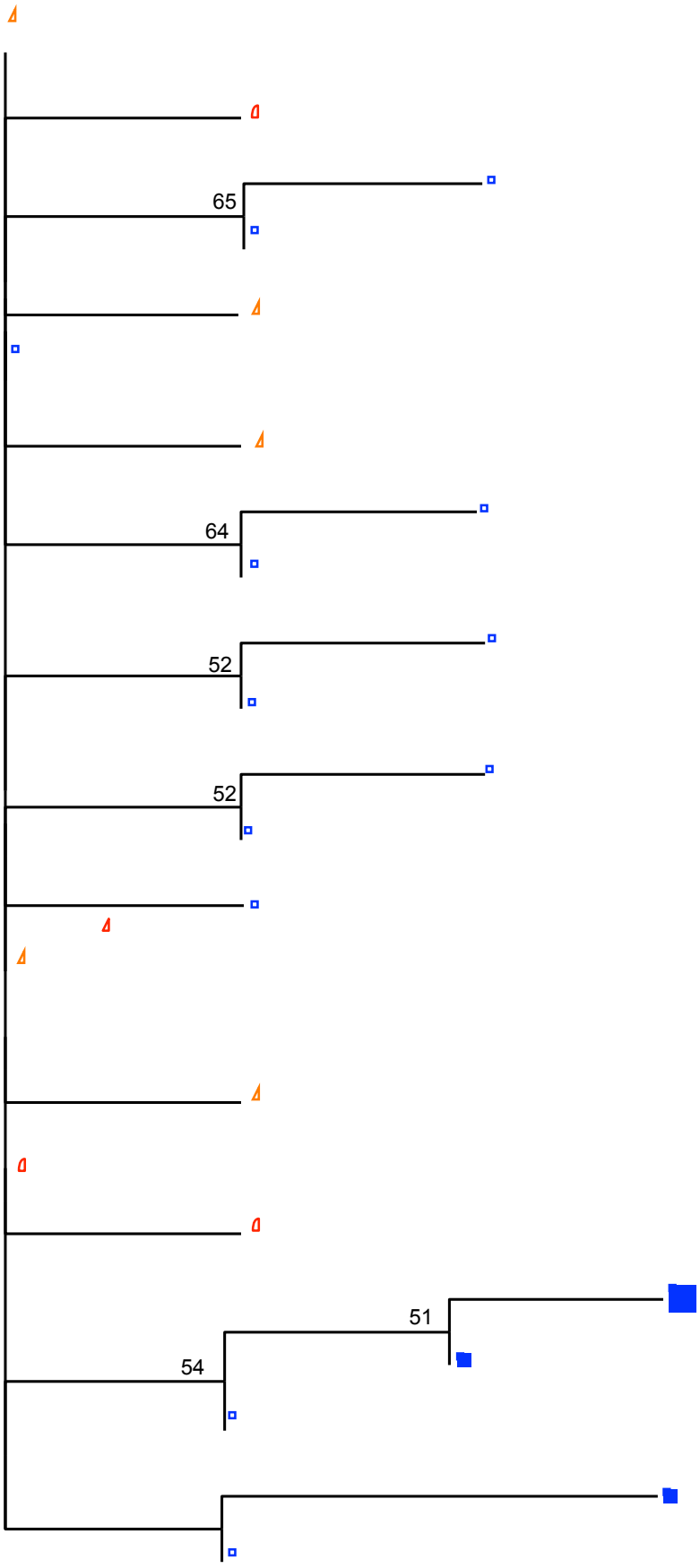

Subject 11

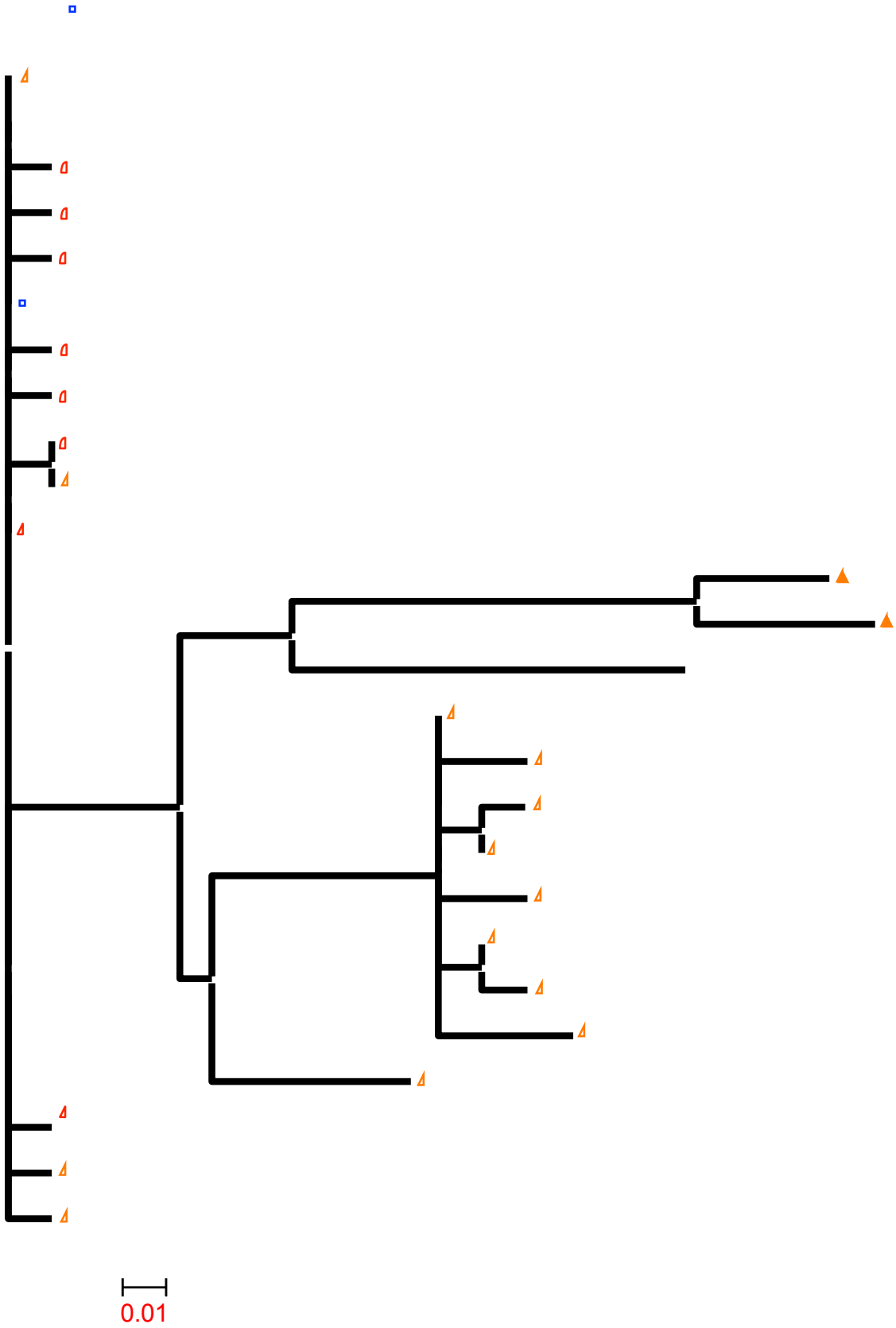

Subject 12

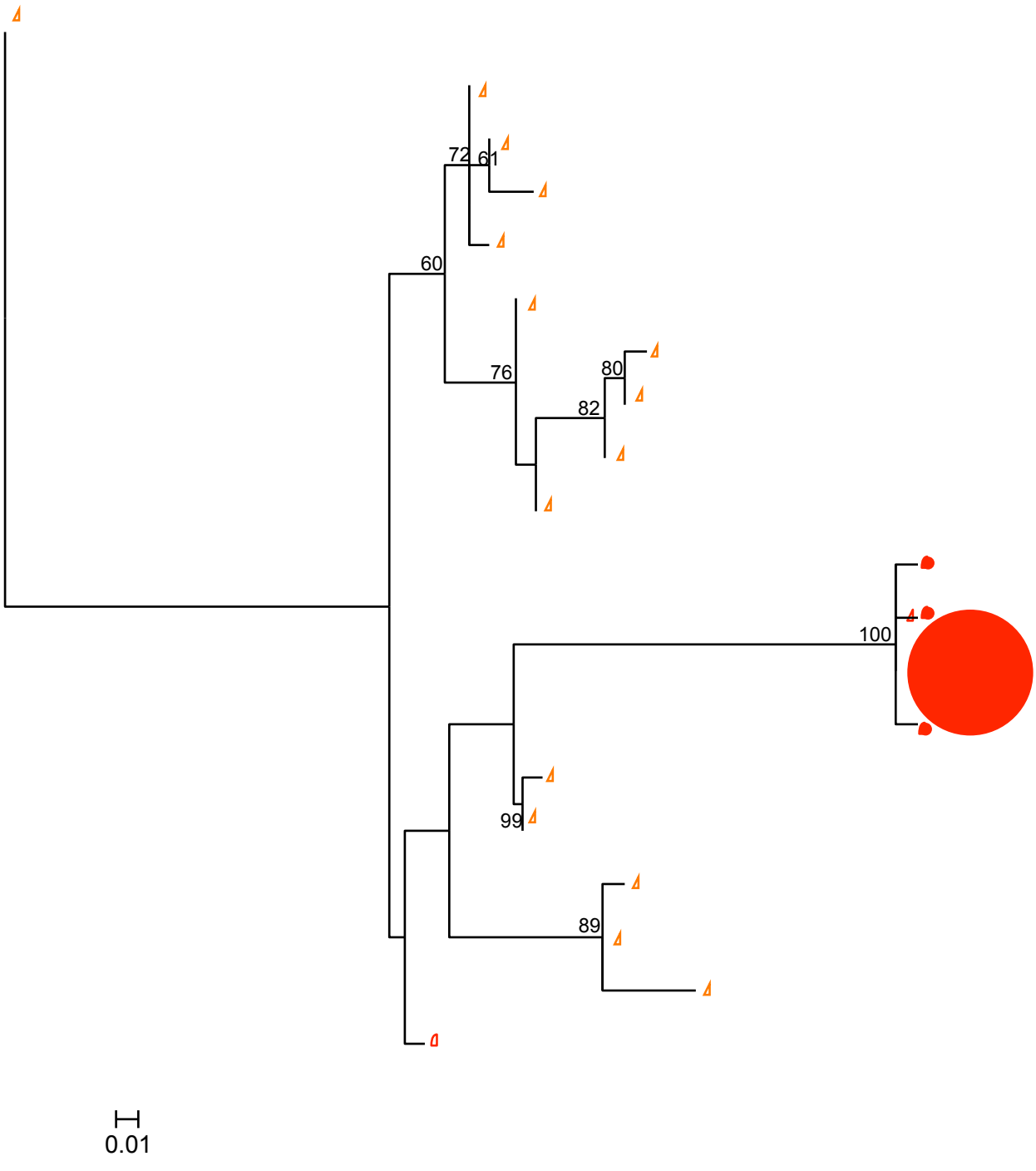

Subject 13

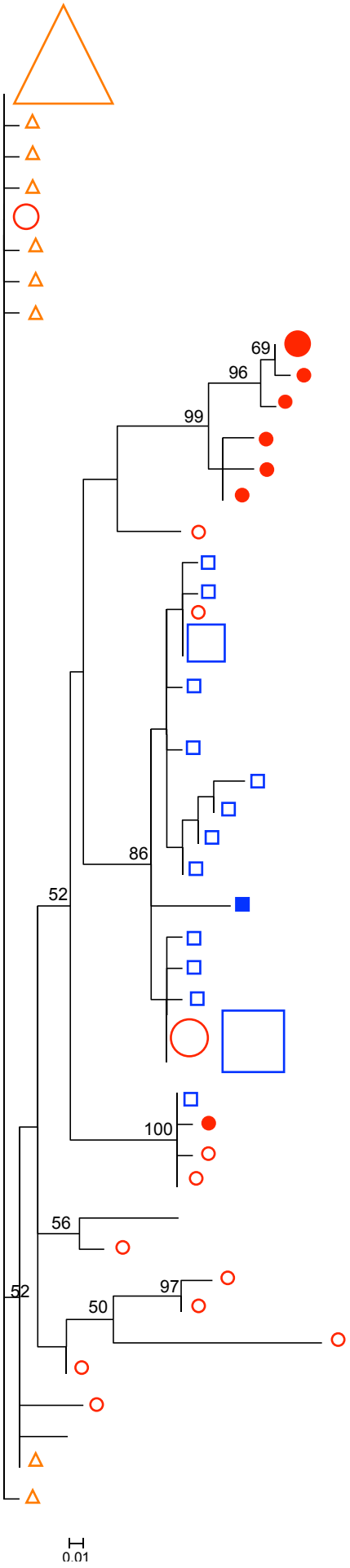

Subject 14

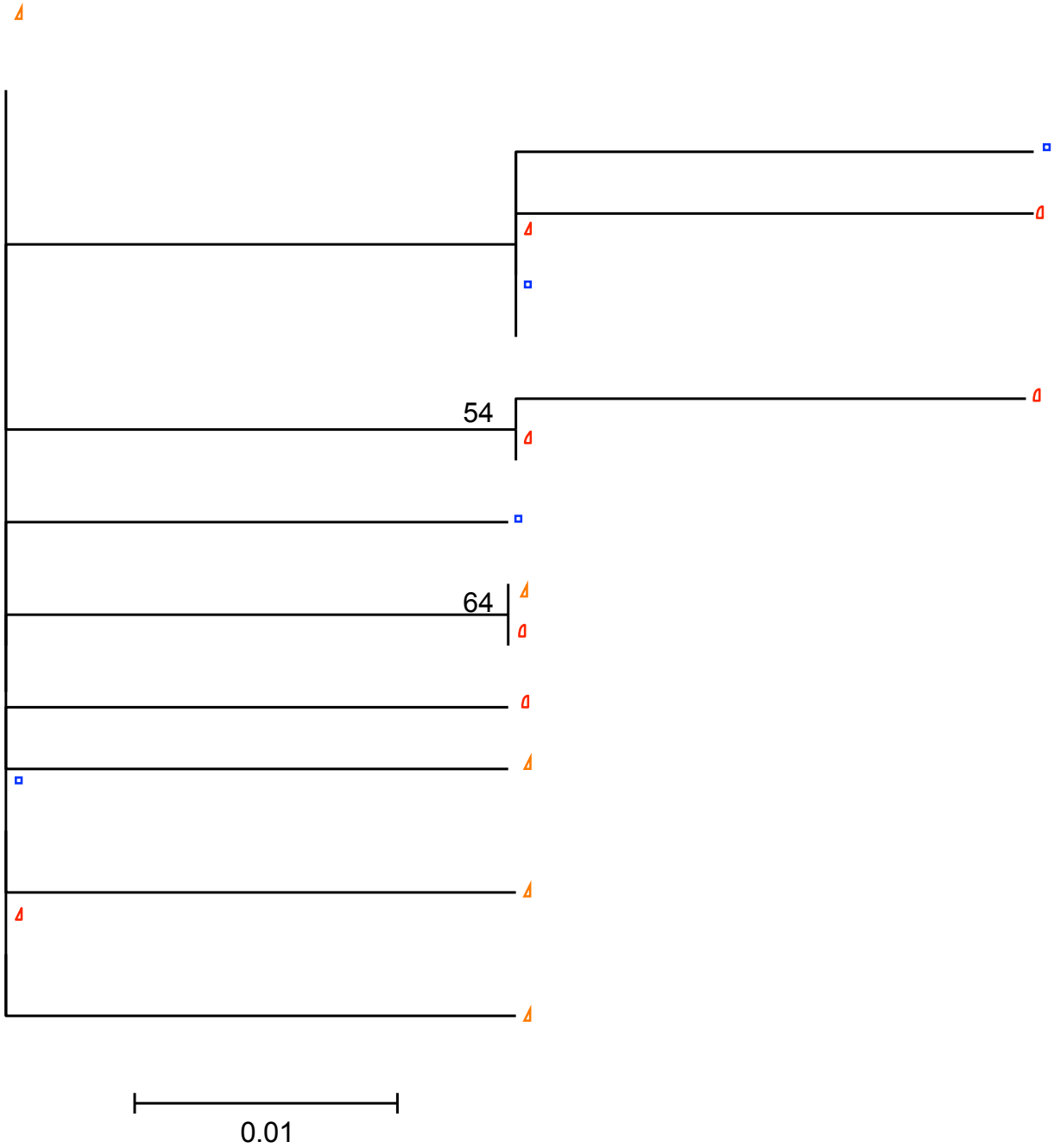

Subject 15

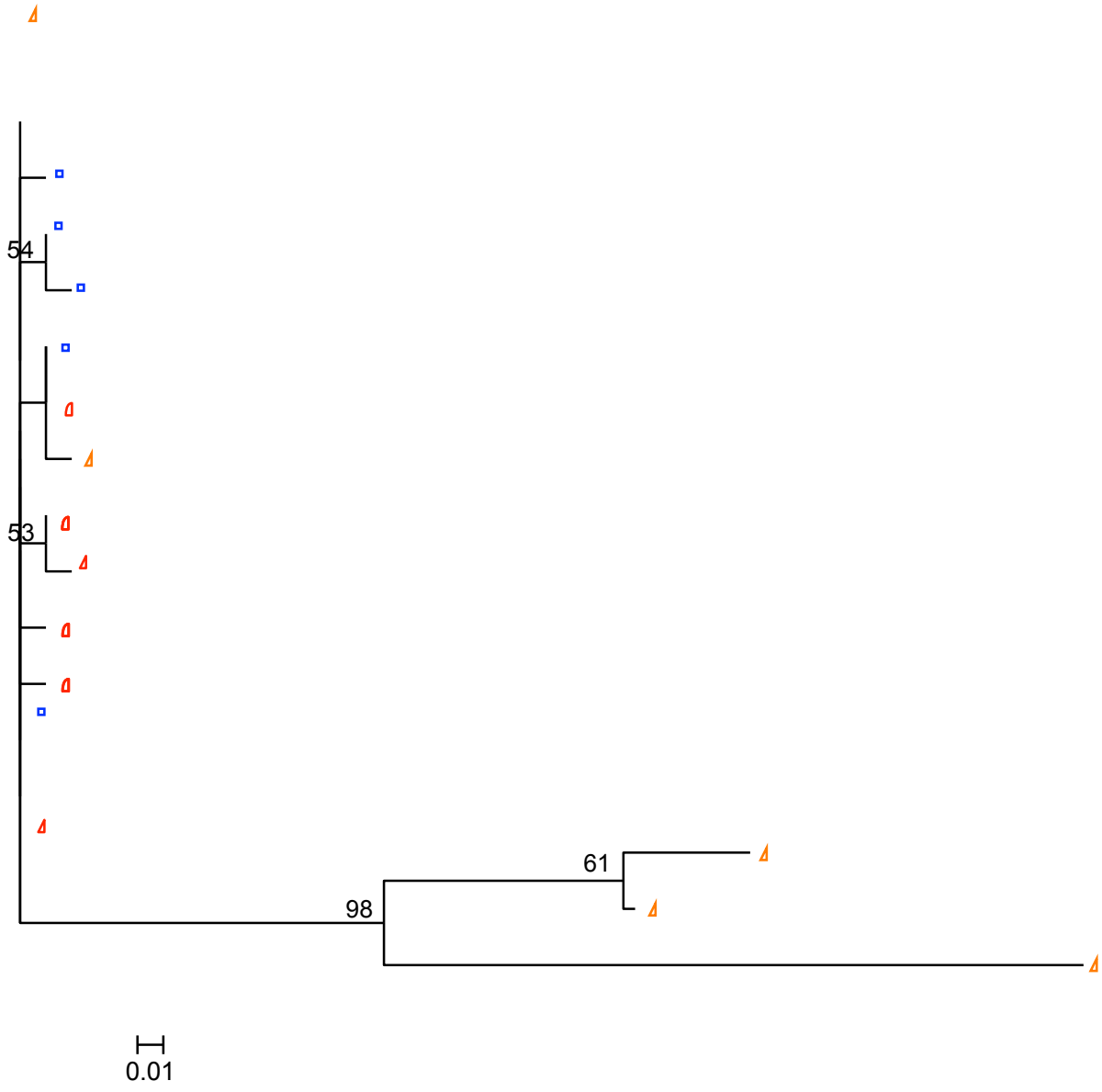

Subject 16

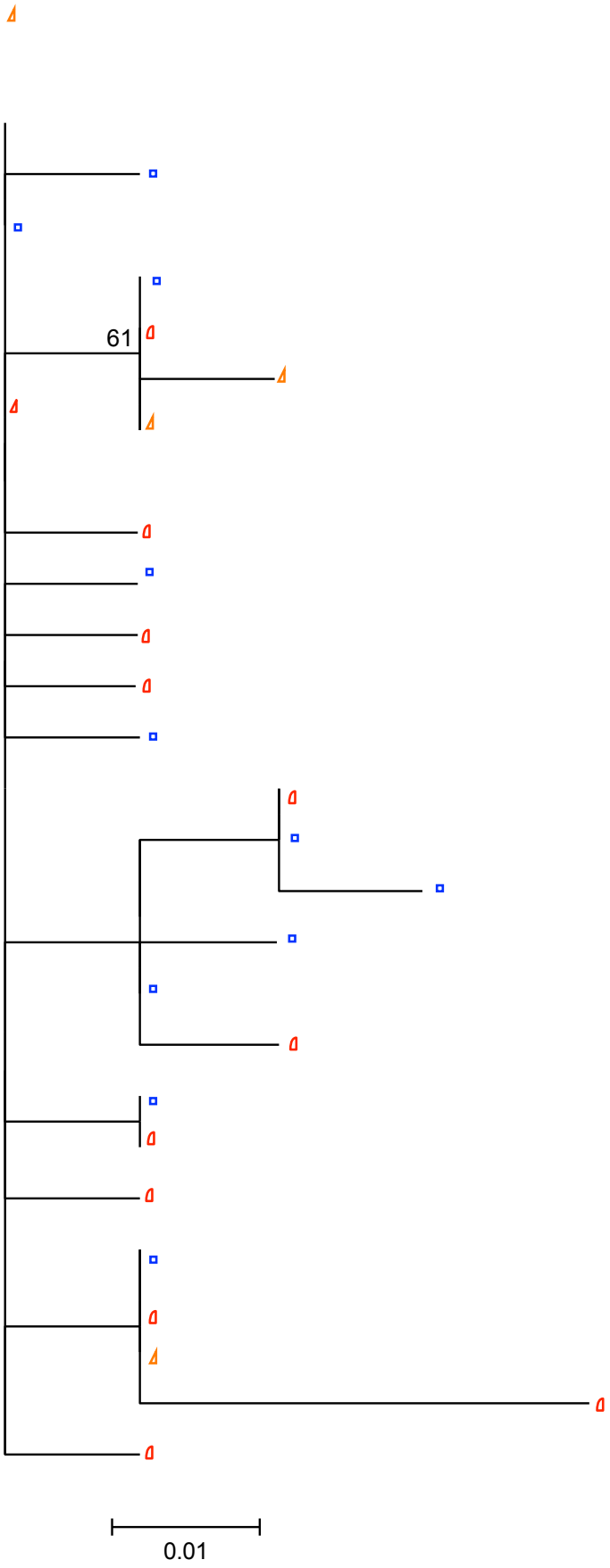

Subject 17

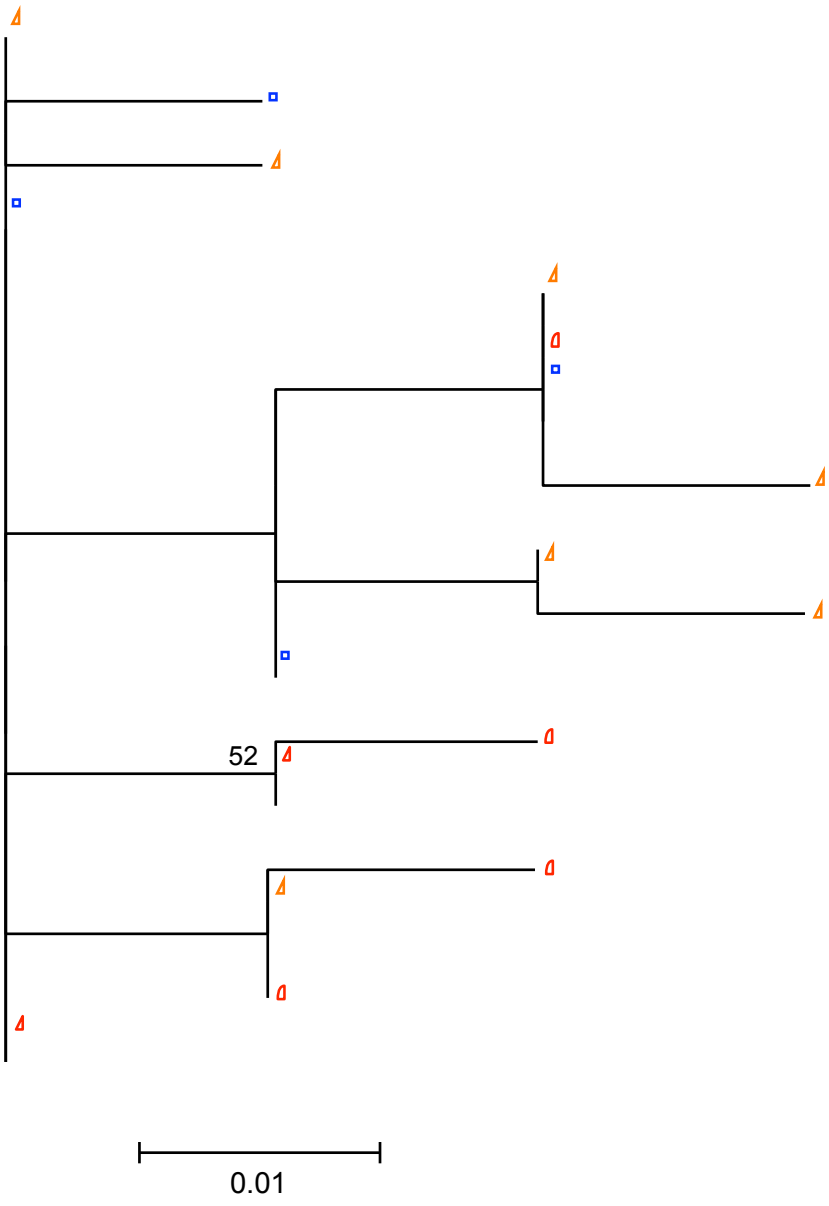

Subject 18

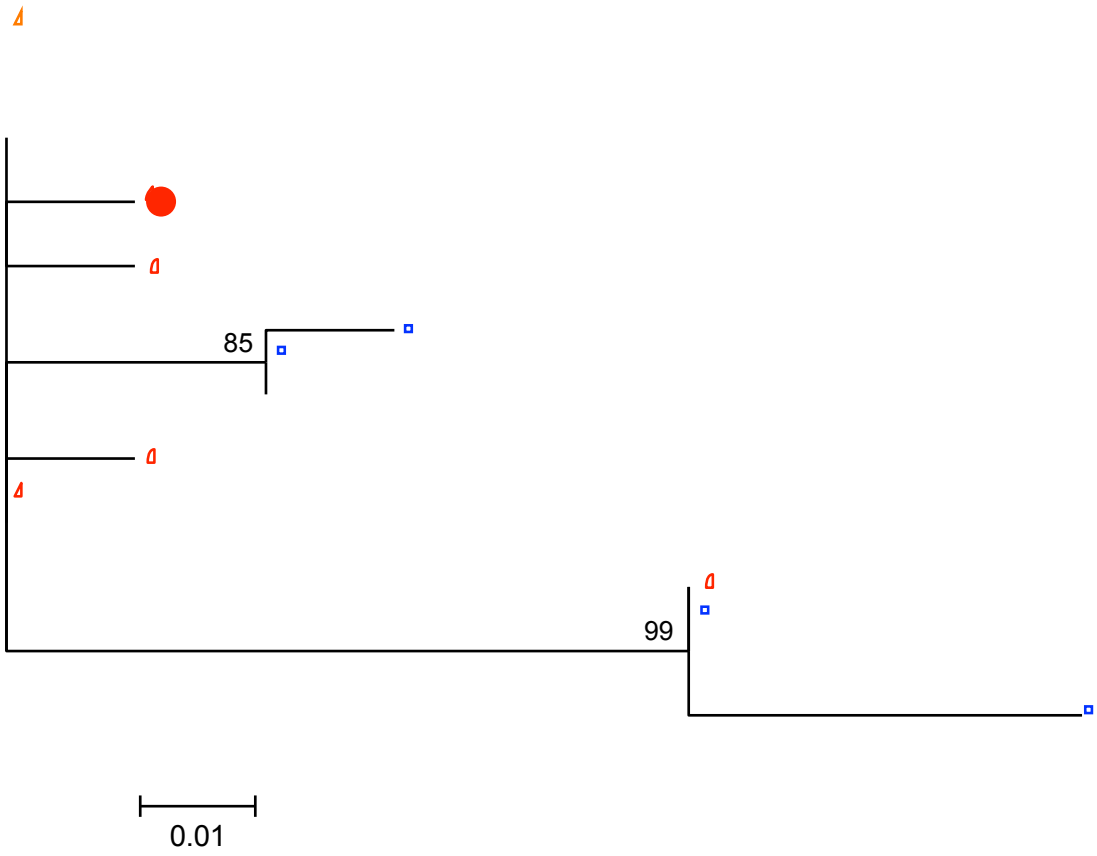

Subject 19

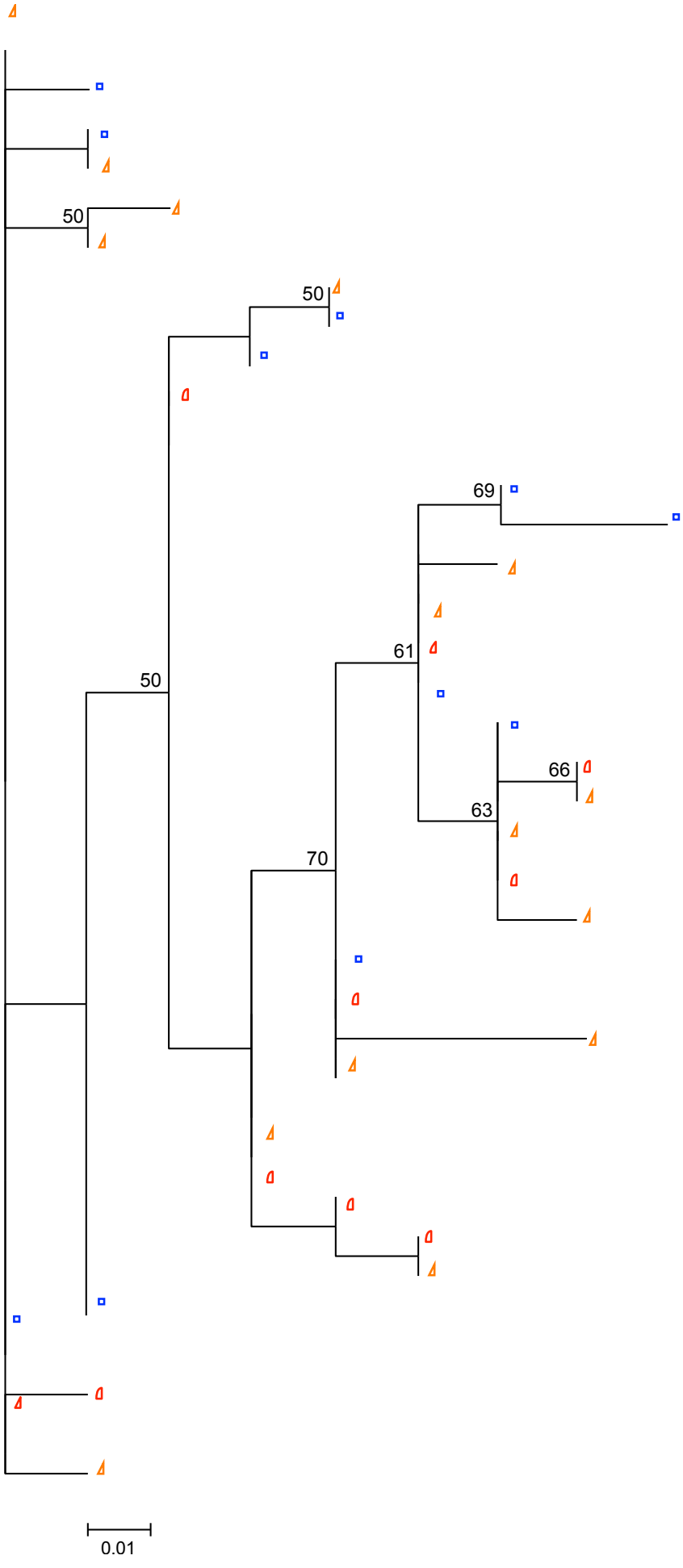

Subject 20

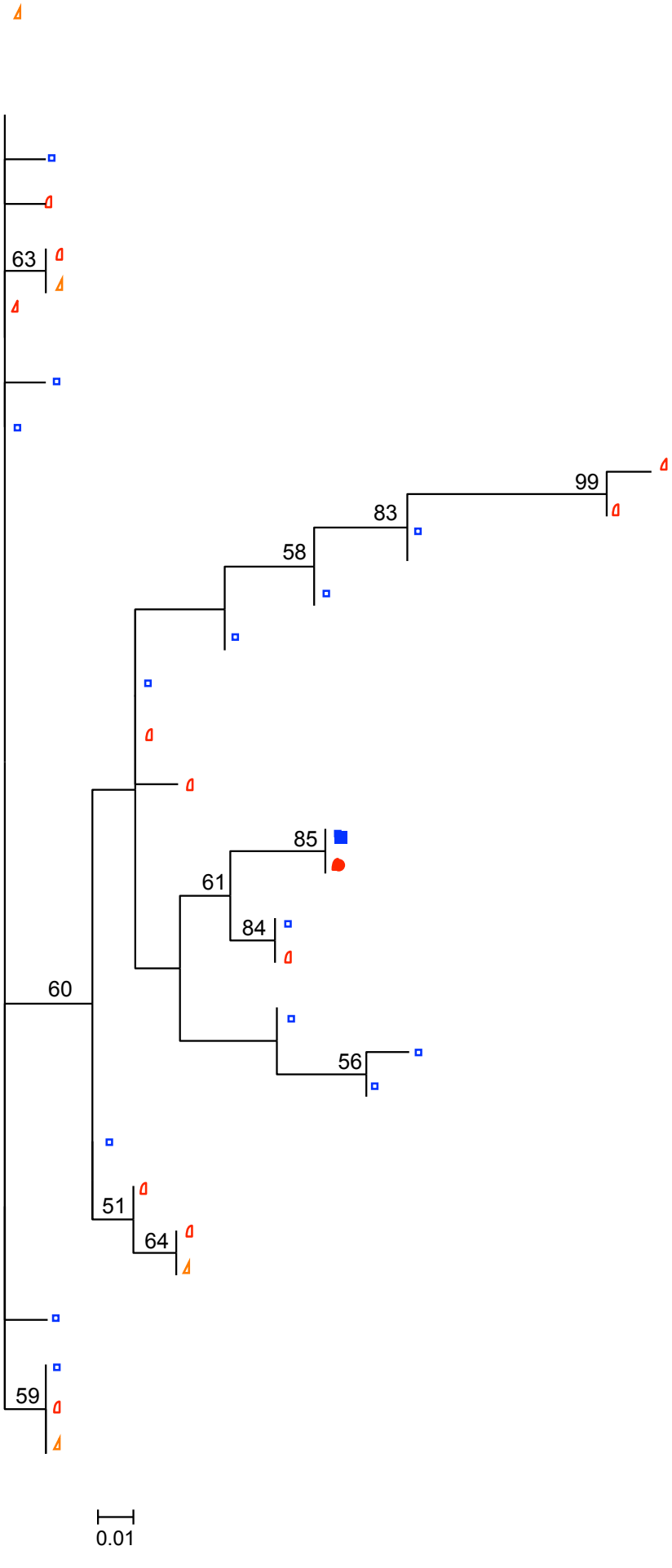

Subject 21

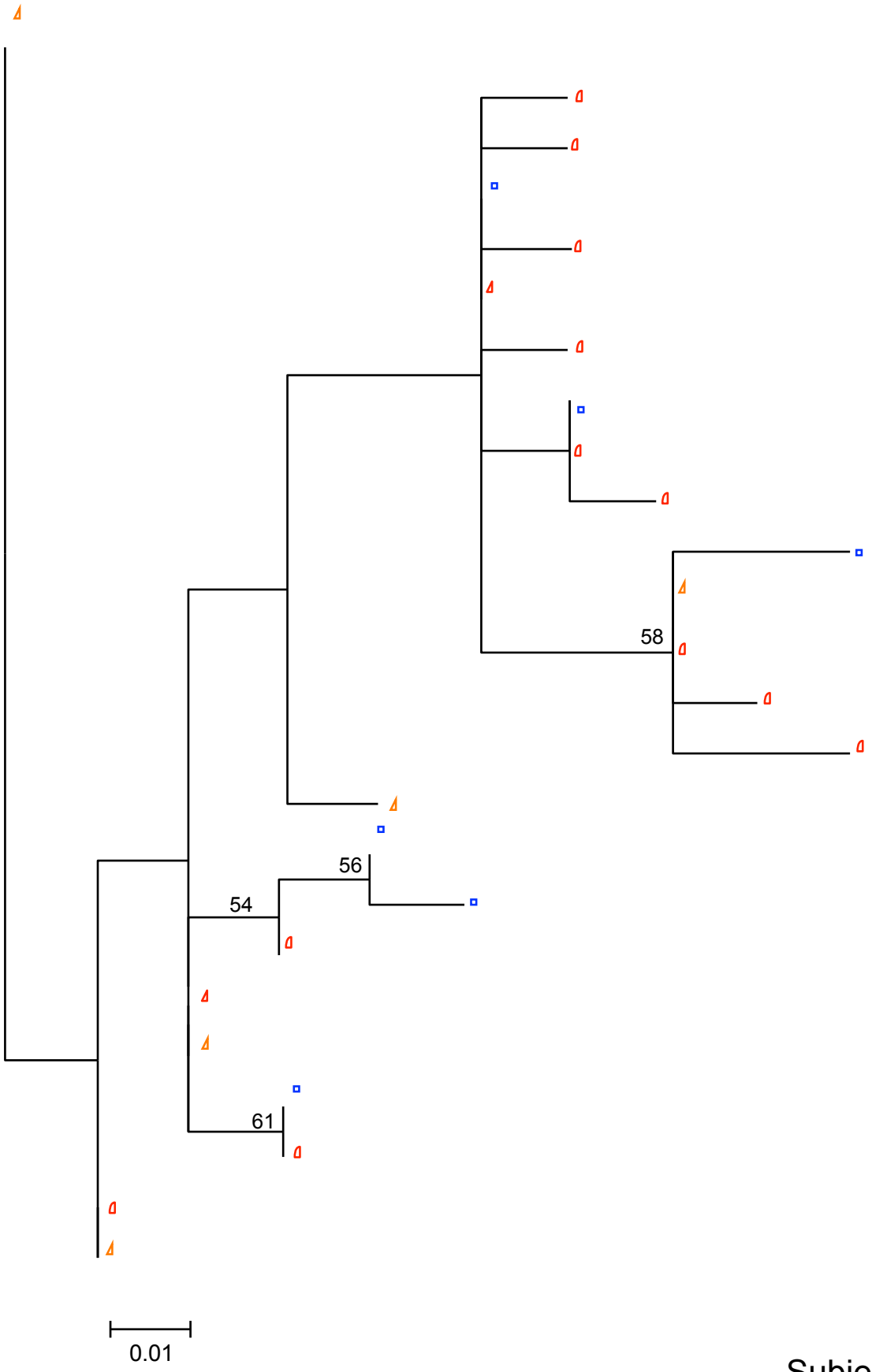

Subject 22

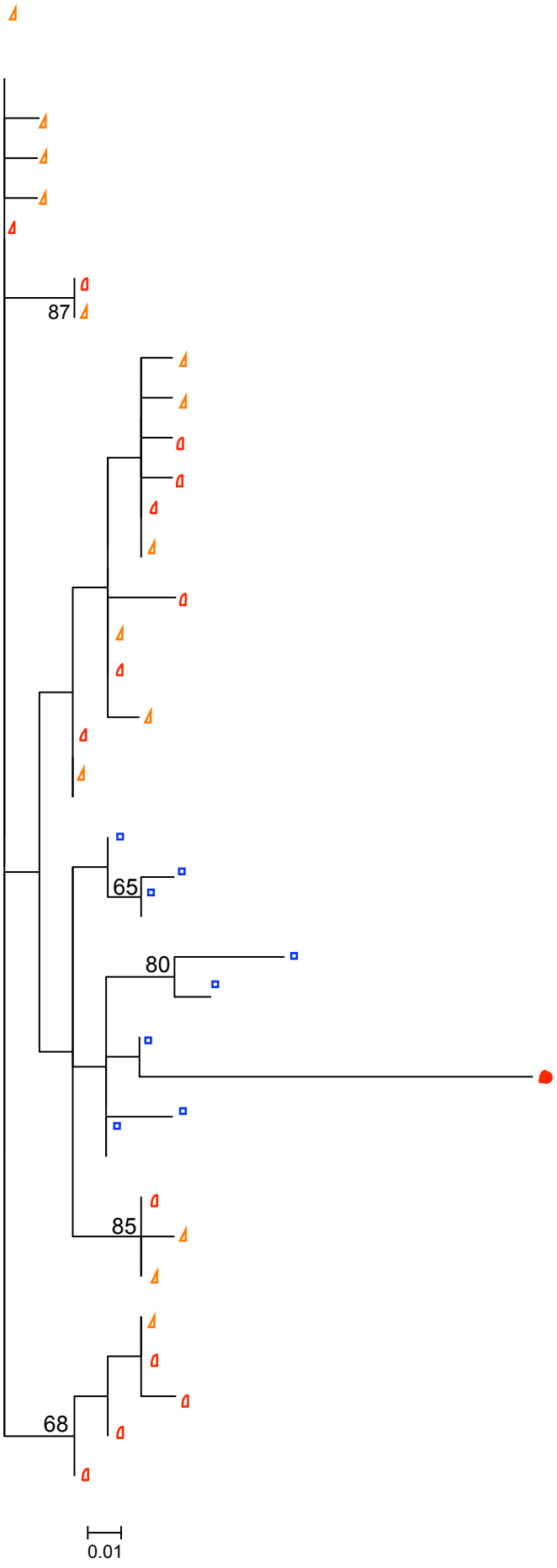

Subject 23

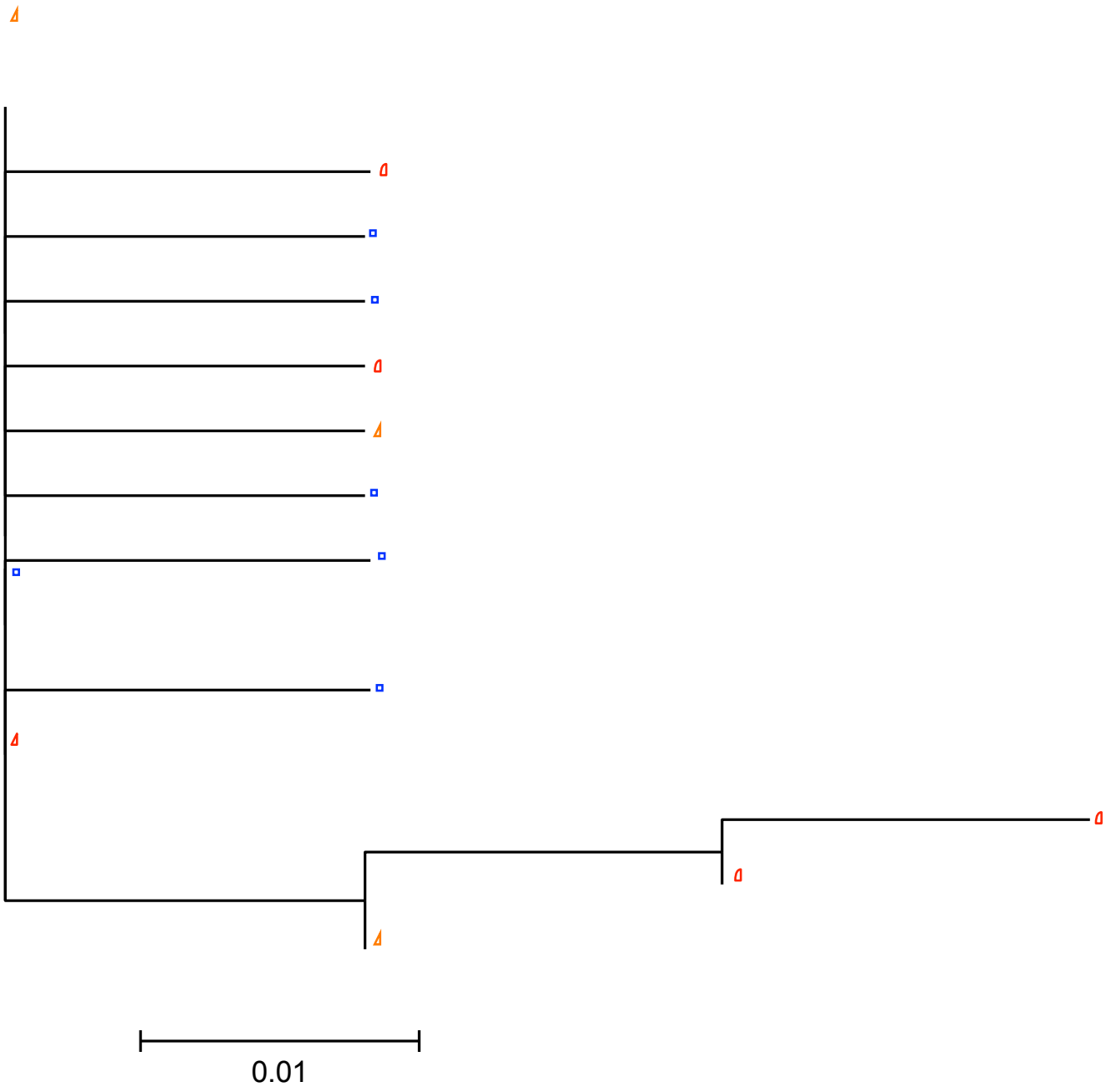

Subject 24

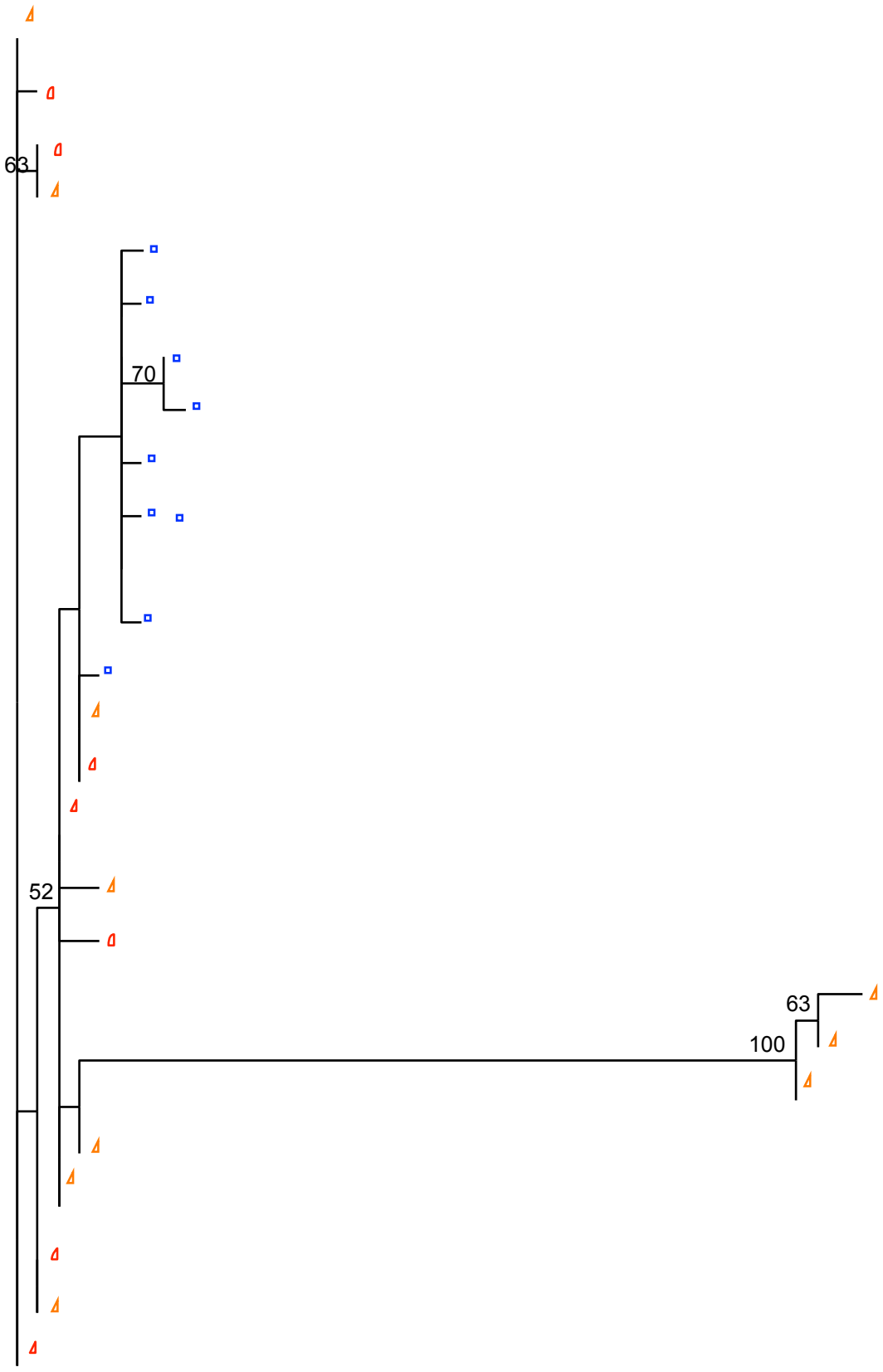

Subject 25

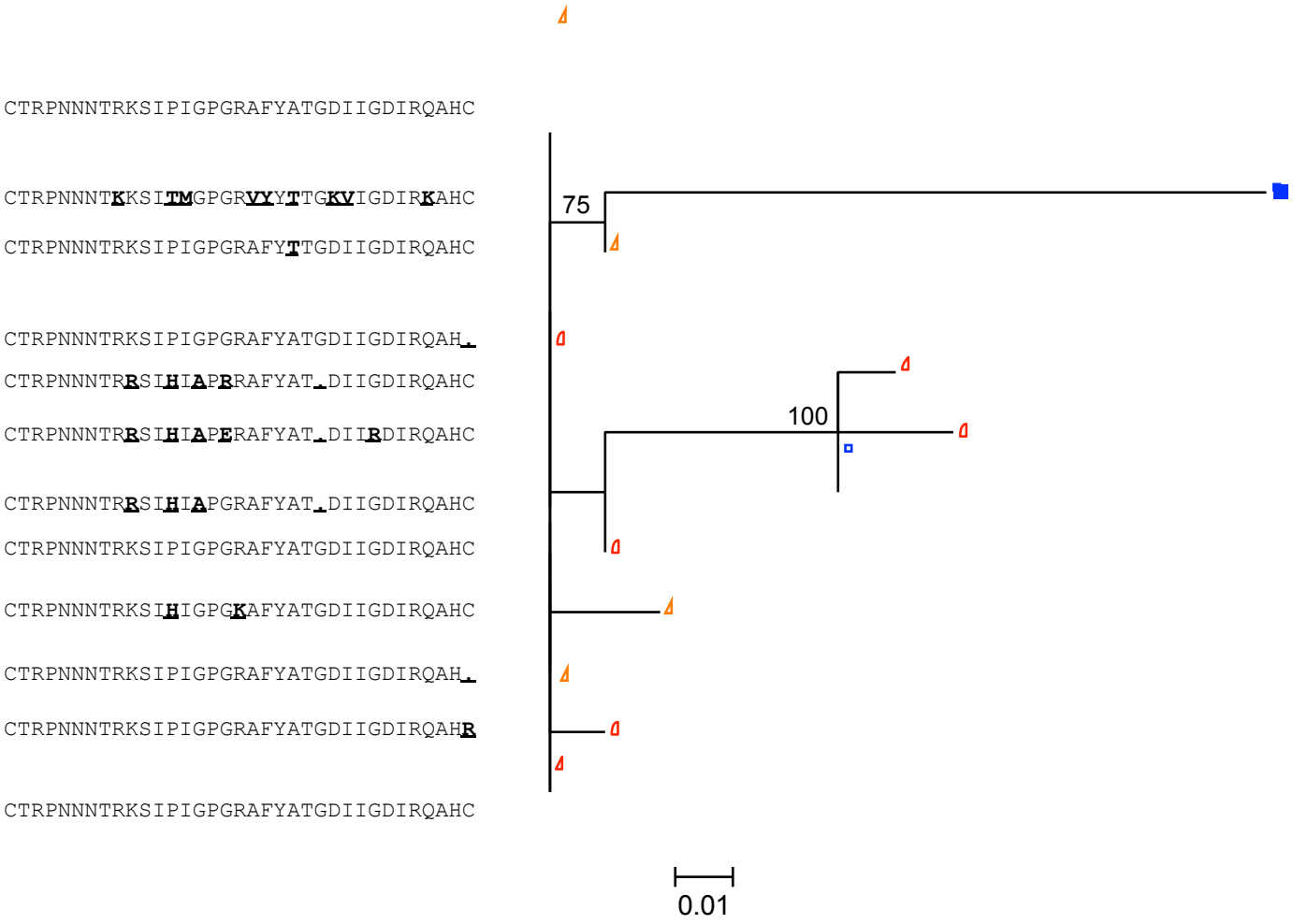
CTRPNNNTRKSIPIGPGRAFYATGDIIGDIRQAHC
CTRPNNNTKKSITMGPGRVYYTTGKVIGDIRKAHC
CTRPNNNTRKSIPIGPGRAFYTTGDIIGDIRQAHC
CTRPNNNTRKSIPIGPGRAFYATGDIIGDIRQAH-
CTRPNNNTRRSIHIAPRRAFYAT-DIIGDIRQAHC
CTRPNNNTRRSIHIAPERAFYAT-DIIRDIRQAHC
CTRPNNNTRRSIHIAPGRAFYAT-DIIGDIRQAHC
CTRPNNNTRKSIPIGPGRAFYATGDIIGDIRQAHC
CTRPNNNTRKSIHIGPGKAFYATGDIIGDIRQAHC
CTRPNNNTRKSIPIGPGRAFYATGDIIGDIRQAH-
CTRPNNNTRKSIPIGPGRAFYATGDIIGDIRQAHR
CTRPNNNTRKSIPIGPGRAFYATGDIIGDIRQAHC
75
100
0.01

Subject 26

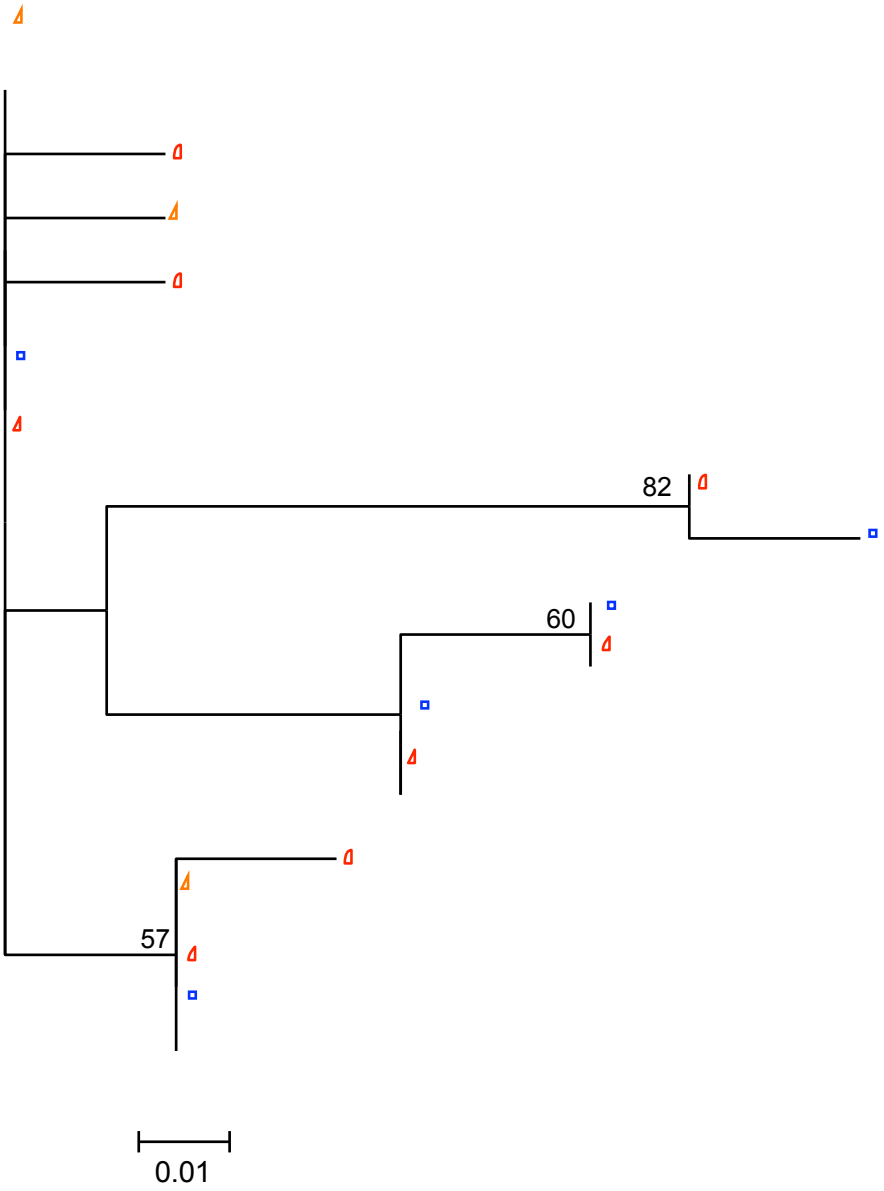

Subject 27

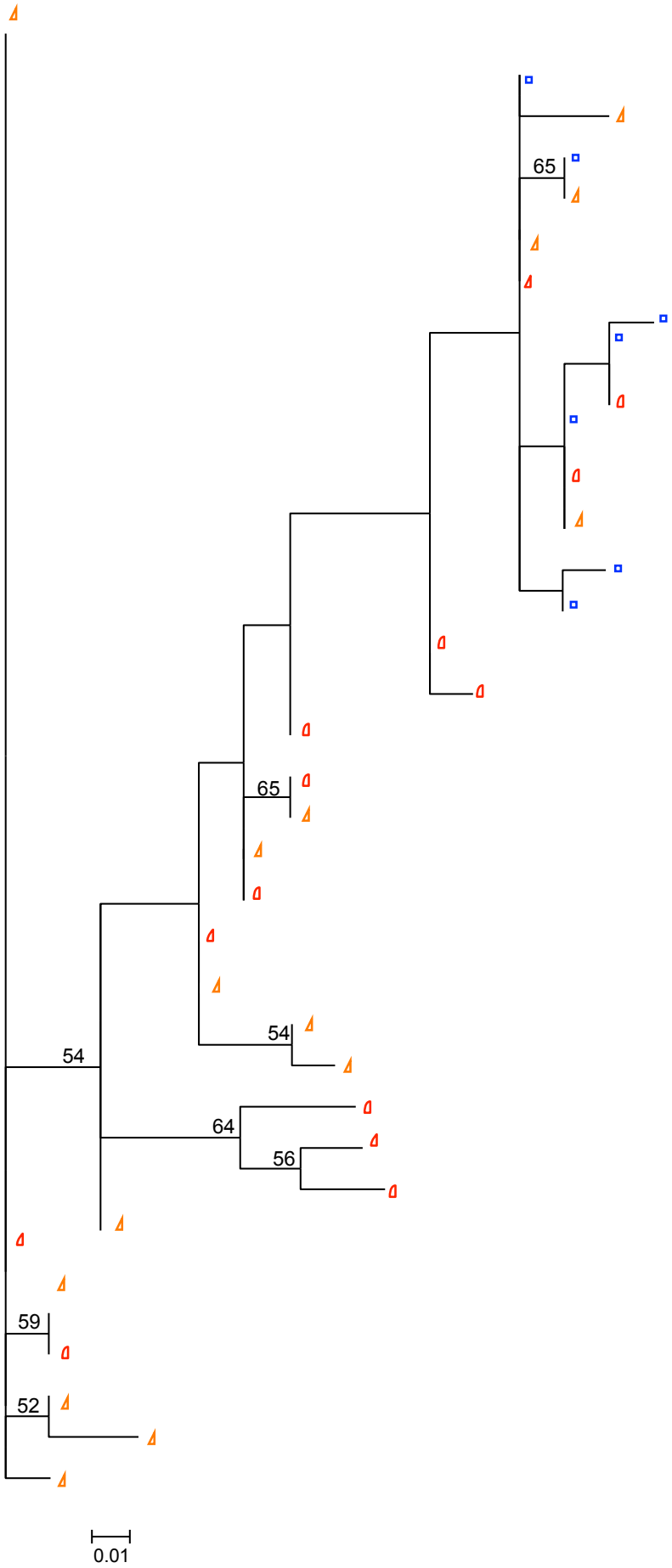

Subject 28

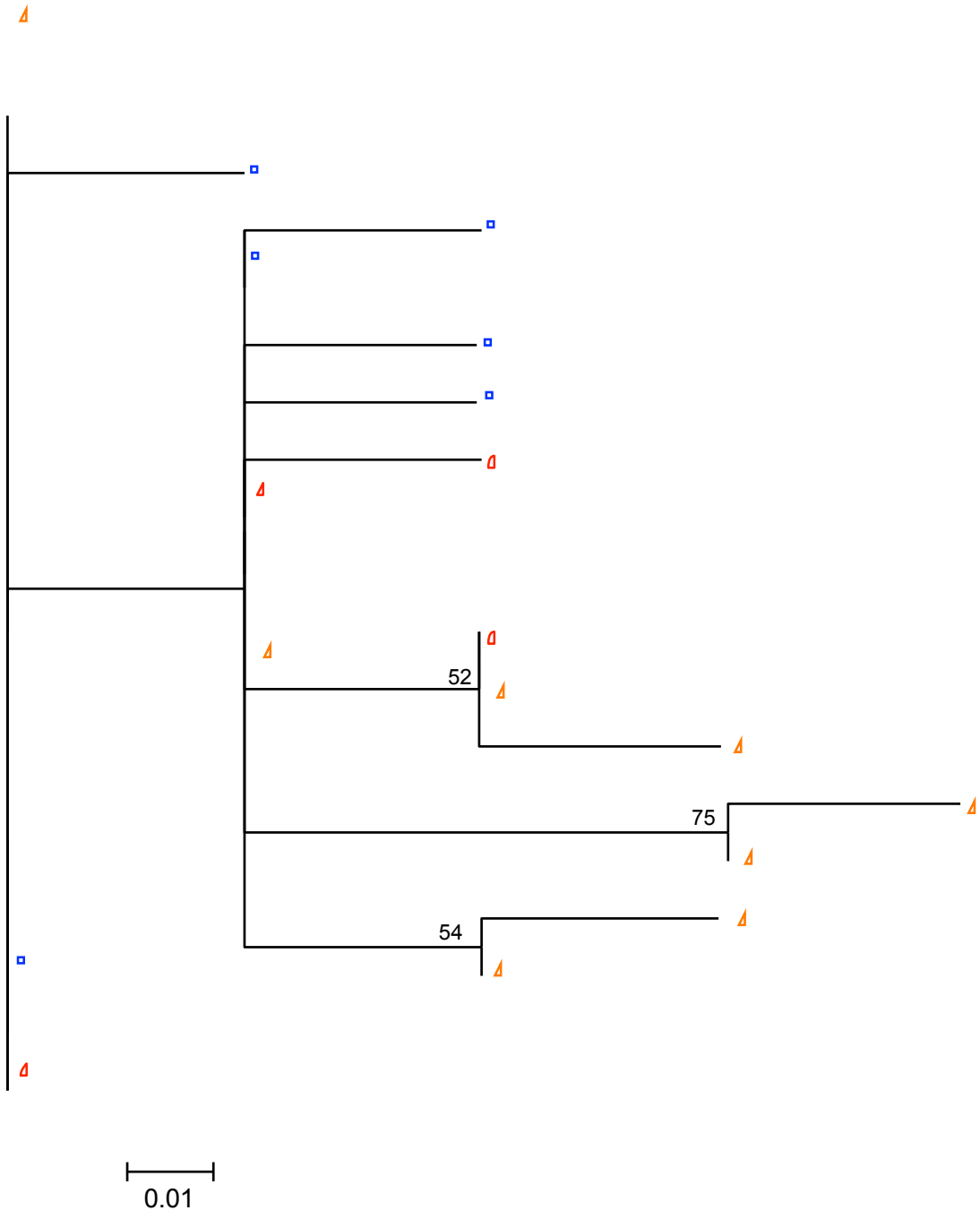

Subject 29

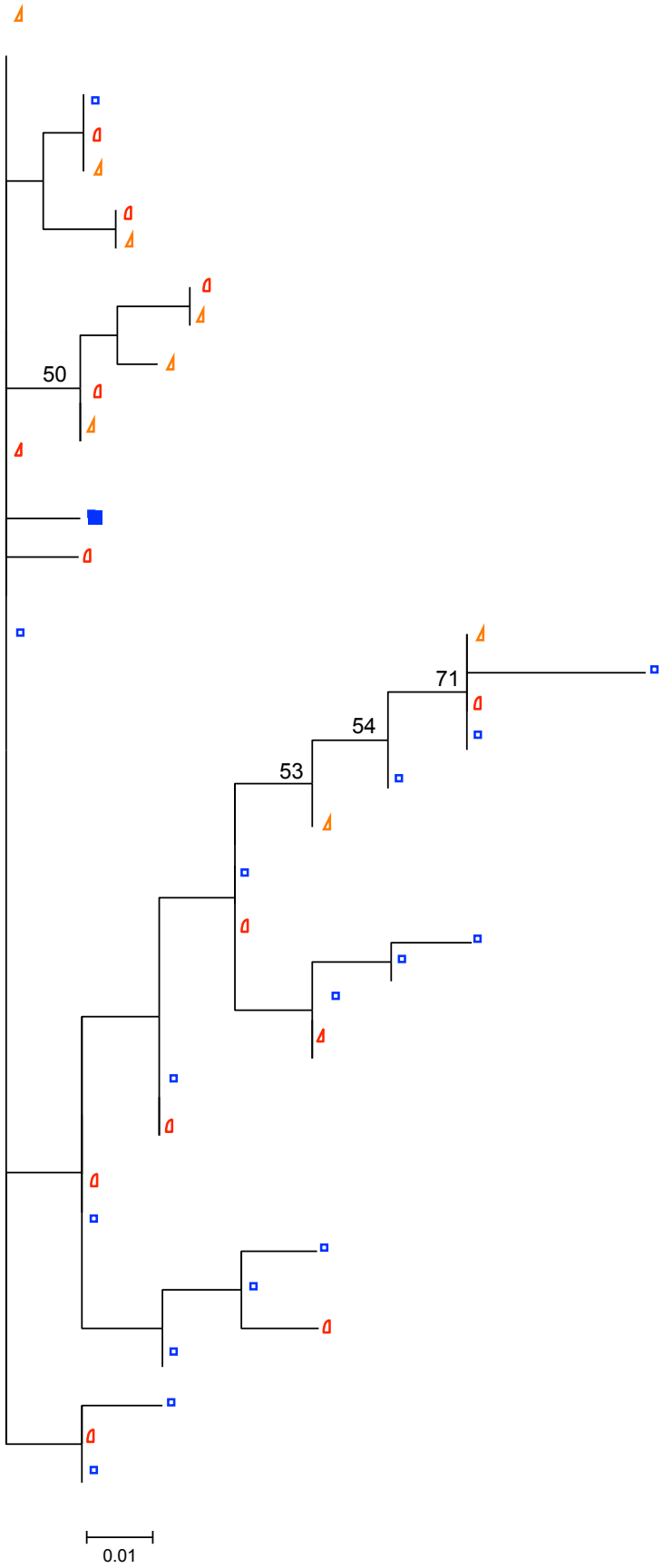

Subject 30

Chapter 2

Switching the third drug of antiretroviral therapy to maraviroc in aviraemic subjects: a pilot, prospective, randomized clinical trial

Anna Bonjoch[1,2*†], Christian Pou[2,3†], Núria Pérez-Álvarez[1,4], Rocío Bellido[2,3], Maria Casadellà[2,3], Jordi Puig[1], Marc Noguera-Julian[2,3], Bonaventura Clotet[1–3], Eugènia Negredo[1,2] and Roger Paredes[1–3]

[1]HIV Unit & Fundació Lluita contra la SIDA, Hospital Universitari Germans Trias i Pujol, Barcelona, Catalonia, Spain; [2]Universitat Autònoma de Barcelona, Barcelona, Catalonia, Spain; [3]IrsiCaixa AIDS Research Institute-HIVACAT, Barcelona, Catalonia, Spain; [4]Universitat Politècnica de Catalunya, Barcelona, Catalonia, Spain

The journal of antimicrobial chemotherapy. 2013 Jun;68(6):1382-7.

Abstract

Objectives: To evaluate the safety and efficacy of switching the third drug of antiretroviral treatment to maraviroc in aviraemic subjects infected with R5 HIV.

Patients and methods: This is a pilot, prospective, randomized clinical trial (ClinicalTrials ID: NCT00966329). Eighty HIV-1-infected aviraemic adults on stable antiretroviral treatment for ≥1 year and no antiretroviral drug resistance were screened for the presence of non-R5 HIV by triplicate proviral V3 population sequencing. From them, 30 subjects with R5 HIV-1 were randomized 1:1 to switch the non-nucleoside reverse transcriptase inhibitor or ritonavir-boosted protease inhibitor to maraviroc (n=15) or to continue the same antiretroviral treatment (controls, n=15). The principal endpoint was the proportion of subjects with HIV-1 RNA <50 copies/ mL at week 48. Ultrasensitive proviral HIV-1 tropism testing (454 sequencing) was performed retrospectively at weeks 0, 4, 12, 24, 36 and 48.

Results: One subject in the maraviroc arm and one control had non-R5 HIV in proviral DNA by retrospective 454 sequencing. The subject receiving maraviroc was the only individual to develop virological failure. However, plasma HIV at failure was R5. Switching to maraviroc was well tolerated and associated with small, but statistically significant, declines in total, high-density lipoprotein and low-density lipoprotein cholesterol. Median (IQR) triglyceride [1 (0.67–1.22) versus 1.6 (1.4–3.1) mmol/L, P=0.003] and total cholesterol [4.3 (4.1–4.72) versus 5.4 (4–5.7) mmol/L, P=0.059] values were lower in the maraviroc arm than in controls at week 48.

Conclusions: In this pilot, prospective, randomized clinical trial, switching the third drug to maraviroc was safe, efficacious and improved lipid parameters.

Keywords: ultrasensitive proviral HIV-1 tropism testing, virally suppressed patients, HIV.

Introduction

It is uncertain if subjects with sustained undetectable HIV-1 RNA levels experiencing antiretroviral-related toxicity could safely switch their current ritonavir-boosted protease inhibitor (PI/r) or non-nucleoside reverse transcriptase inhibitor (NNRTI) drug to maraviroc. This treatment strategy could allow improvements in metabolic profile, efavirenz-related neurotoxicity, hepatotoxicity and gastrointestinal events, and would preserve other drugs with favourable toxicity profiles for future regimens. Nevertheless, for this strategy to be safe, it must be ensured that maraviroc is prescribed to subjects with negligible levels of CXCR4-using (non-R5) HIV[1]. The safety of using population sequencing of the gp120 V3-loop of peripheral blood mononuclear cell (PBMC)-associated HIV-1 to guide maraviroc switches in aviraemic subjects, which is becoming increasingly popular in Europe[2,3], has been evaluated in observational studies[4,5], but not in prospective, randomized clinical trials.

We developed a pilot clinical trial to test the safety and efficacy of switching from a PI/r or an NNRTI to maraviroc in subjects with persistent virological suppression and with R5 viruses by proviral V3-loop population sequencing.

Methods

This was a 48 week, two-arm, prospective, randomized, pilot clinical trial in HIV-1-infected adults receiving care in the outpatient HIV Unit of the Hospital Universitari Germans Trias i Pujol, Badalona, Catalonia, Spain (ClinicalTrials ID: NCT00966329).

Inclusion criteria for screening were being on stable antiretroviral therapy including a PI/r or an NNRTI plus two nucleoside reverse transcriptase inhibitors (NRTIs) for ≥1 year, having HIV-1 RNA <50 copies/mL for ≥6 months, absence of genotypic drug resistance to the NRTI backbone by bulk sequencing and ≥90% self-reported treatment adherence. Exclusion criteria were previous virological failure, previous detection of non-R5 HIV by any tropism test, active acute or uncontrolled chronic infection during the previous 2 months and pregnancy or willingness to become pregnant. The use of lipid-lowering drugs was allowed. The study was approved by the Institutional Review Board of the Hospital Universitari Germans Trias i Pujol. All subjects provided written informed consent to participate in the study.

HIV-1 tropism was inferred from subjects fulfilling the selection criteria from triplicate V3-loop population sequencing of proviral HIV-1 DNA (Supplementary methods, available as Supplementary data at JAC Online). Non-R5 HIV was defined as a false-positive rate value ≤20% in any of the triplicate sequences, using the $Geno2Pheno_{[coreceptor]}$ algorithm. Subjects with R5 HIV were randomized 1:1 to switch

their NNRTI or PI/r to maraviroc (Celsentri®, ViiV Healthcare, 300 mg twice a day) (maraviroc arm) or to continue their previous antiretroviral regimen (control arm).

Study visits were at baseline (day of randomization and maraviroc initiation) and at weeks 4, 8, 12, 24, 36 and 48. Clinical data and fasting blood specimens were collected at every visit. Measurements included a complete blood count and biochemistry, HIV-1 RNA levels (NucliSens EasyQ HIV-1, bioMérieux, Marcy l'Étoile, France) and CD4+ cell counts every 12 weeks. Plasma and PBMC samples were stored at –80ºC. Proviral HIV-1 tropism was retrospectively evaluated in all visits using 454 sequencing and the Geno2Pheno$_{[454]}$ tool (Supplementary methods, available as Supplementary data at JAC Online). Non-R5 HIV was defined as the presence of ≥2% V3 sequences with a false-positive rate ≤3.75[1,6].

Dyslipidaemia was defined as values that exceeded the National Cholesterol Education Programme (NCEP, Adult Treatment Panel III) borderline-high cut-offs[7], i.e.: triglycerides, ≥1.7 mmol/L (≥150 mg/dL); total cholesterol, ≥5.2 mmol/L (≥200 mg/dL); high-density lipoprotein (HDL) cholesterol, <1.03 mmol/L (<40 mg/dL); and low-density lipoprotein (LDL) cholesterol, ≥3.4 mmol/L (≥130 mg/dL). The total cholesterol/HDL cholesterol atherogenic ratio was also determined.

The principal efficacy analysis, i.e. the proportion of subjects with HIV-1 RNA <50 copies/mL at week 48, was performed per protocol and by intention-to-treat, where switching or missing equalled failure. The statistical significance of longitudinal changes in HIV RNA levels and CD4+ counts was evaluated by comparing their slope between treatment groups and according to other relevant baseline factors using Student's t, Wilcoxon or Mann–Whitney tests. The proportion of subjects with dyslipidaemia was compared using Fisher's exact test. All analyses were performed using SPSS version 15.0 (SPSS Inc., Chicago, IL, USA). A bilateral P value <0.05 was considered statistically significant.

Results

Eighty individuals were screened; 37 (46.2%) had non-R5 viruses by population sequencing, 13 did not fulfil the inclusion criteria and 30 entered the study, 15 per arm (Table 1). Subjects had been on antiretroviral treatment for a median of 7.4 (IQR 3.0–12.0) years and had had HIV-1 RNA <50 copies/mL for a median of 5.1 (IQR 2.7–8.8) years. Median (IQR) baseline and nadir CD4+ counts were 737 (515–850) and 336 (250–409) cells/mm^3, respectively. All subjects allocated to the maraviroc arm were on NNRTI-based regimens at randomization: nine were receiving nevirapine and six were receiving efavirenz. Seven subjects allocated to the control arm were on PI/r-containing regimens (four on ritonavir-boosted atazanavir, two on ritonavirboosted lopinavir and

one on ritonavir-boosted fosamprenavir) and eight were on NNRTIs (five on efavirenz and three on nevirapine). The median (IQR) number of variants, reads and quality reads obtained by retrospective 454 sequencing per sample was, respectively: 299 (200–498), 3717 (1930–5850) and 2749 (1619–4282).

One patient in the control arm was lost to follow-up at week 12; one in the maraviroc arm interrupted therapy because of diarrhoea at week 1. There were no other adverse events.

One participant in the maraviroc arm and one control had non-R5 HIV-1 in the retrospective proviral DNA 454 sequencing analysis. See Figure 1(e and f). The subject receiving maraviroc was the only individual developing virological failure during the study (HIV RNA=180 and 170 copies/mL at week 36). This subject had switched from nevirapine to maraviroc on a tenofovir/emtricitabine backbone. Trough drug plasma concentrations 12 h 30 min post-dose were 454 ng/mL for maraviroc (18.2x the target), 78 ng/mL for tenofovir (1.2x the Cmin) and 179 ng/mL for emtricitabine (2×the Cmin) at the time of virological failure. By bulk sequencing, the rebounding virus was R5 ($Geno2Pheno_{[coreceptor]}$ false-positive rate: 52.8%) and had no resistance mutations in protease or reverse transcriptase. The subject regained HIV-1 RNA suppression <50 copies/mL after switching back from maraviroc to nevirapine. All remaining subjects retained HIV-1 RNA <50 copies/mL throughout the study.

Therefore, in the primary efficacy analysis by intention-to-treat, where switching or missing equalled failure, 13 individuals (86%) in the maraviroc arm and 14 (93%) in the control arm achieved HIV-1 RNA <50 copies/mL at week 48. In the per-protocol analysis, only one subject in the maraviroc arm developed virological failure (Figure 1a).

Median CD4+ cell counts remained >500 cells/mm^3 in both arms (Figure 1b). There was a median (IQR) increase of 75.5 (-130 to 190) cells/mm^3 in the maraviroc arm (P=0.397) and a median decrease of 84 (-153.5 to -22.25) cells/mm^3 in the control arm (P=0.035), relative to baseline values. At week 48, differences between groups were not significant (P=0.085).

Four subjects in the maraviroc arm and three controls were on lipid-lowering drugs at baseline; one subject in the control arm began lipid-lowering treatment at week 12; they all continued receiving these drugs until the end of the study. Median lipid values were not significantly different at baseline and remained within the normality range throughout the study in both arms. Subjects in the maraviroc arm showed small, but statistically significant, declines in total cholesterol [from 5 (4.8–5.2) to 4.3 (4.1–4.72) mmol/L, P=0.003], HDL cholesterol [from 1.3 (1.15–1.52) to 1.25 (1.08–1.52) mmol/L, P=0.004] and LDL cholesterol [from 2.9 (2.7–3.2) to 2.5 (2.37–2.66) mmol/L, P=0.005]

between baseline and week 48. There were no significant longitudinal changes in median lipid values in the control group.

At week 48, median (IQR) triglyceride values were significantly lower in the maraviroc arm [1 (0.67–1.22) mmol/L] than in controls [1.6 (1.4–3.1) mmol/L] (P=0.003). Median (IQR) total cholesterol values were also lower in the maraviroc arm [4.3 (4.1–4.72) mmol/L] than in the control arm [5.4 (4–5.7) mmol/L], but only achieved marginal statistical significance (P=0.059) (Figure 1c).

Nine subjects (60%) in each study arm had abnormal lipid values at baseline (Figure 1d). Abnormal triglyceride, total cholesterol, HDL cholesterol and LDL cholesterol values were found in nine versus five, seven versus nine, five versus two and eight versus six in controls and maraviroc switches, respectively. Fewer subjects in the maraviroc arm had hypercholesterolaemia than in the control arm (21.4% versus 64.3%, respectively, P=0.054) at week 48. There were no statistically significant differences between arms in the proportion of subjects with other types of dyslipidaemia (Figure 1d). The total cholesterol/HDL cholesterol atherogenic ratio decreased in the maraviroc arm (from 3.78 to 3.31), but increased in the control group (from 3.93 to 4.44) between baseline and week 48; however, differences between and within groups did not achieve statistical significance.

Median (IQR) glycaemia values remained within the normality range without significant differences between arms.

Discussion

In this pilot, prospective, randomized clinical trial, switching the third drug to maraviroc was safe, efficacious, well tolerated and improved lipid parameters.

The virological efficacy of maraviroc in our study supports genotypic tropism testing of proviral DNA as a suitable tool to guide treatment switches to CCR5 antagonists in aviraemic individuals. If the test had been unable to screen out subjects with significant levels of non-R5 HIV, they would have been exposed to virtual dual-NRTI therapy for 48 weeks. Conceivably, that would have been associated with non-R5 virus evolution, higher rates of virological failure and potential development of NRTI resistance. Importantly, no subject with R5 HIV at baseline developed non-R5 viruses during continued exposure to maraviroc therapy, suggesting that maraviroc-including regimens continued to inhibit viral replication as much as conventional antiretroviral treatment.

The settings used for proviral DNA population sequencing in this study were more conservative than the ones suggested by European tropism guidelines[2,3], but still missed non-R5 HIV in the only subject that eventually developed virological failure. The

clinical implications of this finding are uncertain; however, as the rebounding plasma virus was R5 and had no resistance mutations in protease or reverse transcriptase. Trough drug levels at the time of viraemia rebound were adequate, which rules out major adherence or pharmacokinetic problems as the cause of virological failure. Eventually, the subject regained viraemia suppression when he was switched back to tenofovir/emtricitabine plus nevirapine. Non-R5 levels remained relatively stable in proviral DNA throughout the study follow-up, even at virological failure. This is concordant with the heterogeneous cellular and viral composition of PBMCs, which often includes nonviable or non-replicating viruses, although we cannot rule out the emergence of mutations conferring resistance to maraviroc, as observed in previous studies[8]. Larger studies are needed to clarify whether there is a relationship between levels of non-R5 HIV in PBMCs and virological outcomes to maraviroc therapy in aviraemic subjects, beyond the sensitivity threshold of ultrasensitive genotypic tropism techniques.

As observed in treatment-naive individuals[9], a switch to maraviroc improved lipid parameters, with small, but statistically significant, reductions in median total cholesterol and LDL cholesterol levels, and lower triglyceride and total cholesterol levels relative to controls at the end of the study. This lipid-lowering effect, alongside the putative anti-inflammatory activity of maraviroc[10], could potentially contribute to reduce antiretroviral therapy-related cardiovascular risk[11–14], allowing some patients to avoid lipid-lowering agents and their associated toxicity or drug interactions with antiretrovirals. Indeed, we observed a non-significant trend towards decreasing total cholesterol/HDL cholesterol ratios in subjects switching to maraviroc, relative to controls that should be confirmed in larger studies. Although the study inclusion criteria did not restrict for previous NNRTI or PI use and patients were not stratified according to previous treatment, all subjects who switched to maraviroc in this trial were previously receiving NNRTIs. This could have influenced the lipid results even though lipid levels were not significantly different between the study arms at baseline. Particularly, improvements in the lipid profile might have been more evident in subjects switching to maraviroc from PI/r-containing regimens.

The main limitation of this study was its small sample size, which is justified by its pilot nature, given the risk of this strategy and the lack of prospective, randomized, clinical trials assessing its safety and virological consequences when the study was designed. Although our results cannot be considered definitive, they are highly informative for upcoming, well-powered clinical trials. On the one hand, clinicians should be reassured of the overall good performance of genotypic tropism testing in proviral DNA as a tool to screen for aviraemic subjects suitable to receive CCR5

antagonists. On the other hand, studies should attempt to confirm whether ultrasensitive genotyping techniques could further improve clinical outcomes. Cost-effectiveness analyses as well as more detailed metabolic studies would also be important to define the best clinical use of this treatment strategy. One final limitation, common to all clinical trials, is that the benefits of the approach tested in this study could have been overestimated in comparison with routine clinical practice, as participants in clinical trials usually have higher treatment adherence and motivation to pursue treatments correctly.

In conclusion, this pilot, prospective, randomized clinical trial showed that switching the third drug of antiretroviral therapy to maraviroc in aviraemic subjects is safe, efficacious and improves lipid parameters. Adequately powered studies should corroborate our findings, evaluate the cost-effectiveness of this treatment approach and, in particular, investigate whether detection of pre-existing low-frequency non-R5 HIV-1 in proviral DNA further improves the efficacy of this strategy.

Acknowledgements

This study was presented in part at the International Workshop on HIV & Hepatitis Virus Drug Resistance and Curative Strategies, Sitges, Spain, 2012 (Poster #41).

Funding

This study was supported by an investigator-initiated research grant from ViiV Healthcare, ‘CHAIN, Collaborative HIV and Anti-HIV Drug Resistance Network’, Integrated Project no. 223131, funded by the European Commission Framework 7 Program, and the ‘Gala contra la sida—Barcelona 2011’.

Transparency declarations

A. B. has received lecture fees from Bristol-Myers Squibb. B. C. has been a consultant on advisory boards or participated in speakers’ bureaus or conducted clinical trials with Boehringer-Ingelheim, Abbott, Glaxo-SmithKline, Gilead, Janssen, Merck, Shionogi and ViiV Healthcare. E. N. has received research funding, consultancy fees or lecture sponsorships from Gilead, Roche, Bristol-Myers Squibb, GlaxoSmithKline, Tibotec, Abbott, Merck and Boehringer-Ingelheim. R. P. has received research funding, consultancy fees or lecture sponsorships from Gilead, Pfizer, ViiV Healthcare, Roche Diagnostics, Siemens, Merck and Boehringer-Ingelheim. C. P., N. P.-Á., R. B., M. C., J. P. and M. N.-J. report no competing interests.

Author contributions

A. B., E. N., R. P. and B. C. designed the study and were in charge of the recruitment and monitoring of patients. J. P. performed blood extractions and was responsible for management of the database. R. B. performed V3-loop bulk sequencing for tropism screening. C. P. and M. C. performed V3-loop 454 sequencing. C. P., M. C. and M. N.-J. analysed the 454 sequencing tropism data. N. P.-Á. performed the statistical analysis. A. B., C. P., E. N. and R. P. drafted the manuscript. All authors contributed to reviewing, editing and preparing the final version of the manuscript.

Supplementary data

Supplementary methods are available as Supplementary data at JAC Online (http://jac.oxfordjournals.org/).

References

1 Swenson LC, Mo T, Dong WWet al. Deep V3 sequencing for HIV type 1 tropism in treatment-naive patients: a reanalysis of the MERIT trial of maraviroc. Clin Infect Dis 2011; 53: 732–42.

2 Poveda E, Paredes R, Moreno S et al. Update on clinical and methodological recommendations for genotypic determination of HIV tropism to guide the usage of CCR5 antagonists. AIDS Rev 2012; 14:208–17.

3 Vandekerckhove LP, Wensing AM, Kaiser R et al. European guidelines on the clinical management of HIV-1 tropism testing. Lancet Infect Dis 2011;11: 394–407.

4 Obermeier M, Symons J, Wensing AM. HIV population genotypic tropism testing and its clinical significance. Curr Opin HIV AIDS 2012; 7:470–7.

5 Bellecave P, Paredes R, Anta L et al. Determination of HIV-1 tropism from proviral HIV-1 DNA in patients with suppressed plasma HIV-1 RNA using population based- and deep-sequencing: impact of X4-HIV variants on virologic responses to maraviroc. In: Abstracts of the International Workshop on HIV & Hepatitis Virus Drug Resistance and Curative Strategies, Sitges, Spain, 2012. Abstract 42. Antivir Ther 2012;17 Suppl 1: A53.

6 Swenson LC, Mo T, Dong WW et al. Deep sequencing to infer HIV-1 co-receptor usage: application to three clinical trials of maraviroc in treatment-experienced patients. J Infect Dis 2011; 203: 237–45.

7 Third Report of the National Cholesterol Education Program (NCEP) Expert Panel on Detection, Evaluation, and Treatment of High Blood Cholesterol in Adults (Adult Treatment Panel III) Final Report. Circulation 2002; 106: 3143.

8 Tilton JC, Wilen CB, Didigu CA et al. A maraviroc-resistant HIV-1 with narrow cross-resistance to other CCR5 antagonists depends on both N-terminal and extracellular loop domains of drug-bound CCR5. J Virol 2010; 84: 10863–76.

9 MacInnes A, Lazzarin A, Di Perri G et al. Maraviroc can improve lipid profiles in dyslipidemic patients with HIV: results from the MERIT trial. HIV Clin Trials 2011; 12: 24–36.

10 Funderburg N, Kalinowska M, Eason J et al. Effects of maraviroc and efavirenz on markers of immune activation and inflammation and associations with CD4+ cell rises in HIV-infected patients. PLoS One 2010; 5: e13188.

11 Hsue PY, Ordovas K, Lee T et al. Carotid intima-media thickness among human immunodeficiency virus-infected patients without coronary calcium. Am J Cardiol 2011; 109: 742–7.

12 Ross AC, Rizk N, O'Riordan MA et al. Relationship between inflammatory markers, endothelial activation markers, and carotid intimamedia thickness in HIV-infected patients receiving antiretroviral therapy. Clin Infect Dis 2009; 49: 1119–27.

13 Triant VA, Lee H, Hadigan C et al. Increased acute myocardial infarction rates and cardiovascular risk factors among patients with human immunodeficiency virus disease. J Clin Endocrinol Metab 2007;92: 2506–12.

14 Friis-Moller N, Reiss P, Sabin CA et al. Class of antiretroviral drugs and the risk of myocardial infarction. N Engl J Med 2007; 356:1723–35.

TABLE 1. BASELINE CHARACTERISTICS OF STUDY PARTICIPANTS

	Maraviroc arm	Control arm	P value
Female gender, n (%)	1 (7)	1 (7)	0.759
Caucasian ethnicity, n (%)	15 (100)	15 (100)	1
Age (years)	42 (37–47)	39 (37–49)	0.412
Time since HIV diagnosis (months)	113 (37–187)	99 (63.5–156.7)	0.949
Time on suppressed viral load (years)	5 (2.8–9)	5.5 (2.2–8.8)	0.934
Time on highly active antiretroviral therapy (years)	7.1 (2.9–12.6)	7.7 (4.6–11.9)	0.836
Baseline CD4+ T cell count (cells/mm^3)	639 (430–770)	791 (542–996)	0.098
Nadir CD4+ T cell count (cells/mm^3)	319 (212–373)	342 (263–424)	0.436
Total cholesterol (mmol/L)	5 (4.8–5.2)	4.8 (3.8–5.6)	0.744
HDL cholesterol (mmol/L)	1.3 (1.15–1.5)	1.16 (0.96–1.4)	0.126
LDL cholesterol (mmol/L)	2.9 (2.7–3.2)	3.1 (1.9–3.4)	1
Triglycerides (mmol/L)	1.2 (0.8–1.7)	1.7 (0.9–2.5)	0.202
Glycaemia (mmol/L)	5.3 (5.1–5.5)	4.9 (4.7–5.2)	0.005

Values are shown as median (IQR), unless otherwise indicated.

FIGURE 1. STUDY OUTCOMES

A. Primary efficacy analysis: HIV RNA <50 copies/mL at week 48

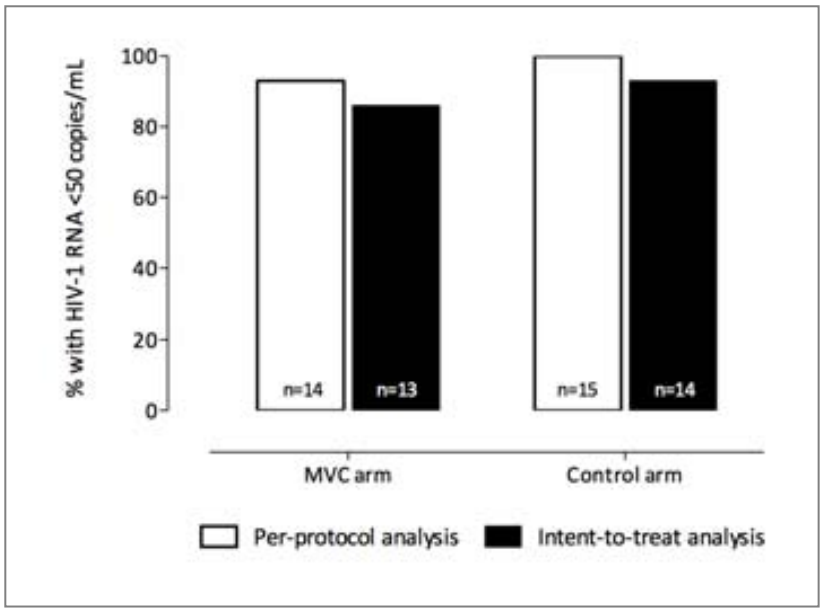

Virological efficacy according to the “per-protocol” or “intention-to-treat”, where switching or missing equalled failure, analyses.

B. CD4+ T cell counts

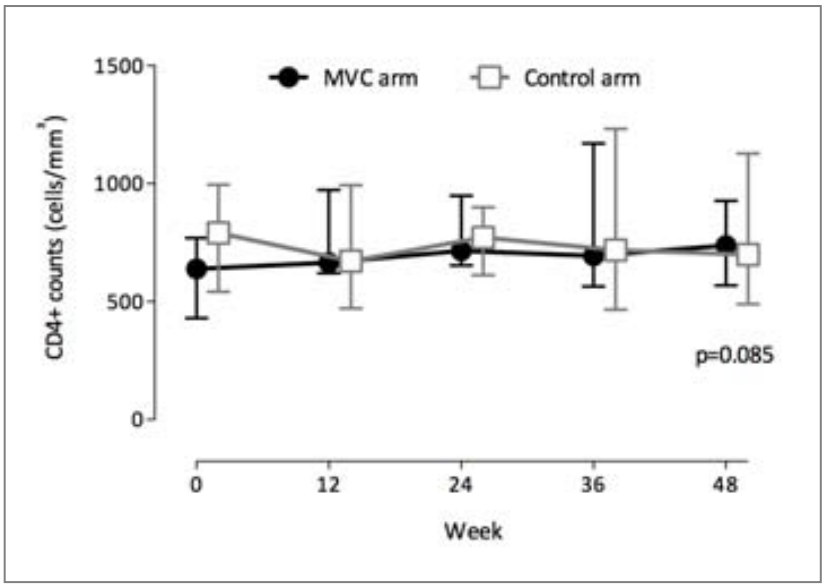

Median and IQR CD4+ counts during the study.

FIGURE 1. STUDY OUTCOMES

C. Median lipid levels at week 0 and 48

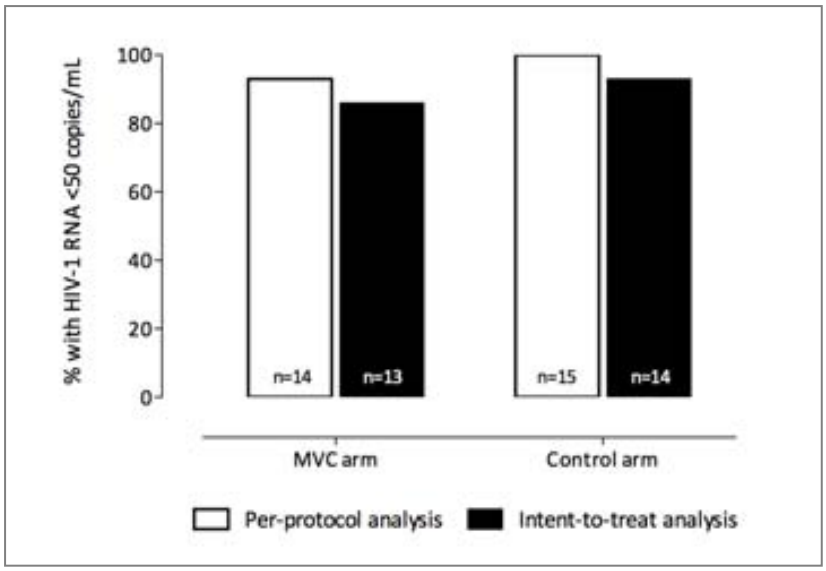

Median lipid values at baseline and week 48.

D. Subjects with abormal fasting lipids

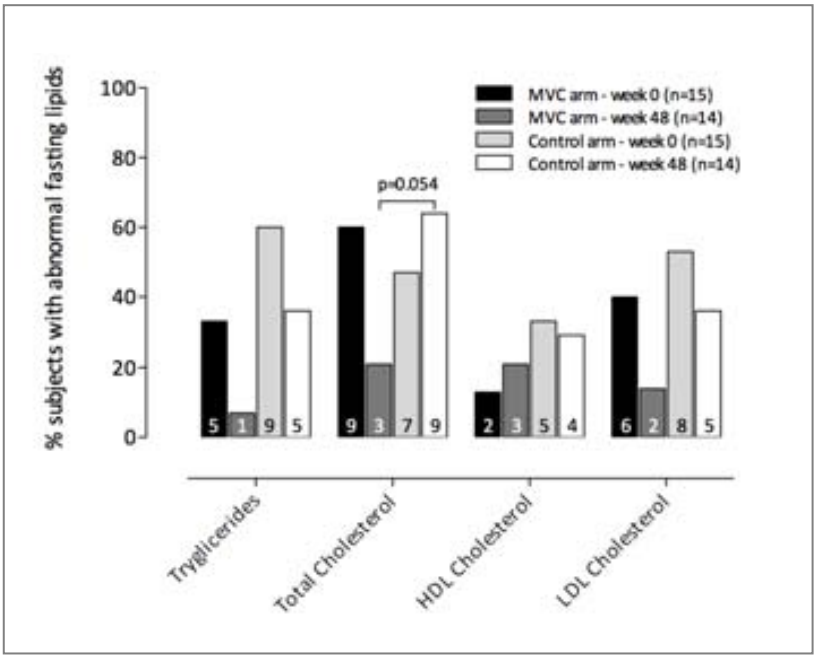

Proportion of subjects with dyslipidaemia, according to the National Cholesterol Education Programme (NCEP, Adult Treatment Panel III) borderline-high cut-offs [i.e. triglycerides, ≥1.7 mmol/L (≥150 mg/dL); total cholesterol, ≥5.2 mmol/L (≥200 mg/dL); HDL cholesterol, <1.03 mmol/L (<40 mg/dL); and LDL cholesterol, ≥3.4 mmol/L (≥130 mg/dL)].

FIGURE 1. STUDY OUTCOMES

E. Levels of non-R5 HIV in the MVC arm by 454 sequencing

F. Levels of non-R5 HIV in controls by 454 sequencing

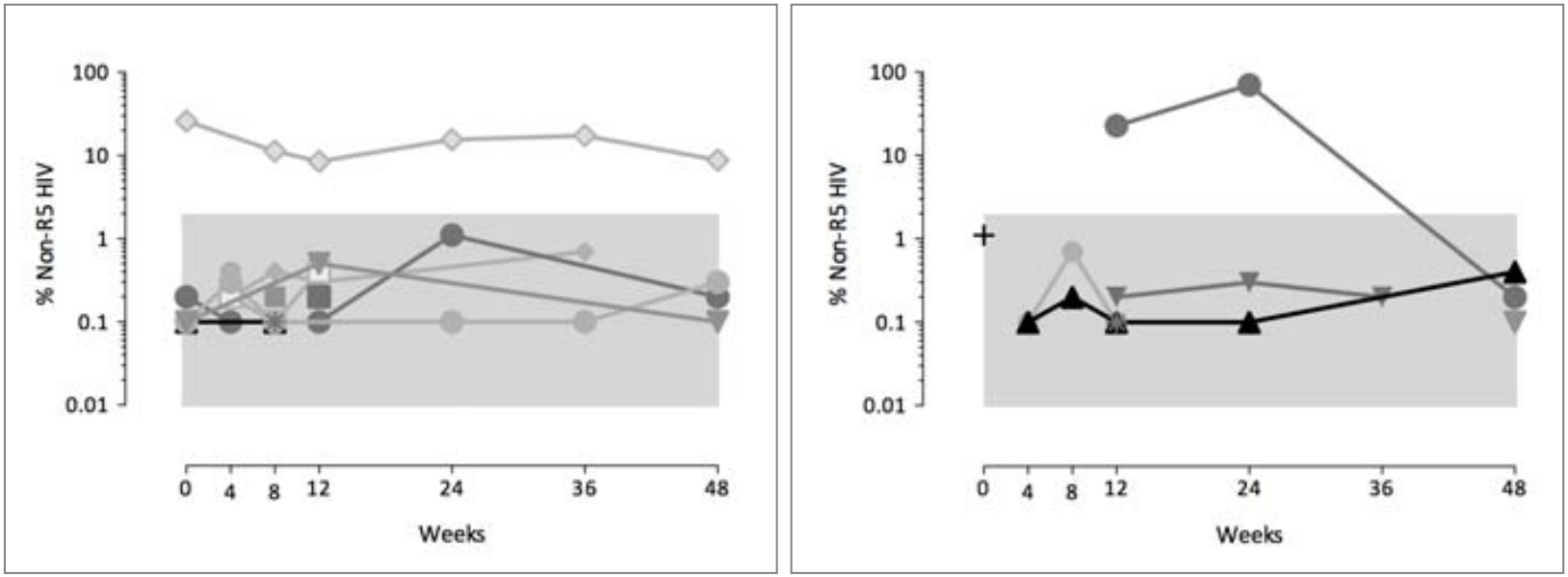

Frequency of non-R5 HIV detected in each individual allocated to the maraviroc and control arms. Different symbols correspond to different subjects. Values coresponding to 0% frequency are not deciped because of the logarithmic scale of this representation. The grey area highlights levels of non-R5 viruses present below the pre-specified 2% detection. In all panels, P values <0.1 are shown. MVC, maraviroc.

Supplementary data

Supplementary methods. Tropism evaluation by proviral DNA V3 population and 454 sequencing

V3-loop population sequencing

Total proviral HIV-1 DNA was extracted from 106 PBMCs using a QIAamp DNA Blood Mini Kit (QIAgen Inc, Valencia, CA, USA). gp160 was PCR-amplified (Platinum® Taq High Fidelity, Life Technologies, Paisley, UK) in triplicate parallel reactions using primers V3-PSOF (HXB2 coordinates 5,858-5,877) 5'-CCC TGG AAG CAT CCA GGA AG-3' and V3-PSOR (HXB2 coordinates 9,064-9,089) 5'-TTT TTA AAA GAA AAG GGG GGA CTG GA-3' with the following cycling conditions: 5 min denaturalization at 94ºC; 30 s at 94ºC, 30 s at 55ºC and 4 min at 68ºC for 30 cycles; and a final elongation step at 68ºC for 5 min. Each PCR product was used as a template for a nested PCR (Platinum® Taq High Fidelity), which was performed with primers V3-PSNF (HXB2 coordinates 5,958-5,983) 5'-TAG GCA TCT CCT ATG GCA GGA AGA AG-3' and V3-PSNR (HXB2 coordinates 8,882-8,904) 5'-GGG TGG GAG CAG TAT CTC GAG AC-3', with the following cycling conditions: 2 min denaturalization at 94ºC; 30 s at 94ºC, 30 s at 55ºC and 3 min at 68ºC for 30 cycles; and a final 5 min elongation step at 68ºC. PCR products were purified (QIAquick PCR Purification Kit, QIAgen Inc.). Bidirectional Sanger sequencing was performed using primers V3-PSeqF (HXB2 coordinates 7,002-7,021) 5'-CTG TTA AAT GGC AGT CTA GC-3' and V3-PSeqR (HXB2 coordinates 7,344-7,363) 5'-CAC AGT TTT AAT TGT GGA GG-3'. Contigs and consensus sequences were created with Sequencher v5.0 (Gene Codes Corporation, Ann Arbor, MI, USA). Coreceptor use was inferred using the $Geno2Pheno_{[coreceptor]}$ tool. Non-R5 HIV was defined as an FPR ≤20% in any of the triplicate sequences evaluated for each study subject.

V3-loop 454 sequencing

Triplicate first-round PCR products described above were pooled and used as a template for a nested PCR (Platinum® Taq High Fidelity) using the following 454-adapted primers: V3-454F (HXB2 coordinates 7,010-7,029) 5'-TGG CAG TCT AGC AGA AGA AG-3' and V3-454R (HXB2 coordinates 7,315-7,332) 5'-CCT CAG GAG GGG ACC CAG-3'. Primers included the corresponding A and B 454 adapters, a 10-mer multiple identifiers and a TCAG sequence tag at the 5' end. Cycling conditions were: 2 min at 94ºC; 30 s at 94ºC, 30 s at 55ºC and 45 s at 68ºC for 30 cycles; and 3 min at 68ºC. PCR products were purified using

AMPure Magnetic Beads (Beckman Coulter Inc., Brea, CA, USA). The concentration and quality of each amplicon was determined by fluorimetry (PicoGreen, Life Technologies) and spectrophotometry (Lab-on-a-Chip, Agilent Technologies, Foster City, CA, USA). Equimolar pools were made to perform emulsion PCR using a 454-FLX sequencing platform with Titanium chemistry (454 Life Sciences/Roche). HIV-1 tropism was determined using the Geno2Pheno$_{[454]}$ tool. Non-R5 HIV was defined as the presence of ≥2% sequences with an FPR ≤3.75.

Discussion

Drug resistance testing is important in the clinical management of HIV-1 infected people. HIV-1 genotyping has substituted phenotypic testing in most situations because of its shorter turnaround time to results, lower cost and the possibility of performing it in a decentralized manner. Population HIV-1 genotyping is utilized in clinical practice to personalize antiretroviral treatment (ART) obtaining good correlations with clinical outcomes. However, its low sensitivity in detecting minority drug resistance mutations (DRM) or minor CXCR4-using viral strains can compromise the efficacy of antiretroviral therapy (ART).

The presence of minority DRM has been associated with poor prognosis in subjects receiving antiretroviral drugs with a low genetic barrier, such as in subjects initiating NNRTI-based ART with minority DRM before treatment administration or subjects presenting minority DRM after exposure to single-dose nevirapine who initiate NNRTI-based ART. On the contrary, the presence of minority DRM in subjects initiating first-line therapy based on antiretroviral agents with high genetic barrier was not associated with a loss of virologic response. Regarding viral tropism, the presence of minority CXCR4-using variants prior to treatment with CCR5 antagonists has also been associated with an increased risk of virologic failure in subjects who initiate CCR5 antagonist-based therapy.

Throughout this thesis, we evaluated the clinical value of ultrasensitive HIV-1 genotyping in the management of ARV treatment-experienced HIV-1 infected subjects in different clinical scenarios. We employed 454 sequencing for ultrasensitive HIV-1 genotyping, determining antiretroviral drug resistance and viral tropism.

In chapter 1 we evaluated whether the same virus populations were inspected during the performing of tropism tests in plasma ARN and PBMC-associated DNA. Based on our results, 454 sequencing obtained the closest diagnostic accuracy to ESTA in plasma ARN, becoming an alternative to the current gold-standard assay. Even though tropism determinations were equivalent between plasma and cellular compartments, phylogenetic analyses from data generated by 454 sequencing revealed sequence compartmentalization in some subjects. Here, virus populations were subtly different in terms of the number of haplotypes and their prevalence. Although previous studies based on HIV-1 DNA-based genotypic methods supported their concordance with clinical outcomes, this sequence compartmentalization might

compromise the prediction of virologic response to maraviroc by HIV-1 genotyping, depending on the compartment examined. The mobilization of different cell sanctuaries, the presence of residual replication and/or the use of a different number of DNA molecules inspected during PCR amplifications could explain this phenomenon. Furthermore, the absence of evolution observed during prolonged periods of aviremia suggested that testing of stored plasma samples would be generally safe and informative.

In recent years, the European Consensus Group on clinical management of tropism testing has recommended the use of population HIV-1 genotyping in plasma ARN for establishing co-receptor tropism. The analysis of PBMC-associated DNA for tropism determinations in subjects with non-detectable viral loads has aroused interest in clinical practice. In chapter 1, the tropism assay achieving the best performance in HIV-1 DNA was population sequencing. The high specificity obtained by population sequencing in HIV-1 DNA led to obtaining the closest accuracy to ESTA. This could be explained because PBMCs contain a historical repository of current and past HIV-1, often accumulating non-replicative minority CXCR4-using forms detected by 454 sequencing.

A validation of population HIV-1 genotyping from PBMC-associated DNA for viral tropism determination was shown in chapter 2. In this prospective and randomized clinical trial, DNA HIV-1 genotyping by triplicate population sequencing allowed the safe switch from the antiretroviral regimen to maraviroc in subjects with sustained undetectable HIV-1 RNA levels experiencing antiretroviral-related toxicity. Although our settings enhanced the possibility of detecting non-R5 strains by population HIV-1 genotyping (triplicate population sequencing reactions and a conservative G2P FPR≤20% to classify non-R5 viruses), some non-R5 strains were still missed. 454 sequencing was able to detect non-R5 HIV-1 strains in one subject in the control arm and one subject in the maraviroc previously classified as R5 by population sequencing.

The subject harboring non-R5 HIV-1 in the maraviroc arm was the only individual who lost virologic response. This subject regained viremia suppression when he was switched back to tenofovir/emtricitabine plus nevirapine. Released viral particles at virologic failure were CCR5-using viruses and did not show drug resistance mutations in protease and reverse transcriptase genes by population HIV-1 genotyping. Nevertheless, we cannot rule out the presence of mutations conferring resistance to maraviroc outside the HIV-1 V3-loop.

Regarding the assessment of antiretroviral drug susceptibility in the *pol* gene, 454 sequencing for ultrasensitive HIV-1 genotyping was technically non-inferior to population HIV-1 genotyping. This technology provided additional genotypic information

beyond population sequencing in most heavily pre-treated individuals tested (6 out of 7) being concordant with previous studies [1]. Nonetheless, the detection of minority DRM only modified a few antiretroviral susceptibility predictions (5%). The switch of drug susceptibility predictions observed in this study mainly affected RT inhibitors, being concordant with findings observed by Varghese et al[2]. The low genetic barrier of these compounds could explain the loss of antiviral drug susceptibility. On the other hand, ultrasensitive HIV-1 genotyping did not consistently provide additional information on PIs or InSTIs drug susceptibility. Because most additional DRM in our study were detected at virologic failure, the clinical value of ultrasensitive HIV-1 genotyping in treatment-experienced subjects might be more useful for assessing the loss of antiviral efficacy after virologic failure than for evaluating pre-existing resistance.

Another application of massive parallel sequencing was to explore the origin of ARV drug resistance mutations present in virologic failure in subjects developing virologic failure. We provided further evidence that HIV-1 can escape from antiretroviral suboptimal drug pressure through the selection of pre-existing drug-resistant mutants. Phylogenetic analyses revealed the emergence of minority drug resistance mutations (Q148R and N155H) during virologic failure from two independent evolutionary clusters. Moreover, ultrasensitive HIV-1 genotyping revealed the coexistence of double mutants Q148R+N155H found in a prevalence of 1.7%, often carrying E138K and G163R mutations on the same genome to compensate viral fitness. These findings emphasized the importance of prescribing fully active antiretroviral regimens to all HIV-1-infected subjects.

Technical aspects of 454 sequencing

In this thesis, 454 sequencing protocols have been designed, optimized and implemented for 454 sequencing strategies tailored to antiviral drug resistance and viral tropism.

454 sequencing has evolved by involving library preparation, sequencing procedure and data analysis. Regarding sample preparation, several changes in “in-house” library preparation improved the quality of the amplicons generated. Gel electrophoresis, PCR purification by column and DNA quantification by spectrophotometry were replaced by lab-on-a-chip technology, purification by magnetic beads and quantification by fluorimetry, respectively. These modifications in the protocol reduced the presence of the primer dimer and permit the inspection of the quality of the amplicons with the highest sensitivity. In parallel, the metallic coating of the PTP^{TM} and the use of smaller DNA capture beads increased the number and length of the reads. Furthermore, the

length of multiple identifiers (MIDs) was also extended to reduce the chance of reassign readouts from one subject to another.

One limitation associated with NGS for applying sequencing to HIV-1 is the requirement of a large amount of DNA for the sequencing procedure. Moreover, reverse transcription is also required for library preparation. During the rounds of PCR amplification, the original diversity of the sample can be altered by the incorporation of nucleotide substitutions, the recombination PCR-mediated and the selection of specific viral strains due to polymorphisms in the primer binding. Because PCR cannot be avoided, some modifications in the protocol would reduce some of the PCR-associated weaknesses. For example, the use of high-fidelity DNA polymerases could reduce the incorporation of nucleotide substitutions. The recombination PCR-mediated could be minimized by a) increasing the primer concentration, b) increasing the extension time, c) decreasing the DNA input, d) decreasing the number of amplification cycles and e) using high-processivity DNA polymerases. Finally, the positioning of the primers in conserved genomic regions reduces the amplification bias. This is often difficult because of the variability of the HIV-1 and the high number of primers utilized for ultrasensitive HIV-1 genotyping in the *pol* gene.

The chance to detect minority virus populations depends on the number of genomes inspected or sampled. The testing of samples with high viral loads (>1,000 c/mL) is crucial to obtain reliable and robust drug resistance report. In contrast, resampling occurs when a few numbers of genomes are inspected, reamplifying the same genomes along the rounds of PCR amplification. It is associated with a low concentration of RNA/DNA input for PCR or polymorphisms in the primer binding site. Therefore, sampling should be monitored to ensure a deep characterization of the viral population. However, the utilization of quantitative PCR for this purpose is not feasible because the regions tested should not be any longer than 200bp. Improvements in quantitative PCR kits could handle the qualification of longer PCR products.

The nature of pyrosequencing makes it difficult to detect DRM located within or adjacent to homopolymers. This particular composition of bases also facilitates the accumulation of mutations due to the stalling of reverse transcriptase during HIV-1 replication or in vitro cDNA synthesis. Bidirectional sequencing was performed in all these studies with the aim of interrogating the same position at both ends of the amplicon facilitating the detection of DRM. The last version of Amplicon Variant Analyzer (AVA) software provided with the 454 Sequencing Systems has incorporated the combination of the frequency of the mutation on the forward and reverse strand. It easy allows the recognition of problematic sequencing regions, giving an idea of the robustness of the assay.

Sequencing of controls in parallel to the samples allowed the monitoring of variability incorporated during the generation of sequence readouts.

Based on HIV-1 clonal sequencing the error rate for in-house 454 sequencing assays has been calculated to be between 0.1 to 0.5%[2-5]. It should be noted that we used a more conservative threshold to filter the error incorporated during reverse transcription, which was not evaluated by our DNA controls. We established two different conservative thresholds for filtering putative wrong sequences in HIV-1 V3-loop and *pol* gene. Here, we identified the percentage of different HIV-1 V3-loop unique sequences obtained after amplifying a commercial pNL4.3 DNA under the same PCR conditions used to generate patient sequences. In chapter 1, no “false” haplotype sequences were found above a frequency of 0.6%, considering valid HIV-1 V3-loop haplotypes if they were present in at least 0.6% of the virus population. In chapters 3 and 4, a conservative cut-off of ≥1% was used to classify one DRM as valid.

Despite the increased sensitivity shown by 454 sequencing beyond the current population genotyping, resistant viral strains in prevalence below the error threshold of the technology can be selected and outgrow when pressure is exercised, compromising the efficacy of ART. This was demonstrated Addendum I and II, where a DRM present at baseline was not detected at virologic failure and a DRM at prevalence below the threshold of sensitivity was selected afterwards, respectively. The design of more sophisticated controls could reduce these limits of sensitivity, incorporating drug resistance mutations or minority non-R5 viral strains that are important for treatment design. Ideally, future controls should be based on mixtures of virus in different proportions to evaluate simultaneously a) error incorporated during reverse transcription and PCR amplifications, b) PCR-mediated recombination and c) accuracy of the assay.

Interpretation of the genotype

In this thesis, algorithms for inferring antiretroviral drug susceptibility were used for the interpretation of the ultrasensitive HIV-1 genotype. However, their utilization for this purpose remains controversial. We assumed that mutations under the error threshold of the technology were not clinically relevant, and that minority mutants had the same weight in genotypic susceptibility interpretation algorithms as if they were present at high prevalence. Future studies are needed to explore the association between the prevalence of DRM and their role in the GSS calculation. Furthermore, not all the antiretroviral agents are evaluated by the algorithms and their role in the genotypic susceptibility score (GSS) calculation is unclear.

Future directions

GS FLX 454 sequencing platforms are suitable for laboratories managing a large number of samples for testing due to the high-throughput sequencing data generated. It should be noted that these laboratories must often combine different projects in the same run for sequencing in a cost-effective manner. In order to bring the technology closer to smaller laboratories, the company released a GS Junior platform in late 2009. It is a more scalable sequencer that substantially reduces the time to results at the expense of the samples tested. Although the scalability seems to be resolved, other bottlenecks associated with 454 sequencing complicate its implementation in routine diagnosis.

454 sequencing requires hard-working library preparation and emPCR for HIV-1 sequencing. These sophisticated processes make the possibility of automating the protocol difficult. In addition, other next-generation sequencing competitors are developing semi-automated protocols to apply these technologies in clinical laboratories. For instance, Illumina® has drastically reduced the time to results by the use of transposons for DNA fragmentation, a semi-automated DNA tagmentation and bridge-amplification of template DNA molecules on a solid surface. Nonetheless, further studies are needed to gain an insight into the effectiveness of other NGS platforms beyond 454 sequencing for HIV-1 genotyping. A recent study evaluated the ability of different NGS platforms (454 sequencing, Illumina®, PacBio®, and Ion Torrent™) to explore the presence of non-R5 viruses within the HIV-1 population. In conclusion, although all NGS the platforms were able to detect the same higher frequency variants, slight variations in the detection of low frequency variants might have an impact on the virologic response to ART.

The use of next-generation sequencing technologies (NNGS) for HIV-1 sequencing would permit the generation of longer readout lengths in a shorter time to result and lower the overall cost. Other benefits associated with NNGS are the possibility of substituting DNA-polymerases by RNA-polymerases for RNA sequencing and the requirement of a smaller amount of DNA/RNA for sequencing.

Another limitation associated with massive parallel sequencing was computational analysis. Several types of open-source marketed software have been developed to bring the technology closer to clinical laboratories. Apart from the inspection of the quality of the sequences and the DRM reporting, they can change the interpretation of the phenotype, haplotype reconstruction or phylogenetic analysis. Moreover, advances in sequencing technology also make demands on the capacity and throughput of storage systems. Here, several network storage systems are being marketed to handle the analysis and storage of data in remote servers out of institutions.

In summary, this thesis has shown the clinical usefulness of ultrasensitive HIV-1 genotyping in ART-experienced HIV-1 infected individuals. 454 sequencing allowed a deep characterization of the HIV-1 diversity within a host, bringing a better understanding of viral evolution and HIV-1 pathogenesis. Moreover, the standardization and automation of 454 sequencing protocols for HIV-1 sequencing would allow the implementation of this technology in HIV-1 diagnosis.

References

1. Le, T., et al., Low-abundance HIV drug-resistant viral variants in treatment-experienced persons correlate with historical antiretroviral use. PLoS One, 2009. 4(6): p. e6079.
2. Varghese, V., et al., Minority variants associated with transmitted and acquired HIV-1 nonnucleoside reverse transcriptase inhibitor resistance: implications for the use of second-generation nonnucleoside reverse transcriptase inhibitors. J Acquir Immune Defic Syndr, 2009. 52(3): p. 309-15.
3. Buzon, M.J., et al., Deep molecular characterization of HIV-1 dynamics under suppressive HAART. PLoS Pathog, 2011. 7(10): p. e1002314.
4. Saliou, A., et al., Concordance between two phenotypic assays and ultradeep pyrosequencing for determining HIV-1 tropism. Antimicrob Agents Chemother, 2011. 55(6): p. 2831-6.
5. Swenson, L.C., et al., Improved detection of CXCR4-using HIV by V3 genotyping: application of population-based and "deep" sequencing to plasma RNA and proviral DNA. J Acquir Immune Defic Syndr, 2010. 54(5): p. 506-10.

Conclusions

1. 454 sequencing is technically non-inferior to bulk sequencing and provides additional genotypic information that could potentially improve treatment decisions in deep salvage therapy, particularly in subjects with suboptimal treatment adherence. However, although additional mutations improved the assessment of genotypic resistance to etravirine, deep sequencing did not consistently provide additional information on darunavir, tipranavir or raltegravir susceptibility relative to population sequencing.
2. Q148R and N155H mutants developing during virologic failure to raltegravir can originate from minority mutants generated spontaneously before treatment exposure, which are selected when selective pressure is exercised.
3. The absence of CXCR4 virus evolution during prolonged periods of viremia suppression suggests that, when available, testing of stored plasma samples is generally safe and informative, provided that HIV-1 RNA levels remain continuously suppressed.
4. Testing of stored pre-therapy plasma samples, when available, may not capture potential virus evolution towards CXCR4-use during ART. The existence of sequence compartmentalization between plasma and PBMCs in some subjects indicates that the genotypic information provided by both compartments might not necessarily be biologically equivalent or be necessarily associated with equivalent clinical outcomes.
5. Switching the third drug to maraviroc is safe, efficacious, well tolerated, and it improves lipid parameters.
6. Genotypic tropism testing in proviral DNA is a suitable tool to guide treatment switches to CCR5 antagonists in aviremic individuals.

Addendum I

Added Value of Deep Sequencing Relative to Population Sequencing in Heavily Pre-Treated HIV-1-Infected Subjects

Francisco M. Codoñer[1,8], Christian Pou[1], Alexander Thielen[3], Federico García[4], Rafael Delgado[5], David Dalmau[6], Miguel Álvarez-Tejado[7], Lidia Ruiz[1], Bonaventura Clotet[1,2], Roger Paredes[1,2]

[1]Institut de Recerca de la SIDA irsiCaixa-HIVACAT and [2]Unitat VIH; Hospital Universitari Germans Trias I Pujol, Badalona, Spain; [3]Max Planck Institute für Informatik, Saarbücken, Germany; [4]Hospital San Cecilio, Granada, Spain; [5]Hospital 12 de Octubre, Madrid, Spain; [6]Hospital Universitari Mutua Terrassa, Terrassa, Spain; [7]Roche Diagnostics SL, Sant Cugat del Vallès, Spain; [8] Present Address: Lifesequencing, S.L., Valencia, Spain.

PLoS One. 2011;6(5):e19461.

Abstract

Objective: To explore the potential of deep HIV-1 sequencing for adding clinically relevant information relative to viral population sequencing in heavily pre-treated HIV-1-infected subjects.

Methods: In a proof-of-concept study, deep sequencing was compared to population sequencing in HIV-1-infected individuals with previous triple-class virological failure who also developed virologic failure to deep salvage therapy including, at least, darunavir, tipranavir, etravirine or raltegravir. Viral susceptibility was inferred before salvage therapy initiation and at virological failure using deep and population sequencing genotypes interpreted with the HIVdb, Rega and ANRS algorithms. The threshold level for mutant detection with deep sequencing was 1%.

Results: 7 subjects with previous exposure to a median of 15 antiretrovirals during a median of 13 years were included. Deep salvage therapy included darunavir, tipranavir, etravirine or raltegravir in 4, 2, 2 and 5 subjects, respectively. Self-reported treatment adherence was adequate in 4 and partial in 2; one individual underwent treatment interruption during follow-up. Deep sequencing detected all mutations found by population sequencing and identified additional resistance mutations in all but one individual, predominantly after virological failure to deep salvage therapy. Additional genotypic information led to consistent decreases in predicted susceptibility to etravirine, efavirenz, nucleoside reverse transcriptase inhibitors and indinavir in 2, 1, 2 and 1 subject, respectively. Deep sequencing data did not consistently modify the susceptibility predictions achieved with population sequencing for darunavir, tipranavir or raltegravir.

Conclusions: In this subset of heavily pre-treated individuals, deep sequencing improved the assessment of genotypic resistance to etravirine, but did not consistently provide additional information on darunavir, tipranavir or raltegravir susceptibility. These data may inform the design of future studies addressing the clinical value of minority drug-resistant variants in treatment-experienced subjects.

Keywords: Deep Sequencing, Antiretroviral therapy, Antiretroviral Resistance, Protease, Reverse Transcriptase, Adherence, Etravirine.

Introduction

The rate of virological failure of the 3 original drug classes is low, but not negligible, and does not appear to diminish over time from starting antiretroviral therapy[1]. If this trend continues, many patients will require newer drugs to maintain viral suppression and accurate resistance tests will be needed to guide clinical management. Deep HIV-1 sequencing (454 Life Sciences/Roche Diagnostics) could potentially improve genotypic resistance assessments because it detects the same range of mutants than Sanger viral population sequencing, but with higher sensitivity[2].

Studies have shown that pre-existing minority drug-resistant mutants increase the risk of virological failure to first-line antiretroviral therapy with non-nucleoside reverse transcriptase inhibitors (NNRTIs)[3,4,5,6,7]. Conversely, low-frequency drug-resistant variants do not affect virological outcomes of first-line therapy including drugs with high genetic barrier, like ritonavir-boosted protease inhibitors (PI/r)[8]. Whereas most studies addressing the role of minority variants have been performed in antiretroviral-naïve subjects[2,3,4,5,6,7,9,10,11,12,13], less information exists on the clinical significance of minority mutants in antiretroviral-experienced individuals[14,15,16].

It is particularly uncertain if ultrasensitive genotypic tests could provide clinically relevant information in heavily pre-treated HIV-1-infected subjects beyond that provided by standard population sequencing genotypic tests. On one hand, detection of additional minority drug-resistant mutants could improve the assessment of viral susceptibility to drugs with intermediate or high drug genetic barrier. On the other hand, the presence of extensive drug resistance could compromise the ability of deep sequencing to add relevant genotypic information to that already obtained with population sequencing, particularly when alternative treatment options are severely limited. Moreover, mutant fixation during virological failure in the presence of ART pressure could potentially complicate the detection of additional low-frequency variants[16].

We therefore sought to explore the potential of deep sequencing to provide additional, clinically relevant genotypic information that could be used to improve treatment decisions in heavily pre-treated HIV-1-infected subjects, relative to population sequencing.

Methods

Subjects

This proof-of-concept observational study included HIV-1-infected adults with previous virological failure (VF) to protease inhibitors (PIs), nucleos(t)ide (NRTIs) and non-nucleoside reverse transcriptase inhibitors (NNRTIs), who developed virological failure to deep salvage therapy including, at least, darunavir, tipranavir, etravirine or raltegravir. Virological failure was defined as the presence of HIV-1 RNA levels > 200 copies/mL 24 weeks after salvage therapy initiation or beyond. Adherence was self-reported by the patient and collected from medical charts. Adequate adherence was defined as intake of all medication doses. Partial adherence was defined as the presence of missed doses during treatment. Treatment interruption meant the complete interruption of therapy during follow-up. The Institutional Review Board of the Hospital Universitari Germans Trias i Pujol, Badalona, Spain, approved the study; participants provided written informed consent for retrospective sample testing.

HIV RNA extraction and reverse transcription

HIV-1 RNA was extracted from 1 mL of plasma within 4 weeks before initiation of deep salvage therapy (baseline) and at virological failure (QIAamp UltraSens Virus Kit™, QIAGEN, Valencia, CA). Three One-Step RT-PCRs (SuperScript® III One-Step RT-PCR System with Platinum® Taq High Fidelity, Invitrogen, Carlsbad, CA) were performed in parallel per each sample. Primers used were 1,571-L23 (HXB2: 1,417→1,440) 5'-ATT TCT CCT ACT GGG ATA GGT GG-3' and 5,464-L27 (HXB2: 5,464→5,438) 5'-CCT TGT TAT GTC CTG CTT GAT ATT CAC-3'. Cycling conditions were: 30 min. at 52ºC, 2 min. at 94ºC; 30 sec. at 94ºC, 30 sec. at 56ºC, 4 min. at 68ºC, for 20 cycles; followed by 5 min. at 68ºC. Triplicate RT-PCR products were pooled, column-purified (QIAquick PCR Purification Kit, QIAGEN, Valencia, CA) and used for both viral population and deep HIV-1 sequencing.

Viral population genotyping

Triplicate nested PCRs were performed in parallel (Platinum® Taq DNA Polymerase High Fidelity, Invitrogen, Carlsbad, CA) with primers 2,084-U26 (HXB2: 2,084→2,109) 5'-ATT TTT TAG GGA AGA TCT GGC CTT CC-3' and 5,456-L26 (HXB2: 5,456→5,431) 5'-TGT CCT GCT TGA TAT TCA CAC CTA GG-3'. Cycling conditions were: 2 min. at 94ºC; 30 sec. at 94ºC, 30 sec. at 56ºC, 4 min. at 68ºC, for 20 cycles; followed by 5 min. at 68ºC. Nested PCR products were pooled and column-purified. Protease (PR), reverse transcriptase (RT) and integrase (IN) were sequenced

in-house (BigDye v3.1, Applied Biosystems, Foster City, CA, USA) and resolved by capillary electrophoresis (ABI 7000, Foster City, CA, USA).

Deep HIV-1 sequencing

Pooled purified RT-PCR products were used as template to generate eight overlapping amplicons covering PR and RT and 3 amplicons covering codons 51 to 215 in IN. Each codon was interrogated by at least 2 independent amplicons, which were generated in triplicate during 20 cycles of PCR amplification (Platinum® Taq DNA Polymerase High Fidelity, Invitrogen, Carlsbad, CA) followed by pooling and purification of triplicate PCR products (QIAquick PCR Purification Kit, QIAGEN, Valencia, CA). PCR reactions were pooled and purified using the Agencourt AMPure Kit (Beckman Coulter, Benried, Germany) to eliminate primer-dimers. The number of molecules was quantified by fluorometry (Quant-iT PicoGreen dsDNA assay kit, Invitrogen, Carlsbad, CA). When amplicon concentrations were below 5ng/mL, amplicon size and primer-dimer content were analysed by spectrometry using BioAnalyzer (Agilent Technologies Inc., Santa Clara, CA). Emulsion PCR was carried out as in[17]. Amplicon Sequencing was performed at 454 Life Sciences, Branford, Connecticut, USA, using a Genome Sequencer FLX. Sequences were extracted and aligned against a consensus sequence from all the reads for each sequences region. Clonal sequences resulting with <90% similarity with the consensus sequence were discarded. Sequencing errors in homopolymeric regions were manually inspected and corrected. Sequences that included a stop codon were removed. Unique sequences (haplotypes) were identified and quantified. The frequency of mutants with a Stanford HIV Database[18] score > 5 was determined.

Using a conservative approach, only mutations present in ≥ 1% of the virus population where considered in this study. An in-house analysis of 992 pNL43 clonal sequences obtained by deep sequencing under the same PCR conditions used to generate patient samples showed a mean (SD) nucleotide mismatch rate of 0.07% (0.13%), which is almost identical to previous reports[14] and corresponds to a variability rate of 1.69×10^{-5}, within the range of the expected PCR error. The mean (SD) error rate for any amino acid mismatch was 0.14% (0.19%), but the mean (SD) error rate for actual drug resistance mutations was 0.03% (0.07%). The 99th percentile of mismatches would establish the threshold for nucleotide errors in 0.61% and the limit for identifying true drug resistance mutations in 0.20%.

Assessment of discrepancies between population and deep sequencing

Genotypes were interpreted with the HIVdb v6.0.8[18], Rega v8.0.2[19] and ANRS v18[20] algorithms. Only mutations with a score ≥ 5 in the Stanford HIV Drug Resistance Database were included in the analysis. Viral susceptibility to each drug was classified as “Sensitive”, “Intermediate” or “Resistant”. Sixty-three paired drug susceptibility predictions (each pair including population and deep sequencing genotypic data) were evaluated per subject and timepoint, 20 for ANRS, 21 for HIVdb v6.0.8 and 22 for Rega v8.0.2.

Results

Subjects

The study included 7 individuals, 2 of them women, with previous exposure to a median of 15 antiretrovirals during a median of 13 years. Their median (interquartilic range, IQR) age was 44 (39; 49) years. The median (IQR) year of HIV diagnosis was 1,988 (1,985; 1,994). Median (IQR) HIV-1 RNA levels and CD4 counts were, respectively, 110,600 (46,550; 370,000) copies/mL and 50 (12; 126) cells/mm^3 at baseline; and 36,700 (2,895; 205,000) copies/mL and 150 (27; 247) cells/mm^3 at virological failure. Median (IQR) nadir CD4 counts were 14 (1; 152) cells/mm^3. Deep salvage therapy included darunavir, tipranavir, etravirine or raltegravir in 4, 2, 2 and 5 subjects, respectively. (Table 1A and Table 1B) Treatment adherence was adequate in 4 individuals (Subjects 1 to 4) (Table 1A) and partial in 2 (Subjects 5 and 6) (Table 1B); one individual (Subject 7) (Table 1B) interrupted antiretroviral therapy during follow-up.

Phenotypic susceptibility predictions by population and deep genotyping

The median (IQR) deep sequencing coverage per base was 3,938 (3,130 – 6,945) sequences at baseline and 3,965 (3,688 – 7,091) sequences at virological failure. Deep sequencing detected all mutations found by population sequencing in all subjects, and found additional mutations in 6 out of 7 individuals. (Table 1A and 1B) Additional mutations were congruent with the treatment history and modified 5.2% of phenotypic susceptibility predictions overall (Figure 1), with no significant differences between interpretation algorithms.

Deep sequencing provided limited additional genotypic information at baseline relative to PS. Baseline DS changed the ANRS predicted susceptibility of lopinavir/r and saquinavir/r from sensitive to intermediate in subject 1 and the ANRS susceptibility of darunavir/r from intermediate to resistant in subject 2 (Table 1A). In subject 7 (Table

1B), however, the detection of minority protease I54L and V82A mutants by deep sequencing in addition to the I54I/V, T74S and L90M detected by population sequencing, consistently decreased the virus susceptibility to indinavir/r across the three algorithms, and led to decreases in predicted susceptibility to saquinavir/r and darunavir/r and to lopinavir/r by the HIVdb and Rega algorithms. The additional detection of the reverse transcriptase M41L and T215Y mutants in this individual led to decreases in susceptibility to different NRTIs by the three algorithms.

Most additional resistance mutations leading to changes in susceptibility predictions were found after virological failure to deep salvage therapy (Table 1A). Consistent decreases in etravirine susceptibility were observed in the two subjects treated with etravirine in this study (subjects 1 and 2). Detection of additional mutations in protease in these two individuals also led to decreased susceptibility to saquinavir/r and lopinavir/r in the ANRS algorithm, respectively. Low-level K103N mutants were detected at virological failure in subject 5. This individual had received efavirenz in the past and was receiving nevirapine at baseline, when he was switched from tenofovir, stavudine, lamivudine and nevirapine, to tenofovir/emtricitabine, darunavir/r and enfuvirtide. The withdrawal of stavudine-mediated pressure over pre-existing K103N mutants might have enabled their emergence and subsequent detection at virological failure. Finally, the detection of minority K219Q and T215Y mutants in subjects 6 and 7, respectively, led to consistent decreases in predicted viral susceptibility to different NRTIs.

Most baseline resistance mutations were lost in subject 7 during treatment interruption becoming undetectable even by deep sequencing at the time of virological failure. No changes in predicted susceptibility were observed for tipranavir or raltegravir, although detection of minority G140S in subject 3 suggested improved fitness of the Q148R mutants detected by population sequencing at virological failure (Table 1B).

Discussion

While being technically non-inferior to population genotyping, deep sequencing enabled the detection of additional resistance mutations with potential clinical significance in 6 out of 7 individuals included in this study. Additional mutations, however, only modified about 5% of antiretroviral susceptibility predictions, including decreased etravirine efficacy in the 2 subjects developing virological failure to this drug, and decreased NRTI, efavirenz and indinavir/r efficacy in 2, 1, and 1 subject,

respectively. Changes in darunavir susceptibility observed in 2 individuals were not consistent across algorithms. Deep sequencing had no impact on susceptibility predictions for tipranavir or raltegravir.

Deep sequencing could modify patient clinical management by avoiding drugs whose resistance may have been underestimated by population sequencing. Indeed, baseline low-frequency PI-resistant mutants were selected during treatment exposure in two subjects: I54T in subject 1, and V32I, Q58E and L89V in subject 2. I54T is a PI-related mutation that appears to be associated with decreased susceptibility to each of the PIs, although its effect has not been well studied. Q58E is a non-polymorphic PI-related mutation associated with reduced susceptibility tipranavir[21,22,23] and possibly to several other PIs. Selection of I54T and Q58E mutations during darunavir therapy may be explained due to residual phenotypic or compensatory effect of such mutations on darunavir susceptibility, genome colinearity with other darunavir-associated mutations, or simple stochastic effects. Interestingly, emergence of I54T in subject 1 was associated with decay in I54A, indicating a possible fitness advantage of I54T over I54A in this particular context. Conversely, substitutions V32I and L89V are nonpolymorphic PI-selected accessory mutations which emerge during treatment with darunavir/ritonavir. Both mutations were associated with decreased response to darunavir/ritonavir in the POWER trials[24], suggesting that they were selected in subject 2 because they conferred additional resistance to darunavir.

Most additional mutants in our study, however, were detected at virological failure. Varghese et al. also detected additional minority variants with major etravirine mutations only in patients failing an NNRTI-containing regimen[14]. Taken together, these results suggest that deep sequencing might be more useful to assess loss of antiviral efficacy after virological failure than to screen for pre-existing resistance in subjects with extensive treatment exposure. As with population sequencing, deep sequencing should also be performed immediately or shortly after virological failure.

The increased sensitivity of deep sequencing could also reassure clinicians about the absence of additional genotypic resistance when making clinical management decisions. This is particularly important for the management of subjects with suboptimal adherence. In our study, deep sequencing provided additional genotypic information in all adherence strata (Table 1 and 2, Figure 1). Deep sequencing, for example, confirmed virus susceptibility to integrase strand-transfer inhibitors in 4 out of 5 subjects who developed virological failure to raltegravir-including regimens, indicating that raltegravir remained a suitable option for subsequent salvage regimens. Similarly, deep sequencing confirmed that subjects 5, 6 and 7 could still be treated with a number of different PIs and suggested higher virus susceptibility to tipranavir than to darunavir

in subject 7 (Figure 1). The absence of resistance mutations by deep sequencing, however, should be interpreted with caution; the loss of most baseline mutants in subject 7 during antiretroviral therapy interruption shows that deep sequencing can also miss clinically relevant resistance mutations present <1% in the viral population.

Detection of low-frequency resistance mutations associated with hypersusceptibility could also improve predicted susceptibility to certain antiretrovirals. For example, the incorporation of a minority T215F mutation in subject 2 changed the HIVdb predicted susceptibility to tenofovir from “resistant” to “intermediate” at virological failure. Therefore, ultrasensitive genotyping also has the potential to refine genotype interpretation rules towards increased virus susceptibility.

Our findings extend those of Le et al.[15], who showed that deep sequencing detected low-frequency mutations unrecognized by Sanger sequencing in 19 out of 22 antiretroviral–experienced individuals experiencing virological failure in routine HIV care between 2004-2007. Additional minority mutants increased a subject’s genotypic resistance to one or more antiretrovirals in 17 of 22 individuals (77%), correlated with the failing drugs in 21% subjects, and with historical antiretroviral use in 79% subjects. In Le’s study, however, samples were collected before etravirine, darunavir or raltegravir became available, so the effect additional minority mutants on HIV susceptibility to these drugs could not be evaluated.

The main limitations of our study are its small sample size, its retrospective observational nature and the fact that adherence was self-reported. This study makes two arguable assumptions: First, that a mutant detected above 1% is clinically relevant. This threshold is clearly above the PCR and 454 sequencing error found in our own and other studies[14,25] and has been shown to predict virological outcomes of first-line NNRTI therapy in treatment–naïve individuals[2]. Moreover, potential PCR-derived recombination should not affect our findings because we did not evaluate mutational linkage. The second assumption is that minority mutants have the same weight in genotypic susceptibility interpretation algorithms as if they were present at higher levels. While biologically plausible, formal studies have not been developed to assess this assumption.

In conclusion, in this subset of heavily pre-treated individuals, deep sequencing showed technical non-inferiority to population sequencing. However, although additional mutations improved the assessment of genotypic resistance to etravirine, deep sequencing did not consistently provide additional information on darunavir, tipranavir or raltegravir susceptibility relative to population sequencing. Further studies should extend our findings and address the clinical impact of ultrasensitive genotyping in HIV-1 infected individuals experiencing virological failure to their first or second-line

antiretroviral therapy. Proper throughput escalation, sample multiplexing and adequate sequence coverage may potentially turn ultrasensitive genotyping into a feasible strategy for HIV drug resistance management in the clinical setting.

Acknowledgements

Roger Paredes wishes to thank Dr. Peter Millard, from the Centro de Saúde San Lucas, Universidade Católica de Moçambique in Beira, for critical review of the manuscript. This work was presented in part at the 17th Conference on Retroviruses and Opportunistic Infections (CROI), San Francisco, 17 February 2010, [abstract # 567].

References

1. Lodwick R, Costagliola D, Reiss P, Torti C, Teira R, et al. (2010) Triple-class virologic failure in HIV-infected patients undergoing antiretroviral therapy for up to 10 years. Arch Intern Med 170: 410-419.
2. Simen BB, Simons JF, Hullsiek KH, Novak RM, Macarthur RD, et al. (2009) Low-abundance drug-resistant viral variants in chronically HIV-infected, antiretroviral treatment-naive patients significantly impact treatment outcomes. J Infect Dis 199: 693-701.
3. Paredes R, Lalama CM, Ribaudo HJ, Schackman BR, Shikuma C, et al. (2010) Pre-existing minority drug-resistant HIV-1 variants, adherence, and risk of antiretroviral treatment failure. J Infect Dis 201: 662-671.
4. Metzner KJ, Giulieri SG, Knoepfel SA, Rauch P, Burgisser P, et al. (2009) Minority quasispecies of drug-resistant HIV-1 that lead to early therapy failure in treatment-naive and -adherent patients. Clin Infect Dis 48: 239-247.
5. Johnson JA, Li JF, Wei X, Lipscomb J, Irlbeck D, et al. (2008) Minority HIV-1 drug resistance mutations are present in antiretroviral treatment-naive populations and associate with reduced treatment efficacy. PLoS Med 5: e158.
6. Goodman DD, Zhou Y, Margot NA, McColl DJ, Zhong L, et al. (2010) Low level of the K103N HIV-1 above a threshold is associated with virological failure in treatment-naive individuals undergoing efavirenz-containing therapy. Aids 25: 325-333.
7. Geretti AM, Fox ZV, Booth CL, Smith CJ, Phillips AN, et al. (2009) Low-frequency K103N strengthens the impact of transmitted drug resistance on virologic responses to first-line efavirenz or nevirapine-based highly active antiretroviral therapy. J Acquir Immune Defic Syndr 52: 569-573.
8. Lataillade M, Chiarella J, Yang R, Schnittman S, Wirtz V, et al. (2010) Prevalence and clinical significance of HIV drug resistance mutations by ultra-deep sequencing in antiretroviral-naive subjects in the CASTLE study. PLoS One 5: e10952.
9. Toni TA, Asahchop EL, Moisi D, Ntemgwa M, Oliveira M, et al. (2009) Detection of human immunodeficiency virus (HIV) type 1 M184V and K103N minority variants in patients with primary HIV infection. Antimicrob Agents Chemother 53: 1670-1672.
10. Balduin M, Oette M, Daumer MP, Hoffmann D, Pfister HJ, et al. (2009) Prevalence of minor variants of HIV strains at reverse transcriptase position 103 in therapy-naive patients and their impact on the virological failure. J Clin Virol 45: 34-38.
11. Peuchant O, Thiebaut R, Capdepont S, Lavignolle-Aurillac V, Neau D, et al. (2008) Transmission of HIV-1 minority-resistant variants and response to first-line antiretroviral therapy. Aids 22: 1417-1423.
12. Metzner KJ, Rauch P, Braun P, Knechten H, Ehret R, et al. (2010) Prevalence of key resistance mutations K65R, K103N, and M184V as minority HIV-1 variants in chronically HIV-1 infected, treatment-naive patients. J Clin Virol 50: 156-161.

13. Jakobsen MR, Tolstrup M, Sogaard OS, Jorgensen LB, Gorry PR, et al. (2010) Transmission of HIV-1 drug-resistant variants: prevalence and effect on treatment outcome. Clin Infect Dis 50: 566-573.

14. Varghese V, Shahriar R, Rhee SY, Liu T, Simen BB, et al. (2009) Minority variants associated with transmitted and acquired HIV-1 nonnucleoside reverse transcriptase inhibitor resistance: implications for the use of second-generation nonnucleoside reverse transcriptase inhibitors. J Acquir Immune Defic Syndr 52: 309-315.

15. Le T, Chiarella J, Simen BB, Hanczaruk B, Egholm M, et al. (2009) Low-abundance HIV drug-resistant viral variants in treatment-experienced persons correlate with historical antiretroviral use. PLoS ONE 4: e6079.

16. D'Aquila RT, Geretti AM, Horton JH, Rouse E, Kheshti A, et al. (2010) Tenofovir (TDF)-Selected or Abacavir (ABC)-Selected Low-Frequency HIV Type 1 Subpopulations During Failure with Persistent Viremia as Detected by Ultradeep Pyrosequencing. AIDS Res Hum Retroviruses 27: 201-209.

17. Margulies M, Egholm M, Altman WE, Attiya S, Bader JS, et al. (2005) Genome sequencing in microfabricated high-density picolitre reactors. Nature 437: 376-380.

18. Rhee SY, Fessel WJ, Zolopa AR, Hurley L, Liu T, et al. (2005) HIV-1 Protease and reverse-transcriptase mutations: correlations with antiretroviral therapy in subtype B isolates and implications for drug-resistance surveillance. J Infect Dis 192: 456-465.

19. Van Laethem K, Geretti A, Camacho R, Vandamme AM Algorithm for the use of genotypic HIV-1 resistance data. Rega v8.0.2 ©, Leuven, 16 June 2009.

20. Shikuma CM, Yang Y, Glesby MJ, Meyer WA, 3rd, Tashima KT, et al. (2007) Metabolic effects of protease inhibitor-sparing antiretroviral regimens given as initial treatment of HIV-1 Infection (AIDS Clinical Trials Group Study A5095). J Acquir Immune Defic Syndr 44: 540-550.

21. Marcelin AG, Masquelier B, Descamps D, Izopet J, Charpentier C, et al. (2008) Tipranavir-ritonavir genotypic resistance score in protease inhibitor-experienced patients. Antimicrob Agents Chemother 52: 3237-3243.

22. Pellegrin I, Breilh D, Ragnaud JM, Boucher S, Neau D, et al. (2006) Virological responses to atazanavir-ritonavir-based regimens: resistance-substitutions score and pharmacokinetic parameters (Reyaphar study). Antivir Ther 11: 421-429.

23. Yates PJ, Hazen R, St Clair M, Boone L, Tisdale M, et al. (2006) In vitro development of resistance to human immunodeficiency virus protease inhibitor GW640385. Antimicrob Agents Chemother 50: 1092-1095.

24. de Meyer S, Vangeneugden T, van Baelen B, de Paepe E, van Marck H, et al. (2008) Resistance profile of darunavir: combined 24-week results from the POWER trials. AIDS Res Hum Retroviruses 24: 379-388.

25. Shao W, Boltz VF, Kearney M, Maldarelli F, Mellors JM, et al. (2009) Characterization of HIV-1 sequence artifacts introduced by bulk PCR and detected by 454 sequencing. XVIII International HIV Drug Resistance Workshop: Basic Principles & Clinical Implications. Fort Myers, FL, USA 9-13 June 2009 (Abstract 104). Antiviral Therapy 14 Suppl 1: A123.

TABLE 1A. ADDITIONAL GENOTYPIC INFORMATION PROVIDED BY DEEP HIV-1 SEQUENCING AND CHANGES IN PREDICTED PHENOTYPIC SUSCEPTIBILITY, RELATIVE TO POPULATION SEQUENCING IN ADEQUATE THERAPY [A, B, C] (SUBJECT 1-2)

SUBJECT	ADHERENCE	ART	BASELINE					VIROLOGICAL FAILURE				
			Mutations by population sequencing	Additional mutations by DS (percent in the viral population)	Change in Predicted Phenotype due to additional DS data			Mutations by population sequencing	Additional mutations by DS (percent in the viral population)	Change in Predicted Phenotype due to additional DS data		
					HIVdb	REGA	ANRS			HIVdb	REGA	ANRS
1	ADEQUATE	TDF FTC DRVr ETR RAL	PI: V11I, V32I, L33F, K43T, I54A, Q58E, T74P, I84V, L89V, L90M	PI: I54T (12.0), V82F (1.1), V82L (1.1)	_	_	LPVr, SQVr: S to I	PR: V11I, V32I, L33F, K43T, I54T, Q58E, T74P, I84V, L89V, L90M	PR: I54A (6.1), V82F (3.5), V82L (3.5)	_	_	SQVr: S to I
			NRTI: M41L, E44D, D67G, L74IV, V75AITV, V118I, L210W, T215Y, K219N	NRTI: none	_	_	_	NRTI: M41L, E44D, D67G, L74IV, V75T, V118I, L210CW, T215Y, K219DN	NRTI: none	_	_	_
			NNRTI: L100I, K103N	NNRTI: none	_	_	_	NNRTI: L100I, K103N	NNRTI: V179D (3.0), Y181C (17.6)	ETR: I to R	ETR: I to R	ETR: S to I
			InSTI: none	InSTI: none	_	_	_	InSTI: none	InSTI: V151I (1.8)	_	_	_
2	ADEQUATE	TDF FTC DRVr ETR RAL	PI: L33F, K43T, M46L, I54V, T74P, V82A, I84V, L90M	PI: V32I (1.6), F53L (1.6), Q58E (8.6), L89V (21.0)	_	_	DRVr: I to R	PI: V11I, V32I, L33F, K43T, I54A, Q58E, T74P, I84V, L89V, L90M	PI: I54T (15.9)	_	_	LPVr: I to R
			NRTI: D67N, T69Li, K70R, Y115F, F116Y, Q151M, M184V, T215V, K219Q	NRTI: T215F (1.8)	_	_	_	NRTI: M41L, E44D, D67N, L74V, V75T, V118I, Q151M, M184V, L210W, T215Y, K219N	NRTI: T215F (1.2)	TDF: R to I	_	_
			NNRTI: K101Q, K103N	NNRTI: none	_	_	_	NNRTI: L100I, K103N	NNRTI: K101E (2.3), Y181C (1.7)	ETR: I to R	ETR: I to R	ETR: S to I
			InSTI: G163K	InSTI: none	_	_	_	InSTI: none	InSTI: V151I (2.3), G163K (21.5)	_	_	_

TABLE 1B. ADDITIONAL GENOTYPIC INFORMATION PROVIDED BY DEEP HIV-1 SEQUENCING AND CHANGES IN PREDICTED PHENOTYPIC SUSCEPTIBILITY, RELATIVE TO POPULATION SEQUENCING IN ADEQUATE THERAPY [A, B, C] (SUBJECT 3-4)

SUBJECT	ADHERENCE	ART	BASELINE					VIROLOGICAL FAILURE				
			Mutations by population sequencing	Additional mutations by DS (percent in the viral population)	Change in Predicted Phenotype due to additional DS data			Mutations by population sequencing	Additional mutations by DS (percent in the viral population)	Change in Predicted Phenotype due to additional DS data		
					HIVdb	REGA	ANRS			HIVdb	REGA	ANRS
3	ADEQUATE	TDF TPVr RAL	PI: V32I, I54M, Q58E, G73S, I84V, L89V, L90M	PI: none	_	_	_	PI: V32I, I54M, Q58E, G73S, I84V, L89V, L90M	PI: none	_	_	_
			NRTI: K70KN, M184V, T215Y	NRTI: none	_	_	_	NRTI: K70KN, M184V, T215Y	NRTI: D67N (8.1)	TDF: S to I	ABC, d4T, ddI: S to I	_
			NNRTI: A98G	NNRTI: none	_	_	_	NNRTI: A98G	NNRTI: none	_	_	_
			InSTI: none	InSTI: none	_	_	_	InSTI: Q148QR, N155NH, G163GR	InSTI: E138K (32.6), G140S (16.1)	_	_	_
4	ADEQUATE	TDF FTC TPVr RAL	PI: M46IL, I54V, G73S, I84V, L90M	PI: none	_	_	_	PI: E35G, M46L, I54V, G73S, I84V, L90M	PI: none	_	_	_
			NRTI: M41L, D67N, L74V, V118I, M184V, L210W, T215Y, K219DN	NRTI: none				NRTI: M41L, D67N, L74V, V118I, M184V, L210W, T215Y, K219N	NRTI: none	_	_	_
			NNRTI: K101P, V179D, G190A	NNRTI: none	_	_	_	NNRTI: K101P, V179D, G190A	NNRTI: none	_	_	_
			InSTI: none	InSTI: none	_	_	_	InSTI: none	InSTI: none	_	_	_

TABLE 1C. ADDITIONAL GENOTYPIC INFORMATION PROVIDED BY DEEP HIV-1 SEQUENCING AND CHANGES IN PREDICTED PHENOTYPIC SUSCEPTIBILITY, RELATIVE TO POPULATION SEQUENCING IN PARTIAL AND ART INTERRUPTION THERAPY [A, B, C] (SUBJECT 5-6)

SUBJECT	ADHERENCE	ART	BASELINE					VIROLOGICAL FAILURE				
			Mutations by population sequencing	Additional mutations by DS (percent in the viral population)	Change in Predicted Phenotype due to additional DS data			Mutations by population sequencing	Additional mutations by DS (percent in the viral population)	Change in Predicted Phenotype due to additional DS data		
					HIVdb	REGA	ANRS			HIVdb	REGA	ANRS
5	PARTIAL	DRVr TDF FTC T20	PI: L23I, L33F, E35G, I54L, Q58E, N88S	PI: none	_	_	_	PI: L23I, L33F, E35G, I54L, Q58E, N88S	PI: none	_	_	_
			NRTI: D67N, K70R, M184V, T215Y, K219E	NRTI: T215F (2.2)	_	_	_	NRTI: D67N, K70R, T215Y, K219E	NRTI: T215F (1.7)	_	_	_
			NNRTI: E138A, Y181V	NNRTI: none	_	_	_	NNRTI: E138A, Y181V	NNRTI: K103N (12.9)	EFV: I to R	_	EFV, NVP: S to R
			InSTI: E157Q	InSTI: none	_	_	_	InSTI: E157Q	InSTI: none	_	_	_
6	PARTIAL	ZDV 3TC ABC ATV RAL	PI: None	PI: none	_	_	_	PI: none	PI: none	_	_	_
			NRTI: D67N, T69DN, K70KR, K219KQ	NRTI: none	_	_	_	NRTI: D67N, T69DN, K70KR,	NRTI: K219Q (1.6)	_	D4T, ZDV: I to R ABC: S to I	D4T, ZDV: S to R
			NNRTI: K103KN	NNRTI: none	_	_	_	NNRTI: K103KN	NNRTI: none	_	_	_
			InSTI: none	InSTI: none	_	_	_	InSTI: none	InSTI: none	_	_	_

TABLE 1D. ADDITIONAL GENOTYPIC INFORMATION PROVIDED BY DEEP HIV-1 SEQUENCING AND CHANGES IN PREDICTED PHENOTYPIC SUSCEPTIBILITY, RELATIVE TO POPULATION SEQUENCING IN PARTIAL AND ART INTERRUPTION THERAPY [A, B, C] (SUBJECT 7)

SUBJECT	ADHERENCE	ART	BASELINE					VIROLOGICAL FAILURE				
			Mutations by population sequencing	Additional mutations by DS (percent in the viral population)	Change in Predicted Phenotype due to additional DS data			Mutations by population sequencing	Additional mutations by DS (percent in the viral population)	Change in Predicted Phenotype due to additional DS data		
					HIVdb	REGA	ANRS			HIVdb	REGA	ANRS
7	ART INTERRUPTION	STARTS AND STOPS TDF FTC DRVr	PI: I54IV, T74S, L90M	PI: I54L (2.4), V82A (13.9)	IDVr, SQVr: I to R DRVr: S to I	IDVr: I to R LPVr: S to I	IDVr: I to R	PI: L90M	PI: none	_	_	_
			NRTI: T215ST	NRTI : M41L (1.4), T215Y (13.7)	ABC, ddI, TDF : S to I	ddI: S to I	D4T, ZDV: I to R ddI: S to R	NRTI: none	NRTI: T215Y (7.9)	d4T, ZDV, ABC, ddI, TDF: S to I	d4T, ZDV: S to I	d4T, ZDV: S to R
			NNRTI: none	NNRTI : none	_	_	_	NNRTI: none	NNRTI: none	_	_	_
			InSTI: none	InSTI: none	_	_	_	InSTI: none	InSTI: none	_	_	_

[a] Only mutations with a score ≥ 5 in the Stanford HIV Drug Resistance Database were included in the analysis.

[b] ART: antiretroviral therapy; DS: deep sequencing; PI: protease inhibitor; NRTI: nucleoside reverse transcriptase inhibitor; NNRTI: non-nucleoside reverse transcriptase inhibitor; InSTI: Integrase Strand Transfer Inhibitor; ZDV: zidovudine; ABC: abacavir; d4T: stavudine; ddI: didanosine; TDF: tenofovir; EFV: efavirenz; NVP: nevirapine; ETR: etravirine; ATV: atazanavir; IDVr: indinavir/ritonavir; FAPVr: fosamprenavir/ritonavir; SQVr: saquinavir/ritonavir; LPVr: lopinavir/ritonavir; DRVr: darunavir/ritonavir; TPVr: tipranavir/ritonavir; ANRS: algorithm of the French ANRS (*Agence Nationale de Recherche sur le SIDA*) AC11 Resistance group, version 18, July 2009, France; HIVdb: HIV db program version 6.0.8, implemented at the Stanford HIV Drug Resistance Database, Stanford University, USA; REGA: Algorithm of the Rega Institute version 8.0.2, University of Leuven, Belgium.

[c] Predicted antiretroviral susceptibility: S: susceptible; I: intermediate; R: Resistant.

FIGURE 1. PREDICTED ANTIRETROVIRAL SUSCEPTIBILITY ACCORDING TO SANGER OR QUANTITATIVE DEEP 454 SEQUENCING (PATIENTS 1-4)

FIGURE 1. PREDICTED ANTIRETROVIRAL SUSCEPTIBILITY ACCORDING TO SANGER OR QUANTITATIVE DEEP 454 SEQUENCING (PATIENTS 5-7)

Color code: Green= Sensitive; Yellow=Intermediate; Red=Resistant. Changes in predicted phenotypic susceptibility between Sanger and 454 sequencing sequencing are highlighted in black boxes. DLV: delavirdine; EFV: efavirenz; ETR: etravirine; NVP: neviapine; 3TC: lamivudine; ABC: abacavir; AZT: zidovudine; d4T: stavudine; ddI: didanosine; FTC: emtricitabine; TDF: tenofovir dippivoxil fumarate; ATV: atazanavir; ATVr: ritonavir-boosted atazanavir; DRVr: ritonavir-boosted darunavir ; FPVr: ritonavir-boosted fosamprenavir; IDVr: ritonavir-boosted indinavir; LPVr: ritonavir-boosted lopinavir; NFV: nelfinavir; SQVr: ritonavir-boosted saquinavir; TPVr: ritonavir-boosted tipranavir; RA: ralegravirL; ELV: elvitegravir.

Addendum II

Dynamic Escape of Pre-Existing Raltegravir-Resistant HIV-1 from Raltegravir Selection Pressure

Francisco M. Codoñer[1], Christian Pou[1], Alexander Thielen[3], Federico García[4], Rafael Delgado[5], David Dalmau[6], José Ramon Santos[2], Maria José Buzón[1], Javier Martínez-Picado[1,7], Miguel Álvarez-Tejado[8], Bonaventura Clotet[1,2], Lidia Ruiz[1], Roger Paredes[1,2]

[1]IrsiCaixa Retrovirology Laboratory-HIVACAT and [2]Lluita Contra la SIDA Foundation; Hospital Universitari Germans Trias i Pujol, Badalona, Spain; [3]Max Planck Institute für Informatik, Saarbücken, Germany; [4]Hospital Universitario San Cecilio, Granada, Spain; [5]Hospital 12 de Octubre, Madrid, Spain; [6]Hospital Universitari Mútua de Terrassa, Terrassa, Spain; [7]Institució Catalana de Recerca i Estudis Avançats (ICREA), Barcelona, Spain; [8]Roche Diagnostics SL, Sant Cugat del Vallès, Spain

Antiviral Research. 2010 Dec;88(3):281-6.

Abstract

Using quantitative deep HIV-1 sequencing in a subject who developed virological failure to deep salvage therapy with raltegravir, we found that most Q148R and N155H mutants detected at the time of virological failure originated from pre-existing minority Q148R and N155H variants through independent evolutionary clusters. Double 148R + N155H mutants were also detected in 1.7% of viruses at virological failure in association with E138K and/or G163R. Our findings illustrate the ability of HIV-1 to escape from suboptimal antiretroviral drug pressure through selection of pre-existing drug-resistant mutants, underscoring the importance of using fully active antiretroviral regimens to treat all HIV-1-infected subjects.

Keywords: HIV-1; antiretroviral resistance; deep sequencing; raltegravir; evolution.

Introduction

Integrase strand transfer inhibitors are a new family of antiretrovirals that reached HIV clinics in 2007 (McColl and Chen, 2010; Steigbigel et al., 2008). Resistance to raltegravir, the first integrase inhibitor available for HIV treatment, evolves through three seemingly exclusive pathways (Fransen et al., 2009) characterized by a signature mutation in the integrase catalytic centre (Y143R/C, Q148R/H/K or N155H) plus several accessory mutations that increase resistance or improve viral replication (Cooper et al., 2008; Paredes and Clotet, 2010). Clonal analyses suggested that Q148R/H/K and N155H mutations did not coexist in individual genomes, which is consistent with the low replication capacity of double Q148R/H/K + N155H mutants *in vitro* (Fransen et al., 2009; McColl and Chen, 2010). The fitness impact of raltegravir resistance mutations, however, may be modulated *in vivo* by accessory mutations in integrase, as well as by epistatic effects of other HIV-1 genes (Buzon et al., 2010).

Clinical Case

We report the case of a 42 year-old male diagnosed with HIV in 1988 (Figure 1) with history of alcoholism and illicit drug use until 1993. He was treated for pulmonary tuberculosis and *Pneumocystiis jirovecii* pneumonia in 1993 and 2004, respectively. Although he had good adherence to antiretrovirals in the recent years, he never achieved HIV-1 RNA suppression <50 copies/mL and his CD4+ T cell counts remained extremely low (the nadir and zenith CD4+ counts were, respectively, 1 and 169 cells/mm^3). After receiving 13 different antiretrovirals during 15 years, he began salvage therapy with tenofovir disoproxil fumarate (245 mg QD), raltegravir (200 mg BID), darunavir (600 mg BID) and ritonavir (100 mg BID) on July 2007. HIV-1 RNA levels decreased 2 $\log_{10}$ four weeks after therapy initiation, but rebounded 1 $\log_{10}$ twenty weeks later. A few weeks after virological failure, the patient was admitted to the intensive care unit and died of acute respiratory distress.

Methods

HIV-1 population and quantitative deep sequencing

HIV-1 RNA was extracted from 1 mL of plasma 3 weeks before initiation of salvage antiretroviral therapy (baseline) and at virological failure (VF), 24 weeks after treatment initiation. Plasma was centrifuged at 35,000 rpm (9,000 x g) during 90 minutes at 4ºC. Viral pellets were resuspended and viral RNA was extracted (QIAamp UltraSens Virus Kit™, QIAGEN, Valencia, CA). Three One-Step RT-PCRs (SuperScript® III One-Step

RT-PCR System with Platinum® Taq High Fidelity, Invitrogen, Carlsbad, CA) were performed in parallel per each sample. Primers used were 1,571-L23 (HXB2: 1,417→1,440) 5'-ATT TCT CCT ACT GGG ATA GGT GG-3' and 5,464-L27 (HXB2: 5,464→5,438) 5'-CCT TGT TAT GTC CTG CTT GAT ATT CAC-3'. Cycling conditions were: 30 min. at 52ºC, 2 min. at 94ºC; 30 sec. at 94ºC, 30 sec. at 56ºC, 4 min. at 68ºC, for 30 cycles; followed by 5 min. at 68ºC. Triplicate RT-PCR products were pooled, column-purified (QIAquick PCR Purification Kit, QIAGEN, Valencia, CA) and used for both viral population and quantitative deep HIV-1 sequencing (QDS).

Viral population genotyping

For population sequencing, triplicate nested PCRs were performed in parallel (Platinum® Taq DNA Polymerase High Fidelity, Invitrogen, Carlsbad, CA) with primers 2,084-U26 (HXB2: 2,084→2,109) 5'-ATT TTT TAG GGA AGA TCT GGC CTT CC-3' and 5,456-L26 (HXB2: 5,456→5,431) 5'-TGT CCT GCT TGA TAT TCA CAC CTA GG-3'. Cycling conditions were: 2 min. at 94ºC; 30 sec. at 94ºC, 30 sec. at 56ºC, 4 min. at 68ºC, for 30 cycles; followed by 5 min. at 68ºC. Again, nested PCR products were pooled and column-purified (QIAquick PCR Purification Kit, QIAGEN, Valencia, CA). Protease, reverse transcriptase and integrase genes were sequenced in-house (BigDye v3.1, Applied Biosystems, Foster City, CA, USA) and resolved by capillary electrophoresis (ABI 7000, Foster City, CA, USA). Genotypes were interpreted automatically with the HIVdb program implemented in the Stanford Drug resistance Database (Liu and Shafer, 2006; Rhee et al., 2003).

Quantitative deep sequencing

Pooled purified RT-PCR products were used as template to generate two overlapping amplicons. Excluding primer sites, amplicon 1 encompassed the integrase codons 91 to 178 (HXB2: 4,499-4,763), whereas amplicon 2 included the integrase codons 132 to 224 (HXB2: 4,621-4,900). The overlapping region between the two amplicons thus encompassed codons 132 to 178 in the Integrase catalytic center (HXB2: 4,621-4,763) Each amplicon was generated in triplicate during 30 cycles of PCR amplification (Platinum® Taq DNA Polymerase High Fidelity, Invitrogen, Carlsbad, CA). Primers for amplicon 1 were Beta-F (HXB2: 4,481→4,499) 5'- AGA AGC AGA AGT TAT TCC A -3' and Beta R (HXB2 4,763→4,780) 5'- TTG TGG ATG AAT ACT GCC -3'; primers for amplicon 2 were Gamma-F (HXB2: 4,606→4,621) 5'- TTA AGG CCG CCT GTT G -3' and Gamma R (HXB2: 4,900→4,917) 5' – TGT CCC TGT AAT AAA CCC -3'. In addition, primers contained 454 sequencing adapters A or B and 8-nucleotide sample identifier tags in the 5'-end. Triplicate PCR products were pooled

and purified (QIAquick PCR Purification Kit, QIAGEN, Valencia, CA). Quantitative Deep Sequencing was performed at 454 Life Sciences, Branford, Connecticut, USA.

Raw output sequences were filtered to ensure high quality (Table 1). The overlapping region between the two amplicons (integrase codons 132 to 178) was extracted. Sequences resulting from extraction were selected if they had more than 90% similarity with the consensus sequence of the run for that subject and region. Sequencing errors in homopolymeric regions were manually inspected and corrected. Sequences that included a stop codon were removed. The sequence coverage was calculated for each aminoacid position. Unique sequences were identified and the percentage of specific mutations in the 143, 148 or 155 positions as well as the percentage of double and triple mutants was calculated only in those sequences surpassing all the above-mentioned quality filters.

An in-house analysis of 992 pNL43 clonal sequences obtained by quantitative deep sequencing under the same PCR conditions used to generate patient samples showed a mean (SD) nucleotide mismatch rate of 0.07% (0.13%), similar to previous reports (Varghese et al., 2009). The mean (SD) error rate for any aminoacid mismatch was 0.14% (0.19%), but the mean (SD) error rate for actual drug resistance mutations was 0.03% (0.07%). The 99th percentile of mismatches would establish the threshold for nucleotide errors in 0.61% and the limit for identifying true drug resistance mutations in 0.20%.

Phylogenetic analysis

Unique overlapping sequences obtained with QDS were used to build a protein Multiple Sequence Alignment (MSA) using Musclev3.7 (Edgar, 2004). Sequence indeterminations were substituted for gaps and were subsequently removed. In addition, a DNA MSA was built concatenating triplets of bases according to the protein MSA. The protein alignment was used to identify the best fit molecular evolutionary model using PROTTEST v2.2 (Abascal et al., 2005). The evolutionary model obtained was used to build a maximum likelihood phylogenetic tree with PHYMLv3.0 (Guindon and Gascuel, 2003). MEGA v4.1 (Kumar et al., 2004) was used to build the tree topology based on a Neighbor-Joining approach, using a pairwise deletion, with the best evolutionary model found by PROTTEST and implemented in MEGA as a distance model. A Simodaira Hasegawa test was used to assess the most likely tree topology to explain the sequence evolution (Simodaira and Hasegawa 1999).

To further investigate the origin of Q148R and N155H mutants detected at the time of VF using an independent phylogenetic method, we used the four-clustering likelihood mapping technique implemented in TREEPUZZLE v 5.2 (Schmidt et al.,

2002). In brief, we constructed 4 clusters of sequences containing, respectively, mutants detected at baseline, mutants present at virological failure, wildtype (wt) viruses found at baseline; and wt viruses observed at virological failure. Wildtype was defined as absence of major integrase inhibitor-resistant mutations at positions 143, 148 and 155. Then, we tested the hypotheses that mutant viruses at virological failure derived from baseline mutants, baseline wt, or wt at virological failure. These analyses were performed separately for Q148R and N155H mutants, excluding sequences with other major integrase resistance mutations than the one being tested.

Genetic linkage between major and accessory mutations was investigated using in-house algorithms.

Results

Pre-treatment viruses were only susceptible to raltegravir and tenofovir (Figure 1). Population sequencing detected the major raltegravir resistant mutations Q148R and N155H and the accessory G163R mutation at virological failure, mixed with the corresponding wild type. All other baseline mutations remained detectable at the time of virological failure.

Out of 3,390 clonal sequences obtained with QDS before raltegravir initiation, nine (0.27%) had the Y143H/C mutation alone, four (0.12%) contained the Q148R mutation, one (0.03%) had the N155H mutation and none (0%) harboured two major mutations together. Of 3,384 clonal sequences obtained with QDS at the time of virological failure, 1,668 (49.29%) were single Q148R mutants, and 1,575 (46.54%) had the N155H alone. Double Q148R + N155H mutants were found in 58 (1.71%) sequences at virological failure. Three baseline Q148R sequences were identical to 79/3,384 (2.34%) sequences at virological failure, whereas the baseline N155H sequence was identical to 83/3,384 (2.45%) sequences at virological failure.

The best evolutionary model obtained with PROTTESTv2.2 (HIVw + Γ with α = 2.921) was used to perform the maximum likelihood tree; a Neighbor Joining distance tree was performed with the second best model detected by PROTTESTv2.2 (JTT + Γ with α = 3.204), given that the best model is not implemented in MEGA4. A Shimodaira and Hasegawa test (Shimodaira and Hasegawa, 1999) considered the Neighbor Joining tree as the one most likely to explain the sequence evolution. The tree topology suggested that Q148R and the N155H mutants evolved in two separate clusters (Figure 2). Most Q148R mutants found at VF originated from pre-existing Q148R mutants whereas N155H mutants found at VF could have originated from either the

baseline N155H mutant or from baseline wildtype viruses. Double Q148R + N155H mutants were found interspersed at the edges of either Q148R or N155H cluster. Single Y143C/H mutants clustered together at baseline but were not found at VF, suggesting that they were less fit, compared to Q148R and/or N155H, in the presence of raltegravir. A four-clustering likelihood mapping technique implemented in TREEPUZZLE v 5.2, independently supported the hypothesis that most Q148R and N155H mutants emerging at virological failure originated, respectively, from pre-existing Q148R and N155H mutants (Figure 2).

No viruses with major raltegravir-resistant mutations had other mutations linked on the same genome before therapy initiation (not shown). Conversely, extensive associations between major and accessory mutations were observed at VF (Table 1). Only 6.5% and 7% of sequences, respectively, contained mutation Q148R and N155H alone at virological failure; all double Q148R+N155H mutants contained other accessory mutations.

Discussion

Our study shows that Q148R and N155H mutants developing during virological failure to raltegravir can originate from minority mutants generated spontaneously before treatment exposure. The spontaneous generation of mutants is predicted by extant models of viral replication in view of HIV-1's high turnover and the error-prone nature of its reverse transcriptase (Coffin, 1995; Najera et al., 1995). Here, mutants could not have been transmitted because integrase inhibitors had just been commercialized. The high antiviral potency of raltegravir (McColl and Chen, 2010) in a context of virtual dual therapy exerted potent selective pressure over pre-existing resistant viruses, as predicted from mathematical modeling of HIV resistance (Nowak et al., 1997).

Pre-existing mutants, however, were found below the error threshold of the technology; point errors at drug resistance sites converting a wildtype to a resistant mutation were 0.2% in our own controls and in previous studies (Shao et al., 2009; Wang et al., 2007). Nevertheless, two independent phylogenetic analyses indicated that pre-existing mutants were the most likely origin of Q148R and N155H mutants at virological failure; indeed, sequences identical to the baseline mutants were found in about 2% of viruses at virological failure. Using various technologies, other studies found pre-existing Q148R/H mutants at similar levels (Ceccherini-Silberstein et al., 2009; Charpentier et al., 2009).

Whereas baseline mutants did not incorporate other mutations in the genome region explored, more than 90% of viruses evolving during virological failure had accumulated accessory mutations in their genome. We cannot completely rule out that the presence of double Q148R + N155H mutants in 1.7% of viruses was due to PCR recombination, (Shao et al., 2009) although it seems unlikely. The two mutations lie 6 codons apart and were found in similar proportions in two overlapping amplicons generated independently through separate triplicate PCRs. Interestingly, dual mutants often carried mutations E138K and G163R on the same genome. The ability of such accessory mutations to restore the impaired fitness of double Q148R + N155H mutants *in vivo* (Fransen et al., 2009) merits further investigation.

This case study provides further evidence that HIV-1 can escape from antiretroviral drug pressure through selection of pre-existing drug-resistant mutants. Our findings underscore the importance of prescribing fully active antiretroviral regimens to all HIV-1-infected subjects, as well as the need of developing more sensitive assays to detect transmitted as well as spontaneously-generated drug-resistant minority variants.

Acknowledgements

This study was supported by the CDTI (Centro para el Desarrollo Tecnológico Industrial), Spanish Ministry of of Science and Innovation (IDI-20080843); the Spanish AIDS network 'Red Temática Cooperativa de Investigación en SIDA' (RD06/0006), 'The European AIDS Treatment Network' (NEAT – European Commission FP6 Program, contract LSHP-CT-2006-037570) and 'CHAIN, Collaborative HIV and Anti-HIV Drug Resistance Network', Integrated Project no. 223131, funded by the European Commission Framework 7 Program. FMC was supported by the Marie Curie European Reintegration Grant number 238885, 'HIV Coevolution', also funded by the European Commission Framework 7 Program. This work was presented in part at the 8th European HIV Drug Resistance Workshop, 17-19 March 2010, Sorrento, Italy (Poster #51).

Conflicts of interest

F García has been a consultant on advisory boards, or has participated in speakers' bureaus, with Roche, Boehringer-Ingelheim, BMS, GSK, Gilead, Janssen, Merck and Pfizer. R Delgado has received consulting fees and grant support from Abbott, BMS, Gilead and Roche. D Dalmau has been a consultant on advisory boards, has participated in speakers' bureaus, or has conducted clinical trials with Roche, Boehringer-Ingelheim, Abbott, BMS, GSK, Gilead, Tibotec, Janssen, Merck and Pfizer. J Martínez-Picado has received research funding, consultancy fees, or lecture sponsorships from GlaxoSmithKline, Merck and Roche. M Álvarez-Tejado works for Roche Diagnostics S.L., Spain, which commercialises the 454 sequencing

technology in Spain. B Clotet has been a consultant on advisory boards, has participated in speakers' bureaus, or has conducted clinical trials with Roche, Boehringer-Ingelheim, Abbott, BMS, GSK, Gilead, Tibotec, Janssen, Merck, Pfizer, Siemens, Monogram Biosciences, and Panacos. R Paredes has received consulting fees from Pfizer and grant support from Pfizer, Siemens, Merck and Boehringer Ingelheim. FM. Codoñer, C Pou, A Thielen, MJ Buzón, JR Santos and L Ruiz report no conflicts of interest relevant to this article. No other potential conflict of interest relevant to this article was reported.

References

Abascal, F., Zardoya, R., Posada, D., 2005. ProtTest: selection of best-fit models of protein evolution. Bioinformatics 21, 2104-2105.

Buzon, M.J., Dalmau, J., Puertas, M.C., Puig, J., Clotet, B., Martinez-Picado, J., 2010. The HIV-1 integrase genotype strongly predicts raltegravir susceptibility but not viral fitness of primary virus isolates. Aids 24, 17-25.

Ceccherini-Silberstein, F., Armenia, D., D'Arrigo, R., Vandenbroucke, I., Van Baelen, K., Van Marck, H., Stuyver, L., Rizzardini, G., Antinori, A., Perno, C., 2009. Baseline Variability of HIV-1 Integrase in Multi-experienced Patients Treated with Raltegravir: A Refined Analysis by Pyrosequencing, 16th Conference on Retroviruses and Opportunistic Infections, Montreal, Canada.

Charpentier, C., Piketty, C., Tisserand, P., Bélec, L., Laureillard, D., Karmochkine, M., Si-Mohamed, A., Weiss, L., 2009. Allele-specific Real-time Polymerase Chain Reaction of the Presence of Q148H, Q148R, and N155H Minority Variants at Baseline of a Raltegravir-based Regimen, 16th Conference on Retroviruses and Opportunistic Infections, Montreal, Canada.

Coffin, J.M., 1995. HIV population dynamics in vivo: implications for genetic variation, pathogenesis, and therapy. Science 267, 483-489.

Cooper, D.A., Steigbigel, R.T., Gatell, J.M., Rockstroh, J.K., Katlama, C., Yeni, P., Lazzarin, A., Clotet, B., Kumar, P.N., Eron, J.E., Schechter, M., Markowitz, M., Loutfy, M.R., Lennox, J.L., Zhao, J., Chen, J., Ryan, D.M., Rhodes, R.R., Killar, J.A., Gilde, L.R., Strohmaier, K.M., Meibohm, A.R., Miller, M.D., Hazuda, D.J., Nessly, M.L., DiNubile, M.J., Isaacs, R.D., Teppler, H., Nguyen, B.Y., 2008. Subgroup and resistance analyses of raltegravir for resistant HIV-1 infection. N Engl J Med 359, 355-365.

Edgar, R.C., 2004. MUSCLE: multiple sequence alignment with high accuracy and high throughput. Nucleic Acids Res 32, 1792-1797.

Fransen, S., Gupta, S., Danovich, R., Hazuda, D., Miller, M., Witmer, M., Petropoulos, C.J., Huang, W., 2009. Loss of raltegravir susceptibility by human immunodeficiency virus type 1 is conferred via multiple nonoverlapping genetic pathways. J Virol 83, 11440-11446.

Guindon, S., Gascuel, O., 2003. A simple, fast, and accurate algorithm to estimate large phylogenies by maximum likelihood. Syst Biol 52, 696-704.

Kumar, S., Tamura, K., Nei, M., 2004. MEGA3: Integrated software for Molecular Evolutionary Genetics Analysis and sequence alignment. Brief Bioinform 5, 150-163.

Liu, T.F., Shafer, R.W., 2006. Web resources for HIV type 1 genotypic-resistance test interpretation. Clin Infect Dis 42, 1608-1618.

McColl, D.J., Chen, X., 2010. Strand transfer inhibitors of HIV-1 integrase: bringing IN a new era of antiretroviral therapy. Antiviral Res 85, 101-118.

Najera, I., Holguin, A., Quinones-Mateu, M.E., Munoz-Fernandez, M.A., Najera, R., Lopez-Galindez, C., Domingo, E., 1995. Pol gene quasispecies of human immunodeficiency virus: mutations associated with drug resistance in virus from patients undergoing no drug therapy. J Virol 69, 23-31.

Nowak, M.A., Bonhoeffer, S., Shaw, G.M., May, R.M., 1997. Anti-viral drug treatment: dynamics of resistance in free virus and infected cell populations. J Theor Biol 184, 203-217.

Paredes, R., Clotet, B., 2010. Clinical management of HIV-1 resistance. Antiviral Res 85, 245-265.

Rhee, S.Y., Gonzales, M.J., Kantor, R., Betts, B.J., Ravela, J., Shafer, R.W., 2003. Human immunodeficiency virus reverse transcriptase and protease sequence database. Nucleic Acids Res 31, 298-303.

Schmidt, H.A., Strimmer, K., Vingron, M., von Haeseler, A., 2002. TREE-PUZZLE: maximum likelihood phylogenetic analysis using quartets and parallel computing. Bioinformatics 18, 502-504.

Shao, W., Boltz, V.F., Kearney, M., Maldarelli, F., Mellors, J.M., Stewart, C., Levitsky, A., Volfovsky, N., Stephens, R.M., Coffin, J.M., 2009. Characterization of HIV-1 sequence artifacts introduced by bulk PCR and detected by 454 sequencing. XVIII International HIV Drug Resistance Workshop: Basic Principles & Clinical Implications. Fort Myers, FL, USA 9-13 June 2009 (Abstract 104). Antiviral Therapy 14 Suppl 1, A123.

Shimodaira, H., Hasegawa, M., 1999. Multiple Comparisons of Log-Likelihoods with Applications to Phylogenetic Inference. Mol Biol Evol 16, 1114-1116.

Steigbigel, R.T., Cooper, D.A., Kumar, P.N., Eron, J.E., Schechter, M., Markowitz, M., Loutfy, M.R., Lennox, J.L., Gatell, J.M., Rockstroh, J.K., Katlama, C., Yeni, P., Lazzarin, A., Clotet, B., Zhao, J., Chen, J., Ryan, D.M., Rhodes, R.R., Killar, J.A., Gilde, L.R., Strohmaier, K.M., Meibohm, A.R., Miller, M.D., Hazuda, D.J., Nessly, M.L., DiNubile, M.J., Isaacs, R.D., Nguyen, B.Y., Teppler, H., 2008. Raltegravir with optimized background therapy for resistant HIV-1 infection. N Engl J Med 359, 339-354.

Varghese, V., Shahriar, R., Rhee, S.Y., Liu, T., Simen, B.B., Egholm, M., Hanczaruk, B., Blake, L.A., Gharizadeh, B., Babrzadeh, F., Bachmann, M.H., Fessel, W.J., Shafer, R.W., 2009. Minority variants associated with transmitted and acquired HIV-1 nonnucleoside reverse transcriptase inhibitor resistance: implications for the use of second-generation nonnucleoside reverse transcriptase inhibitors. J Acquir Immune Defic Syndr 52, 309-315.

Wang, C., Mitsuya, Y., Gharizadeh, B., Ronaghi, M., Shafer, R.W., 2007. Characterization of mutation spectra with ultra-deep pyrosequencing: application to HIV-1 drug resistance. Genome Res 17, 1195-1201.

TABLE 1. FILTERING OF SEQUENCES OBTAINED BY QUANTITATIVE DEEP SEQUENCING

		HXB2 position range*	Integrase codon range*	Reads	Sequences filtered out (homology < 90%)	Sequences left	Unique sequences
Baseline	Amplicon 1	4499-4763	91-178	1951	312	1639	N/A
	Amplicon 2	4621-4900	132-224	1852	100	1752	N/A
	Overlap **	4621-4763	132-178	3803	412	3391	222
Virological failure	Amplicon 1	4499-4763	91-178	2506	456	2050	N/A
	Amplicon 2	4621-4900	132-224	1409	75	1334	N/A
	Overlap **	4621-4763	132-178	3915	531	3384	311

** excluding primer sites.*

*** overlapping regions of the 2 amplicons; N/A, not applicable.*

TABLE 2. LINKAGE ANALYSIS OF MAJOR AND ACCESSORY INTEGRASE INHIBITOR RESISTANCE MUTATIONS AT VIROLOGICAL FAILURE BY QUANTITATIVE DEEP SEQUENCING

Major Mutation	Accessory mutations in integrase codons					# clones	% relative to clones with the major mutation	% relative to total clones at virological failure
	138	140	151	163	Other*			
Consensus B	E	G	V	G	N/A			
Q148R	K	.	.	.	.	895	53.56	26.45
	.	S	.	.	.	357	21.36	10.55
	.	S	.	R	.	143	8.56	4.23
	.	.	.	.	.	109	6.52	3.22
	K	.	.	R	.	93	5.57	2.75
	.	.	.	.	X	74	4.43	2.19
N155H	.	.	.	R	.	1,353	85.47	39.98
	.	.	.	.	.	111	7.01	3.28
	K	.	.	R	.	41	2.59	1.21
	.	.	.	.	X	78	4.93	2.31
Q148R + N155H	K	.	.	R	.	31	53.43	0.92
	.	.	.	R	.	9	15.53	0.27
	.	S	.	R	.	9	15.53	0.27
	K	.	.	.	.	7	12.07	0.21
	.	.	.	.	.	1	1.73	0.03
	.	S	.	.	.	1	1.73	0.03
Y143H + Q148R	K	.	.	.	.	1	33.33	0.03
	K	.	.	R	.	1	33.33	0.03
	.	S	.	R	.	1	33.33	0.03
Y143C + N155H	.	.	.	R	.	3	100	0.09
Y143H + N155H	.	.	.	R	.	8	100	0.24

** only clones representing > 1% of the total sequences obtained by quantitative deep sequencing at virological failure are shown for single Q148R and N155H major mutants; all clones are shown for dual major mutants. "Other" includes the sum of all clones being detected in less than 1% of the total sequences at virological failure that show mutation combinations different from the ones presented in the table; other combinations are represented by "X".*

*** N/A, not applicable.*

FIGURE 1. ANTIRETROVIRAL TREATMENT HISTORY AND VIROLOGICAL AND IMMUNOLOGICAL EVOLUTION

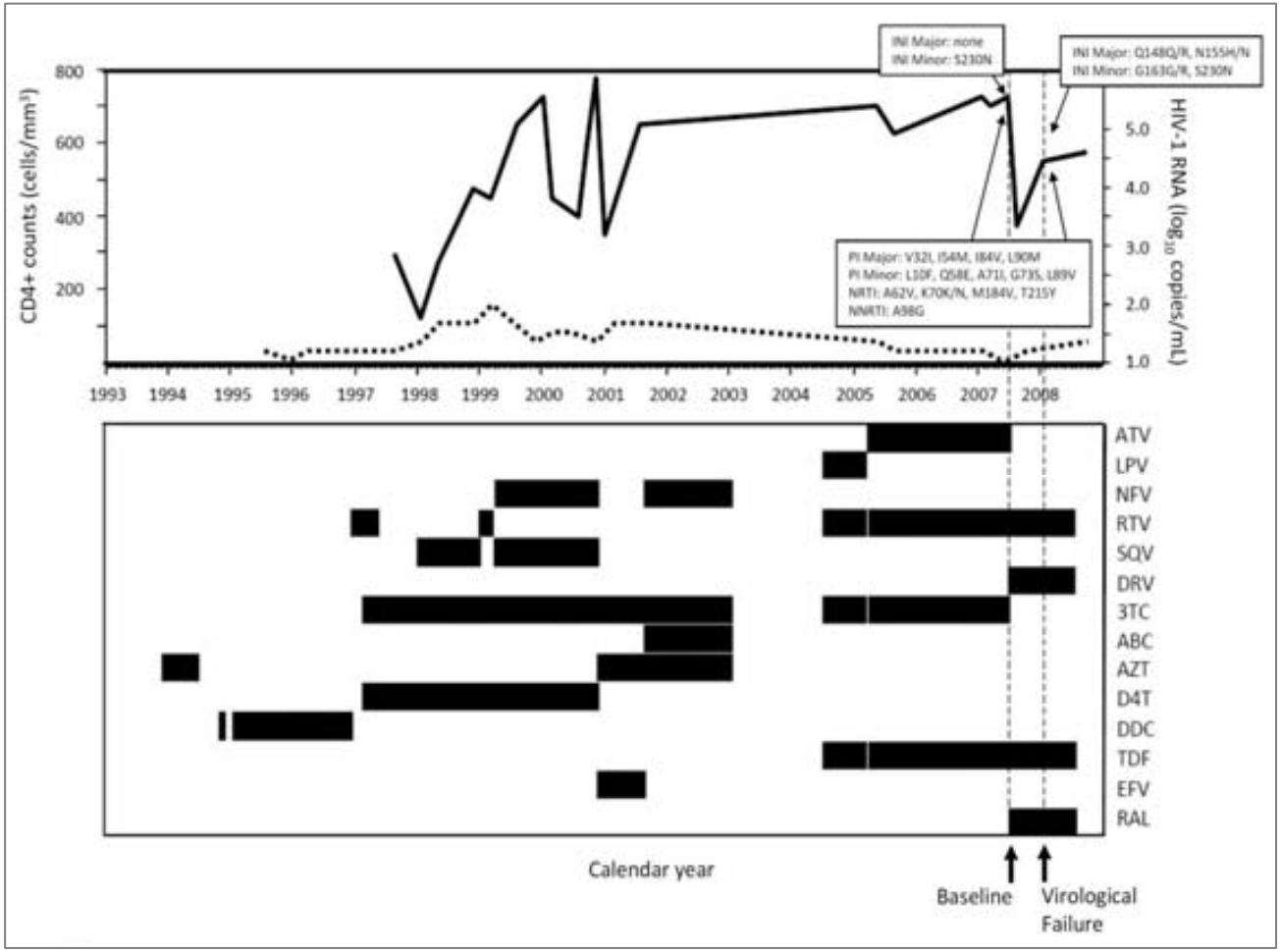

The continuous line in the upper graph represents HIV-1 RNA levels in copies/mL transformed in a logarithmic scale; the dashed line in the upper graph represents CD4+ T-cell counts (CD4 counts) in cells/mm3. Horizontal bars in the lower graph represent the time period during which a given antiretroviral drug was prescribed. Vertical dashed lines represent the timepoints when population and quantitative dep sequencing was performed; i.e., baseline and virological failure. Boxes include resistance mutations detected by population sequencing at baseline and virological failure. PI: protease inhibitor; NRTI: nucleoside reverse transcriptase inhibitor; NNRTI: non-nucleoside reverse transcriptase inhibitor; IN: integrase; ATV: atazanavir; LPV: lopinavir; NFV: nelfinavir; RTV: ritonavir; SQV: saquinavir; DRV: darunavir; 3TC: lamivudine; ABC: abacavir; AZT: zidovudine; D4T: stavudine; DDC: zalcitabine; TDF: tenofovir diprivoxil fumarate; EFV: efavirenz; RAL: raltegravir; None: antiretroviral treatment interruption. Graph developed with and adapted from the ART-AiDE (Antiretroviral Therapy - Acquisition & Display Engine) Program, Stanford HIV Drug Resistance Database.

FIGURE 2. ORIGIN OF VIRUSES ESCAPING RALTEGRAVIR PRESSURE. LEFT PANEL: EVOLUTION OF INTEGRASE SEQUENCES OBTAINED BY QUANTITATIVE DEEP SEQUENCING

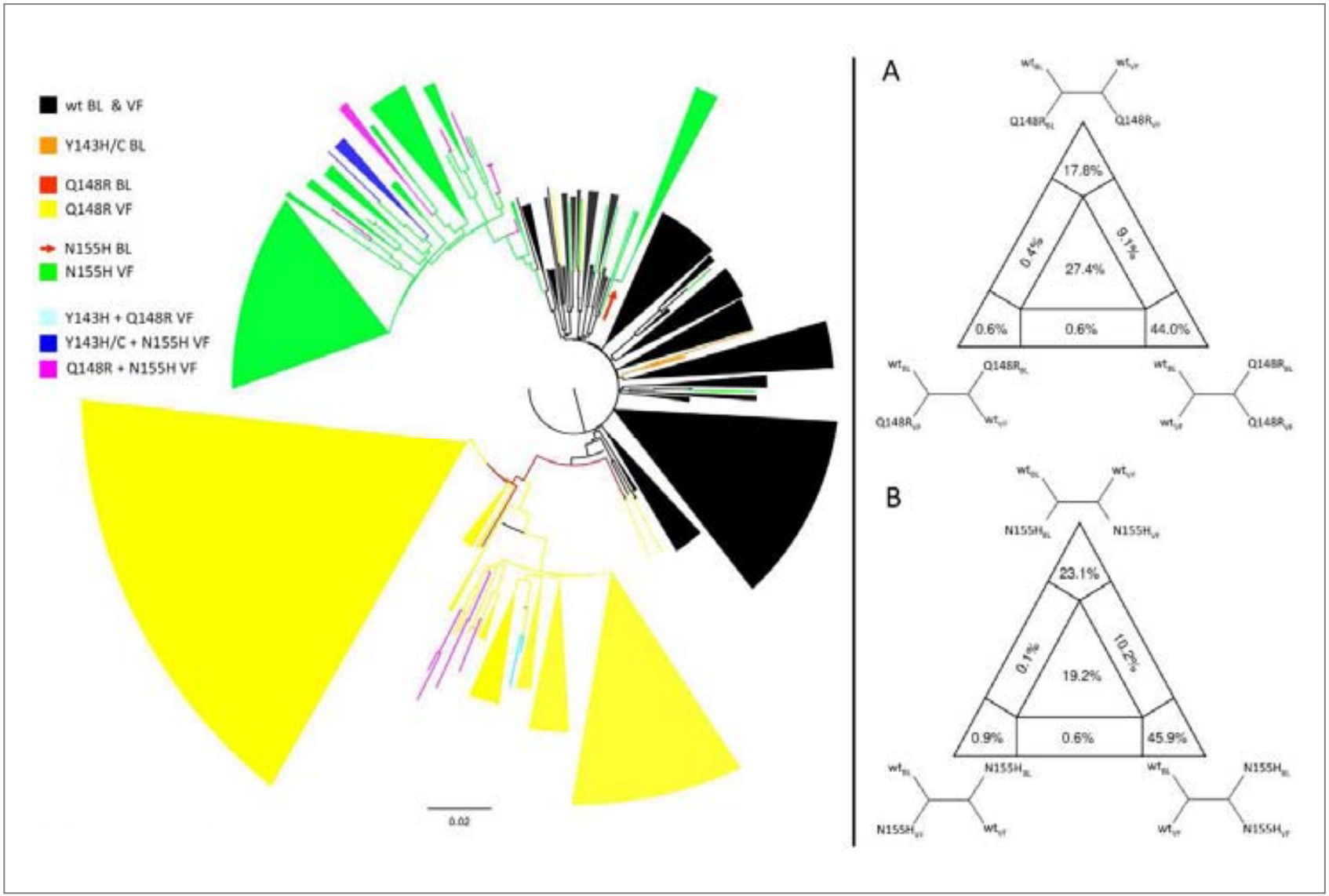

Neighbor Joining Tree with branch lengths computed according to a heterogeneous JTT + Γ model of protein evolution. This was the most likely tree to explain sequence evolution according to a Shimodaira-Hasegawa test.(Shimodaira and Hasegawa, 1999) For clarity, monophyletic groups of sequences containing the same major integrase resistance mutation or combination of mutations were collapsed into a cartoon with colours indicating the explored mutation and the size of the cartoon being proportional to the number of sequences included. Right panels: Quartet likelihood mapping analysis of the origin of Q148R and N155H raltegravir-resistant viruses detected at virological failure. Four clusters of sequences containing, respectively, mutants at baseline (BL), mutants at virological failure (VF), wildtype (wt) viruses at BL; and wt viruses at VF were created. All possible quartets of sequences containing one sequence from each cluster were generated. A distance phylogenetic tree was then calculated for each sequence quartet and was compared with the phylogeny of each of our three hypotheses, shown in the triangle vertices. Numbers in the triangle show the proportion of quartet phylogenetic trees matching each hypothesis. The percentage of solved phylogenies is shown in the triangle vertices; unsolved phylogenies are represented in intermediate regions of the triangle. Separate analyses were performed for single Q148R (panel A) and single N155H (panel B) mutants at virological failure. Wildtype was defined as absence of major integrase inhibitor-resistant mutations at positions 143, 148 and 155.

Addendum III

Published Manuscripts in Portable Document Format (PDF)

OPEN ACCESS Freely available online

PLOS ONE

HIV-1 Tropism Testing in Subjects Achieving Undetectable HIV-1 RNA: Diagnostic Accuracy, Viral Evolution and Compartmentalization

Christian Pou[1]*, Francisco M. Codoñer[1], Alexander Thielen[3], Rocío Bellido[1], Susana Pérez-Álvarez[1], Cecilia Cabrera[1], Judith Dalmau[1], Marta Curriu[1], Yolanda Lie[5], Marc Noguera-Julian[1], Jordi Puig[2], Javier Martínez-Picado[1,4], Julià Blanco[1], Eoin Coakley[5], Martin Däumer[6], Bonaventura Clotet[1,2], Roger Paredes[1,2]*

1 Institut de Recerca de la SIDA irsiCaixa–HIVACAT, Hospital Universitari Germans Trias i Pujol, Universitat Autònoma de Barcelona, Catalonia, Spain, **2** HIV Unit-Fundació Lluita contra la SIDA, Hospital Universitari Germans Trias i Pujol, Universitat Autònoma de Barcelona, Catalonia, Spain, **3** Max-Planck-Institut für Informatik, Saarbücken, Germany, **4** Institució Catalana de Recerca i Estudis Avançats (ICREA), Barcelona, Spain, **5** Monogram Biosciences Inc., South San Francisco, California, United States of America, **6** Institut für Immunologie und Genetik, Kaiserlautern, Germany

Abstract

Background: Technically, HIV-1 tropism can be evaluated in plasma or peripheral blood mononuclear cells (PBMCs). However, only tropism testing of plasma HIV-1 has been validated as a tool to predict virological response to CCR5 antagonists in clinical trials. The preferable tropism testing strategy in subjects with undetectable HIV-1 viremia, in whom plasma tropism testing is not feasible, remains uncertain.

Methods & Results: We designed a proof-of-concept study including 30 chronically HIV-1-infected individuals who achieved HIV-1 RNA <50 copies/mL during at least 2 years after first-line ART initiation. First, we determined the diagnostic accuracy of 454 and population sequencing of gp120 V3-loops in plasma and PBMCs, as well as of MT-2 assays before ART initiation. The Enhanced Sensitivity Trofile Assay (ESTA) was used as the technical reference standard. 454 sequencing of plasma viruses provided the highest agreement with ESTA. The accuracy of 454 sequencing decreased in PBMCs due to reduced specificity. Population sequencing in plasma and PBMCs was slightly less accurate than plasma 454 sequencing, being less sensitive but more specific. MT-2 assays had low sensitivity but 100% specificity. Then, we used optimized 454 sequence data to investigate viral evolution in PBMCs during viremia suppression and only found evolution of R5 viruses in one subject. No *de novo* CXCR4-using HIV-1 production was observed over time. Finally, Slatkin-Maddison tests suggested that plasma and cell-associated V3 forms were sometimes compartmentalized.

Conclusions: The absence of tropism shifts during viremia suppression suggests that, when available, testing of stored plasma samples is generally safe and informative, provided that HIV-1 suppression is maintained. Tropism testing in PBMCs may not necessarily produce equivalent biological results to plasma, because the structure of viral populations and the diagnostic performance of tropism assays may sometimes vary between compartments. Thereby, proviral DNA tropism testing should be specifically validated in clinical trials before it can be applied to routine clinical decision-making.

Citation: Pou C, Codoñer FM, Thielen A, Bellido R, Pérez-Álvarez S, et al. (2013) HIV-1 Tropism Testing in Subjects Achieving Undetectable HIV-1 RNA: Diagnostic Accuracy, Viral Evolution and Compartmentalization. PLoS ONE 8(8): e67085. doi:10.1371/journal.pone.0067085

Editor: Alan Landay, Rush University, United States of America

Received November 21, 2012; **Accepted** May 15, 2013; **Published** August 1, 2013

Funding: This study was supported through an unrestricted research grant from Pfizer, 'CHAIN, Collaborative HIV and Anti-HIV Drug Resistance Network', Integrated Project number 223131, funded by the European Commission Framework 7 Program, the Spanish AIDS network 'Red Temática Cooperativa de Investigación en SIDA' (RD06/0006), and the 'Gala contra la sida – Barcelona 2011'. FMC was supported by the Marie Curie European Reintegration Grant number 238885, 'HIV Coevolution', European Commission Framework 7 Program. None of the funding bodies had any role in the design, collection, analysis, or interpretation of data, in the writing of the manuscript, or in the decision to submit the manuscript for publication.

Competing Interests: JMP has received research funding, consultancy fees, or lecture sponsorships from GlaxoSmithKline, Merck. JB has received research funding from Merck and consultancy fees from GlaxoSmithKline. YL and EC are employees of Monogram Biosciences, South San Francisco California, United States of America. BC has been a consultant on advisory boards or participated in speakers' bureaus or conducted clinical trials with Boehringer-Ingelheim, Abbott, GlaxoSmithKline, Gilead, Janssen, Merck, Shionogi and ViiV. RP has received consulting fees from Pfizer and grant support from Pfizer, Roche Diagnostics, Siemens, Merck and Boehringer-Ingelheim. CP, FMC, AT, RB, SPA, CC, JD, MC, JP, MN and MD report no competing interests. This does not alter the authors' adherence to all the PLOS ONE policies on sharing data and materials.

* E-mail: cpou@irsicaixa.es (CP); rparedes@irsicaixa.es (RP)

Introduction

The efficacy of CCR5 antagonist therapy depends on the accurate characterization of HIV-1 tropism. A major cause of virological failure to CCR5-antagonist therapy is the emergence of pre-existing CXCR4-using viruses, often missed by tropism assays [1,2]. Retrospective reanalyses of pre-treatment plasma samples from maraviroc trials in treatment-naïve [3] and -experienced [4,5,6] individuals found that population and 454 sequencing (454 Life Sciences/Roche) of the V3 loop of gp120 were able to predict

virological response to maraviroc as accurately as Trofile™ and the enhanced sensitivity version of Trofile™ (ESTA), respectively [7,8]. In the MERIT trial, first-line therapy with maraviroc in treatment naïve individuals only achieved non-inferiority to efavirenz when the ESTA [3] or 454 sequencing [9] and not the former, less sensitive version of Trofile™ were used to assess presence of CXCR4-using virus at screening. Moreover, the risk of virological failure to maraviroc-including therapy was directly proportional to the amount of CXCR4-using viruses in the viral population in other studies [10]. Presence of as little as 2% CXCR4-using viruses in the population conferred an increased risk of virological failure to maraviroc-including therapy. As with other regimens, lower CD4+ counts, resistance to other drugs or inclusion of less than 3 active drugs in the regimen further increased the risk of virological failure to maraviroc regimens.

Tropism assays validated in clinical trials to date characterize plasma viruses from subjects with detectable HIV-1 RNA. Maraviroc clinical trials enrolled individuals with HIV-1 RNA ≥2000 copies/mL (MERIT Study in ART-naïve individuals) and ≥5000 copies/mL (MOTIVATE 1&2 studies in treatment – experienced subjects). However, most HIV-1-infected individuals who could potentially benefit from the favorable toxicity and drug-drug-interaction profile of CCR5 antagonists have undetectable HIV-1 RNA levels under antiretroviral therapy (ART). The optimal strategy to evaluate HIV tropism in aviremic subjects, in whom plasma tropism testing is not feasible, remains uncertain. Testing of stored pre-therapy plasma samples, when available, may not capture potential virus evolution towards CXCR4-use during ART. Conversely, proviral DNA testing might assess different virus populations than those circulating simultaneously in plasma, implying that both tests may not necessarily provide equivalent genotypic or phenotypic information for clinical decision-making and may need to be validated independently in clinical trials.

We designed this study to gain further insight into the aforementioned questions. First, we investigated the ability of different state-of-the-art genotypic and phenotypic tropism tests in proviral DNA and plasma RNA to detect CXCR4-using viruses relative to the ESTA in 30 subjects before they initiated first-line ART without CCR5 antagonists. Then, we examined if virus evolution occurred after at least 2 years of persistent HIV-1 RNA suppression under ART in these same individuals. Finally, we used population differentiation tests to investigate if pre-treatment PBMC V3 form populations were different from a) those simultaneously observed in plasma and b) those observed in PBMCs after at least 2 years of continuous HIV-1 RNA suppression.

Materials and Methods

Study design and participants

This was a retrospective proof-of-concept study that included chronically HIV-1-infected adults who achieved persistent HIV-1 RNA levels <50 copies/mL during at least 2 years after starting first-line ART without CCR5 antagonists. Subjects had to have cryopreserved samples available for testing within 6 months before ART initiation (baseline, T1) and after at least 2 years of undetectable viremia (persistent viremia suppression, T2). (Figure 1) The Institutional Review Board of the Hospital Universitari Germans Trias i Pujol, Badalona, Spain, approved the study; participants provided written informed consent for retrospective sample testing. Tropism tests performed at T1 included the *Enhanced-Sensitivity Trofile™Assay* (ESTA), direct cocultivation of patient-derived PBMCs with MT2 cells (MT2 assay), and population and 454 sequencing of the V3-loop in plasma RNA and proviral DNA. Tropism tests performed at T2 included population and 454 sequencing in PBMCs and the MT2 assay. HIV-1 RNA levels (NucliSens EasyQ HIV-1, Biomerieux, Marcy l'Etoile, France), CD4+ and CD8+ cells counts were determined at regular 3 to 4-month intervals as part of the routine clinical follow-up of subjects.

Tropism testing

The ESTA was performed in Monogram Biosciences, South San Francisco, USA, blinded for clinical characteristics or other tropism testing results. ESTA was considered the technical reference standard for comparison with the remaining tropism assays because a) it has been used in most CCR5 antagonist clinical trials, b) is widely recognized as a sensitive, accurate and robust tropism test. c) is the only FDA-approved and CLIA-certified HIV tropism test and d) is readily available to HIV clinics worldwide. For the MT2 assay, HIV-1 was isolated by direct cocultivation with $1–5\times10^6$ patient-derived cryopreserved PBMCs with 1×10^6 MT2 cell line, in duplicate, as in [11]. Functional CXCR4-using viruses were defined by their ability to grow in MT2 cocultures, as confirmed by p24 production. Virus growth ability was evaluated with cocultures of 1×10^6 patient-derived PHA-stimulated PBMCs and PHA-stimulated PBMC from healthy seronegative donors. For population and 454 V3 loop sequencing, HIV-1 RNA was extracted from 1 mL of plasma after ultracentrifugation at 30,000 rpm during 1.5 hours; HIV-1 DNA was extracted from 10 million PBMCs. Reverse transcription and DNA amplification were performed in triplicate parallel reactions followed by pooling of PCR products to avoid founder effects. First-round PCR products were used for both population and 454 V3-loop sequencing. The V3-loop of functional viruses extracted from the supernatant of positive MT2 assays was also sequenced for comparison with 454 sequencing. The combined error threshold for PCR amplification and 454 sequencing was established identifying the percentage of different V3-loop unique sequences (haplotypes) obtained after amplifying a commercial pNL4.3 DNA clone under the same PCR conditions used to generate patient samples and using the same filtering steps. A total of 2,702 V3-loop pNL4.3 clonal sequences and 154 different haplotypes were obtained by 454 sequencing, which followed a Poisson-like distribution. The 99th percentile of such distribution established the threshold for detecting "valid" V3-loop haplotypes at ≥0.6% of the viral population. The percentage of valid V3-loop haplotypes with predicted CXCR4-using tropism was then calculated.

Statistical analyses

Mean and 95% confidence intervals of the sensitivity, specificity, positive and negative predictive value and accuracy of each assay were calculated assuming a binomial distribution of the data. "Accuracy" (also known as "Fraction Correct") was defined as: (True positives + True negatives)/Total. V3 loop genotypes derived from population and 454 sequencing were interpreted using Geno2Pheno$_{[coreceptor]}$ [12] at false positive rates (FPR) ranging from 3.5% to 20%. The FPR cut-off providing better diagnostic performance relative to the ESTA was used to define viral tropism in subsequent analyses. HIV subtype was determined with the Geno2Pheno$_{[coreceptor]}$ tool. The prevalence of subjects with CXCR4-using viruses was determined with each assay and setting; differences relative to ESTA were tested for significance using a two-sided exact binomial test. Statistical analyses were performed with *R* [13].

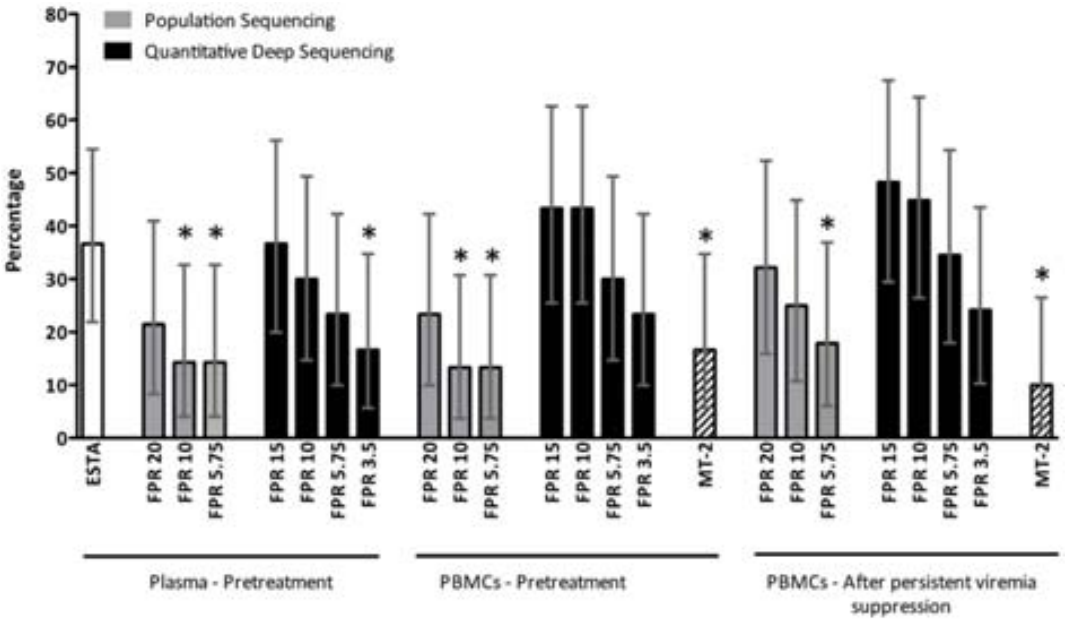

Figure 1. Prevalence of CXCR4-using viruses using different tropism assays and settings. Bar plot showing the mean and 95% confidence intervals of the prevalence of subjects with CXCR4-using viruses using different tropism assays and settings. The Geno2Pheno$_{[coreceptor]}$ clinical model was only used in pre-treatment bulk sequences derived from plasma RNA; otherwise, the clonal model was used. ESTA, Enhanced-Sensitivity Trofile^{TM} Assay; FPR, Geno2Pheno$_{[coreceptor]}$ false positive rate used to assign tropism; MT-2, Direct cocultivation of patient-derived peripheral blood mononuclear cells with MT-2 cells. * p-value$<$0.05, two-sided exact binomial tst.
doi:10.1371/journal.pone.0067085.g001

Phylogenetic analyses

The phylogenetic relatedness between viruses present in plasma and PBMCs at T1 and in PBMCs at T2 was determined using valid 454 sequencing V3-loop haplotypes. Sequences were codon-aligned with HIValign; the optimal nucleotide evolution model was determined with FindModel (http://www.hiv.lanl.gov). Maximum likelihood trees were constructed with PhyML [14] and were edited with Mega v4.0 [15,16]; node reliability was evaluated with 1,000 bootstraps. Tree labels were manually edited to make their size proportional to the sequence representation in the virus population. Trees were rooted at the most prevalent plasma V3-loop haplotype present before antiretroviral treatment initiation. Patterns of temporal and CXCR4-using clustering were investigated in subjects with 454 sequencing data available from the three compartments (plasma at T1 and PBMC at T1 and T2). The presence or absence of CXCR4-using clustering was only evaluated in subjects with at least two CXCR4-using viruses in any compartment. CXCR4-using clustering was defined as the presence of at least one cluster of at least two CXCR4-using haplotypes, supported by a bootstrap value or 70% or higher. Temporal clustering was defined as the grouping of all V3-loop haplotypes from one timepoint into a single cluster, supported by a bootstrap value or 70% or higher.

Population differentiation

Population differentiation was assessed using the tree topology-based Slatkin-Maddison test [17] implemented in HYPHY [18]. The Slatkin-Maddison test compares tree topologies without taking into account haplotype frequency in the population. In previous controls, no compartmentalization was observed between duplicate measurements of 6 different PBMC samples by the Slatkin-Maddison test. However, an analysis of molecular variance (AMOVA) [19] provided statistically significant differences between duplicate samples, indicating that AMOVA can provide false positive results when deep sequencing data is used to estimate frequencies of closely related viral variants and, therefore, is not suitable for this analysis.

Sequence Data Sets

V3-loop population and 454 sequences were deposited in GenBank (http://www.ncbi.nlm.nih.gov/genbank/index.html) and the Sequence Read Archive (http://www.ncbi.nlm.nih.gov/sra/), respectively, accession numbers: JF297475-JF297561 and SRP018530. Descriptions of biological source materials used in experimental assays are available in the Biosample database (http://www.ncbi.nlm.nih.gov/biosample) under consecutive accession numbers SAMN01914993 to SAMN01915082. The BioProject (http://www.ncbi.nlm.nih.gov/bioproject) code for this work is PRJNA188778.

Results

Subjects' characteristics

Thirty-five chronically HIV-1-infected adults were recruited for this study in Badalona, Spain, between June and October 2008. Subjects had to have stored samples available for tropism testing within 6 months before ART initiation (baseline, T1) and after at least 2 years of undetectable viremia (T2). (Figure 1) Five individuals were excluded from the analysis due to non-interpretable ESTA results (n = 1), treatment interruption during follow-up (n = 1), lack of amplification by any genotypic method (n = 1) and absence of sufficient sample material for testing (n = 2). The median age of the 30 individuals providing data was 44 years; they were mostly men and had acquired HIV through sexual practices (Table 1). The median time between T1 and T2 were 45 months. The median T1 viremia and CD4+ counts were 58,500 copies/mL and 224 cells/mm^3, respectively; median nadir CD4+ counts

Table 1. Subjects' Characteristics.[a]

Age, median (IQR)	44 (39; 49)
Gender, n (%)	
Male	20 (67.7)
Female	10 (33.3)
Transmission route, n (%)	
Heterosexual	11 (36.7)
Homosexual	11 (36.7)
IVDU	2 (6.7)
IVDU + Homosexual	1 (3.3)
Transfusion of blood derivatives	1 (3.3)
Unknown	4 (13.3)
Pre-treatment HIV-1 RNA copies/mL, median (IQR)	58,500 (7,925; 107,500)
Pre-treatment CD4+ T cell count (cells/mm^3)	
Absolute, median (IQR)	224 (120; 326)
Percentage, median (IQR)	15 (10; 19)
Nadir, median (IQR)	216 (86; 267)
CD4+ T cell count (cells/mm^3) after >2 years of viremia suppression	
Absolute, median (IQR)	560 (416; 788)
Percentage, median (IQR)	29 (25; 37)
Pre-treatment CD8+ T cell count (cells/mm^3)	
Absolute, median (IQR)	886 (657; 1,196)
Percentage, median (IQR)	41 (38; 51)
CD8+ T cell count (cells/mm^3) >2 years of viremia suppression	
Absolute, median (IQR)	959 (665; 1,120)
Percentage, median (IQR)	62 (56; 71)
Antiretroviral treatment initiated, n (%)	
2 NRTIs + PIr	14 (46.7)
2 NRTIs + NNRTI	12 (40)
2 NRTIs + NNRTI + PIr	3 (10)
2 NRTIs	1 (3.3)
Time in months between events	
HIV diagnosis and T1, median (IQR)	2 (1;8)
T1 and T2, median (IQR)	45 (32;72)
ART initiation and T2, median (IQR)	33 (25; 51)

[a]IQR, 25th–75th interquartile range; ART, Antiretroviral treatment; IVDU, Intravenous Drug User; NRTI, Nucleoside reverse transcriptase inhibitor; NNRTI, Non-nucleoside reverse transcriptase inhibitor; PIr, Ritonavir-boosted Protease Inhibitor; T1, first timepoint when tropism was measured (i.e. before ART initiation); T2, second timepoint when tropism was measured (i.e., after >2 years of HIV-1 RNA suppression).

doi:10.1371/journal.pone.0067085.t001

were 215 cells/mm^3. Median CD4+ counts increased to 560 cells/mm^3 at T2 while HIV-1 RNA levels remained <50 copies/mL. Five individuals developed one HIV-1 RNA blip each during follow-up (HIV-1 RNA range: 125–275 copies/mL, incidence rate 1.7 blips/1,000 person-years). 454 sequencing produced a median (interquartile range, IQR) number of total, valid and unique V3-loop sequences of 5,366 (3,228 ; 6,553), 4,591 (2,751 ; 5,371) and 7 (4 ; 15) in plasma at T1; 3,983 (3,042 ; 5,256), 3,315 (2,238 ; 3,963) and 8 (6 ; 14) in PBMCs at T1; and 3,498 (2,444 ; 4,512), 2,562 (1,718 ; 3,509) and 8 (6 ; 15) in PBMCs at T2, respectively. All subjects were infected with subtype B HIV.

Accuracy of tropism assays relative to ESTA

The accuracy of tropism tests in plasma and PBMCs was only evaluated before ART initiation, when all assays could be simultaneously compared to the technical reference standard in the same clinical conditions. (Table 2)

454 sequencing of plasma viruses provided the best agreement with ESTA, particularly at a Geno2Pheno$_{[coreceptor]}$ False Positive Rate (FPR) of 10% (73% sensitivity, 95% specificity, 87% accuracy). Increasing the FPR to 15% did not improve the sensitivity but worsened the specificity; decreasing the FPR improved the specificity to 100%, but decreased the sensitivity to levels overlapping those of population sequencing. (Figure 1, Table 2) Interestingly, 454 sequencing was less accurate in proviral DNA than in plasma HIV-1 RNA, being similarly sensitive but less specific. Increases in specificity could be achieved by decreasing the FPR cut-off, but this also decreased the assay's sensitivity considerably. Moreover, the PBMC X4 load in subjects with detectable CXCR4-using HIV in PBMCs by 454 but R5

Table 2. Accuracy of Tropism Assays Relative to the Enhanced-Sensitivity Trofile™ Assay.[a]

	Tests performed in pre-treatment Plasma RNA							Tests performed in pre-treatment Proviral DNA							
	Population V3-loop sequencing[b]			454 V3-loop sequencing				Population V3-loop sequencing[b]			454 V3-loop sequencing				MT-2[c]
G2P FPR[b]	**20**	**10**	**5.75**	**15**	**10**	**5.75**	**3.5**	**20**	**10**	**5.75**	**15**	**10**	**5.75**	**3.5**	
Sensitivity	60	40	40	72.7	72.7	63.6	45.5	63.6	36.4	36.4	72.7	72.7	54.5	45.5	45.5
	(26.2–87.4)	(12.1–73.8)	(12.1–73.8)	(39–94)	(39–94)	(30.8–89.1)	(16.7–76.6)	(30.8–89.1)	(10.9–69.2)	(10.9–69.2)	(39–94)	(39–94)	(23.4–83.3)	(16.7–76.6)	(16.7–76.6)
Specificity	100	100	94.4	84.2	94.7	100	100	100	100	100	73.7	73.7	84.2	89.5	100
	(74–100)	(74–100)	(74–100)	(60.4–96.6)	(74–99.9)	(75.1–100)	(75.1–100)	(75.1–100)	(75.1–100)	(75.1–100)	(48.8–90.9)	(48.8–90.9)	(60.4–96.6)	(66.9–98.7)	(75.1–100)
PPV[d]	100	100	100	72.7	88.9	100	100	100	100	100	61.5	61.5	66.7	71.4	100
	(42.1–100)	(28.4–100)	(28.4–100)	(30–94)	(51.8–99.7)	(47.3–100)	(35.9–100)	(47.3–100)	(28.4–100)	(28.4–100)	(31.6–86.1)	(31.6–86.1)	(29.9–92.5)	(29–96.3)	(35.9–100)
NPV[e]	81.8	75	75	84.2	85.7	82.6	76	82.6	73.1	73.1	82.4	82.4	76.2	73.9	76
	(59.7–94.8)	(53.3–90.2)	(53.3–90.2)	(60.4–96.6)	(63.7–97)	(61.2–95)	(54.9–90.6)	(61.2–95)	(52.2–88.4)	(52.2–88.4)	(56.6–96.2)	(56.6–96.2)	(52.8–91.8)	(51.6–89.8)	(54.9–90.6)
Accuracy[f]	85.7	78.6	78.6	80	86.7	86.7	80	86.7	76.7	76.7	73.3	73.3	73.3	73.3	80
	(67.3–96)	(59–91.7)	(59–91.7)	(61.4–92.3)	(69.3–96.2)	(69.3–96.2)	(61.4–92.3)	(69.3–96.2)	(57.7–90.1)	(57.7–90.1)	(54.1–87.7)	(54.1–87.7)	(54.1–87.7)	(54.1–87.7)	(61.4–92.3)

[a]Values are mean percentages (95% confidence interval of the mean), calculated assuming a binomial distribution of the data.
[b]*G2P FPR*, Geno2Pheno$_{[coreceptor]}$ false positive rate used for population and 454 sequencing to assign CXCR4 use . The Geno2Pheno$_{[coreceptor]}$ clonal model was always used.
[c]*MT-2*, Direct cocultivation of patient-derived peripheral blood mononuclear cells with MT-2 cells.
[d]*PPV*, Positive Predictive Value.
[e]*NPV*, Negative Predictive Value.
[f]"Accuracy" is defined as: (True positives + True negatives)/Total.
doi:10.1371/journal.pone.0067085.t002

Table 3. Longitudinal tropism testing results per subject.[a,b,c]

Subject ID	Before ART initiation (T1)								≥2 years of HIV-1 RNA suppression (T2)			
	HIV-1 RNA (cop/mL)	CD4+ count (c/mm^3)	Tropism in Plasma RNA			Tropism in Proviral DNA			CD4+ count (c/mm^3)	Tropism in Proviral DNA		
			ESTA	Pop Seq	454 (% X4)	Pop Seq	454 (% X4)	MT2		Pop Seq	454 (% X4)	MT2
1	300,000	191	DM	X4	100	X4	100	SI	326	X4	29	SI
2	60,000	88	DM	X4	100	X4	98.1	SI	272	X4	30.4	-
3	29,000	55	DM	X4	100	X4	90.1	SI	904	X4	79.4	SI
4	130,000	345	DM	X4	67.7	X4	93.9	SI	655	X4	100	SI
5	1,300,000	82	DM	-	12.2	-	15.7	SI	368	X4	16	-
6	40,000	231	DM	-	1.8	X4	68.9	-	950	X4	61.5	-
7	6,800	262	DM	-	2.8	-	-	-	528	X4	19.3	-
8	52,000	259	DM	X4	7.6	X4	15.4	-	872	X4	22.6	-
9	65,000	214	DM	X4	-	X4	1.8	-	471	X4	-	-
10	80,000	35	DM	NA	NA	-	-	-	488	-	-	-
11	89,000	379	DM	-	-	-	-	-	684	-	18.1	-
12	65,000	213	-	-	16.3	-	-	-	502	-	-	-
13	88,000	614	-	NA	-	-	99	-	1,384	NA	NA	-
14	2,300	265	-	-	-	-	36	-	665	-	3.3	-
15	1,220	418	-	-	-	-	-	-	760	-	-	-
16	1,290	281	-	-	-	-	-	-	298	-	-	-
17	57,000	539	-	-	-	-	-	-	1,232	-	-	-
18	860,000	52	-	-	-	-	-	-	608	-	-	-
19	180,000	131	-	-	-	-	11.4	-	1,056	-	-	-
20	226,195	182	-	-	-	-	-	-	490	-	-	-
21	1,600	64	-	-	-	-	7.3	-	283	-	1.2	-
22	1,000	331	-	-	-	-	-	-	1,001	NA	-	-
23	1,400	335	-	-	-	-	1.1	-	590	-	-	-
24	100,000	325	-	-	-	-	-	-	420	-	-	-
25	8,300	217	-	-	-	-	-	-	529	-	-	-
26	200,000	284	-	-	-	-	-	-	614	-	1.3	-
27	87,000	269	-	-	-	-	-	-	673	-	-	-
28	43,000	184	-	-	-	-	-	-	524	-	-	-
29	16,000	158	-	-	-	-	-	-	403	-	-	-
30	32,000	39	-	-	-	-	-	-	382	-	1.9	-

[a]*ESTA, Enhanced-Sensitivity Trofile™ Assay*; *Pop Seq*, population sequencing of the V3-loop; *454*, 454 sequencing of the V3-loop; *MT2*, direct co-cultivation of patient-derived peripheral blood mononuclear cells with MT-2 cells. HIV-1 RNA levels are in copies/mL; CD4+ cell counts are in cells/mm^3.

[b]Population and 454 sequencing data shown here used the Geno2Pheno$_{[coreceptor]}$ false positive rate cut-off providing highest accuracy when assigning HIV-1 tropism, i.e.: 20% and 10%, respectively. Based on internal error controls, only V3 forms present in ≥0.6% of viruses were considered for tropism prediction with 454 sequencing.

[c]Tests detecting CXCR4-using HIV are reported as "*dual-mixed, DM*" for ESTA, "*X4*" for population sequencing, "*percent of X4 viruses*" for 454, and "*syncytium-inducing, SI*" for MT-2 assays; for clarity, viruses only using CCR5 are shown as dashes; NA, tropism test result not available due to lack of amplification.

doi:10.1371/journal.pone.0067085.t003

HIV-1 by ESTA (Table 3, subjects 13, 14, 19, 21 and 23) was usually high enough to suggest a different HIV population structure in plasma and PBMCs, rather than fluctuations around the sensitivity threshold of each technology amenable to fine-tuning.

Population sequencing was invariably less sensitive than 454 sequencing although it retained high specificity. No differences in accuracy were observed using either 10% or 5.75% FPR cut-offs. However, increasing the FPR threshold to 20% improved the sensitivity of the assay without compromising its specificity. Of note, population sequencing achieved similar accuracy in proviral DNA than in plasma HIV-1 RNA. All subjects with CXCR4-using viruses by population sequencing except one had CXCR4-using virus levels above 15% by 454 sequencing in proviral DNA, further supporting the idea that clinically relevant CXCR4-using cut-off levels might be different for plasma and PBMCs.

The MT-2 assays had low sensitivity but high specificity. As observed elsewhere [20], internal controls of direct cocultivation of patient and healthy donor PBMCs indicated that we were only capable of obtaining productive HIV infection from about 50% of subjects overall (not shown).

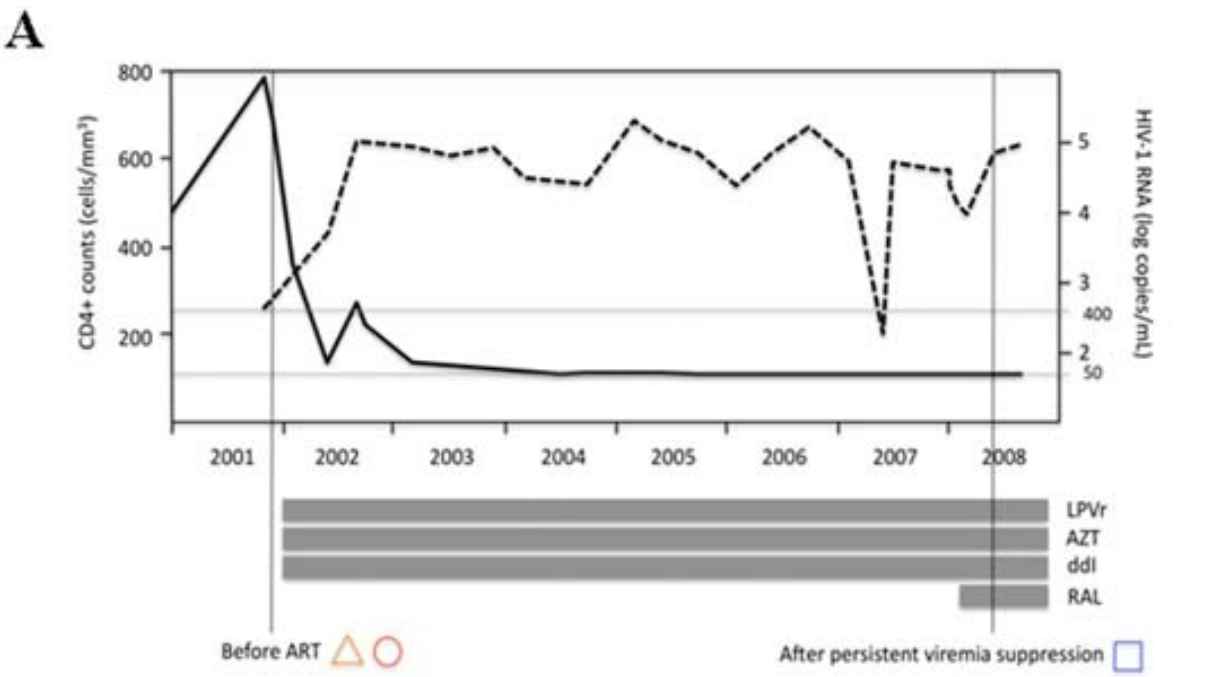

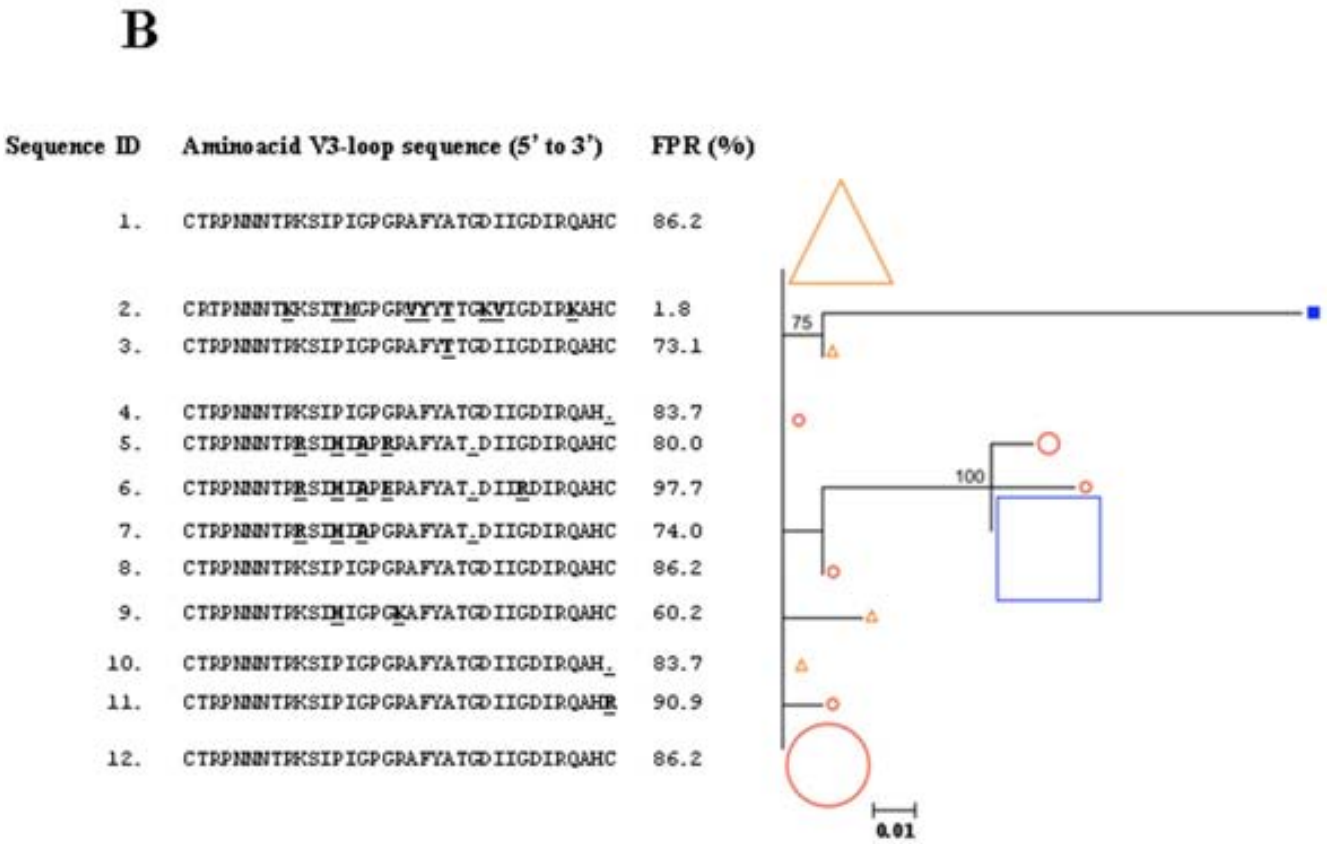

Figure 2. Selection of a CXCR4-using variant above the 454 sequencing error threshold during persistent viremia suppression in Subject 26. ***Panel A, antiretroviral treatment history, virological and immunological evolution.*** Continuous line, HIV-1 RNA levels; dashed line, CD4+ counts; horizontal bars, time period during which a given antiretroviral drug was prescribed. Vertical lines indicate the timepoints when 454 sequencing was performed. LPVr, lopinavir/ritonavir; AZT, zidovudine; ddI, didanosine; RAL, raltegravir. ***Panel B, maximum likelihood nucleotide-based phylogenetic tree*** including V3-loop haplotypes present at a frequency ≥0.6% in the virus population in plasma (triangles), PBMCs before therapy initiation (circles) and PBMCs after persistent viremia suppression (squares). The tree is rooted at the most frequent plasma sequence before

antiretroviral treatment initiation. Filled symbols show predicted CXCR4-using viruses; open symbols show predicted CCR5-using viruses. Symbol size increases proportionally to the V3-loop haplotype frequency in the virus population in 10% intervals. Node reliability was tested using 1000 bootstraps; bootstrap values ≥50% are shown. The V3-loop aminoacid sequence translation is shown next to each taxon. Aminoacid changes relative to the predominant sequence in plasma are highlighted in bold and underlined. Gaps correspond to aminoacid indeterminations. A Geno2Pheno $_{[coreceptor]}$ false positive rate (FPR) equal or lower than 10% was used to define CXCR4 use. The actual false positive rate of each sequence is shown. *Sequence #2 was identical to one detected in 0.04% of PBMC-associated viruses, below the error threshold, before treatment initiation.
doi:10.1371/journal.pone.0067085.g002

The prevalence of subjects with a CXCR4-using virus varied among tropism tests and settings (Figure 1). ESTA detected CXCR4-using viruses in 36.7% of subjects. The prevalence of CXCR4-using HIV was significantly underestimated by plasma 454 sequencing using a FPR of 3.5%, population sequencing of plasma and PBMC V3 forms using FPRs of 10% or 5.75%, and by the MT-2 assay ($p<0.05$ for all comparisons with ESTA, two-sided exact binomial test). No statistically significant differences in CXCR4-using prevalence were observed between plasma and PBMCs.

Viral evolution during viremia suppression and population differentiation

Overall, there was good individual agreement in the longitudinal detection of CXCR4-using HIV (Table 3), but slightly more CXCR4-using viruses were detected in PBMCs after at least two years of viremia suppression (Table 3, Figure 1). To evaluate if viruses evolved in PBMCs during suppressive ART, we used V3 forms generated by 454 sequencing present in ≥0.6% in the virus population. Based on the previous accuracy assessments, a FPR ≤10% was chosen to define CXCR4 use. Twenty-eight subjects had 454 sequencing data available from plasma at T1, PBMCs at T1 and PBMCs at T2 (Figure 2, File S1).

We only observed evolution of CCR5 viruses in one individual (Subject 7), who showed bootstrap-supported temporal clustering of new CCR5 viruses at T2. Apparently, another subject seemed to have developed CXCR4-using HIV-1 *de novo* during viremia suppression (subject 26). The emerging CXCR4-using V3-loop form (sequence ID 2; Figure 2B), however, was present before therapy in 0.04% of PBMC-associated viruses, suggesting that detection of such CXCR4-using virus was more likely due to fluctuations around the sensitivity threshold of 454 sequencing than to a true emergence of a CXCR4-using virus *de novo*. Subject 30 (Table 3) also had low-frequency CXCR4-using HIV detected only at T2. Phylogenetic analysis (File S1) confirmed that such variant clustered with pre-treatment viruses. This indicates that this was a pre-existing which was detected at T2 due to fluctuations around the sensitivity threshold of 454 sequencing, rather than to true virus evolution. Of the remaining individuals, 9 (32.1%) showed bootstrap-supported CXCR4-using HIV-1 clustering across timepoints and compartments, 3 (10.7%) had non-significant CXCR4-using virus clustering and 15 (53.6%) had only R5 viruses detected in all timepoints and compartments. Interestingly, the V3-loop sequence of syncytium-inducing viruses grown in all positive MT-2 assays was identical to one of the predominant V3-loop haplotypes simultaneously detected by 454 sequencing in proviral DNA and/or plasma RNA (Figure 3), suggesting that 454 sequencing can detect V3 forms that are also present in functional CXCR4-using viruses.

There were no differences in nucleotide variability (π) among compartments in any subject. (Table 4) The Slatkin-Maddison test indicated the presence of sequence compartmentalization between plasma and PBMCs at T1 in 2/28 (7%) individuals, and between PBMCs at T1 and T2 in 6/28 (21%) individuals.

Discussion

Only assays assessing tropism of plasma HIV-1 have been validated in clinical trials. Given that tropism cannot be routinely assessed in plasma of subjects with HIV-1 RNA levels <500–1,000 copies/mL, the optimal tropism testing strategy for clinical decision-making in these individuals remains unclear. To better understand the advantages and limitations of different tropism testing strategies in aviremic subjects, we first evaluated the diagnostic performance of various state-of-the-art tropism tests relative to the ESTA. The latter was chosen as the technical reference standard for this study because it is widely recognized as a sensitive and robust assay, it is CLIA-validated, and has been used in most previous clinical trials of CCR5 antagonists [3,4,5,6,21], including those leading to the approval of maraviroc [3,4,5].

In our hands, the tropism assay providing closest diagnostic accuracy to ESTA was 454 sequencing of plasma RNA. The highest accuracy of this assay was obtained after applying strict PCR and 454 sequencing error controls, considering only V3 forms present in at least 0.6% of the virus population and using a Geno2Pheno $_{[coreceptor]}$ FPR cut-off of 10% to define CXCR4-using viruses. Such settings provided 73% sensitivity, 95% specificity and 87% accuracy. Using a 2% level of minor CXCR4-using variants and a 3.5% Geno2Pheno $_{[coreceptor]}$ FPR to define non-R5 use, other authors found that 454 sequencing of plasma HIV-1 was able to accurately predict virological response to maraviroc-including regimens in retrospective reanalyses of maraviroc trials [4,5,6,7]. However, applying such settings to our own dataset (including the assessment of tropism by Geno2Pheno$_{[454]}$ starting from raw sequence data) resulted in decreased sensitivity and accuracy of the assay (50% sensitivity, 95% specificity and 79% accuracy). Consequently, the settings chosen for 454 sequencing in our study might potentially provide a more accurate assessment of phenotypic tropism; proper validation of our 454 settings in larger datasets including clinical endpoints is however warranted before they can be routinely used to predict virological outcomes to CCR5 antagonists.

454 sequencing was remarkably less accurate in proviral DNA than in plasma, mainly due to reduced specificity. In fact, population sequencing in proviral DNA was slightly less sensitive but more specific and, overall, more accurate than 454 sequencing in PBMCs. The reasons for such discrepancy are not fully understood. On one hand, tropism prediction engines have been trained and validated using data from plasma viruses, and might require different settings in other compartments. Peripheral blood mononuclear cells contain a historical repository of current and past HIV, some of which might be defective or unable to replicate. Also, identical V3 forms are often present at different frequency in plasma and PBMCs; whether this has an impact on treatment outcomes remains unclear. Even if identical V3 forms can be identified simultaneously in plasma RNA, proviral DNA and in syncytium-inducing viruses growing in MT-2 cells, as observed in this study, such V3 loops may be present in viruses with different genetic backgrounds and, thus, have different phenotypic tropism. Mutations in gp120 outside V3 loop and in gp41 [22], as well as

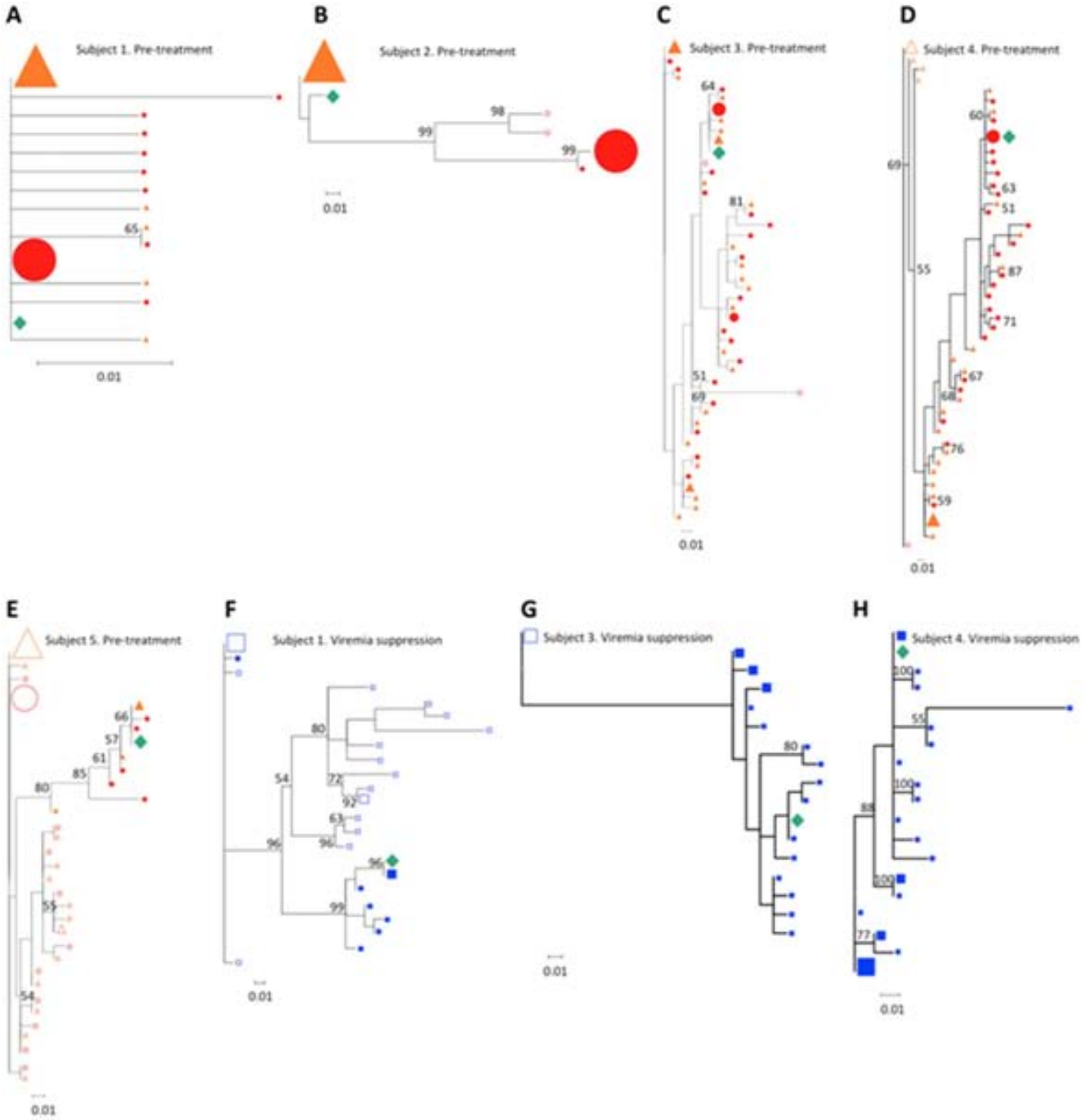

Figure 3. V3-loop haplotypes detected by quantitative deep sequencing are also found in CXCR4-using viruses growing in MT2 assays. Maximum likelihood phylogenetic trees showing that the V3-loop sequence of syncytium-inducing viruses grown in MT-2 assays (diamond) is identical to one of the predominant V3-loop haplotypes detected with quantitative deep sequencing in proviral DNA and/or plasma RNA before antiretroviral therapy initiation (Trees A to E) or after at least 2 years of persistent viremia suppression (trees F to H). Trees include V3-loop haplotypes present at a frequency ≥0.6% in the virus population in plasma (triangles), PBMCs before therapy initiation (circles) and PBMCs after persistent viremia suppression (squares); trees are rooted at the predominant plasma (trees A to E) or PBMC (trees G to H) V3-loop haplotype. Filled symbols represent CXCR4-using viruses; open symbols show R5 viruses. Symbol size increases proportionally to the V3-loop haplotype frequency in the virus population in 10% intervals. Node reliability was tested using 1,000 bootstraps; bootstrap values ≥50% are shown. CXCR4 use was defined by a Geno2Pheno $_{[coreceptor]}$ false positive rate ≤10%.
doi:10.1371/journal.pone.0067085.g003

differences in env glycosylation patterns [23] can modulate the viral tropism in a minority of subjects. This is a limitation of most genotypic techniques based on V3 loop sequencing. However, although mutations in gp41 are correlated with coreceptor tropism, they do not improve tropism prediction methods substantially [24].

The accuracy of population sequencing of plasma or PBMC-associated HIV in our study was similar to that of other studies

Table 4. Population structure analysis of plasma and PBMC V3 forms detected by 454 sequencing.[a]

Subject ID	Intracompartment Variability (Π)			Slatkin-Madison Test	
	Plasma T1	PBMC T1	PBMC T2	Plasma T1 vs PBMC T1	PBMC T1 vs PBMC T2
1	0.0156	0.0097	0.1469	2	2
2	NC	0.1190	0.1052	1	4
3	0.0351	0.0476	0.0457	18	7**
4	0.0645	0.0591	0.0276	13	13
5	0.0476	0.0606	0.0622	14	16
6	0.0271	0.0277	0.0307	4	4
7	0.0362	0.0293	0.0923	6	3*
8	0.0329	0.0286	0.0349	20	16
9	0.0130	0.0171	0.0779	3	1**
11	0.0116	0.0096	0.0274	4	3
12	0.1184	0.0170	0.0000	4*	2
14	0.0176	0.1509	0.0728	2**	6**
15	0.0156	0.0187	0.0163	4	4
16	0.1598	0.0169	0.0157	3	4
17	0.0167	0.0244	0.0230	3	8
18	0.0214	0.0208	0.0162	5	3
19	NC	0.0317	0.0605	1	2
20	0.0379	0.0286	0.0360	9	8
21	0.0264	0.0560	0.0472	4	10
22	0.0337	0.0342	0.0483	5	5
23	0.0425	0.0539	0.0424	12	2**
24	0.0130	0.0177	0.0163	3	4
25	0.1163	0.0225	0.0271	7	2**
26	0.0108	0.0306	0.1447	4	2
27	0.0129	0.0262	0.0262	2	6
28	0.0502	0.0552	0.0184	10	4
29	0.0222	0.0145	0.0182	4	4
30	0.0347	0.0321	0.0346	8	11

[a]The intracompartment variability (*Π*) of each sample is measured with the best evolutionary model found with *Findmodel* (www.hiv.lanl.gov); it corresponds to the average number of nucleotide differences per site between sequences. Migration events with *p-value*, and F_{ST} with *p-value* are indicated for Slatkin-Madison population structure tests. *NA* indicates comparisons where the tests were not applicable. *NC* indicates that variability cannot be calculated because there is only one haplotype.
*p-value between 0.05 and 0.01;
**p-value$<$0.01 and 10^{-6}.
Statistically significant p-values are colored; the color intensity is proportional to the p-value. Note that a complete dataset was not available for subjects 10 and 13, which were, therefore, not included in this analysis.
doi:10.1371/journal.pone.0067085.t004

that also used the ESTA as the reference standard [25,26]. Interestingly, although population sequencing was less sensitive than plasma 454, it was more specific and, overall, just slightly less accurate, particularly when a 20% FPR was used. This suggests that population sequencing might be an acceptable alternative to 454 sequencing in settings without access to next-generation sequencing provided that high FPR cutoffs are used.

One particular interest of our study was to evaluate to which extent tropism tests in plasma and PBMCs provide equivalent biological results. The observation of sequence compartmentalization in some subjects suggests that, although plasma and PBMCs often provide similar tropism reports [27], their biological or clinical meaning might not be necessarily equivalent. Indeed, in a retrospective reanalysis of pretreatment samples of the MOTIVATE and A4001029 studies, HIV DNA-based methods were generally good predictors of virological response to maraviroc regimens, but virologic response was better predicted by plasma compared to PBMC 454 sequencing [28]. Contrasting with our dataset, the PBMC compartment harbored more variable V3 forms than plasma. Concordance between plasma and PBMC tropism by 454 sequencing ranged from 74% amongst samples with CD4+ counts $<$50 cells/mm^3 to 100% concordance at CD4+ counts $>$350 cells/mm^3, suggesting that, in addition to the sequence compartmentalization observed in our study, a CD4+ count-dependant bias in DNA input might also affect PBMC results. Moreover, the existence of V3 compartmentalization between PBMCs at T1 and T2 in the absence of overt viral evolution during prolonged viremia suppression suggests the presence of drifts in PBMC composition that may further affect DNA sampling for tropism testing.

We also sought to explore if HIV-1 tropism shifts were frequently observed during persistent viremia suppression, which

would be informative of the clinical feasibility of using stored plasma samples collected before ART initiation for tropism testing. The absence of CXCR4 virus evolution during prolonged periods of viremia suppression suggests that, when available, testing of stored plasma samples is generally safe and informative, provided that HIV-1 RNA levels remain continuously suppressed. Our findings are in agreement with previous publications using population sequencing of proviral DNA [29,30]. Importantly, subjects in this study did not receive CCR5 antagonists; it remains largely unexplored if HIV-1 tropism may still evolve under the selective pressure of CCR5 antagonists if continuous viremia suppression is achieved.

This study represents a comprehensive comparison of the main state-of-the-art tropism tests with potential application to HIV clinical management and fulfills the Standards for Reporting of Diagnostic Accuracy (STARD) [31]. The study design allowed investigating population differentiation and longitudinal CXCR4-using evolution in different compartments, which is informative of the optimal timing and source for tropism testing in subjects with undetectable HIV-1 RNA levels. The main weaknesses of the study are its small sample size, its retrospective nature, the lack of association of tropism data with outcomes to CCR5 antagonist therapy, and the use of cryopreserved PBMCs for MT-2 assays. This last factor, and the fact that subjects had had HIV RNA <50 copies/mL during more than 2 years of ART at T2, likely reduced our ability to recover infectious viruses, leading to a decreased performance of MT2 assays relative to previous publications [32]. We only used Geno2Pheno$_{[coreceptor]}$ to interpret genotypic data because previous comparisons demonstrated equivalence with other interpretation systems [33,34] and it is extensively used in our setting. Differences in FPR settings observed in this study were sometimes due to a small number of patients, which is reflected in the wide confidence intervals of our diagnostic accuracy estimations.

Conclusions

Although plasma and PBMCs may often provide similar tropism reports, [27] tropism testing in PBMCs may not necessarily produce equivalent biological results to plasma, because the structure of viral populations and the diagnostic performance of tropism assays vary between compartments. Thereby, proviral DNA tropism testing should be specifically validated in clinical trials before it can be applied to routine clinical decision-making. Clinically relevant cut-offs and settings should be identified for clonal and population genotypic tropism testing in proviral DNA. The absence of tropism shifts during viremia suppression suggests that, when available, testing of stored plasma samples is generally safe and informative, provided that HIV suppression is maintained. Next-generation sequencing technologies have the potential to be a cost-effective alternative to assess viral tropism and provide essential information to increase the efficacy of HIV therapeutics and advance our understanding of HIV pathogenesis.

Supporting Information

File S1 Phylogenetic relatedness of V3 forms before treatment initiation and after 2 years in each subject. Maximum-likelihood phylogenetic trees including V3-loop haplotypes present at a frequency $\geq$0.6% in the virus population in plasma (triangles), PBMCs before therapy initiation (circles) and PBMCs after persistent viremia suppression (squares). One tree is shown per each subject. Trees are rooted at the most frequent plasma sequence before antiretroviral treatment initiation. Filled symbols show predicted CXCR4-using viruses; open symbols show predicted CCR5-using viruses. Symbol size increases proportionally to the V3-loop haplotype frequency in the virus population in 10% intervals. Node reliability was tested using 1000 bootstraps; bootstrap values $\geq$50% are shown. A Geno2Pheno $_{[coreceptor]}$ false positive rate (FPR) equal or lower than 10% was used to define CXCR4 use.
(PDF)

Acknowledgments

This study was presented in part at the 17th Conference on Retroviruses and Opportunistic Infections, San Francisco, USA, February 16–19, 2010, Abstract# 544; and 18th Conference on Retroviruses and Opportunistic Infections, Boston, USA, February 27–March 2, 2011, Abstract# 669.

Author Contributions

Conceived and designed the experiments: CP FMC JMP JB BC RP. Performed the experiments: CP RB CC JD MC YL EC MD. Analyzed the data: CP FMC AT RB MD RP. Contributed reagents/materials/analysis tools: FMC AT SPA MNJ JP JMP JB MD BC RP. Wrote the paper: CP RP. Reviewed, edited, and approved the article: CP FMC AT RB SPA CC JD MC YL MNJ JP JMP JB EC MD BC RP.

References

1. Tsibris AM, Sagar M, Gulick RM, Su Z, Hughes M, et al. (2008) In vivo emergence of vicriviroc resistance in a human immunodeficiency virus type 1 subtype C-infected subject. J Virol 82: 8210–8214.
2. Westby M, Lewis M, Whitcomb J, Youle M, Pozniak AL, et al. (2006) Emergence of CXCR4-using human immunodeficiency virus type 1 (HIV-1) variants in a minority of HIV-1-infected patients following treatment with the CCR5 antagonist maraviroc is from a pretreatment CXCR4-using virus reservoir. J Virol 80: 4909–4920.
3. Cooper DA, Heera J, Goodrich J, Tawadrous M, Saag M, et al. (2010) Maraviroc versus efavirenz, both in combination with zidovudine-lamivudine, for the treatment of antiretroviral-naive subjects with CCR5-tropic HIV-1 infection. J Infect Dis 201: 803–813.
4. Gulick RM, Lalezari J, Goodrich J, Clumeck N, DeJesus E, et al. (2008) Maraviroc for previously treated patients with R5 HIV-1 infection. N Engl J Med 359: 1429–1441.
5. Fatkenheuer G, Nelson M, Lazzarin A, Konourina I, Hoepelman AI, et al. (2008) Subgroup analyses of maraviroc in previously treated R5 HIV-1 infection. N Engl J Med 359: 1442–1455.
6. Saag M, Goodrich J, Fatkenheuer G, Clotet B, Clumeck N, et al. (2009) A double-blind, placebo-controlled trial of maraviroc in treatment-experienced patients infected with non-R5 HIV-1. J Infect Dis 199: 1638–1647.
7. Swenson L, Dong W, Mo T, Thielen A, Jensen M, et al. (2010) Large-scale Application of Deep Sequencing Using 454 Technology to HIV Tropism Screening. 17th Conference on Retroviruses and Opportunistic Infections. San Francisco, USA.
8. McGovern RA, Thielen A, Mo T, Dong W, Woods CK, et al. (2010) Population-based V3 genotypic tropism assay: a retrospective analysis using screening samples from the A4001029 and MOTIVATE studies. AIDS 24: 2517–2525.
9. Swenson LC, Mo T, Dong WW, Zhong X, Woods CK, et al. (2011) Deep Third Variable Sequencing for HIV Type 1 Tropism in Treatment-Naive Patients: A Reanalysis of the MERIT Trial of Maraviroc. Clin Infect Dis 53: 732–742.
10. Heera J, Harrigan PR, Lewis M, Chapman D, Biswas P, et al. (February 27–March 2, 2011) Predicting MVC Responses According to Absolute Number vs. Proportion of CXCR4-Using Virus Among Treatment-experienced Patients. 18th Conference on Retroviruses and Opportunistic Infections. Boston.
11. Koot M, Vos AH, Keet RP, de Goede RE, Dercksen MW, et al. (1992) HIV-1 biological phenotype in long-term infected individuals evaluated with an MT-2 cocultivation assay. AIDS 6: 49–54.
12. Sing T, Low AJ, Beerenwinkel N, Sander O, Cheung PK, et al. (2007) Predicting HIV coreceptor usage on the basis of genetic and clinical covariates. Antivir Ther 12: 1097–1106.
13. R_Development_Core_Team (2009) R: A language and environment for statistical computing. In: Computing RFfS, editor. Austria, Vienna: R Foundation for Statistical Computing.

14. Guindon S, Gascuel O (2003) A simple, fast, and accurate algorithm to estimate large phylogenies by maximum likelihood. Syst Biol 52: 696–704.
15. Tamura K, Dudley J, Nei M, Kumar S (2007) MEGA4: Molecular Evolutionary Genetics Analysis (MEGA) software version 4.0. Mol Biol Evol 24: 1596–1599.
16. Kumar S, Nei M, Dudley J, Tamura K (2008) MEGA: a biologist-centric software for evolutionary analysis of DNA and protein sequences. Brief Bioinform 9: 299–306.
17. Slatkin M, Maddison WP (1989) A cladistic measure of gene flow inferred from the phylogenies of alleles. Genetics 123: 603–613.
18. Kosakovsky Pond SL, Frost SD (2005) Not so different after all: a comparison of methods for detecting amino acid sites under selection. Mol Biol Evol 22: 1208–1222.
19. Excoffier L, Laval G, Schneider S (2005) Arlequin (version 3.0): an integrated software package for population genetics data analysis. Evol Bioinform Online 1: 47–50.
20. Hosoya N, Su Z, Wilkin T, Gulick RM, Flexner C, et al. (2009) Assessing human immunodeficiency virus type 1 tropism: Comparison of assays using replication-competent virus versus plasma-derived pseudotyped virions. J Clin Microbiol 47: 2604–2606.
21. Gulick RM, Su Z, Flexner C, Hughes MD, Skolnik PR, et al. (2007) Phase 2 study of the safety and efficacy of vicriviroc, a CCR5 inhibitor, in HIV-1-Infected, treatment-experienced patients: AIDS clinical trials group 5211. J Infect Dis 196: 304–312.
22. Huang W, Toma J, Fransen S, Stawiski E, Reeves JD, et al. (2008) Coreceptor tropism can be influenced by amino acid substitutions in the gp41 transmembrane subunit of human immunodeficiency virus type 1 envelope protein. J Virol 82: 5584–5593.
23. Ogert RA, Lee MK, Ross W, Buckler-White A, Martin MA, et al. (2001) N-linked glycosylation sites adjacent to and within the V1/V2 and the V3 loops of dualtropic human immunodeficiency virus type 1 isolate DH12 gp120 affect coreceptor usage and cellular tropism. J Virol 75: 5998–6006.
24. Thielen A, Lengauer T, Swenson LC, Dong WW, McGovern RA, et al. (2011) Mutations in gp41 are correlated with coreceptor tropism but do not improve prediction methods substantially. Antivir Ther 16: 319–328.
25. Prosperi MC, Bracciale L, Fabbiani M, Di Giambenedetto S, Razzolini F, et al. (2010) Comparative determination of HIV-1 co-receptor tropism by Enhanced Sensitivity Trofile, gp120 V3-loop RNA and DNA genotyping. Retrovirology 7: 56.
26. Svicher V, D'Arrigo R, Alteri C, Andreoni M, Angarano G, et al. (2010) Performance of genotypic tropism testing in clinical practice using the enhanced sensitivity version of Trofile as reference assay: results from the OSCAR Study Group. New Microbiol 33: 195–206.
27. Raymond S, Delobel P, Mavigner M, Cazabat M, Encinas S, et al. (2010) CXCR4-using viruses in plasma and peripheral blood mononuclear cells during primary HIV-1 infection and impact on disease progression. AIDS 24: 2305–2312.
28. Swenson LC, McGovern RA, James I, Demarest J, Chapman D, et al. (February 27–March 2, 2011) Analysis of Cellular HIV V3 DNA to Predict Virologic Response to Maraviroc: Performance of Population-based and 454 Deep V3 Sequencing. 18th Conference on Retroviruses and Opportunistic Infections. Boston.
29. Soulie C, Lambert-Niclot S, Wirden M, Simon A, Valantin MA, et al. (2011) Low frequency of HIV-1 tropism evolution in patients successfully treated for at least 2 years. AIDS 25: 537–539.
30. Seclen E, Del Mar Gonzalez M, De Mendoza C, Soriano V, Poveda E (2010) Dynamics of HIV tropism under suppressive antiretroviral therapy: implications for tropism testing in subjects with undetectable viraemia. J Antimicrob Chemother 65: 1493–1496.
31. Bossuyt PM, Reitsma JB, Bruns DE, Gatsonis CA, Glasziou PP, et al. (2003) Towards complete and accurate reporting of studies of diagnostic accuracy: the STARD initiative. BMJ 326: 41–44.
32. Coakley E, Reeves JD, Huang W, Mangas-Ruiz M, Maurer I, et al. (2009) Comparison of human immunodeficiency virus type 1 tropism profiles in clinical samples by the Trofile and MT-2 assays. Antimicrob Agents Chemother 53: 4686–4693.
33. Abbate I, Rozera G, Tommasi C, Bruselles A, Bartolini B, et al. (2010) Analysis of co-receptor usage of circulating viral and proviral HIV genome quasispecies by ultra-deep pyrosequencing in patients who are candidates for CCR5 antagonist treatment. Clin Microbiol Infect.
34. Recordon-Pinson P, Soulie C, Flandre P, Descamps D, Lazrek M, et al. (2010) Evaluation of the genotypic prediction of HIV-1 coreceptor use versus a phenotypic assay and correlation with the virological response to maraviroc: the ANRS GenoTropism study. Antimicrob Agents Chemother 54: 3335–3340.

Supplementary File S1: Phylogenetic analyses of all subjects

HIV-1 Tropism Testing in Subjects Achieving Undetectable HIV-1 RNA: Diagnostic Accuracy, Viral Evolution and Compartmentalization

Christian Pou[1*], Francisco M. Codoñer[1], Alexander Thielen[3], Rocío Bellido[1], Susana Pérez-Álvarez[1], Cecilia Cabrera[1], Judith Dalmau[1], Marta Curriu[1], Yolanda Lie[5], Marc Noguera[1], Jordi Puig[2], Javier Martinez-Picado[2,4], Julià Blanco[1], Eoin Coakley[5], Martin Däumer[6], Bonaventura Clotet[1,2], Roger Paredes[1,2*].

[1]Institut de Recerca de la SIDA irsiCaixa - HIVACAT & [2]HIV Unit-Fundació Lluita contra la SIDA, Hospital Universitari Germans Trias i Pujol, Universitat Autònoma de Barcelona, Catalonia, Spain; [3]Max-Planck-Institut für Informatik, Saarbücken, Germany; [4]Institució Catalana de Recerca i Estudis Avançats (ICREA), Barcelona, Spain; [5]Monogram Biosciences Inc., South San Francisco, California, USA, [6]Institut für Immunologie und Genetik, Kaiserlautern, Germany.

Maximum-likelihood phylogenetic trees were constructed for each subject using PhyML and the best nucleotide evolution model identified by Modeltest. Trees included V3-loop haplotypes present at a frequency ≥0.6% in the virus population in plasma (triangles), PBMCs before therapy initiation (circles) and PBMCs after persistent viremia suppression (squares). One tree is shown per each subject. Trees are rooted at the most frequent plasma sequence before antiretroviral treatment initiation. Filled symbols show predicted CXCR4-using viruses; open symbols show predicted CCR5-using viruses. Symbol size increases proportionally to V3-loop haplotype frequency in the virus population in 10% intervals. Node reliability was tested using 1000 bootstraps; bootstrap values ≥ 50% are shown. A Geno2Pheno $_{[coreceptor]}$ false positive rate (FPR) equal or lower than 10% was used to define CXCR4 use.

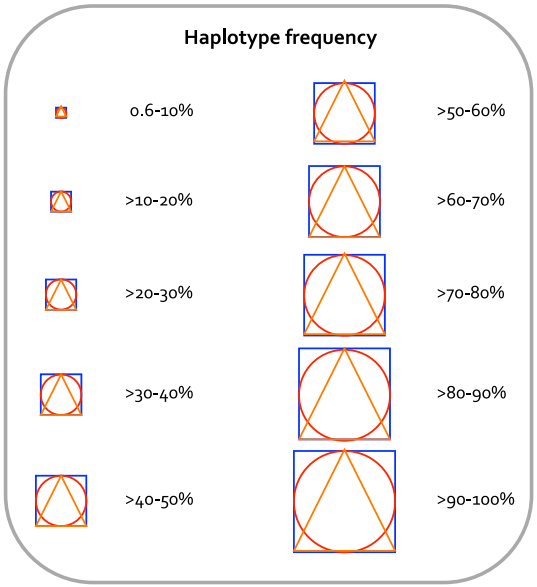

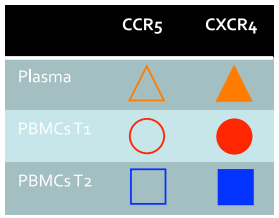

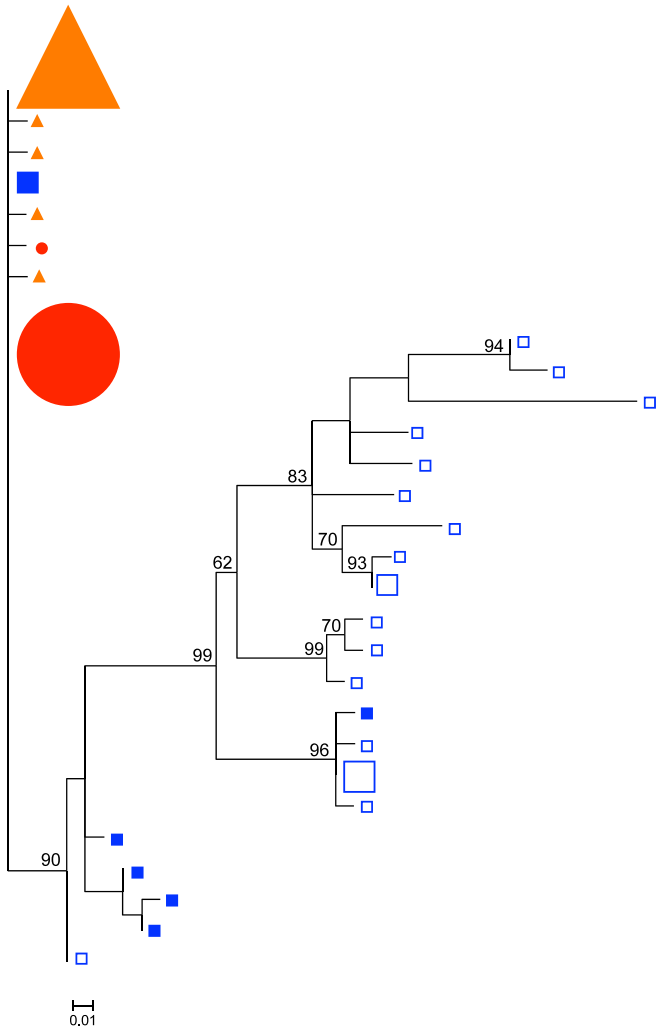

Subject 1

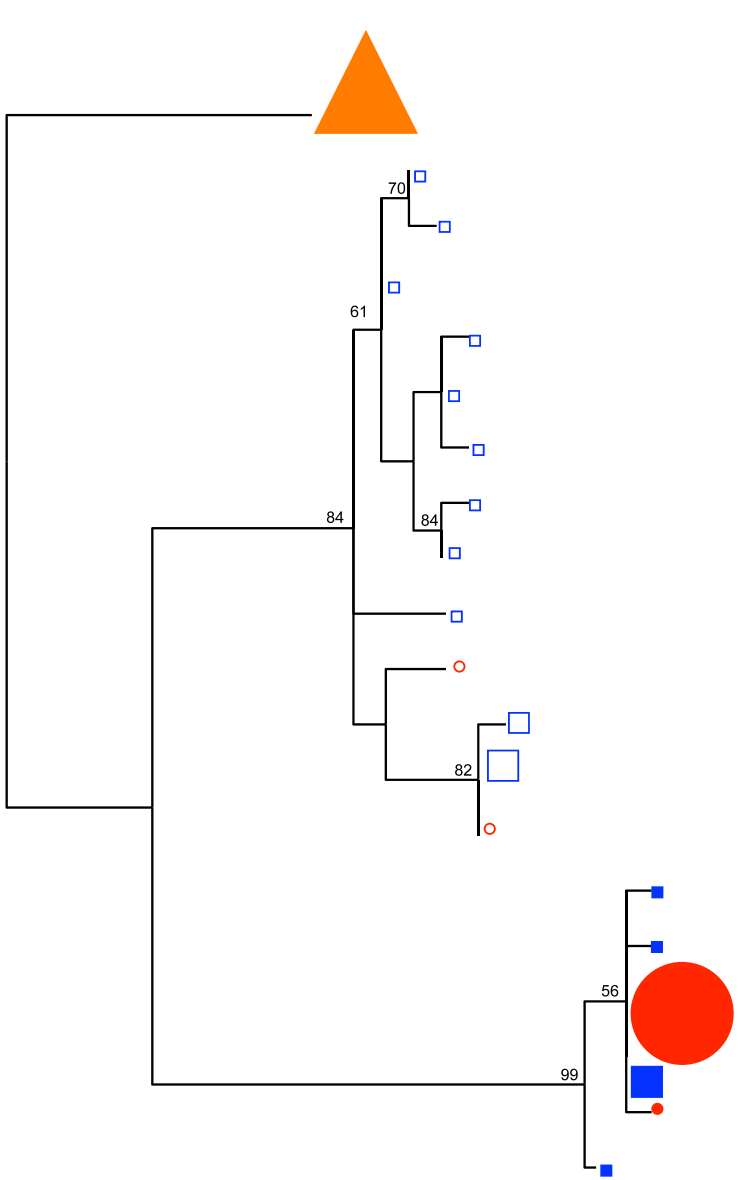

Subject 2

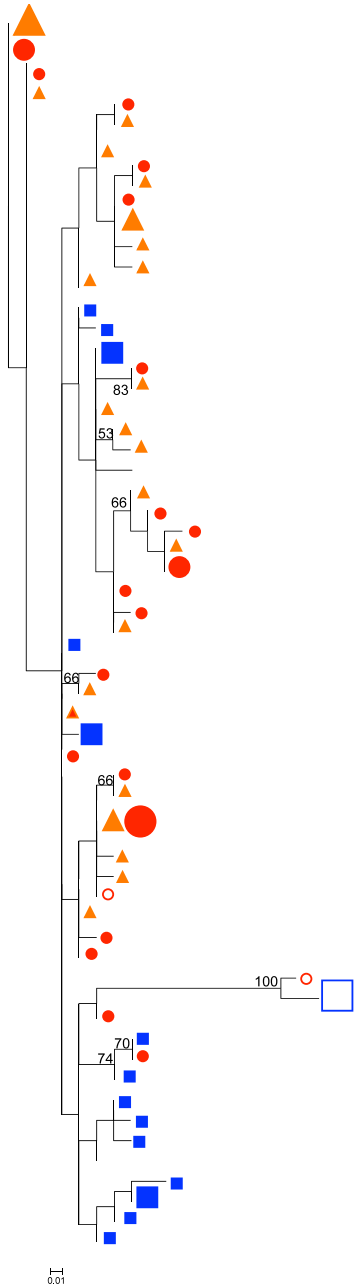

Subject 3

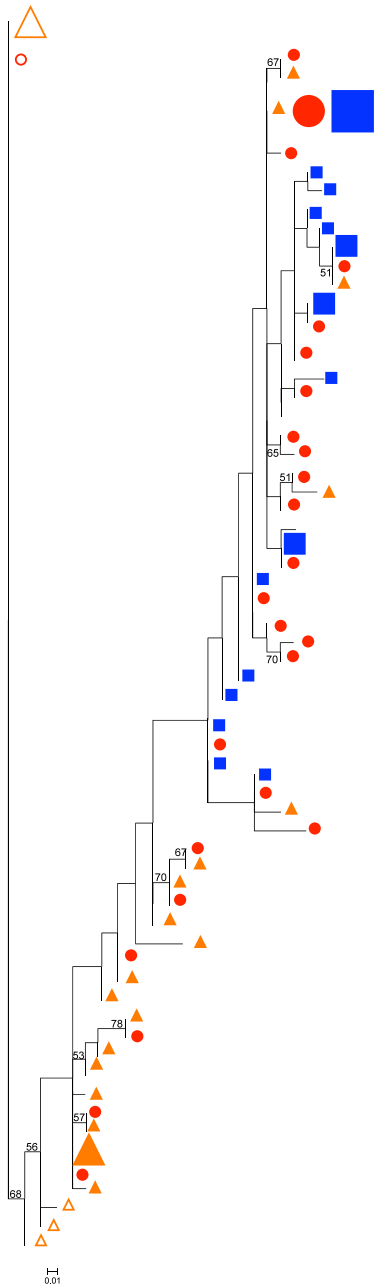

Subject 4

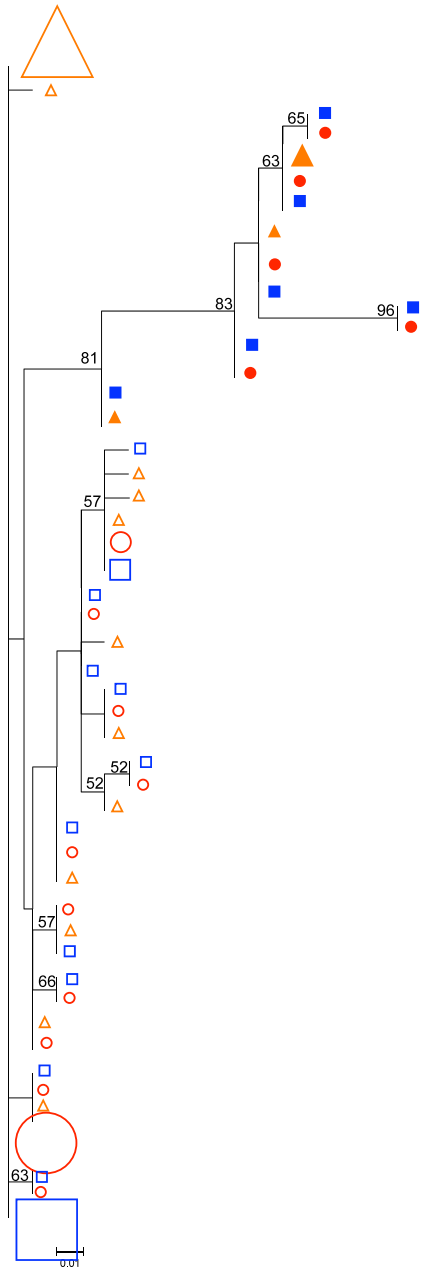

Subject 5

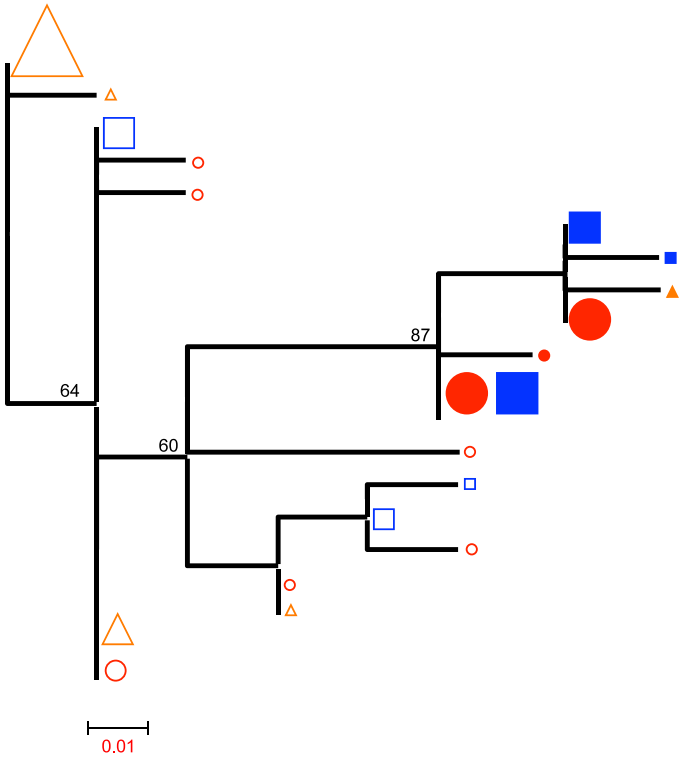

Subject 6

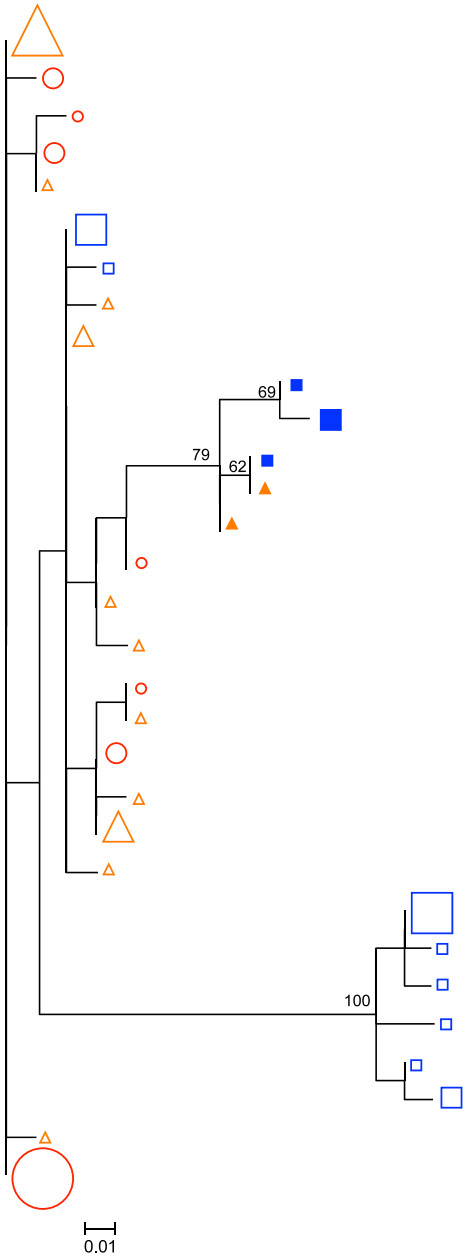

Subject 7

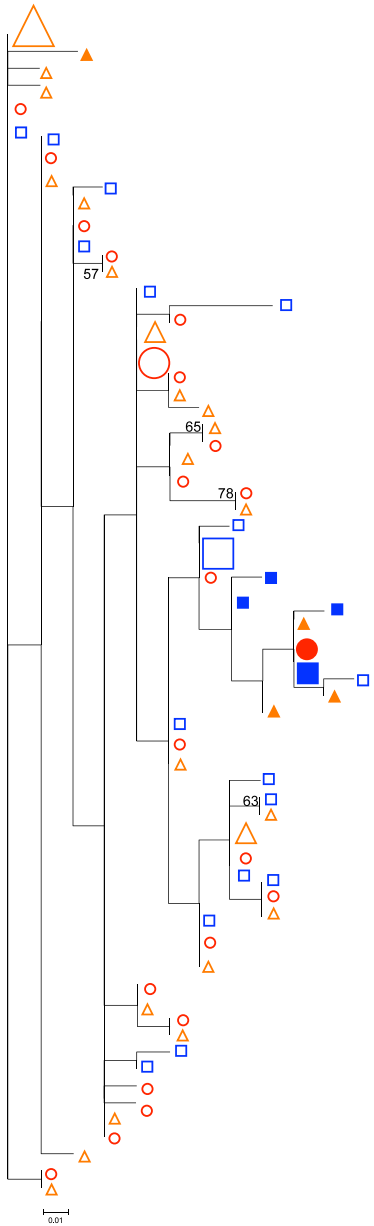

Subject 8

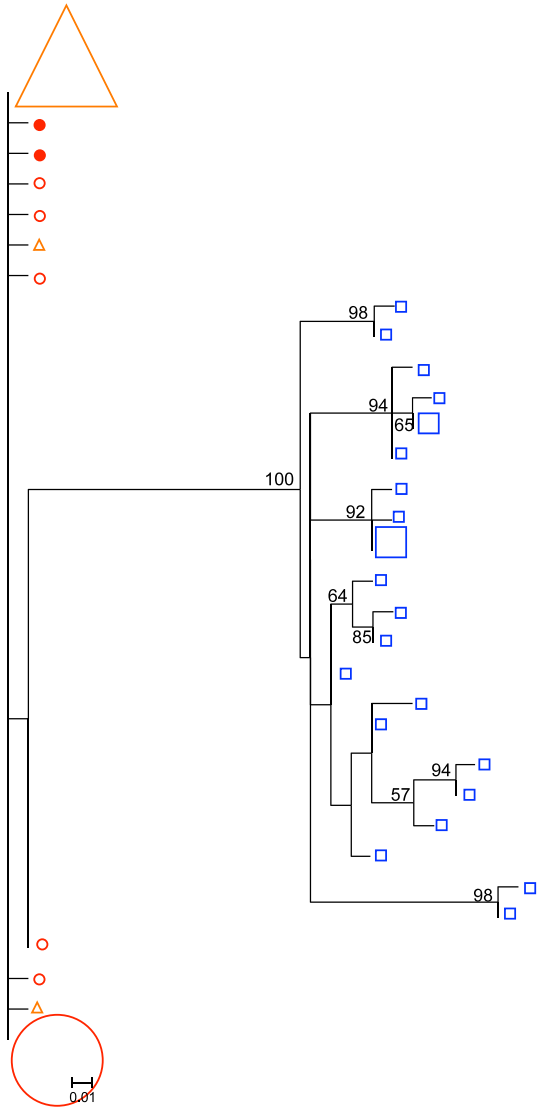

Subject 9

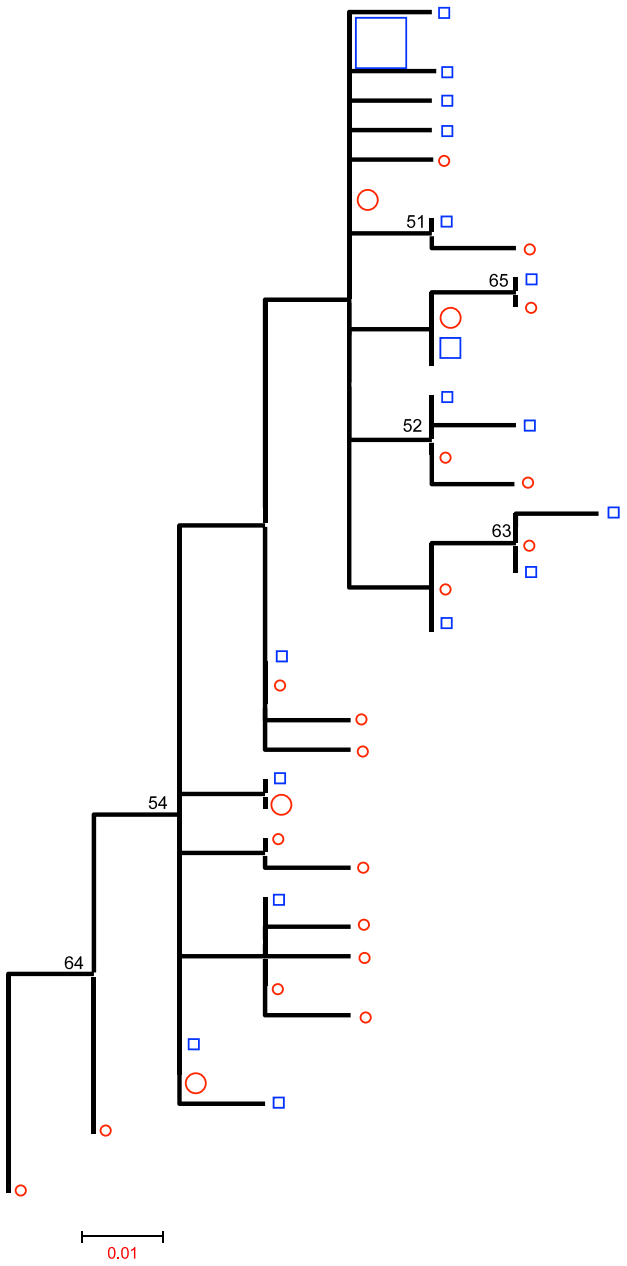

Subject 10

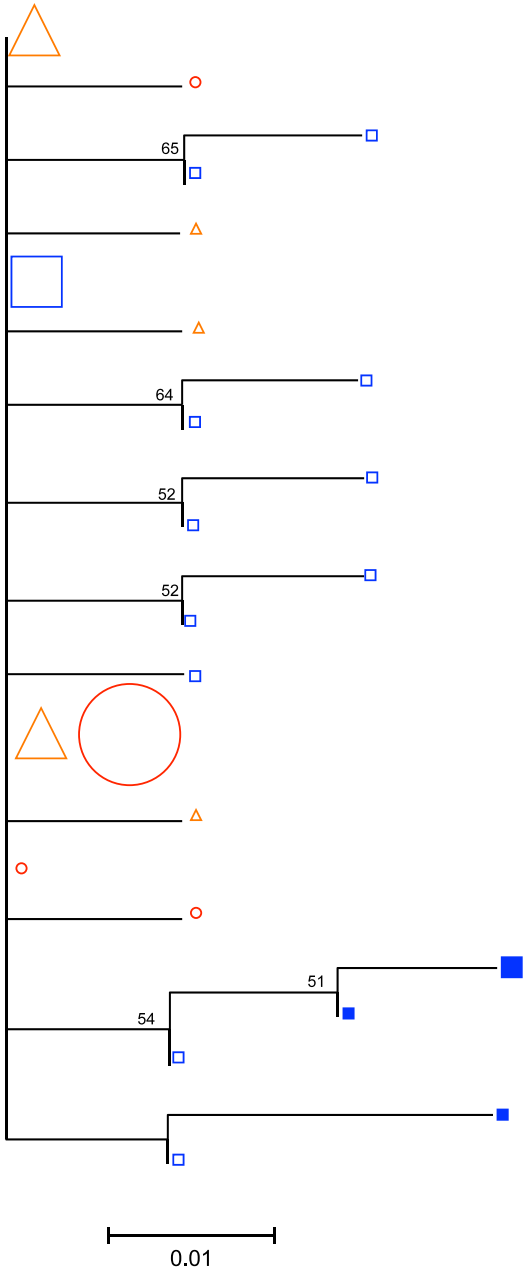

Subject 11

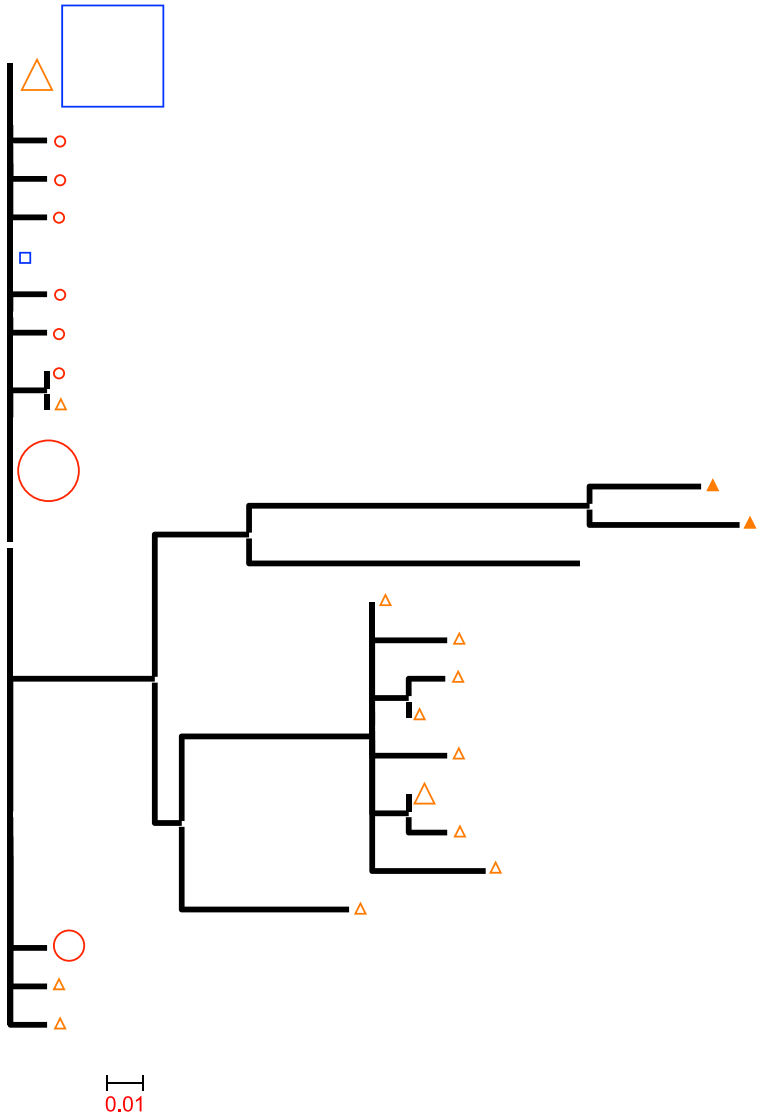

Subject 12

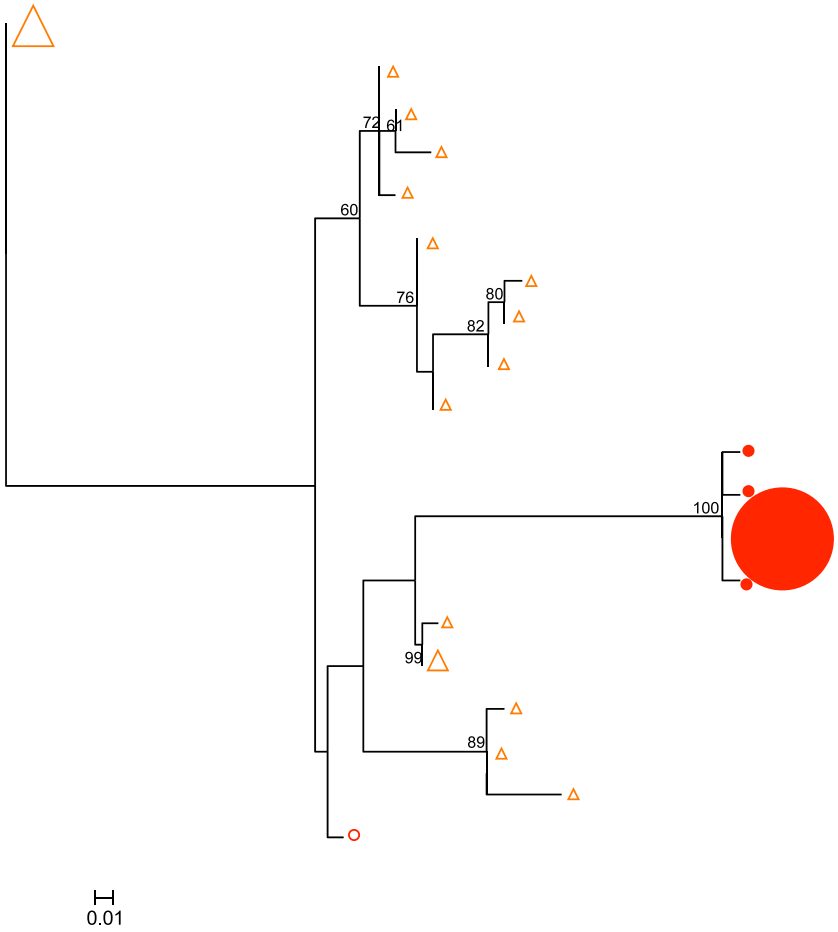

Subject 13

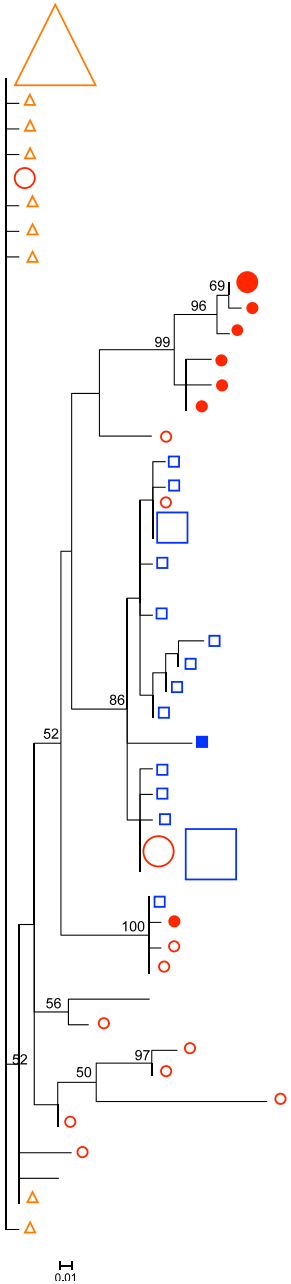

Subject 14

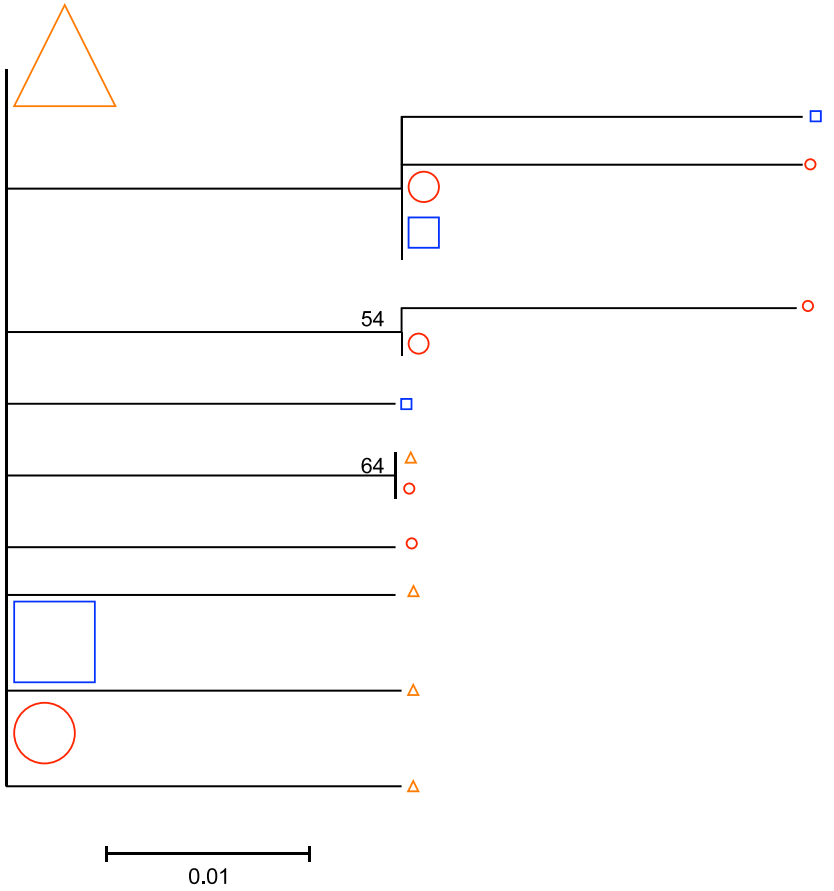

Subject 15

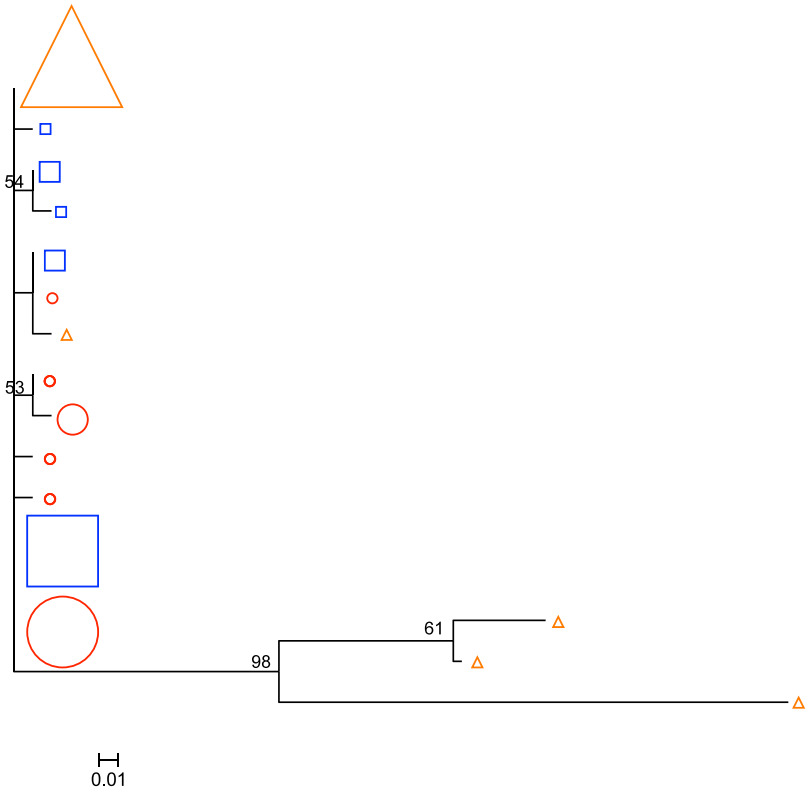

Subject 16

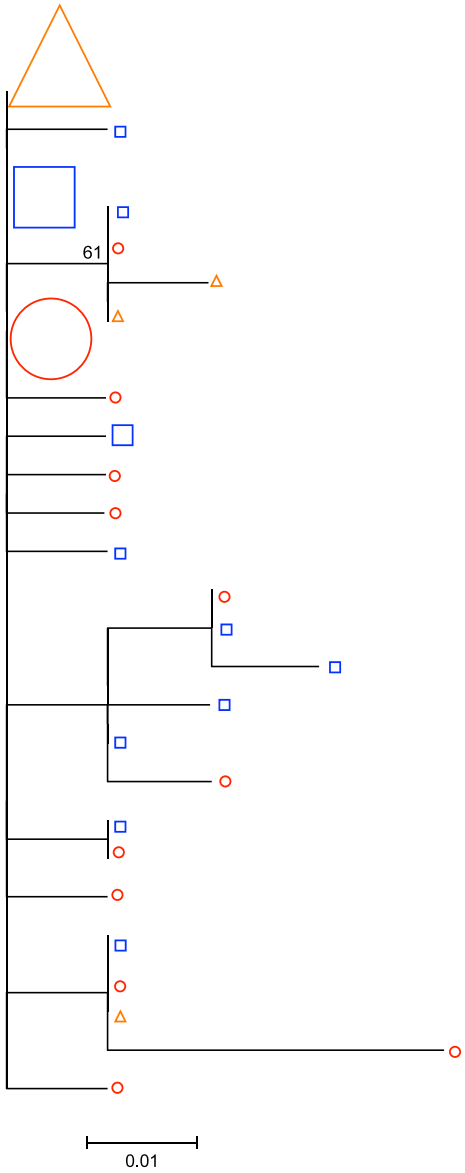

Subject 17

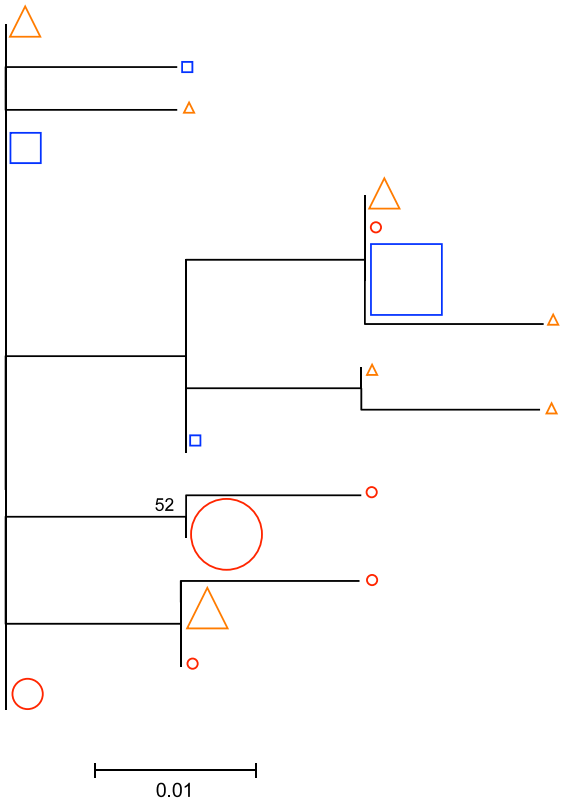

Subject 18

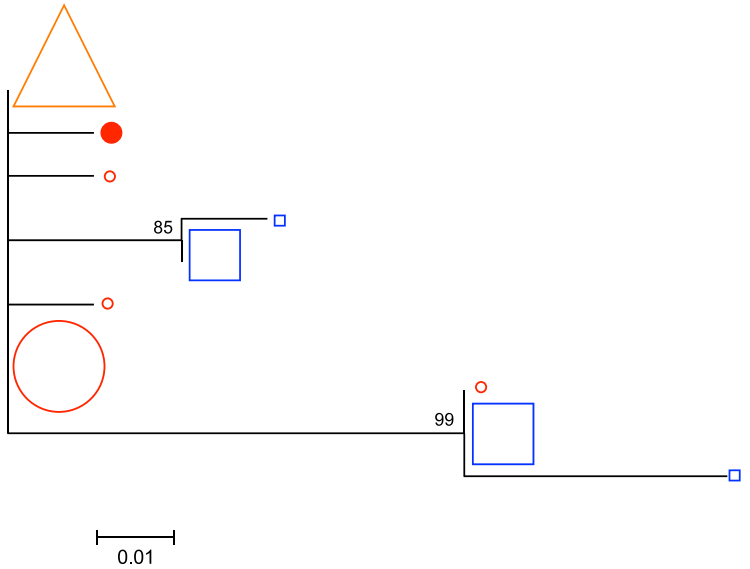

Subject 19

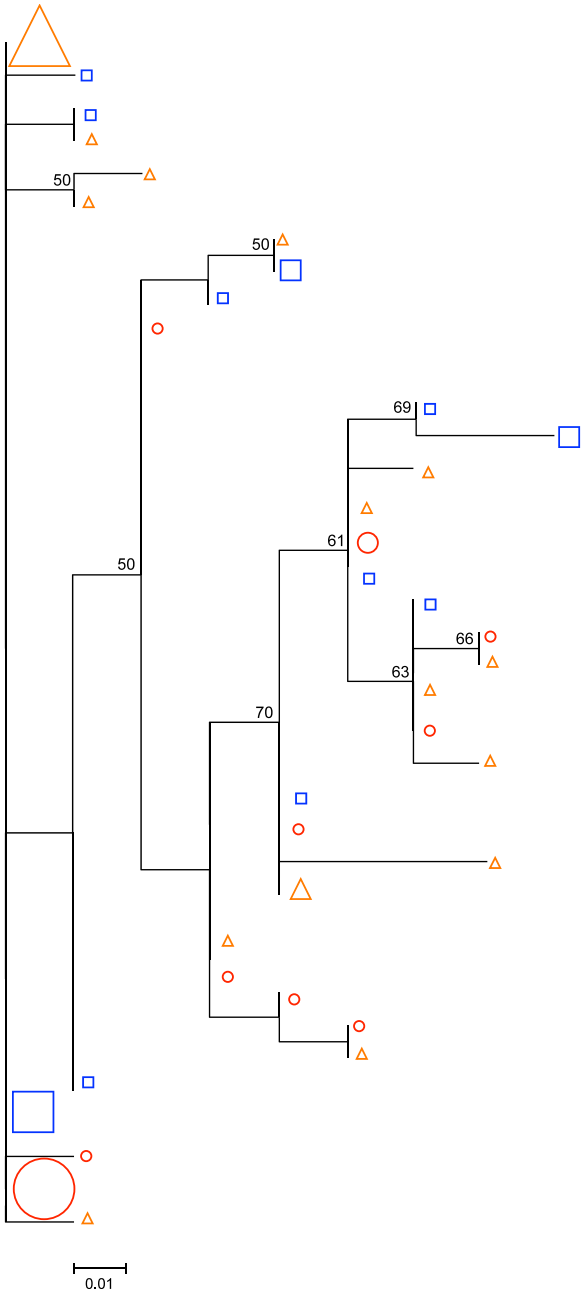

Subject 20

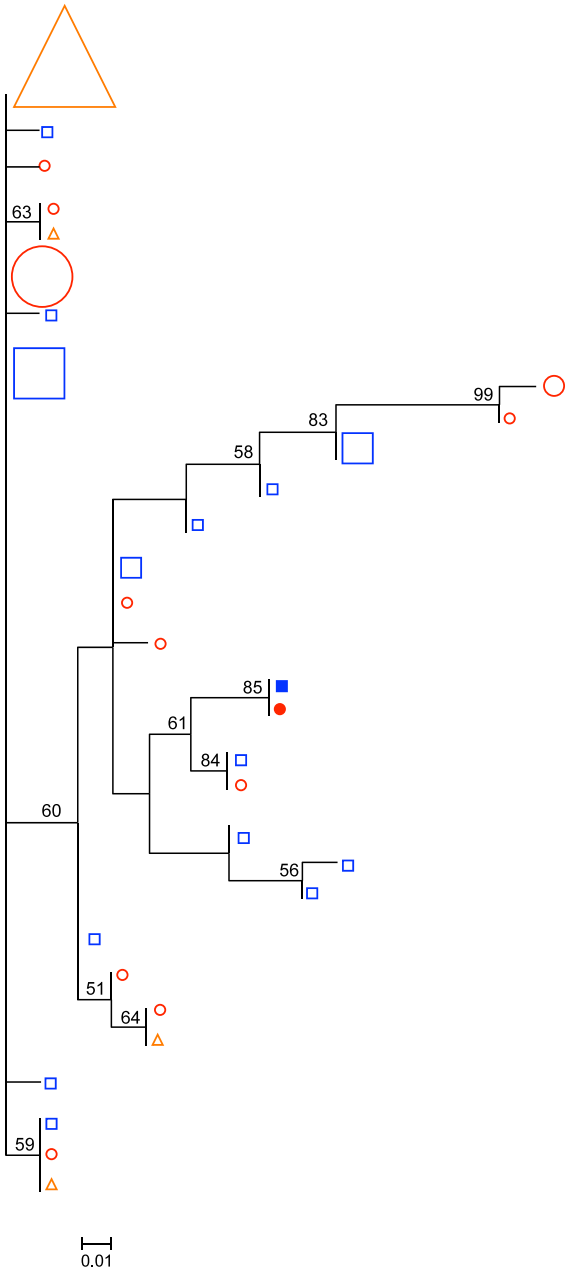

Subject 21

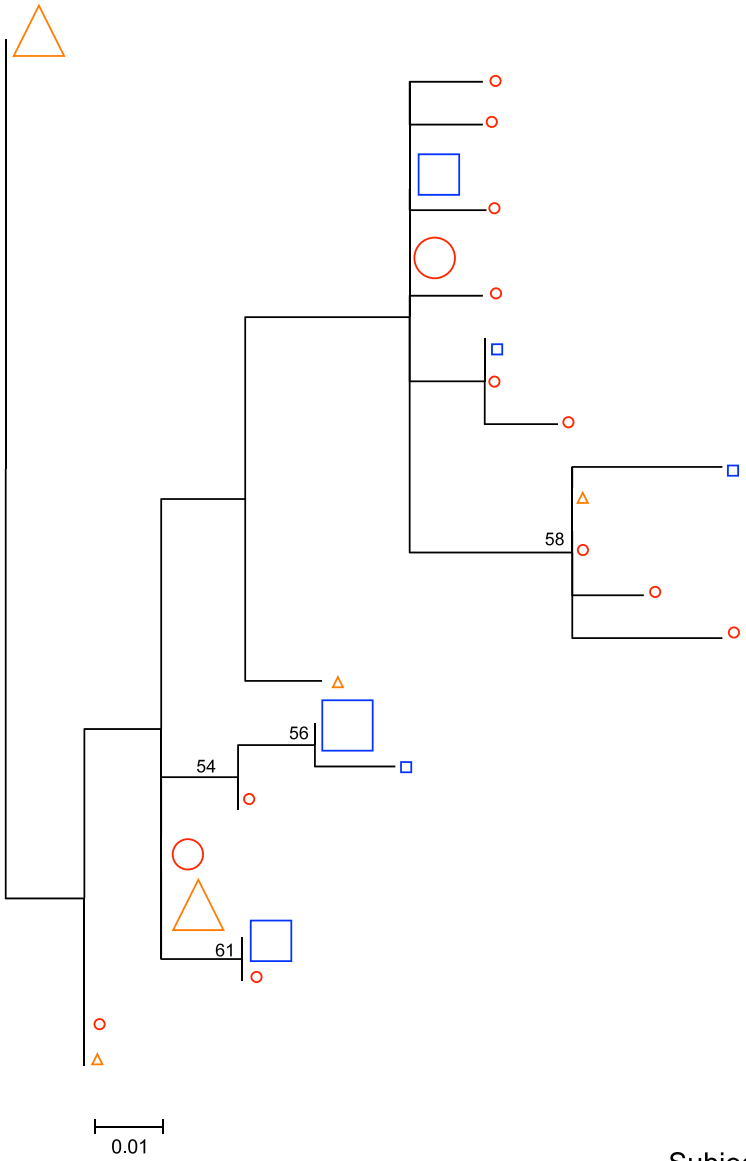

Subject 22

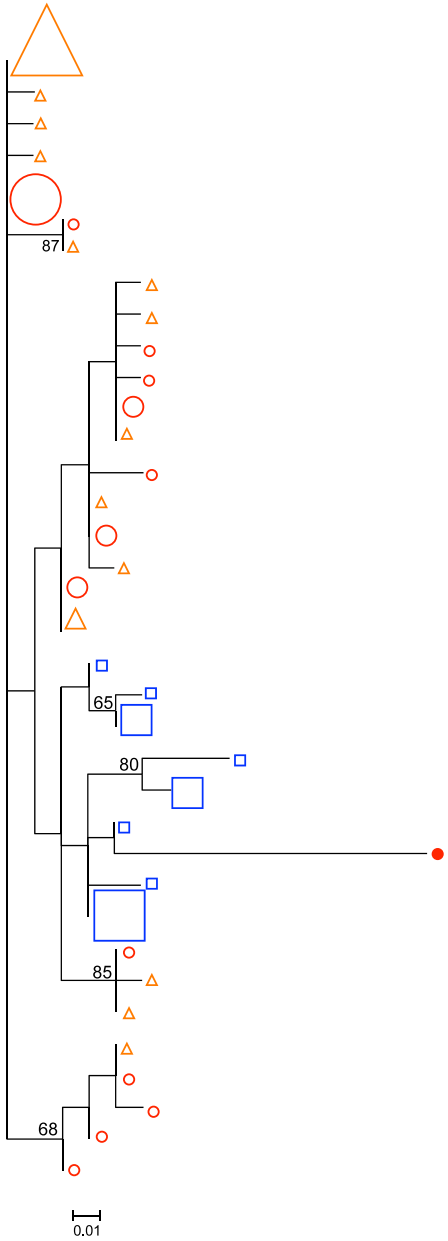

Subject 23

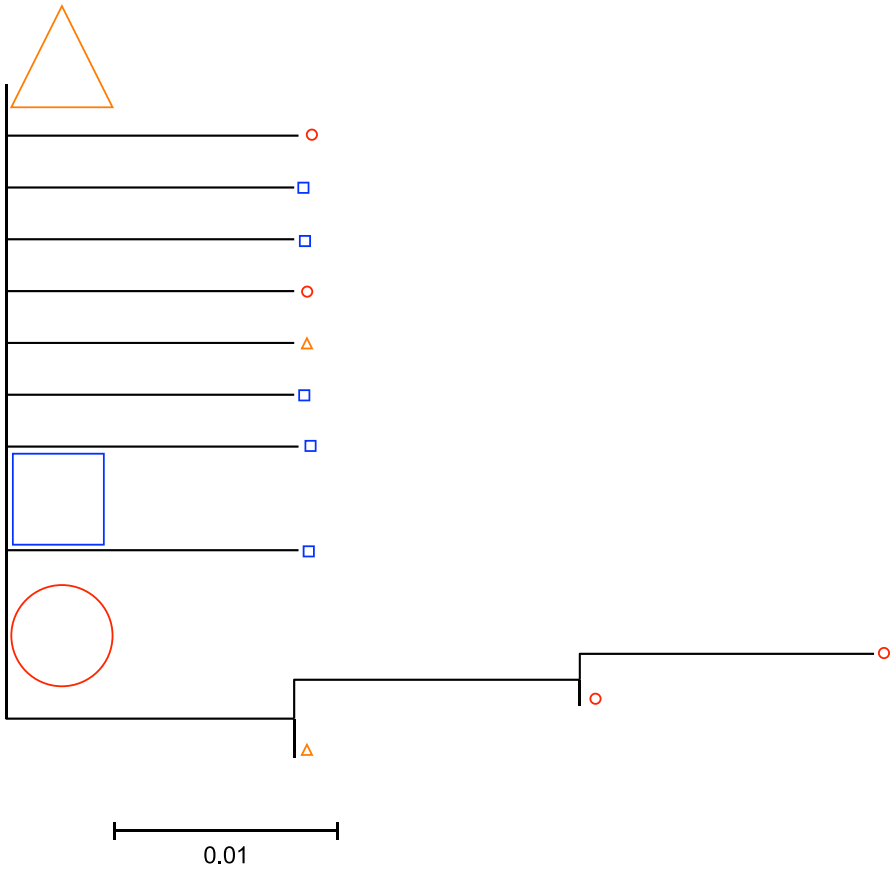

Subject 24

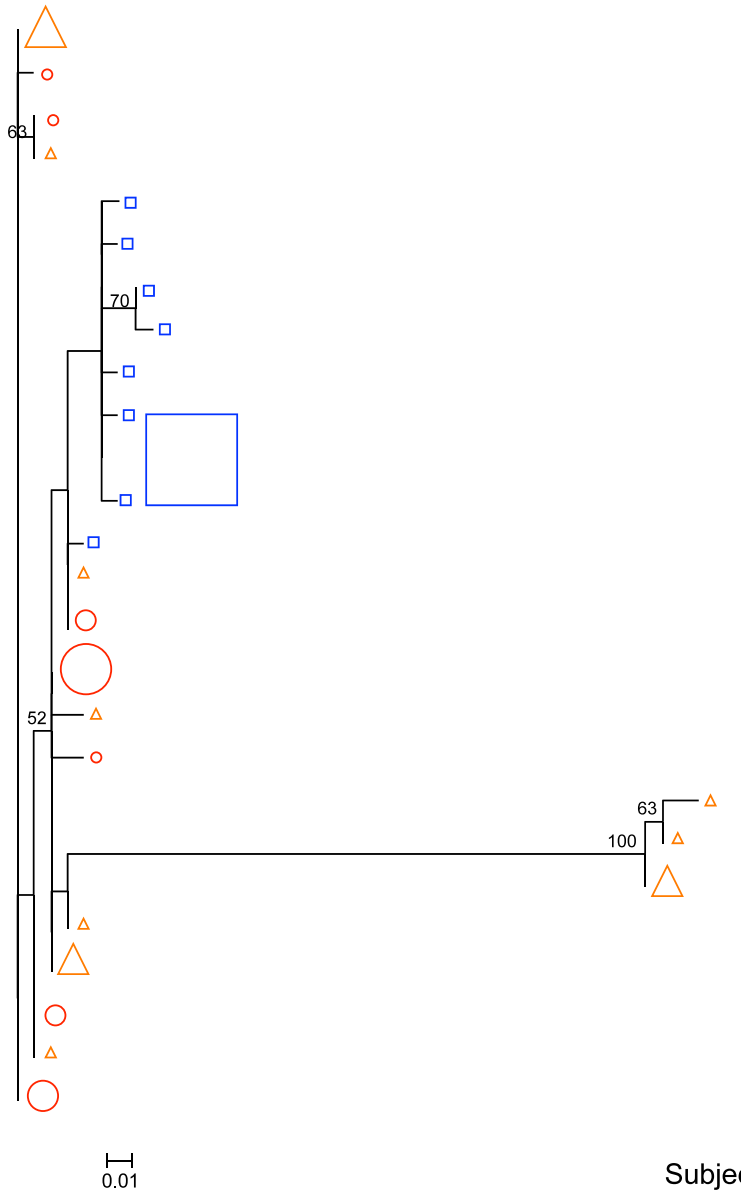

Subject 25

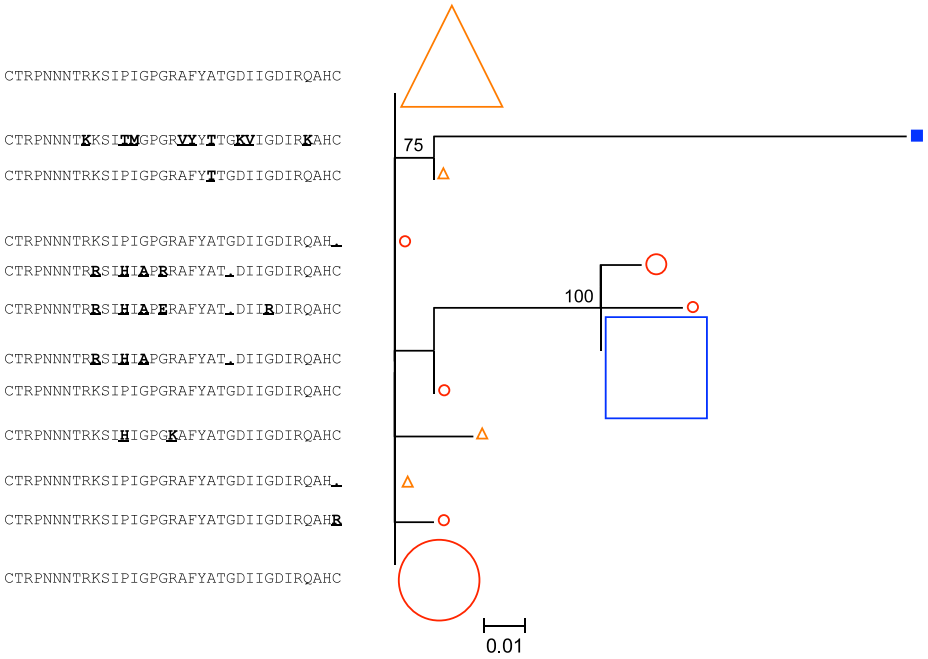

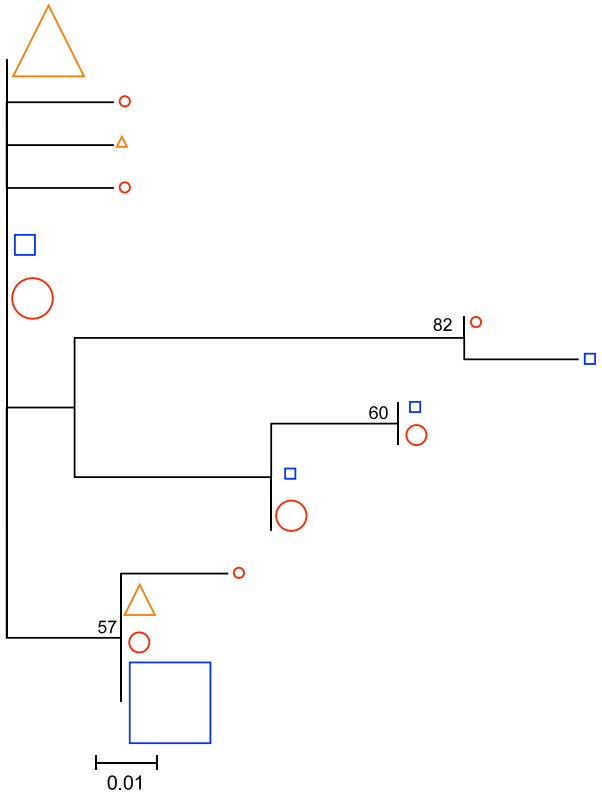

Subject 26

Subject 27

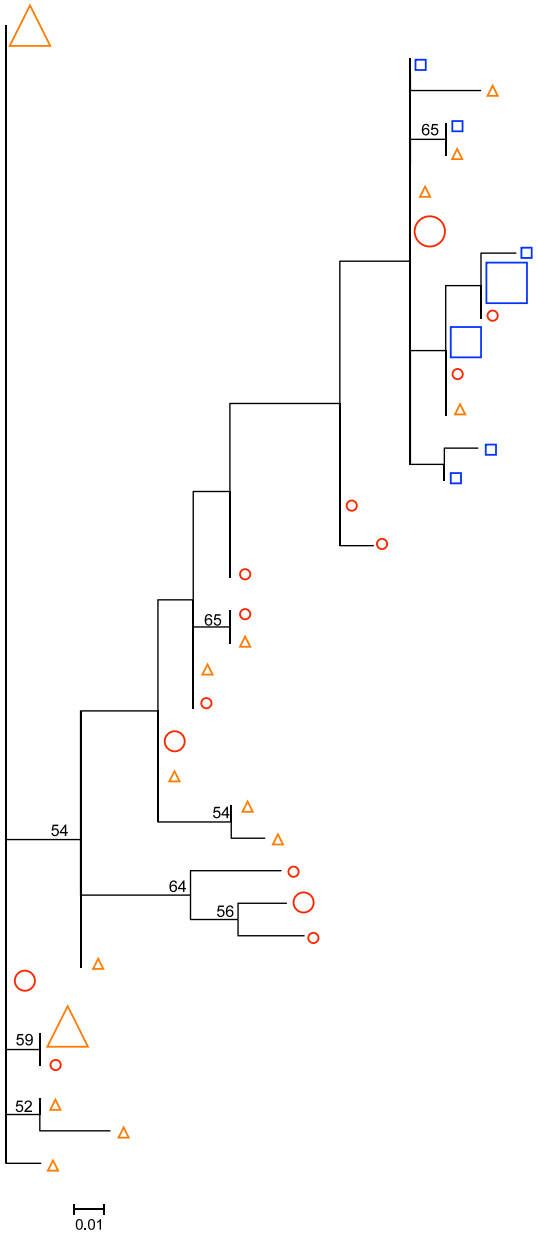

Subject 28

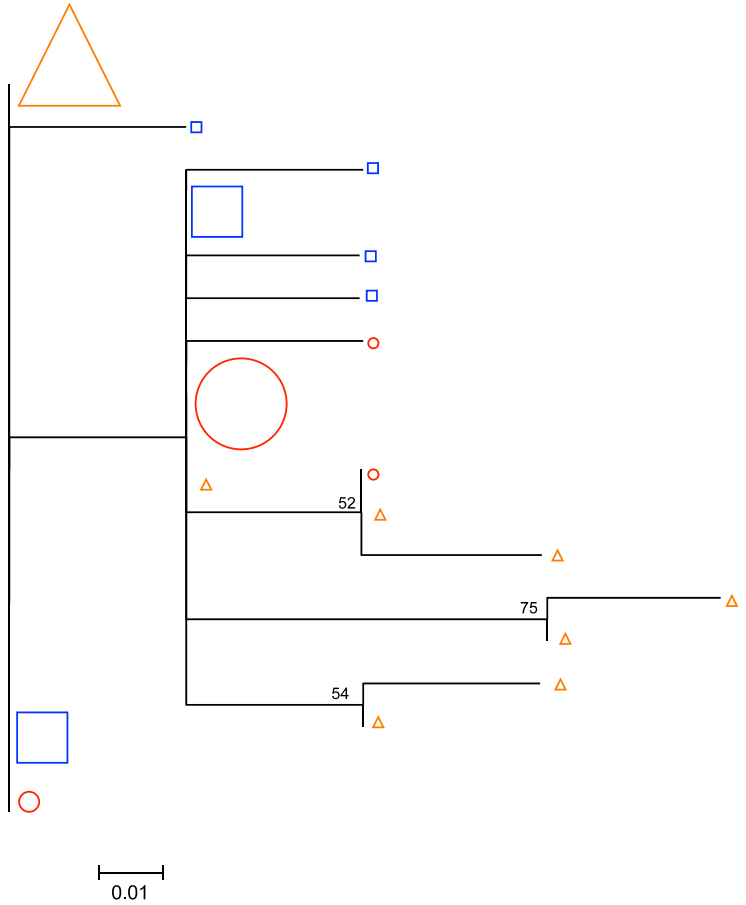

Subject 29

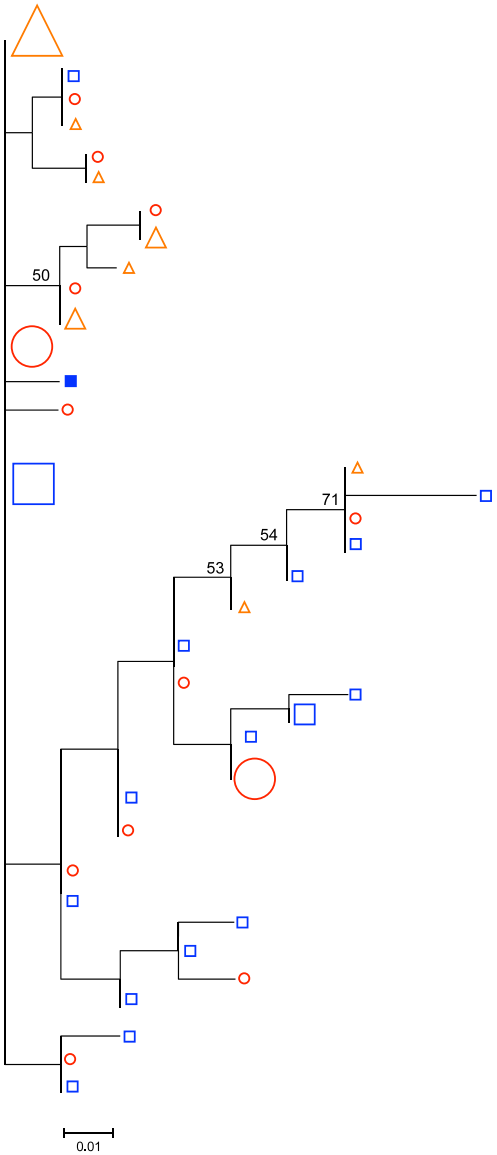

Subject 30

J Antimicrob Chemother
doi:10.1093/jac/dks539

Journal of Antimicrobial Chemotherapy

Switching the third drug of antiretroviral therapy to maraviroc in aviraemic subjects: a pilot, prospective, randomized clinical trial

Anna Bonjoch[1,2]*†, Christian Pou[2,3]†, Núria Pérez-Álvarez[1,4], Rocío Bellido[2,3], Maria Casadellà[2,3], Jordi Puig[1], Marc Noguera-Julian[2,3], Bonaventura Clotet[1–3], Eugènia Negredo[1,2] and Roger Paredes[1–3]

[1]HIV Unit & Fundació Lluita contra la SIDA, Hospital Universitari Germans Trias i Pujol, Barcelona, Catalonia, Spain; [2]Universitat Autònoma de Barcelona, Barcelona, Catalonia, Spain; [3]IrsiCaixa AIDS Research Institute-HIVACAT, Barcelona, Catalonia, Spain; [4]Universitat Politècnica de Catalunya, Barcelona, Catalonia, Spain

*Corresponding author. Fundació Lluita contra la SIDA, Hospital Universitari Germans Trias i Pujol, Ctra de Canyet s/n, 08916 Badalona, Barcelona, Catalonia, Spain. Tel: +34-93-4978887; Fax: +34-93-4657602; E-mail: abonjoch@flsida.org
†Both authors contributed equally.

Received 23 October 2012; returned 22 November 2012; revised 10 December 2012; accepted 21 December 2012

Objectives: To evaluate the safety and efficacy of switching the third drug of antiretroviral treatment to maraviroc in aviraemic subjects infected with R5 HIV.

Patients and methods: This is a pilot, prospective, randomized clinical trial (ClinicalTrials ID: NCT00966329). Eighty HIV-1-infected aviraemic adults on stable antiretroviral treatment for ≥1 year and no antiretroviral drug resistance were screened for the presence of non-R5 HIV by triplicate proviral V3 population sequencing. From them, 30 subjects with R5 HIV-1 were randomized 1:1 to switch the non-nucleoside reverse transcriptase inhibitor or ritonavir-boosted protease inhibitor to maraviroc ($n=15$) or to continue the same antiretroviral treatment (controls, $n=15$). The principal endpoint was the proportion of subjects with HIV-1 RNA <50 copies/mL at week 48. Ultrasensitive proviral HIV-1 tropism testing (454 sequencing) was performed retrospectively at weeks 0, 4, 12, 24, 36 and 48.

Results: One subject in the maraviroc arm and one control had non-R5 HIV in proviral DNA by retrospective 454 sequencing. The subject receiving maraviroc was the only individual to develop virological failure. However, plasma HIV at failure was R5. Switching to maraviroc was well tolerated and associated with small, but statistically significant, declines in total, high-density lipoprotein and low-density lipoprotein cholesterol. Median (IQR) triglyceride [1 (0.67–1.22) versus 1.6 (1.4–3.1) mmol/L, $P=0.003$] and total cholesterol [4.3 (4.1–4.72) versus 5.4 (4–5.7) mmol/L, $P=0.059$] values were lower in the maraviroc arm than in controls at week 48.

Conclusions: In this pilot, prospective, randomized clinical trial, switching the third drug to maraviroc was safe, efficacious and improved lipid parameters.

Keywords: ultrasensitive proviral HIV-1 tropism testing, virally suppressed patients, HIV

Introduction

It is uncertain if subjects with sustained undetectable HIV-1 RNA levels experiencing antiretroviral-related toxicity could safely switch their current ritonavir-boosted protease inhibitor (PI/r) or non-nucleoside reverse transcriptase inhibitor (NNRTI) drug to maraviroc. This treatment strategy could allow improvements in metabolic profile, efavirenz-related neurotoxicity, hepatotoxicity and gastrointestinal events, and would preserve other drugs with favourable toxicity profiles for future regimens. Nevertheless, for this strategy to be safe, it must be ensured that maraviroc is prescribed to subjects with negligible levels of CXCR4-using (non-R5) HIV.[1] The safety of using population sequencing of the gp120 V3-loop of peripheral blood mononuclear cell (PBMC)-associated HIV-1 to guide maraviroc switches in aviraemic subjects, which is becoming increasingly popular in Europe,[2,3] has been evaluated in observational studies,[4,5] but not in prospective, randomized clinical trials.

We developed a pilot clinical trial to test the safety and efficacy of switching from a PI/r or an NNRTI to maraviroc in subjects with persistent virological suppression and with R5 viruses by proviral V3-loop population sequencing.

Methods

This was a 48 week, two-arm, prospective, randomized, pilot clinical trial in HIV-1-infected adults receiving care in the outpatient HIV Unit of the Hospital Universitari Germans Trias i Pujol, Badalona, Catalonia, Spain (ClinicalTrials ID: NCT00966329).

Inclusion criteria for screening were being on stable antiretroviral therapy including a PI/r or an NNRTI plus two nucleoside reverse transcriptase inhibitors (NRTIs) for ≥1 year, having HIV-1 RNA <50 copies/mL for ≥6 months, absence of genotypic drug resistance to the NRTI backbone by bulk sequencing and ≥90% self-reported treatment adherence. Exclusion criteria were previous virological failure, previous detection of non-R5 HIV by any tropism test, active acute or uncontrolled chronic infection during the previous 2 months and pregnancy or willingness to become pregnant. The use of lipid-lowering drugs was allowed. The study was approved by the Institutional Review Board of the Hospital Universitari Germans Trias i Pujol. All subjects provided written informed consent to participate in the study.

HIV-1 tropism was inferred from subjects fulfilling the selection criteria from triplicate V3-loop population sequencing of proviral HIV-1 DNA (Supplementary methods, available as Supplementary data at *JAC* Online). Non-R5 HIV was defined as a false-positive rate value ≤20% in any of the triplicate sequences, using the Geno2Pheno$_{[coreceptor]}$ algorithm. Subjects with R5 HIV were randomized 1:1 to switch their NNRTI or PI/r to maraviroc (Celsentri®, ViiV Healthcare, 300 mg twice a day) (maraviroc arm) or to continue their previous antiretroviral regimen (control arm).

Study visits were at baseline (day of randomization and maraviroc initiation) and at weeks 4, 8, 12, 24, 36 and 48. Clinical data and fasting blood specimens were collected at every visit. Measurements included a complete blood count and biochemistry, HIV-1 RNA levels (NucliSens EasyQ HIV-1, bioMérieux, Marcy l'Étoile, France) and CD4+ cell counts every 12 weeks. Plasma and PBMC samples were stored at −80°C. Proviral HIV-1 tropism was retrospectively evaluated in all visits using 454 sequencing and the Geno2Pheno$_{[454]}$ tool (Supplementary methods, available as Supplementary data at *JAC* Online). Non-R5 HIV was defined as the presence of ≥2% V3 sequences with a false-positive rate ≤3.75.[1,6]

Dyslipidaemia was defined as values that exceeded the National Cholesterol Education Programme (NCEP, Adult Treatment Panel III) borderline-high cut-offs,[7] i.e.: triglycerides, ≥1.7 mmol/L (≥150 mg/dL); total cholesterol, ≥5.2 mmol/L (≥200 mg/dL); high-density lipoprotein (HDL) cholesterol, <1.03 mmol/L (<40 mg/dL); and low-density lipoprotein (LDL) cholesterol, ≥3.4 mmol/L (≥130 mg/dL). The total cholesterol/HDL cholesterol atherogenic ratio was also determined.

The principal efficacy analysis, i.e. the proportion of subjects with HIV-1 RNA <50 copies/mL at week 48, was performed per protocol and by intention-to-treat, where switching or missing equalled failure. The statistical significance of longitudinal changes in HIV RNA levels and CD4+ counts was evaluated by comparing their slope between treatment groups and according to other relevant baseline factors using Student's *t*, Wilcoxon or Mann–Whitney tests. The proportion of subjects with dyslipidaemia was compared using Fisher's exact test. All analyses were performed using SPSS version 15.0 (SPSS Inc., Chicago, IL, USA). A bilateral *P* value <0.05 was considered statistically significant.

Results

Eighty individuals were screened; 37 (46.2%) had non-R5 viruses by population sequencing, 13 did not fulfil the inclusion criteria and 30 entered the study, 15 per arm (Table 1). Subjects had been on antiretroviral treatment for a median of 7.4 (IQR 3.0–12.0) years and had had HIV-1 RNA <50 copies/mL for a median of 5.1 (IQR 2.7–8.8) years. Median (IQR) baseline and nadir CD4+ counts were 737 (515–850) and 336 (250–409) cells/mm^3, respectively. All subjects allocated to the maraviroc arm were on NNRTI-based regimens at randomization: nine were receiving nevirapine and six were receiving efavirenz. Seven subjects allocated to the control arm were on PI/r-containing regimens (four on ritonavir-boosted atazanavir, two on ritonavir-boosted lopinavir and one on ritonavir-boosted fosamprenavir) and eight were on NNRTIs (five on efavirenz and three on nevirapine). The median (IQR) number of variants, reads and quality reads obtained by retrospective 454 sequencing per sample was, respectively: 299 (200–498), 3717 (1930–5850) and 2749 (1619–4282).

One patient in the control arm was lost to follow-up at week 12; one in the maraviroc arm interrupted therapy because of diarrhoea at week 1. There were no other adverse events.

One participant in the maraviroc arm and one control had non-R5 HIV-1 in the retrospective proviral DNA 454 sequencing analysis. See Figure 1(e and f). The subject receiving maraviroc

Table 1. Baseline characteristics of study participants

	Maraviroc arm	Control arm	*P* value
Female gender, *n* (%)	1 (7)	1 (7)	0.759
Caucasian ethnicity, *n* (%)	15 (100)	15 (100)	1
Age (years)	42 (37–47)	39 (37–49)	0.412
Time since HIV diagnosis (months)	113 (37–187)	99 (63.5–156.7)	0.949
Time on suppressed viral load (years)	5 (2.8–9)	5.5 (2.2–8.8)	0.934
Time on highly active antiretroviral therapy (years)	7.1 (2.9–12.6)	7.7 (4.6–11.9)	0.836
Baseline CD4+ T cell count (cells/mm^3)	639 (430–770)	791 (542–996)	0.098
Nadir CD4+ T cell count (cells/mm^3)	319 (212–373)	342 (263–424)	0.436
Total cholesterol (mmol/L)	5 (4.8–5.2)	4.8 (3.8–5.6)	0.744
HDL cholesterol (mmol/L)	1.3 (1.15–1.5)	1.16 (0.96–1.4)	0.126
LDL cholesterol (mmol/L)	2.9 (2.7–3.2)	3.1 (1.9–3.4)	1
Triglycerides (mmol/L)	1.2 (0.8–1.7)	1.7 (0.9–2.5)	0.202
Glycaemia (mmol/L)	5.3 (5.1–5.5)	4.9 (4.7–5.2)	0.005

Values are shown as median (IQR), unless otherwise indicated.

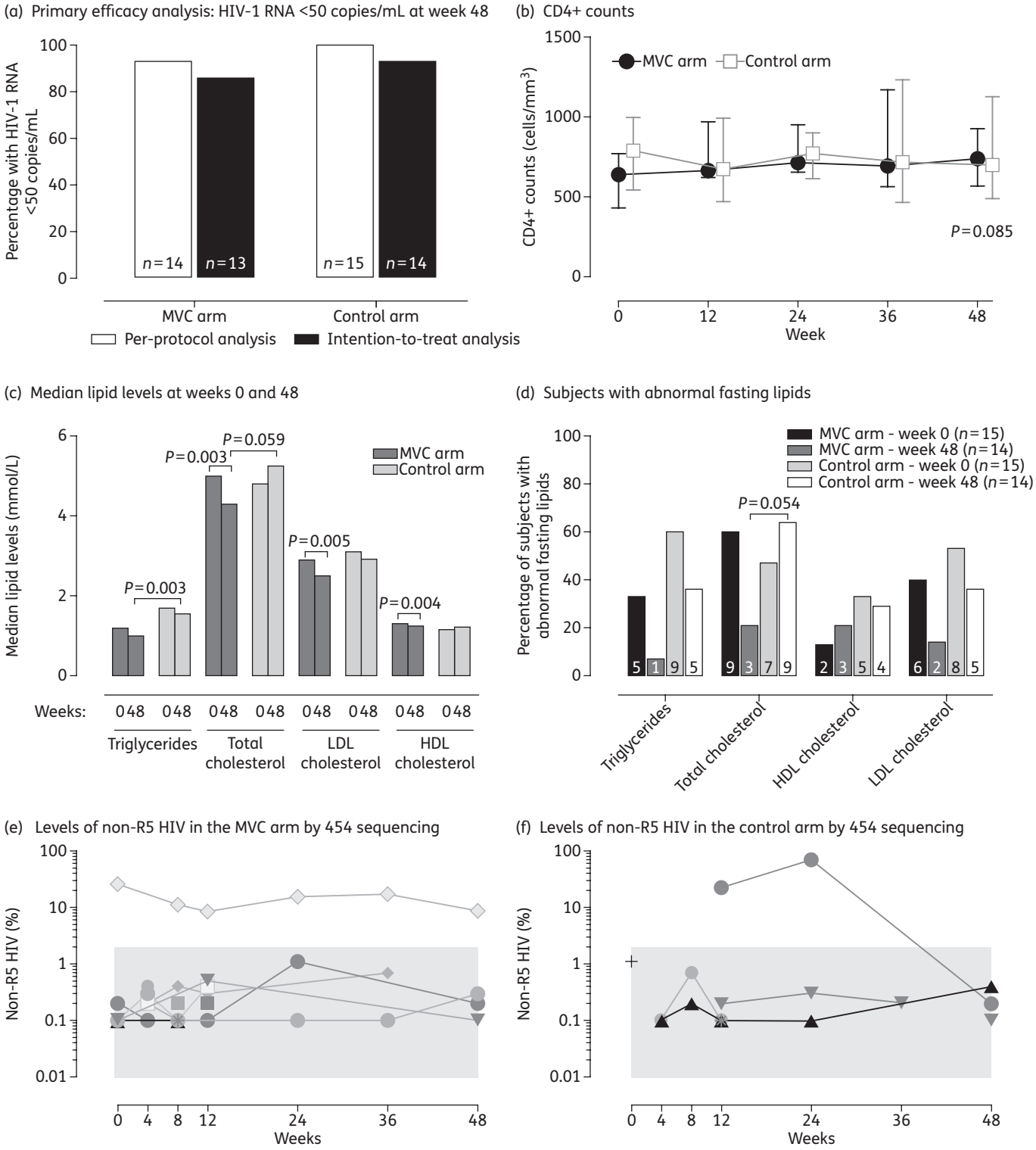

Figure 1. Study outcomes. The main results of the study are shown, i.e.: virological efficacy according to the 'per-protocol' or 'intention-to-treat, where switching or missing equalled failure, analyses (a); median and IQR CD4+ counts during the study (b); median lipid values at baseline and week 48 (c); and proportion of subjects with dyslipidaemia, according to the National Cholesterol Education Programme (NCEP, Adult Treatment Panel III) borderline-high cut-offs [i.e. triglycerides, ≥1.7 mmol/L (≥150 mg/dL); total cholesterol, ≥5.2 mmol/L (≥200 mg/dL); HDL cholesterol, <1.03 mmol/L (<40 mg/dL); and LDL cholesterol, ≥3.4 mmol/L (≥130 mg/dL)] (d). (e and f) Frequency of non-R5 HIV detected in each individual allocated to the maraviroc and control arms, respectively. Different symbols correspond to different subjects. Values corresponding to 0% frequency are not depicted because of the logarithmic scale of this representation. The grey area highlights levels of non-R5 viruses present below the pre-specified 2% detection limit. In all panels, *P* values <0.1 are shown. MVC, maraviroc.

was the only individual developing virological failure during the study (HIV RNA=180 and 170 copies/mL at week 36). This subject had switched from nevirapine to maraviroc on a tenofovir/emtricitabine backbone. Trough drug plasma concentrations 12 h 30 min post-dose were 454 ng/mL for maraviroc (18.2× the target), 78 ng/mL for tenofovir (1.2× the C_{min}) and 179 ng/mL for emtricitabine (2× the C_{min}) at the time of virological failure. By bulk sequencing, the rebounding virus was R5 (Geno2Pheno$_{[coreceptor]}$ false-positive rate: 52.8%) and had no resistance mutations in protease or reverse transcriptase. The subject regained HIV-1 RNA suppression <50 copies/mL after switching back from maraviroc to nevirapine. All remaining subjects retained HIV-1 RNA <50 copies/mL throughout the study.

Therefore, in the primary efficacy analysis by intention-to-treat, where switching or missing equalled failure, 13 individuals (86%) in the maraviroc arm and 14 (93%) in the control arm achieved HIV-1 RNA <50 copies/mL at week 48. In the per-protocol analysis, only one subject in the maraviroc arm developed virological failure (Figure 1a).

Median CD4+ cell counts remained >500 cells/mm^3 in both arms (Figure 1b). There was a median (IQR) increase of 75.5 (−130 to 190) cells/mm^3 in the maraviroc arm (P=0.397) and a median decrease of 84 (−153.5 to −22.25) cells/mm^3 in the control arm (P=0.035), relative to baseline values. At week 48, differences between groups were not significant (P=0.085).

Four subjects in the maraviroc arm and three controls were on lipid-lowering drugs at baseline; one subject in the control arm began lipid-lowering treatment at week 12; they all continued receiving these drugs until the end of the study. Median lipid values were not significantly different at baseline and remained within the normality range throughout the study in both arms. Subjects in the maraviroc arm showed small, but statistically significant, declines in total cholesterol [from 5 (4.8–5.2) to 4.3 (4.1–4.72) mmol/L, P=0.003], HDL cholesterol [from 1.3 (1.15–1.52) to 1.25 (1.08–1.52) mmol/L, P=0.004] and LDL cholesterol [from 2.9 (2.7–3.2) to 2.5 (2.37–2.66) mmol/L, P=0.005] between baseline and week 48. There were no significant longitudinal changes in median lipid values in the control group.

At week 48, median (IQR) triglyceride values were significantly lower in the maraviroc arm [1 (0.67–1.22) mmol/L] than in controls [1.6 (1.4–3.1) mmol/L] (P=0.003). Median (IQR) total cholesterol values were also lower in the maraviroc arm [4.3 (4.1–4.72) mmol/L] than in the control arm [5.4 (4–5.7) mmol/L], but only achieved marginal statistical significance (P=0.059) (Figure 1c).

Nine subjects (60%) in each study arm had abnormal lipid values at baseline (Figure 1d). Abnormal triglyceride, total cholesterol, HDL cholesterol and LDL cholesterol values were found in nine versus five, seven versus nine, five versus two and eight versus six in controls and maraviroc switches, respectively. Fewer subjects in the maraviroc arm had hypercholesterolaemia than in the control arm (21.4% versus 64.3%, respectively, P=0.054) at week 48. There were no statistically significant differences between arms in the proportion of subjects with other types of dyslipidaemia (Figure 1d). The total cholesterol/HDL cholesterol atherogenic ratio decreased in the maraviroc arm (from 3.78 to 3.31), but increased in the control group (from 3.93 to 4.44) between baseline and week 48; however, differences between and within groups did not achieve statistical significance.

Median (IQR) glycaemia values remained within the normality range without significant differences between arms.

Discussion

In this pilot, prospective, randomized clinical trial, switching the third drug to maraviroc was safe, efficacious, well tolerated and improved lipid parameters.

The virological efficacy of maraviroc in our study supports genotypic tropism testing of proviral DNA as a suitable tool to guide treatment switches to CCR5 antagonists in aviraemic individuals. If the test had been unable to screen out subjects with significant levels of non-R5 HIV, they would have been exposed to virtual dual-NRTI therapy for 48 weeks. Conceivably, that would have been associated with non-R5 virus evolution, higher rates of virological failure and potential development of NRTI resistance. Importantly, no subject with R5 HIV at baseline developed non-R5 viruses during continued exposure to maraviroc therapy, suggesting that maraviroc-including regimens continued to inhibit viral replication as much as conventional antiretroviral treatment.

The settings used for proviral DNA population sequencing in this study were more conservative than the ones suggested by European tropism guidelines,[2,3] but still missed non-R5 HIV in the only subject that eventually developed virological failure. The clinical implications of this finding are uncertain, however, as the rebounding plasma virus was R5 and had no resistance mutations in protease or reverse transcriptase. Trough drug levels at the time of viraemia rebound were adequate, which rules out major adherence or pharmacokinetic problems as the cause of virological failure. Eventually, the subject regained viraemia suppression when he was switched back to tenofovir/emtricitabine plus nevirapine. Non-R5 levels remained relatively stable in proviral DNA throughout the study follow-up, even at virological failure. This is concordant with the heterogeneous cellular and viral composition of PBMCs, which often includes non-viable or non-replicating viruses, although we cannot rule out the emergence of mutations conferring resistance to maraviroc, as observed in previous studies.[8] Larger studies are needed to clarify whether there is a relationship between levels of non-R5 HIV in PBMCs and virological outcomes to maraviroc therapy in aviraemic subjects, beyond the sensitivity threshold of ultrasensitive genotypic tropism techniques.

As observed in treatment-naive individuals,[9] a switch to maraviroc improved lipid parameters, with small, but statistically significant, reductions in median total cholesterol and LDL cholesterol levels, and lower triglyceride and total cholesterol levels relative to controls at the end of the study. This lipid-lowering effect, alongside the putative anti-inflammatory activity of maraviroc,[10] could potentially contribute to reduce antiretroviral therapy-related cardiovascular risk,[11–14] allowing some patients to avoid lipid-lowering agents and their associated toxicity or drug interactions with antiretrovirals. Indeed, we observed a non-significant trend towards decreasing total cholesterol/HDL cholesterol ratios in subjects switching to maraviroc, relative to controls that should be confirmed in larger studies. Although the study inclusion criteria did not restrict for previous

NNRTI or PI use and patients were not stratified according to previous treatment, all subjects who switched to maraviroc in this trial were previously receiving NNRTIs. This could have influenced the lipid results even though lipid levels were not significantly different between the study arms at baseline. Particularly, improvements in the lipid profile might have been more evident in subjects switching to maraviroc from PI/r-containing regimens.

The main limitation of this study was its small sample size, which is justified by its pilot nature, given the risk of this strategy and the lack of prospective, randomized, clinical trials assessing its safety and virological consequences when the study was designed. Although our results cannot be considered definitive, they are highly informative for upcoming, well-powered clinical trials. On the one hand, clinicians should be reassured of the overall good performance of genotypic tropism testing in proviral DNA as a tool to screen for aviraemic subjects suitable to receive CCR5 antagonists. On the other hand, studies should attempt to confirm whether ultrasensitive genotyping techniques could further improve clinical outcomes. Cost-effectiveness analyses as well as more detailed metabolic studies would also be important to define the best clinical use of this treatment strategy. One final limitation, common to all clinical trials, is that the benefits of the approach tested in this study could have been overestimated in comparison with routine clinical practice, as participants in clinical trials usually have higher treatment adherence and motivation to pursue treatments correctly.

In conclusion, this pilot, prospective, randomized clinical trial showed that switching the third drug of antiretroviral therapy to maraviroc in aviraemic subjects is safe, efficacious and improves lipid parameters. Adequately powered studies should corroborate our findings, evaluate the cost-effectiveness of this treatment approach and, in particular, investigate whether detection of pre-existing low-frequency non-R5 HIV-1 in proviral DNA further improves the efficacy of this strategy.

Acknowledgements

This study was presented in part at the International Workshop on HIV & Hepatitis Virus Drug Resistance and Curative Strategies, Sitges, Spain, 2012 (Poster #41).

Funding

This study was supported by an investigator-initiated research grant from ViiV Healthcare, 'CHAIN, Collaborative HIV and Anti-HIV Drug Resistance Network', Integrated Project no. 223131, funded by the European Commission Framework 7 Program, and the 'Gala contra la sida—Barcelona 2011'.

Transparency declarations

A. B. has received lecture fees from Bristol-Myers Squibb. B. C. has been a consultant on advisory boards or participated in speakers' bureaus or conducted clinical trials with Boehringer-Ingelheim, Abbott, GlaxoSmithKline, Gilead, Janssen, Merck, Shionogi and ViiV Healthcare. E. N. has received research funding, consultancy fees or lecture sponsorships from Gilead, Roche, Bristol-Myers Squibb, GlaxoSmithKline, Tibotec, Abbott, Merck and Boehringer-Ingelheim. R. P. has received research funding, consultancy fees or lecture sponsorships from Gilead, Pfizer, ViiV Healthcare, Roche Diagnostics, Siemens, Merck and Boehringer-Ingelheim. C. P., N. P.-Á., R. B., M. C., J. P. and M. N.-J. report no competing interests.

Author contributions

A. B., E. N., R. P. and B. C. designed the study and were in charge of the recruitment and monitoring of patients. J. P. performed blood extractions and was responsible for management of the database. R. B. performed V3-loop bulk sequencing for tropism screening. C. P. and M. C. performed V3-loop 454 sequencing. C. P., M. C. and M. N.-J. analysed the 454 sequencing tropism data. N. P.-Á. performed the statistical analysis. A. B., C. P., E. N. and R. P. drafted the manuscript. All authors contributed to reviewing, editing and preparing the final version of the manuscript.

Supplementary data

Supplementary methods are available as Supplementary data at *JAC* Online (http://jac.oxfordjournals.org/).

References

1 Swenson LC, Mo T, Dong WW *et al*. Deep V3 sequencing for HIV type 1 tropism in treatment-naive patients: a reanalysis of the MERIT trial of maraviroc. *Clin Infect Dis* 2011; **53**: 732–42.

2 Poveda E, Paredes R, Moreno S *et al*. Update on clinical and methodological recommendations for genotypic determination of HIV tropism to guide the usage of CCR5 antagonists. *AIDS Rev* 2012; **14**: 208–17.

3 Vandekerckhove LP, Wensing AM, Kaiser R *et al*. European guidelines on the clinical management of HIV-1 tropism testing. *Lancet Infect Dis* 2011; **11**: 394–407.

4 Obermeier M, Symons J, Wensing AM. HIV population genotypic tropism testing and its clinical significance. *Curr Opin HIV AIDS* 2012; **7**: 470–7.

5 Bellecave P, Paredes R, Anta L *et al*. Determination of HIV-1 tropism from proviral HIV-1 DNA in patients with suppressed plasma HIV-1 RNA using population based- and deep-sequencing: impact of X4-HIV variants on virologic responses to maraviroc. In: *Abstracts of the International Workshop on HIV & Hepatitis Virus Drug Resistance and Curative Strategies, Sitges, Spain, 2012*. Abstract 42. *Antivir Ther* 2012; **17** Suppl 1: A53.

6 Swenson LC, Mo T, Dong WW *et al*. Deep sequencing to infer HIV-1 co-receptor usage: application to three clinical trials of maraviroc in treatment-experienced patients. *J Infect Dis* 2011; **203**: 237–45.

7 Third Report of the National Cholesterol Education Program (NCEP) Expert Panel on Detection, Evaluation, and Treatment of High Blood Cholesterol in Adults (Adult Treatment Panel III) Final Report. *Circulation* 2002; **106**: 3143.

8 Tilton JC, Wilen CB, Didigu CA *et al*. A maraviroc-resistant HIV-1 with narrow cross-resistance to other CCR5 antagonists depends on both N-terminal and extracellular loop domains of drug-bound CCR5. *J Virol* 2010; **84**: 10863–76.

9 MacInnes A, Lazzarin A, Di Perri G *et al*. Maraviroc can improve lipid profiles in dyslipidemic patients with HIV: results from the MERIT trial. *HIV Clin Trials* 2011; **12**: 24–36.

10 Funderburg N, Kalinowska M, Eason J *et al*. Effects of maraviroc and efavirenz on markers of immune activation and inflammation and associations with CD4+ cell rises in HIV-infected patients. *PLoS One* 2010; **5**: e13188.

11 Hsue PY, Ordovas K, Lee T *et al*. Carotid intima-media thickness among human immunodeficiency virus-infected patients without coronary calcium. *Am J Cardiol* 2011; **109**: 742–7.

12 Ross AC, Rizk N, O'Riordan MA *et al*. Relationship between inflammatory markers, endothelial activation markers, and carotid intima-media thickness in HIV-infected patients receiving antiretroviral therapy. *Clin Infect Dis* 2009; **49**: 1119–27.

13 Triant VA, Lee H, Hadigan C *et al*. Increased acute myocardial infarction rates and cardiovascular risk factors among patients with human immunodeficiency virus disease. *J Clin Endocrinol Metab* 2007; **92**: 2506–12.

14 Friis-Moller N, Reiss P, Sabin CA *et al*. Class of antiretroviral drugs and the risk of myocardial infarction. *N Engl J Med* 2007; **356**: 1723–35.

Supplementary data

Supplementary methods

Tropism evaluation by proviral DNA V3 population and 454 sequencing

V3-loop population sequencing

Total proviral HIV-1 DNA was extracted from 10^6 PBMCs using a QIAamp DNA Blood Mini Kit (QIAgen Inc, Valencia, CA, USA). gp160 was PCR-amplified (Platinum® Taq High Fidelity, Life Technologies, Paisley, UK) in triplicate parallel reactions using primers V3-PSOF (HXB2 coordinates 5858-5877) 5'-CCC TGG AAG CAT CCA GGA AG-3' and V3-PSOR (HXB2 coordinates 9064-9089) 5'-TTT TTA AAA GAA AAG GGG GGA CTG GA-3' with the following cycling conditions: 5 min denaturalization at 94ºC; 30 s at 94ºC, 30 s at 55ºC and 4 min at 68ºC for 30 cycles; and a final elongation step at 68ºC for 5 min. Each PCR product was used as a template for a nested PCR (Platinum® Taq High Fidelity), which was performed with primers V3-PSNF (HXB2 coordinates 5958-5983) 5'-TAG GCA TCT CCT ATG GCA GGA AGA AG-3' and V3-PSNR (HXB2 coordinates 8882-8904) 5'-GGG TGG GAG CAG TAT CTC GAG AC-3', with the following cycling conditions: 2 min denaturalization at 94ºC; 30 s at 94ºC, 30 s at 55ºC and 3 min at 68ºC for 30 cycles; and a final 5 min elongation step at 68ºC. PCR products were purified (QIAquick PCR Purification Kit, QIAgen Inc.). Bidirectional Sanger sequencing was performed using primers V3-PSeqF (HXB2 coordinates 7002-7021) 5'-CTG TTA AAT GGC AGT CTA GC-3' and V3-PSeqR (HXB2 coordinates 7344-7363) 5'-CAC AGT TTT AAT TGT GGA GG-3'.

Contigs and consensus sequences were created with Sequencher v5.0 (Gene Codes Corporation, Ann Arbor, MI, USA). Coreceptor use was inferred using the Geno2Pheno$_{[coreceptor]}$ tool. Non-R5 HIV was defined as an FPR ≤20% in any of the triplicate sequences evaluated for each study subject.

V3-loop 454 sequencing

Triplicate first-round PCR products described above were pooled and used as a template for a nested PCR (Platinum® Taq High Fidelity) using the following 454-adapted primers: V3-454F (HXB2 coordinates 7010-7029) 5'-TGG CAG TCT AGC AGA AGA AG-3' and V3-454R (HXB2 coordinates 7315-7332) 5'-CCT CAG GAG GGG ACC CAG-3'. Primers included the corresponding A and B 454 adapters, a 10-mer multiple identifier and a TCAG sequence tag at the 5' end. Cycling conditions were: 2 min at 94ºC; 30 s at 94ºC, 30 s at 55ºC and 45 s at 68ºC for 30 cycles; and 3 min at 68ºC. PCR products were purified using AMPure Magnetic Beads (Beckman Coulter Inc., Brea, CA, USA). The concentration and quality of each amplicon was determined by fluorimetry (PicoGreen, Life Technologies) and spectrophotometry (Lab-on-a-Chip, Agilent Technologies, Foster City, CA, USA). Equimolar pools were made to perform emulsion PCR using a 454-FLX sequencing platform with Titanium chemistry (454 Life Sciences/Roche). HIV-1 tropism was determined using the Geno2Pheno$_{[454]}$ tool. Non-R5 HIV was defined as the presence of ≥2% sequences with an FPR ≤3.75.

OPEN ACCESS Freely available online

PLoS one

Added Value of Deep Sequencing Relative to Population Sequencing in Heavily Pre-Treated HIV-1-Infected Subjects

Francisco M. Codoñer[1*¤], Christian Pou[1], Alexander Thielen[3], Federico García[4], Rafael Delgado[5], David Dalmau[6], Miguel Álvarez-Tejado[7], Lidia Ruiz[1], Bonaventura Clotet[1,2], Roger Paredes[1,2*]

1 Institut de Recerca de la SIDA irsiCaixa-HIVACAT, Badalona, Spain, **2** Unitat VIH, Hospital Universitari Germans Trias I Pujol, Badalona, Spain, **3** Max Planck Institute für Informatik, Saarbücken, Germany, **4** Hospital San Cecilio, Granada, Spain, **5** Hospital 12 de Octubre, Madrid, Spain, **6** Hospital Universitari Mutua Terrassa, Terrassa, Spain, **7** Roche Diagnostics SL, Sant Cugat del Vallès, Spain

Abstract

Objective: To explore the potential of deep HIV-1 sequencing for adding clinically relevant information relative to viral population sequencing in heavily pre-treated HIV-1-infected subjects.

Methods: In a proof-of-concept study, deep sequencing was compared to population sequencing in HIV-1-infected individuals with previous triple-class virological failure who also developed virologic failure to deep salvage therapy including, at least, darunavir, tipranavir, etravirine or raltegravir. Viral susceptibility was inferred before salvage therapy initiation and at virological failure using deep and population sequencing genotypes interpreted with the HIVdb, Rega and ANRS algorithms. The threshold level for mutant detection with deep sequencing was 1%.

Results: 7 subjects with previous exposure to a median of 15 antiretrovirals during a median of 13 years were included. Deep salvage therapy included darunavir, tipranavir, etravirine or raltegravir in 4, 2, 2 and 5 subjects, respectively. Self-reported treatment adherence was adequate in 4 and partial in 2; one individual underwent treatment interruption during follow-up. Deep sequencing detected all mutations found by population sequencing and identified additional resistance mutations in all but one individual, predominantly after virological failure to deep salvage therapy. Additional genotypic information led to consistent decreases in predicted susceptibility to etravirine, efavirenz, nucleoside reverse transcriptase inhibitors and indinavir in 2, 1, 2 and 1 subject, respectively. Deep sequencing data did not consistently modify the susceptibility predictions achieved with population sequencing for darunavir, tipranavir or raltegravir.

Conclusions: In this subset of heavily pre-treated individuals, deep sequencing improved the assessment of genotypic resistance to etravirine, but did not consistently provide additional information on darunavir, tipranavir or raltegravir susceptibility. These data may inform the design of future studies addressing the clinical value of minority drug-resistant variants in treatment-experienced subjects.

Citation: Codoñer FM, Pou C, Thielen A, García F, Delgado R, et al. (2011) Added Value of Deep Sequencing Relative to Population Sequencing in Heavily Pre-Treated HIV-1-Infected Subjects. PLoS ONE 6(5): e19461. doi:10.1371/journal.pone.0019461

Editor: Esper Georges Kallas, University of Sao Paulo, Brazil

Received January 17, 2011; **Accepted** March 30, 2011; **Published** May 13, 2011

Funding: This study was supported by the CDTI (Centro para el Desarrollo Tecnológico Industrial), Spanish Ministry of Science and Innovation (IDI-20080843) and 'CHAIN, Collaborative HIV and Anti-HIV Drug Resistance Network', Integrated Project no. 223131, funded by the European Commission Framework 7 Program. FMC was supported by Marie Curie European Reintegration Grant number 238885, 'HIV Coevolution', funded by the European Commission Framework 7 Program. Miguel Álvarez-Tejado works for Roche Diagnostics, S.L. The funders had no role in study design, data collection and analysis, decision to publish, or preparation of the manuscript.

Competing Interests: F. García has been a consultant on advisory boards, or has participated in speakers' bureaus, with Roche, Boehringer-Ingelheim, BMS, GSK, Gilead, Janssen, Merck and Pfizer. R. Delgado has received consulting fees and grant support from Abbott, BMS, Gilead and Roche. D. Dalmau has been a consultant on advisory boards, has participated in speakers' bureaus, or has conducted clinical trials with Roche, Boehringer-Ingelheim, Abbott, BMS, GSK, Gilead, Tibotec, Janssen, Merck and Pfizer. M. Álvarez-Tejado works for Roche Diagnostics S.L., Spain, which commercializes the 454 sequencing technology in Spain. B. Clotet has been a consultant on advisory boards, has participated in speakers' bureaus, or has conducted clinical trials with Roche, Boehringer-Ingelheim, Abbott, BMS, GSK, Gilead, Tibotec, Janssen, Merck, Pfizer, Siemens, Monogram Biosciences, and Panacos. R. Paredes has received consulting fees from Pfizer and grant support from Pfizer, Siemens, Merck and Boehringer Ingelheim. This does not alter the authors' adherence to all the PLoS ONE policies on sharing data and materials. F.M. Codoñer, C. Pou, A. Thielen, and L. Ruiz report no conflicts of interest relevant to this article. No other potential conflict of interest relevant to this article was reported.

* E-mail: fcodoner@gmail.com (FMC); rparedes@irsicaixa.es (RP)

¤ Current address: Lifesequencing, S.L., Valencia, Spain

Introduction

The rate of virological failure of the 3 original drug classes is low, but not negligible, and does not appear to diminish over time from starting antiretroviral therapy.[1] If this trend continues, many patients will require newer drugs to maintain viral suppression and accurate resistance tests will be needed to guide clinical management. Deep HIV-1 sequencing (454 Life Sciences/

Roche Diagnostics) could potentially improve genotypic resistance assessments because it detects the same range of mutants than Sanger viral population sequencing, but with higher sensitivity [2].

Studies have shown that pre-existing minority drug-resistant mutants increase the risk of virological failure to first-line antiretroviral therapy with non-nucleoside reverse transcriptase inhibitors (NNRTIs) [3,4,5,6,7]. Conversely, low-frequency drug-resistant variants do not affect virological outcomes of first-line therapy including drugs with high genetic barrier, like ritonavir-boosted protease inhibitors (PIr) [8]. Whereas most studies addressing the role of minority variants have been performed in antiretroviral-naïve subjects [2,3,4,5,6,7,9,10,11,12,13], less information exists on the clinical significance of minority mutants in antiretroviral-experienced individuals. [14,15,16]

It is particularly uncertain if ultrasensitive genotypic tests could provide clinically relevant information in heavily pre-treated HIV-1-infected subjects beyond that provided by standard population sequencing genotypic tests. On one hand, detection of additional minority drug-resistant mutants could improve the assessment of viral susceptibility to drugs with intermediate or high drug genetic barrier. On the other hand, the presence of extensive drug resistance could compromise the ability of deep sequencing to add relevant genotypic information to that already obtained with population sequencing, particularly when alternative treatment options are severely limited. Moreover, mutant fixation during virological failure in the presence of ART pressure could potentially complicate the detection of additional low-frequency variants [16].

We therefore sought to explore the potential of deep sequencing to provide additional, clinically relevant genotypic information that could be used to improve treatment decisions in heavily pre-treated HIV-1-infected subjects, relative to population sequencing.

Methods

Subjects

This proof-of-concept observational study included HIV-1-infected adults with previous virological failure (VF) to protease inhibitors (PIs), nucleos(t)ide (NRTIs) and non-nucleoside reverse transcriptase inhibitors (NNRTIs), who developed virological failure to deep salvage therapy including, at least, darunavir, tipranavir, etravirine or raltegravir. Virological failure was defined as the presence of HIV-1 RNA levels >200 copies/mL 24 weeks after salvage therapy initiation or beyond. Adherence was self-reported by the patient and collected from medical charts. Adequate adherence was defined as intake of all medication doses. Partial adherence was defined as the presence of missed doses during treatment. Treatment interruption meant the complete interruption of therapy during follow-up. The Institutional Review Board of the Hospital Universitari Germans Trias i Pujol, Badalona, Spain, approved the study; participants provided written informed consent for retrospective sample testing.

HIV RNA extraction and reverse transcription

HIV-1 RNA was extracted from 1 mL of plasma within 4 weeks before initiation of deep salvage therapy (baseline) and at virological failure (QIAamp UltraSens Virus Kit™, QIAGEN, Valencia, CA). Three One-Step RT-PCRs (SuperScript® III One-Step RT-PCR System with Platinum® Taq High Fidelity, Invitrogen, Carlsbad, CA) were performed in parallel per each sample. Primers used were 1571-L23 (HXB2: 1417→1440) 5′-ATT TCT CCT ACT GGG ATA GGT GG-3′ and 5464-L27 (HXB2: 5464→5438) 5′-CCT TGT TAT GTC CTG CTT GAT ATT CAC-3′. Cycling conditions were: 30 min. at 52°C, 2 min. at 94°C; 30 sec. at 94°C, 30 sec. at 56°C, 4 min. at 68°C, for 20 cycles; followed by 5 min. at 68°C. Triplicate RT-PCR products were pooled, column-purified (QIAquick PCR Purification Kit, QIAGEN, Valencia, CA) and used for both viral population and deep HIV-1 sequencing.

Viral population genotyping

Triplicate nested PCRs were performed in parallel (Platinum® Taq DNA Polymerase High Fidelity, Invitrogen, Carlsbad, CA) with primers 2084-U26 (HXB2: 2084→2109) 5′-ATT TTT TAG GGA AGA TCT GGC CTT CC-3′ and 5456-L26 (HXB2: 5456→5431) 5′-TGT CCT GCT TGA TAT TCA CAC CTA GG-3′. Cycling conditions were: 2 min. at 94°C; 30 sec. at 94°C, 30 sec. at 56°C, 4 min. at 68°C, for 20 cycles; followed by 5 min. at 68°C. Nested PCR products were pooled and column-purified. Protease (PR), reverse transcriptase (RT) and integrase (IN) were sequenced in-house (BigDye v3.1, Applied Biosystems, Foster City, CA, USA) and resolved by capillary electrophoresis (ABI 7000, Foster City, CA, USA).

Deep HIV-1 sequencing

Pooled purified RT-PCR products were used as template to generate eight overlapping amplicons covering PR and RT and 3 amplicons covering codons 51 to 215 in IN. Each codon was interrogated by at least 2 independent amplicons, which were generated in triplicate during 20 cycles of PCR amplification (Platinum® Taq DNA Polymerase High Fidelity, Invitrogen, Carlsbad, CA) followed by pooling and purification of triplicate PCR products (QIAquick PCR Purification Kit, QIAGEN, Valencia, CA). PCR reactions were pooled and purified using the Agencourt AMPure Kit (Beckman Coulter, Benried, Germany) to eliminate primer-dimers. The number of molecules was quantified by fluorometry (Quant-iT PicoGreen dsDNA assay kit, Invitrogen, Carlsbad, CA). When amplicon concentrations were below 5 ng/mL, amplicon size and primer-dimer content were analysed by spectrometry using BioAnalyzer (Agilent Technologies Inc., Santa Clara, CA). Emulsion PCR was carried out as in [17]. Amplicon Sequencing was performed at 454 Life Sciences, Branford, Connecticut, USA, using a Genome Sequencer FLX. Sequences were extracted and aligned against a consensus sequence from all the reads for each sequences region. Clonal sequences resulting with <90% similarity with the consensus sequence were discarded. Sequencing errors in homopolymeric regions were manually inspected and corrected. Sequences that included a stop codon were removed. Unique sequences (haplotypes) were identified and quantified. The frequency of mutants with a Stanford HIV Database [18] score > 5 was determined.

Using a conservative approach, only mutations present in ≥ 1% of the virus population where considered in this study. An in-house analysis of 992 pNL43 clonal sequences obtained by deep sequencing under the same PCR conditions used to generate patient samples showed a mean (SD) nucleotide mismatch rate of 0.07% (0.13%), which is almost identical to previous reports [14] and corresponds to a variability rate of 1.69×10^{-5}, within the range of the expected PCR error. The mean (SD) error rate for any aminoacid mismatch was 0.14% (0.19%), but the mean (SD) error rate for actual drug resistance mutations was 0.03% (0.07%). The 99th percentile of mismatches would establish the threshold for nucleotide errors in 0.61% and the limit for identifying true drug resistance mutations in 0.20%.

Assessment of discrepancies between population and deep sequencing

Genotypes were interpreted with the HIVdb v6.0.8 [18], Rega v8.0.2 [19] and ANRS v18 [20] algorithms. Only mutations with a

score ≥ 5 in the Stanford HIV Drug Resistance Database were included in the analysis. Viral susceptibility to each drug was classified as "Sensitive", "Intermediate" or "Resistant". Sixty-three paired drug susceptibility predictions (each pair including population and deep sequencing genotypic data) were evaluated per subject and timepoint, 20 for ANRS, 21 for HIVdb v6.0.8 and 22 for Rega v8.0.2.

Results

Subjects

The study included 7 individuals, 2 of them women, with previous exposure to a median of 15 antiretrovirals during a median of 13 years. Their median (interquartilic range, IQR) age was 44 (39; 49) years. The median (IQR) year of HIV diagnosis was 1988 (1985; 1994). Median (IQR) HIV-1 RNA levels and CD4 counts were, respectively, 110,600 (46,550; 370,000) copies/mL and 50 (12; 126) cells/mm^3 at baseline; and 36,700 (2,895; 205,000) copies/mL and 150 (27; 247) cells/mm^3 at virological failure. Median (IQR) nadir CD4 counts were 14 (1; 152) cells/mm^3. Deep salvage therapy included darunavir, tipranavir, etravirine or raltegravir in 4, 2, 2 and 5 subjects, respectively. (Table S1) Treatment adherence was adequate in 4 individuals (Subjects 1 to 4) (Table S1) and partial in 2 (Subjects 5 and 6), one individual (Subject 7) (Table S1) interrupted antiretroviral therapy during follow-up.

Phenotypic susceptibility predictions by population and deep genotyping

The median (IQR) deep sequencing coverage per base was 3938 (3130 – 6945) sequences at baseline and 3965 (3688 – 7091) sequences at virological failure. Deep sequencing detected all mutations found by population sequencing in all subjects, and found additional mutations in 6 out of 7 individuals. (Table S1) Additional mutations were congruent with the treatment history and modified 5.2% of phenotypic susceptibility predictions overall (Table S2), with no significant differences between interpretation algorithms.

Deep sequencing provided limited additional genotypic information at baseline relative to PS. Baseline DS changed the ANRS predicted susceptibility of lopinavir/r and saquinavir/r from sensitive to intermediate in subject 1 and the ANRS susceptibility of darunavir/r from intermediate to resistant in subject 2 (Table S1). In subject 7 (Table S1), however, the detection of minority protease I54L and V82A mutants by deep sequencing in addition to the I54I/V, T74S and L90M detected by population sequencing, consistently decreased the virus susceptibility to indinavir/r across the three algorithms, and led to decreases in predicted susceptibility to saquinavir/r and darunavir/r and to lopinavir/r by the HIVdb and Rega algorithms. The additional detection of the reverse transcriptase M41L and T215Y mutants in this individual led to decreases in susceptibility to different NRTIs by the three algorithms.

Most additional resistance mutations leading to changes in susceptibility predictions were found after virological failure to deep salvage therapy (Table S1). Consistent decreases in etravirine susceptibility were observed in the two subjects treated with etravirine in this study (subjects 1 and 2). Detection of additional mutations in protease in these two individuals also led to decreased susceptibility to saquinavir/r and lopinavir/r in the ANRS algorithm, respectively. Low-level K103N mutants were detected at virological failure in subject 5. This individual had received efavirenz in the past and was receiving nevirapine at baseline, when he was switched from tenofovir, stavudine, lamivudine and nevirapine, to tenofovir/emtricitabine, darunavir/r and enfuvirtide. The withdrawal of stavudine-mediated pressure over pre-existing K103N mutants might have enabled their emergence and subsequent detection at virological failure. Finally, the detection of minority K219Q and T215Y mutants in subjects 6 and 7, respectively, led to consistent decreases in predicted viral susceptibility to different NRTIs.

Most baseline resistance mutations were lost in subject 7 during treatment interruption becoming undetectable even by deep sequencing at the time of virological failure. No changes in predicted susceptibility were observed for tipranavir or raltegravir, although detection of minority G140S in subject 3 suggested improved fitness of the Q148R mutants detected by population sequencing at virological failure (Table S1).

Discussion

While being technically non-inferior to population genotyping, deep sequencing enabled the detection of additional resistance mutations with potential clinical significance in 6 out of 7 individuals included in this study. Additional mutations, however, only modified about 5% of antiretroviral susceptibility predictions, including decreased etravirine efficacy in the 2 subjects developing virological failure to this drug, and decreased NRTI, efavirenz and indinavir/r efficacy in 2, 1, and 1 subject, respectively. Changes in darunavir susceptibility observed in 2 individuals were not consistent across algorithms. Deep sequencing had no impact on susceptibility predictions for tipranavir or raltegravir.

Deep sequencing could modify patient clinical management by avoiding drugs whose resistance may have been underestimated by population sequencing. Indeed, baseline low-frequency PI-resistant mutants were selected during treatment exposure in two subjects: I54T in subject 1, and V32I, Q58E and L89V in subject 2. I54T is a PI-related mutation that appears to be associated with decreased susceptibility to each of the PIs, although its effect has not been well studied. Q58E is a non-polymorphic PI-related mutation associated with reduced susceptibility tipranavir [21,22,23] and possibly to several other PIs. Selection of I54T and Q58E mutations during darunavir therapy may be explained due to residual phenotypic or compensatory effect of such mutations on darunavir susceptibility, genome colinearity with other darunavir-associated mutations, or simple stochastic effects. Interestingly, emergence of I54T in subject 1 was associated with decay in I54A, indicating a possible fitness advantage of I54T over I54A in this particular context. Conversely, substitutions V32I and L89V are nonpolymorphic PI-selected accessory mutations which emerge during treatment with darunavir/ritonavir. Both mutations were associated with decreased response to darunavir/ritonavir in the POWER trials [24], suggesting that they were selected in subject 2 because they conferred additional resistance to darunavir.

Most additional mutants in our study, however, were detected at virological failure. Varghese et al. also detected additional minority variants with major etravirine mutations only in patients failing an NNRTI-containing regimen [14]. Taken together, these results suggest that deep sequencing might be more useful to assess loss of antiviral efficacy after virological failure than to screen for pre-existing resistance in subjects with extensive treatment exposure. As with population sequencing, deep sequencing should also be performed immediately or shortly after virological failure.

The increased sensitivity of deep sequencing could also reassure clinicians about the absence of additional genotypic resistance when making clinical management decisions. This is particularly important for the management of subjects with suboptimal

adherence. In our study, deep sequencing provided additional genotypic information in all adherence strata. (Table S1, Table S2) Deep sequencing, for example, confirmed virus susceptibility to integrase strand-transfer inhibitors in 4 out of 5 subjects who developed virological failure to raltegravir-including regimens, indicating that raltegravir remained a suitable option for subsequent salvage regimens. Similarly, deep sequencing confirmed that subjects 5, 6 and 7 could still be treated with a number of different PIs and suggested higher virus susceptibility to tipranavir than to darunavir in subject 7. (Table S2) The absence of resistance mutations by deep sequencing, however, should be interpreted with caution; the loss of most baseline mutants in subject 7 during antiretroviral therapy interruption shows that deep sequencing can also miss clinically relevant resistance mutations present $<1\%$ in the viral population.

Detection of low-frequency resistance mutations associated with hypersusceptibility could also improve predicted susceptibility to certain antiretrovirals. For example, the incorporation of a minority T215F mutation in subject 2 changed the HIVdb predicted susceptibility to tenofovir from "resistant" to "intermediate" at virological failure. Therefore, ultrasensitive genotyping also has the potential to refine genotype interpretation rules towards increased virus susceptibility.

Our findings extend those of Le et al. [15], who showed that deep sequencing detected low-frequency mutations unrecognized by Sanger sequencing in 19 out of 22 antiretroviral–experienced individuals experiencing virological failure in routine HIV care between 2004-2007. Additional minority mutants increased a subject's genotypic resistance to one or more antiretrovirals in 17 of 22 individuals (77%), correlated with the failing drugs in 21% subjects, and with historical antiretroviral use in 79% subjects. In Le's study, however, samples were collected before etravirine, darunavir or raltegravir became available, so the effect additional minority mutants on HIV susceptibility to these drugs could not be evaluated.

The main limitations of our study are its small sample size, its retrospective observational nature and the fact that adherence was self-reported. This study makes two arguable assumptions: First, that a mutant detected above 1% is clinically relevant. This threshold is clearly above the PCR and 454 sequencing error found in our own and other studies [14,25] and has been shown to predict virological outcomes of first-line NNRTI therapy in treatment–naïve individuals.[2] Moreover, potential PCR-derived recombination should not affect our findings because we did not evaluate mutational linkage. The second assumption is that minority mutants have the same weight in genotypic susceptibility interpretation algorithms as if they were present at higher levels. While biologically plausible, formal studies have not been developed to assess this assumption.

In conclusion, in this subset of heavily pre-treated individuals, deep sequencing showed technical non-inferiority to population sequencing. However, although additional mutations improved the assessment of genotypic resistance to etravirine, deep sequencing did not consistently provide additional information on darunavir, tipranavir or raltegravir susceptibility relative to population sequencing. Further studies should extend our findings and address the clinical impact of ultrasensitive genotyping in HIV-1 infected individuals experiencing virological failure to their first or second-line antiretroviral therapy. Proper throughput escalation, sample multiplexing and adequate sequence coverage may potentially turn ultrasensitive genotyping into a feasible strategy for HIV drug resistance management in the clinical setting.

Supporting Information

Table S1 Additional genotypic information provided by deep HIV-1 sequencing and changes in predicted phenotypic susceptibility, relative to population sequencing [a, b, c]. [a] Only mutations with a score ≥ 5 in the Stanford HIV Drug Resistance Database were included in the analysis. [b] ART: antiretroviral therapy; DS: deep sequencing; PI: protease inhibitor; NRTI: nucleoside reverse transcriptase inhibitor; NNRTI: non-nucleoside reverse transcriptase inhibitor; InSTI: Integrase Strand Transfer Inhibitor; ZDV: zidovudine; ABC: abacavir; d4T: stavudine; ddI: didanosine; TDF: tenofovir; EFV: efavirenz; NVP: nevirapine; ETR: etravirine; ATV: atazanavir; IDVr: indinavir/ritonavir; FAPVr: fosamprenavir/ritonavir; SQVr: saquinavir/ritonavir; LPVr: lopinavir/ritonavir; DRVr: darunavir/ritonavir; TPVr: tipranavir/ritonavir; ANRS: algorithm of the French ANRS (*Agence Nationale de Recherche sur le SIDA*) AC11 Resistance group, version 18, July 2009, France; HIVdb: HIV db program version 6.0.8, implemented at the Stanford HIV Drug Resistance Database, Stanford University, USA; REGA: Algorithm of the Rega Institute version 8.0.2, University of Leuven, Belgium. [c] Predicted antiretroviral susceptibility: S: susceptible; I: intermediate; R: Resistant.
(DOC)

Table S2 Predicted antiretroviral susceptibility according to Sanger or quantitative deep 454 sequencing. Color code: Green = Sensitive; Yellow = Intermediate; Red = Resistant. Changes in predicted phenotypic susceptibility between Sanger and 454 sequencing sequencing are highlighted in black boxes. DLV: delavirdine; EFV: efavirenz; ETR: etravirine; NVP: neviapine; 3TC: lamivudine; ABC: abacavir; AZT: zidovudine; d4T: stavudine; ddI: didanosine; FTC: emtricitabine; TDF: tenofovir dippivoxil fumarate; ATV: atazanavir; ATVr: ritonavir-boosted atazanavir; DRVr: ritonavir-boosted darunavir; FPVr: ritonavir-boosted fosamprenavir; IDVr: ritonavir-boosted indinavir; LPVr: ritonavir-boosted lopinavir; NFV: nelfinavir; SQVr: ritonavir-boosted saquinavir; TPVr: ritonavir-boosted tipranavir; RA: ralegravirL; ELV: elvitegravir.
(XLS)

Acknowledgments

Roger Paredes wishes to thank Dr. Peter Millard, from the Centro de Saúde San Lucas, Universidade Católica de Moçambique in Beira, for critical review of the manuscript. This work was presented in part at the 17th Conference on Retroviruses and Opportunistic Infections (CROI), San Francisco, 17 February 2010, [abstract # 567].

Author Contributions

Conceived and designed the experiments: LR BC RP. Performed the experiments: FMC CP RP. Analyzed the data: FMC AT RP. Contributed reagents/materials/analysis tools: FMC AT FG RD DD MA-T LR BC RP. Wrote the paper: FMC CP RP. Contributed to the study design: FG RD DD MA-T.

References

1. Lodwick R, Costagliola D, Reiss P, Torti C, Teira R, et al. (2010) Triple-class virologic failure in HIV-infected patients undergoing antiretroviral therapy for up to 10 years. Arch Intern Med 170: 410–419.
2. Simen BB, Simons JF, Hullsiek KH, Novak RM, Macarthur RD, et al. (2009) Low-abundance drug-resistant viral variants in chronically HIV-infected, antiretroviral treatment-naive patients significantly impact treatment outcomes. J Infect Dis 199: 693–701.
3. Paredes R, Lalama CM, Ribaudo HJ, Schackman BR, Shikuma C, et al. (2010) Pre-existing minority drug-resistant HIV-1 variants, adherence, and risk of antiretroviral treatment failure. J Infect Dis 201: 662–671.

4. Metzner KJ, Giulieri SG, Knoepfel SA, Rauch P, Burgisser P, et al. (2009) Minority quasispecies of drug-resistant HIV-1 that lead to early therapy failure in treatment-naive and -adherent patients. Clin Infect Dis 48: 239–247.
5. Johnson JA, Li JF, Wei X, Lipscomb J, Irlbeck D, et al. (2008) Minority HIV-1 drug resistance mutations are present in antiretroviral treatment-naive populations and associate with reduced treatment efficacy. PLoS Med 5: e158.
6. Goodman DD, Zhou Y, Margot NA, McColl DJ, Zhong L, et al. (2010) Low level of the K103N HIV-1 above a threshold is associated with virological failure in treatment-naive individuals undergoing efavirenz-containing therapy. Aids 25: 325–333.
7. Geretti AM, Fox ZV, Booth CL, Smith CJ, Phillips AN, et al. (2009) Low-frequency K103N strengthens the impact of transmitted drug resistance on virologic responses to first-line efavirenz or nevirapine-based highly active antiretroviral therapy. J Acquir Immune Defic Syndr 52: 569–573.
8. Lataillade M, Chiarella J, Yang R, Schnittman S, Wirtz V, et al. (2010) Prevalence and clinical significance of HIV drug resistance mutations by ultra-deep sequencing in antiretroviral-naive subjects in the CASTLE study. PLoS One 5: e10952.
9. Toni TA, Asahchop EL, Moisi D, Ntemgwa M, Oliveira M, et al. (2009) Detection of human immunodeficiency virus (HIV) type 1 M184V and K103N minority variants in patients with primary HIV infection. Antimicrob Agents Chemother 53: 1670–1672.
10. Balduin M, Oette M, Daumer MP, Hoffmann D, Pfister HJ, et al. (2009) Prevalence of minor variants of HIV strains at reverse transcriptase position 103 in therapy-naive patients and their impact on the virological failure. J Clin Virol 45: 34–38.
11. Peuchant O, Thiebaut R, Capdepont S, Lavignolle-Aurillac V, Neau D, et al. (2008) Transmission of HIV-1 minority-resistant variants and response to first-line antiretroviral therapy. Aids 22: 1417–1423.
12. Metzner KJ, Rauch P, Braun P, Knechten H, Ehret R, et al. (2010) Prevalence of key resistance mutations K65R, K103N, and M184V as minority HIV-1 variants in chronically HIV-1 infected, treatment-naive patients. J Clin Virol 50: 156–161.
13. Jakobsen MR, Tolstrup M, Sogaard OS, Jorgensen LB, Gorry PR, et al. (2010) Transmission of HIV-1 drug-resistant variants: prevalence and effect on treatment outcome. Clin Infect Dis 50: 566–573.
14. Varghese V, Shahriar R, Rhee SY, Liu T, Simen BB, et al. (2009) Minority variants associated with transmitted and acquired HIV-1 nonnucleoside reverse transcriptase inhibitor resistance: implications for the use of second-generation nonnucleoside reverse transcriptase inhibitors. J Acquir Immune Defic Syndr 52: 309–315.
15. Le T, Chiarella J, Simen BB, Hanczaruk B, Egholm M, et al. (2009) Low-abundance HIV drug-resistant viral variants in treatment-experienced persons correlate with historical antiretroviral use. PLoS ONE 4: e6079.
16. D'Aquila RT, Geretti AM, Horton JH, Rouse E, Kheshti A, et al. (2010) Tenofovir (TDF)-Selected or Abacavir (ABC)-Selected Low-Frequency HIV Type 1 Subpopulations During Failure with Persistent Viremia as Detected by Ultradeep Pyrosequencing. AIDS Res Hum Retroviruses 27: 201–209.
17. Margulies M, Egholm M, Altman WE, Attiya S, Bader JS, et al. (2005) Genome sequencing in microfabricated high-density picolitre reactors. Nature 437: 376–380.
18. Rhee SY, Fessel WJ, Zolopa AR, Hurley L, Liu T, et al. (2005) HIV-1 Protease and reverse-transcriptase mutations: correlations with antiretroviral therapy in subtype B isolates and implications for drug-resistance surveillance. J Infect Dis 192: 456–465.
19. Van Laethem K, Geretti A, Camacho R, Vandamme AM. Algorithm for the use of genotypic HIV-1 resistance data. Rega v8.0.2© Leuven, 16 June 2009.
20. Shikuma CM, Yang Y, Glesby MJ, Meyer WA, 3rd, Tashima KT, et al. (2007) Metabolic effects of protease inhibitor-sparing antiretroviral regimens given as initial treatment of HIV-1 Infection (AIDS Clinical Trials Group Study A5095). J Acquir Immune Defic Syndr 44: 540–550.
21. Marcelin AG, Masquelier B, Descamps D, Izopet J, Charpentier C, et al. (2008) Tipranavir-ritonavir genotypic resistance score in protease inhibitor-experienced patients. Antimicrob Agents Chemother 52: 3237–3243.
22. Pellegrin I, Breilh D, Ragnaud JM, Boucher S, Neau D, et al. (2006) Virological responses to atazanavir-ritonavir-based regimens: resistance-substitutions score and pharmacokinetic parameters (Reyaphar study). Antivir Ther 11: 421–429.
23. Yates PJ, Hazen R, St Clair M, Boone L, Tisdale M, et al. (2006) In vitro development of resistance to human immunodeficiency virus protease inhibitor GW640385. Antimicrob Agents Chemother 50: 1092–1095.
24. de Meyer S, Vangeneugden T, van Baelen B, de Paepe E, van Marck H, et al. (2008) Resistance profile of darunavir: combined 24-week results from the POWER trials. AIDS Res Hum Retroviruses 24: 379–388.
25. Shao W, Boltz VF, Kearney M, Maldarelli F, Mellors JM, et al. (2009) Characterization of HIV-1 sequence artifacts introduced by bulk PCR and detected by 454 sequencing. XVIII International HIV Drug Resistance Workshop: Basic Principles & Clinical Implications. Fort Myers, FL, USA 9-13 June 2009 (Abstract 104). Antiviral Therapy 14(Suppl 1): A123.

SUBJECT	ADHERENCE	ART	BASELINE					VIROLOGICAL FAILURE				
			Mutations by population sequencing	Additional mutations by DS (percent in the viral population)	Change in Predicted Phenotype due to additional DS data			Mutations by population sequencing	Additional mutations by DS (percent in the viral population)	Change in Predicted Phenotype due to additional DS data		
					HIVdb	REGA	ANRS			HIVdb	REGA	ANRS
1	ADEQUATE	TDF FTC DRVr ETR RAL	PI: V11I, V32I, L33F, K43T, I54A, Q58E, T74P, I84V, L89V, L90M	PI: I54T (12.0), V82F (1.1), V82L (1.1)	_	_	LPVr, SQVr: S to I	PR: V11I, V32I, L33F, K43T, I54T, Q58E, T74P, I84V, L89V, L90M	PR: I54A (6.1), V82F (3.5), V82L (3.5)	_	_	SQVr: S to I
			NRTI: M41L, E44D, D67G, L74IV, V75AITV, V118I, L210W, T215Y, K219N	NRTI: none	_	_	_	NRTI: M41L, E44D, D67G, L74IV, V75T, V118I, L210CW, T215Y, K219DN	NRTI: none	_	_	_
			NNRTI: L100I, K103N	NNRTI: none	_	_	_	NNRTI: L100I, K103N	NNRTI: V179D (3.0), Y181C (17.6)	ETR: I to R	ETR: I to R	ETR: S to I
			InSTI: none	InSTI: none	_	_	_	InSTI: none	InSTI: V151I (1.8)	_	_	_
2	ADEQUATE	TDF FTC DRVr ETR RAL	PI: L33F, K43T, M46L, I54V, T74P, V82A, I84V, L90M	PI: V32I (1.6), F53L (1.6), Q58E (8.6), L89V (21.0)	_	_	DRVr: I to R	PI: V11I, V32I, L33F, K43T, I54A, Q58E, T74P, I84V, L89V, L90M	PI: I54T (15.9)	_	_	LPVr: I to R
			NRTI: D67N, T69Li, K70R, Y115F, F116Y, Q151M, M184V, T215V, K219Q	NRTI: T215F (1.8)	_	_	_	NRTI: M41L, E44D, D67N, L74V, V75T, V118I, Q151M, M184V, L210W, T215Y, K219N	NRTI: T215F (1.2)	TDF: R to I	_	_
			NNRTI: K101Q, K103N	NNRTI: none	_	_	_	NNRTI: L100I, K103N	NNRTI: K101E (2.3), Y181C (1.7)	ETR: I to R	ETR: I to R	ETR: S to I
			InSTI: G163K	InSTI: none	_	_	_	InSTI: none	InSTI: V151I (2.3), G163K (21.5)	_	_	_
3	ADEQUATE	TDF TPVr RAL	PI: V32I, I54M, Q58E, G73S, I84V, L89V, L90M	PI: none	_	_	_	PI: V32I, I54M, Q58E, G73S, I84V, L89V, L90M	PI: none	_	_	_
			NRTI: K70KN, M184V, T215Y	NRTI: none	_	_	_	NRTI: K70KN, M184V, T215Y	NRTI: D67N (8.1)	TDF: S to I	ABC, d4T, ddI: S to I	_
			NNRTI: A98G	NNRTI: none	_	_	_	NNRTI: A98G	NNRTI: none	_	_	_
			InSTI: none	InSTI: none	_	_	_	InSTI: Q148QR, N155NH, G163GR	InSTI: E138K (32.6), G140S (16.1)	_	_	_
4	ADEQUATE	TDF FTC TPVr RAL	PI: M46IL, I54V, G73S, I84V, L90M	PI: none	_	_	_	PI: E35G, M46L, I54V, G73S, I84V, L90M	PI: none	_	_	_
			NRTI: M41L, D67N, L74V, V118I, M184V, L210W, T215Y, K219DN	NRTI: none				NRTI: M41L, D67N, L74V, V118I, M184V, L210W, T215Y, K219N	NRTI: none	_	_	_
			NNRTI: K101P, V179D, G190A	NNRTI: none	_	_	_	NNRTI: K101P, V179D, G190A	NNRTI: none	_	_	_
			InSTI: none	InSTI: none	_	_	_	InSTI: none	InSTI: none	_	_	_
5	PARTIAL	DRVr TDF	PI: L23I, L33F, E35G, I54L, Q58E,	PI: none	_	_	_	PI: L23I, L33F, E35G, I54L, Q58E, N88S	PI: none	_	_	_

		FTC T20	N88S									
			NRTI: D67N, K70R, M184V, T215Y, K219E	NRTI: T215F (2.2)	_	_	_	NRTI: D67N, K70R, T215Y, K219E	NRTI: T215F (1.7)	_	_	_
			NNRTI: E138A, Y181V	NNRTI: none	_	_	_	NNRTI: E138A, Y181V	NNRTI: K103N (12.9)	EFV: I to R	_	EFV, NVP: S to R
			InSTI: E157Q	InSTI: none	_	_	_	InSTI: E157Q	InSTI: none	_	_	_
6	PARTIAL	ZDV 3TC ABC ATV RAL	PI: None	PI: none	_	_	_	PI: none	PI: none	_	_	_
			NRTI: D67N, T69DN, K70KR, K219KQ	NRTI: none	_	_	_	NRTI: D67N, T69DN, K70KR,	NRTI: K219Q (1.6)	_	D4T, ZDV: I to R ABC: S to I	D4T, ZDV: S to R
			NNRTI: K103KN	NNRTI: none	_	_	_	NNRTI: K103KN	NNRTI: none	_	_	_
			InSTI: none	InSTI: none	_	_	_	InSTI: none	InSTI: none	_	_	_
7	ART INTERRUPTION	STARTS AND STOPS TDF FTC DRVr	PI: I54IV, T74S, L90M	PI: I54L (2.4), V82A (13.9)	IDVr, SQVr: I to R DRVr: S to I	IDVr: I to R LPVr: S to I	IDVr: I to R	PI: L90M	PI: none	_	_	_
			NRTI: T215ST	NRTI : M41L (1.4), T215Y (13.7)	ABC, ddI, TDF : S to I	ddI: S to I	D4T, ZDV: I to R ddI: S to R	NRTI: none	NRTI: T215Y (7.9)	d4T, ZDV, ABC, ddI, TDF: S to I	d4T, ZDV: S to I	d4T, ZDV: S to R
			NNRTI: none	NNRTI : none	_	_	_	NNRTI: none	NNRTI: none	_	_	_
			InSTI: none	InSTI: none	_	_	_	InSTI: none	InSTI: none	_	_	_

1

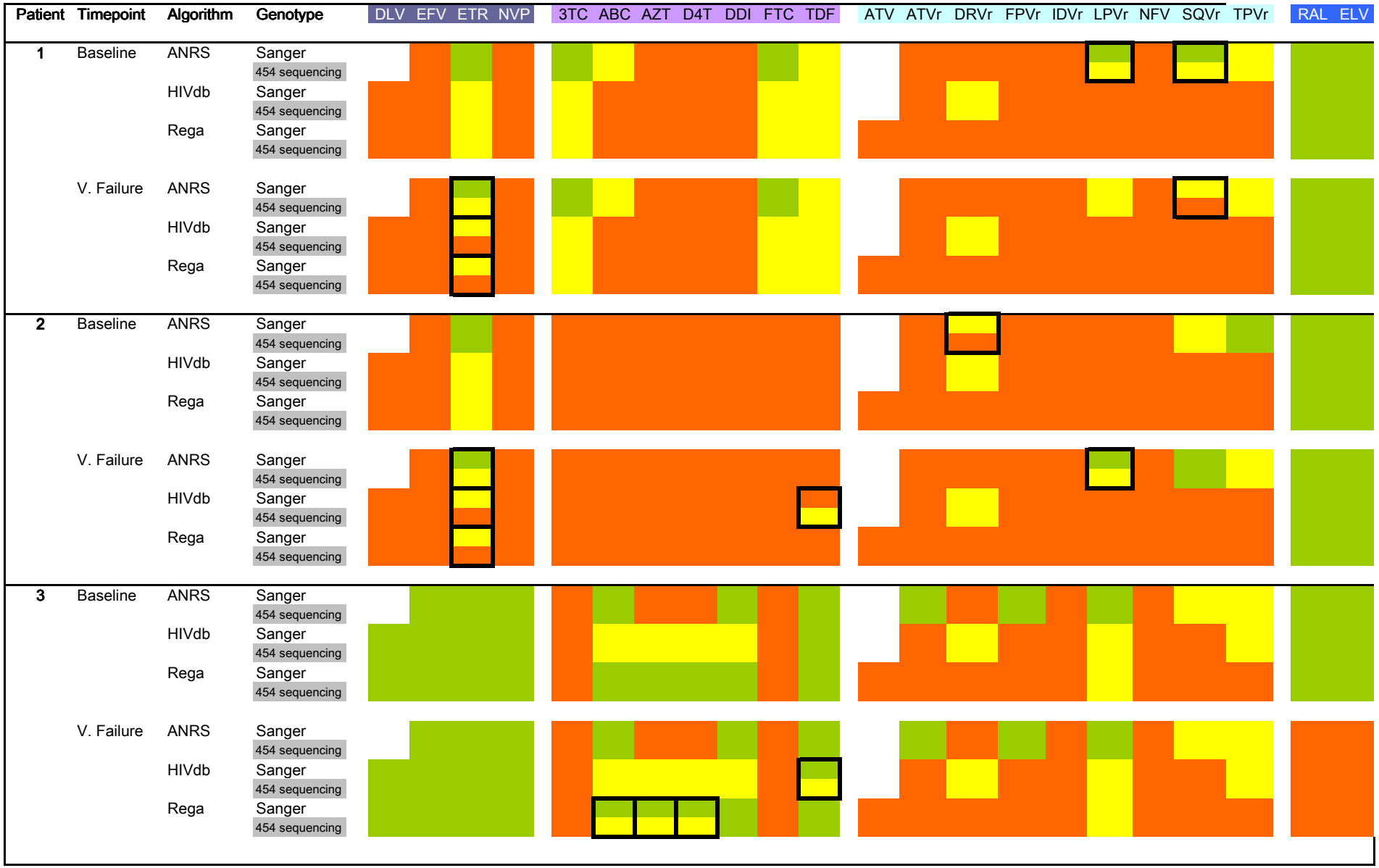
Patient
Timepoint
Algorithm
Genotype
DLV EFV ETR NVP
3TC ABC AZT D4T DDI FTC TDF
ATV ATVr DRVr FPVr IDVr LPVr NFV SQVr TPVr
RAL ELV
1
Baseline
ANRS
Sanger
454 sequencing
HIVdb
Sanger
454 sequencing
Rega
Sanger
454 sequencing
V. Failure
ANRS
Sanger
454 sequencing
HIVdb
Sanger
454 sequencing
Rega
Sanger
454 sequencing
2
Baseline
ANRS
Sanger
454 sequencing
HIVdb
Sanger
454 sequencing
Rega
Sanger
454 sequencing
V. Failure
ANRS
Sanger
454 sequencing
HIVdb
Sanger
454 sequencing
Rega
Sanger
454 sequencing
3
Baseline
ANRS
Sanger
454 sequencing
HIVdb
Sanger
454 sequencing
Rega
Sanger
454 sequencing
V. Failure
ANRS
Sanger
454 sequencing
HIVdb
Sanger
454 sequencing
Rega
Sanger
454 sequencing

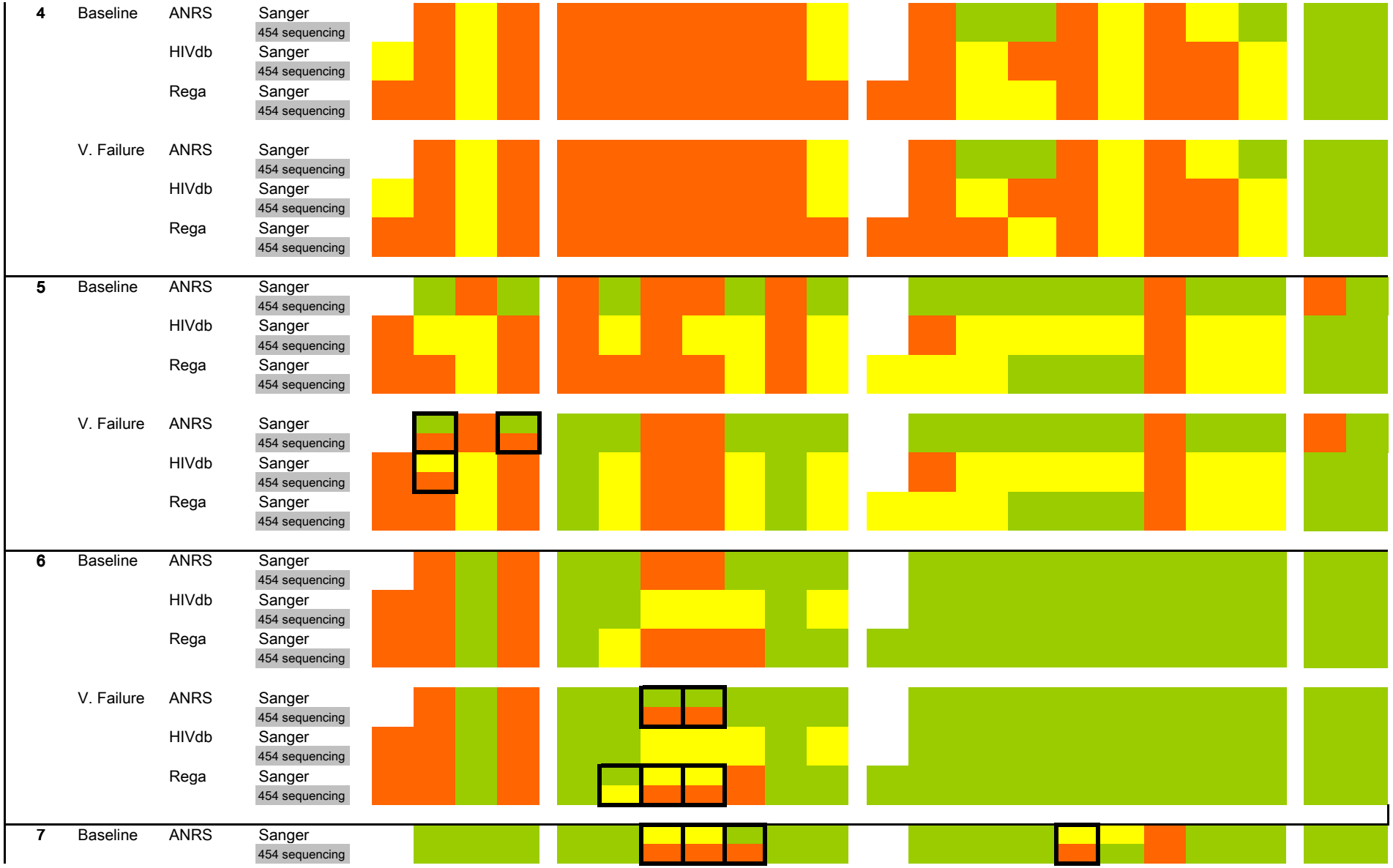
4
Baseline
ANRS
Sanger
454 sequencing
HIVdb
Sanger
454 sequencing
Rega
Sanger
454 sequencing
V. Failure
ANRS
Sanger
454 sequencing
HIVdb
Sanger
454 sequencing
Rega
Sanger
454 sequencing
5
Baseline
ANRS
Sanger
454 sequencing
HIVdb
Sanger
454 sequencing
Rega
Sanger
454 sequencing
V. Failure
ANRS
Sanger
454 sequencing
HIVdb
Sanger
454 sequencing
Rega
Sanger
454 sequencing
6
Baseline
ANRS
Sanger
454 sequencing
HIVdb
Sanger
454 sequencing
Rega
Sanger
454 sequencing
V. Failure
ANRS
Sanger
454 sequencing
HIVdb
Sanger
454 sequencing
Rega
Sanger
454 sequencing
7
Baseline
ANRS
Sanger
454 sequencing

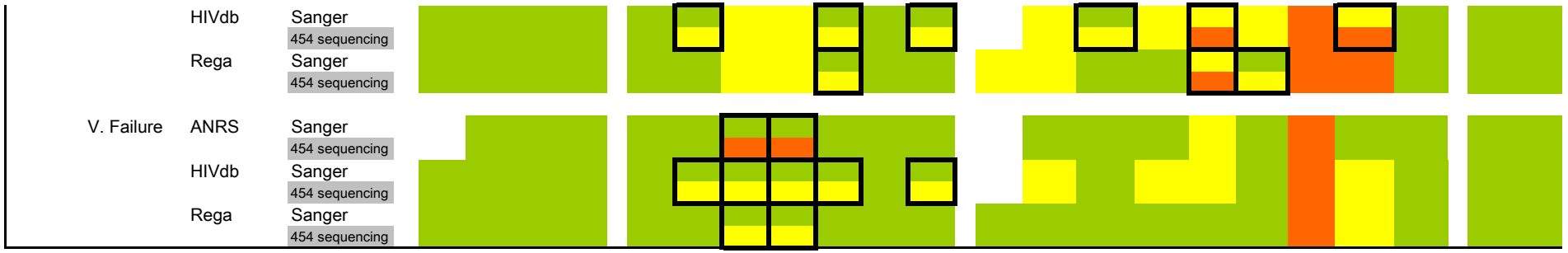
HIVdb
Sanger
454 sequencing
Rega
Sanger
454 sequencing
V. Failure
ANRS
Sanger
454 sequencing
HIVdb
Sanger
454 sequencing
Rega
Sanger
454 sequencing

Antiviral Research 88 (2010) 281–286

Contents lists available at ScienceDirect

Antiviral Research

journal homepage: www.elsevier.com/locate/antiviral

Dynamic escape of pre-existing raltegravir-resistant HIV-1 from raltegravir selection pressure

Francisco M. Codoñer[a], Christian Pou[a], Alexander Thielen[c], Federico García[d], Rafael Delgado[e], David Dalmau[f], José Ramon Santos[b], Maria José Buzón[a], Javier Martínez-Picado[a,g], Miguel Álvarez-Tejado[h], Bonaventura Clotet[a,b], Lidia Ruiz[a], Roger Paredes[a,b,*]

[a] *IrsiCaixa Retrovirology Laboratory-HIVACAT, Hospital Universitari Germans Trias i Pujol, Badalona, Spain*
[b] *Lluita Contra la SIDA Foundation, Hospital Universitari Germans Trias i Pujol, Badalona, Spain*
[c] *Max Planck Institute für Informatik, Saarbücken, Germany*
[d] *Hospital Universitario San Cecilio, Granada, Spain*
[e] *Hospital 12 de Octubre, Madrid, Spain*
[f] *Hospital Universitari Mútua de Terrassa, Terrassa, Spain*
[g] *Institució Catalana de Recerca i Estudis Avançats (ICREA), Barcelona, Spain*
[h] *Roche Diagnostics SL, Sant Cugat del Vallès, Spain*

ARTICLE INFO

Article history:
Received 13 August 2010
Received in revised form
17 September 2010
Accepted 21 September 2010

Keywords:
HIV-1
Antiretroviral resistance
Deep sequencing
Raltegravir
Evolution

ABSTRACT

Using quantitative deep HIV-1 sequencing in a subject who developed virological failure to deep salvage therapy with raltegravir, we found that most Q148R and N155H mutants detected at the time of virological failure originated from pre-existing minority Q148R and N155H variants through independent evolutionary clusters. Double 148R + N155H mutants were also detected in 1.7% of viruses at virological failure in association with E138K and/or G163R. Our findings illustrate the ability of HIV-1 to escape from suboptimal antiretroviral drug pressure through selection of pre-existing drug-resistant mutants, underscoring the importance of using fully active antiretroviral regimens to treat all HIV-1-infected subjects.

1. Introduction

Integrase strand transfer inhibitors are a new family of antiretrovirals that reached HIV clinics in 2007 (McColl and Chen, 2010; Steigbigel et al., 2008). Resistance to raltegravir, the first integrase inhibitor available for HIV treatment, evolves through three seemingly exclusive pathways (Fransen et al., 2009) characterized by a signature mutation in the integrase catalytic centre (Y143R/C, Q148R/H/K or N155H) plus several accessory mutations that increase resistance or improve viral replication (Cooper et al., 2008; Paredes and Clotet, 2010). Clonal analyses suggested that Q148R/H/K and N155H mutations did not coexist in individual genomes, which is consistent with the low replication capacity of double Q148R/H/K + N155H mutants *in vitro* (Fransen et al., 2009; McColl and Chen, 2010). The fitness impact of raltegravir resistance mutations, however, may be modulated *in vivo* by accessory mutations in integrase, as well as by epistatic effects of other HIV-1 genes (Buzon et al., 2010).

2. Clinical case

We report the case of a 42 year-old male diagnosed with HIV in 1988 (Fig. 1) with history of alcoholism and illicit drug use until 1993. He was treated for pulmonary tuberculosis and *Pneumocystiis jirovecii* pneumonia in 1993 and 2004, respectively. Although he had good adherence to antiretrovirals in the recent years, he never achieved HIV-1 RNA suppression <50 copies/mL and his CD4+ T cell counts remained extremely low (the nadir and zenith CD4+ counts were, respectively, 1 and 169 cells/mm^3). After receiving 13 different antiretrovirals during 15 years, he began salvage therapy with tenofovir disoproxil fumarate (245 mg QD), raltegravir (200 mg BID), darunavir (600 mg BID) and ritonavir (100 mg BID) on July 2007. HIV-1 RNA levels decreased 2 $\log_{10}$ four weeks after

* Corresponding author at: HIV Unit & Institut de Recerca de la SIDA – IrsiCaixa, Hospital Universitari Germans Trias i Pujol, Universitat Autònoma de Barcelona, Crta. de Canyet s/n, Planta 2a, 08916 Badalona, Catalonia, Spain.
Tel.: +34 93 465 6374x162; fax: +34 93 465 3968.
E-mail address: rparedes@irsicaixa.es (R. Paredes).

0166-3542/$ – see front matter © 2010 Elsevier B.V. All rights reserved.
doi:10.1016/j.antiviral.2010.09.016

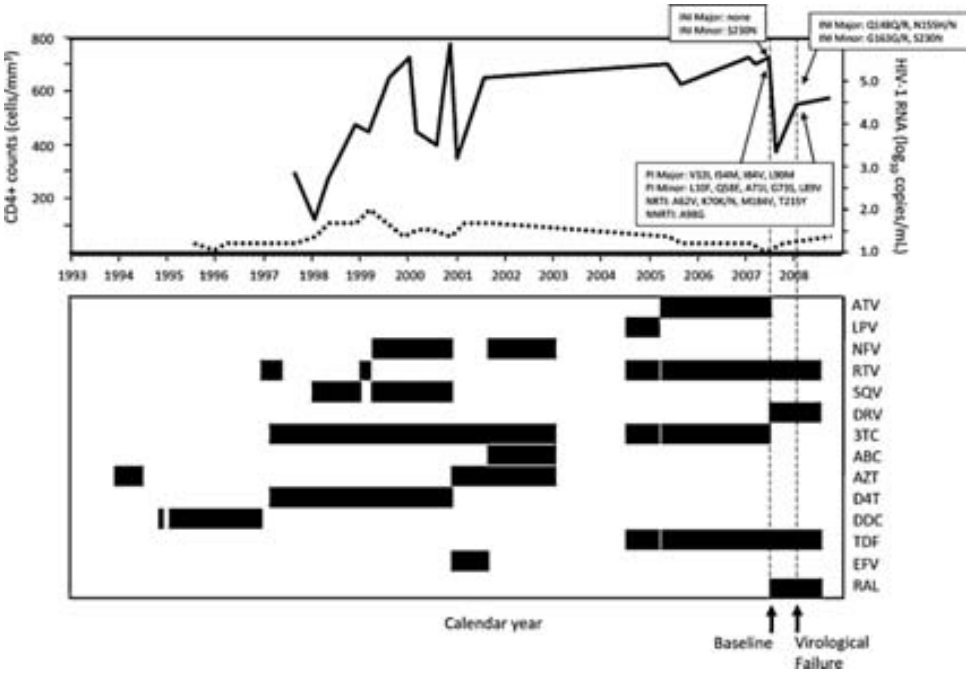

Fig. 1. Antiretroviral treatment history and virological and immunological evolution. The continuous line in the upper graph represents HIV-1 RNA levels in copies/mL transformed in a logarithmic scale; the dashed line in the upper graph represents CD4+ T-cell counts (CD4 counts) in cells/mm^3. Horizontal bars in the lower graph represent the time period during which a given antiretroviral drug was prescribed. Vertical dashed lines represent the timepoints when population and quantitative deep sequencing was performed; i.e., baseline and virological failure. Boxes include resistance mutations detected by population sequencing at baseline and virological failure. PI: protease inhibitor; NRTI: nucleoside reverse transcriptase inhibitor; NNRTI: non-nucleoside reverse transcriptase inhibitor; IN: integrase; ATV: atazanavir; LPV: lopinavir; NFV: nelfinavir; RTV: ritonavir; SQV: saquinavir; DRV: darunavir; 3TC: lamivudine; ABC: abacavir; AZT: zidovudine; D4T: stavudine; DDC: zalcitabine; TDF: tenofovir diprivoxil fumarate; EFV: efavirenz; RAL: raltegravir; None: antiretroviral treatment interruption. Graph developed with and adapted from the ART-AiDE (Antiretroviral Therapy – Acquisition & Display Engine) Program, Stanford HIV Drug Resistance Database.

therapy initiation, but rebounded 1 $\log_{10}$ twenty weeks later. A few weeks after virological failure, the patient was admitted to the intensive care unit and died of acute respiratory distress.

3. Methods

3.1. HIV-1 population and quantitative deep sequencing

HIV-1 RNA was extracted from 1 mL of plasma 3 weeks before initiation of salvage antiretroviral therapy (baseline) and at virological failure (VF), 24 weeks after treatment initiation. Plasma was centrifuged at 35,000 rpm (9000 × *g*) during 90 min at 4 °C. Viral pellets were resuspended and viral RNA was extracted (QIAamp UltraSens Virus Kit™, QIAGEN, Valencia, CA). Three One-Step RT-PCRs (SuperScript® III One-Step RT-PCR System with Platinum® Taq High Fidelity, Invitrogen, Carlsbad, CA) were performed in parallel per each sample. Primers used were 1571-L23 (HXB2: 1417 → 1440) 5′-ATT TCT CCT ACT GGG ATA GGT GG-3′ and 5464-L27 (HXB2: 5464 → 5438) 5′-CCT TGT TAT GTC CTG CTT GAT ATT CAC-3′. Cycling conditions were: 30 min at 52 °C, 2 min at 94 °C; 30 s at 94 °C, 30 s at 56 °C, 4 min at 68 °C, for 30 cycles; followed by 5 min at 68 °C. Triplicate RT-PCR products were pooled, column-purified (QIAquick PCR Purification Kit, QIAGEN, Valencia, CA) and used for both viral population and quantitative deep HIV-1 sequencing (QDS).

3.1.1. Viral population genotyping

For population sequencing, triplicate nested PCRs were performed in parallel (Platinum® Taq DNA Polymerase High Fidelity, Invitrogen, Carlsbad, CA) with primers 2084-U26 (HXB2: 2084 → 2109) 5′-ATT TTT TAG GGA AGA TCT GGC CTT CC-3′ and 5456-L26 (HXB2: 5456 → 5431) 5′-TGT CCT GCT TGA TAT TCA CAC CTA GG-3′. Cycling conditions were: 2 min at 94 °C; 30 s at 94 °C, 30 s at 56 °C, 4 min at 68 °C, for 30 cycles; followed by 5 min at 68 °C. Again, nested PCR products were pooled and column-purified (QIAquick PCR Purification Kit, QIAGEN, Valencia, CA). Protease, reverse transcriptase and integrase genes were sequenced in-house (BigDye v3.1, Applied Biosystems, Foster City, CA, USA) and resolved by capillary electrophoresis (ABI 7000, Foster City, CA, USA). Genotypes were interpreted automatically with the HIVdb program implemented in the Stanford drug resistance database (Liu and Shafer, 2006; Rhee et al., 2003).

3.1.2. Quantitative deep sequencing

Pooled purified RT-PCR products were used as template to generate two overlapping amplicons. Excluding primer sites, amplicon 1 encompassed the integrase codons 91 to 178 (HXB2: 4499–4763), whereas amplicon 2 included the integrase codons 132 to 224 (HXB2: 4621–4900). The overlapping region between the two amplicons thus encompassed codons 132–178 in the Integrase catalytic center (HXB2: 4621–4763). Each amplicon was generated in triplicate during 30 cycles of PCR amplification (Platinum® Taq DNA Polymerase High Fidelity, Invitrogen, Carlsbad, CA). Primers for amplicon 1 were Beta-F (HXB2: 4481 → 4499) 5′- AGA AGC AGA AGT TAT TCC A -3′ and Beta R (HXB2 4763 → 4780) 5′-TTG TGG ATG AAT ACT GCC-3′; primers for amplicon 2 were Gamma-F (HXB2: 4606 → 4621) 5′- TTA AGG CCG CCT GTT G -3′ and Gamma R (HXB2: 4900 → 4917) 5′-TGT CCC TGT AAT AAA CCC-3′. In addition, primers contained 454 sequencing adapters A or B and 8-nucleotide sample identifier tags in the 5′-end. Triplicate PCR products were pooled and purified (QIAquick PCR Purification Kit, QIAGEN, Valencia, CA). Quantitative Deep Sequencing was performed at 454 Life Sciences, Branford, CT, USA.

Raw output sequences were filtered to ensure high quality (Table 1). The overlapping region between the two amplicons (integrase codons 132–178) was extracted. Sequences resulting

Table 1
Filtering of sequences obtained by quantitative deep sequencing.

		HXB2 position range[a]	Integrase codon range[a]	Reads	Sequences filtered out (homology < 90%)	Sequences left	Unique sequences
Baseline	Amplicon 1	4499–4763	91–178	1951	312	1639	N/A
	Amplicon 2	4621–4900	132–224	1852	100	1752	N/A
	Overlap[b]	4621–4763	132–178	3803	412	3391	222
Virological failure	Amplicon 1	4499–4763	91–178	2506	456	2050	N/A
	Amplicon 2	4621–4900	132–224	1409	75	1334	N/A
	Overlap[b]	4621–4763	132–178	3915	531	3384	311

[a] Excluding primer sites.
[b] Overlapping regions of the 2 amplicons; N/A, not applicable.

from extraction were selected if they had more than 90% similarity with the consensus sequence of the run for that subject and region. Sequencing errors in homopolymeric regions were manually inspected and corrected. Sequences that included a stop codon were removed. The sequence coverage was calculated for each aminoacid position. Unique sequences were identified and the percentage of specific mutations in the 143, 148 or 155 positions as well as the percentage of double and triple mutants was calculated only in those sequences surpassing all the abovementioned quality filters.

An in-house analysis of 992 pNL43 clonal sequences obtained by quantitative deep sequencing under the same PCR conditions used to generate patient samples showed a mean (SD) nucleotide mismatch rate of 0.07% (0.13%), similar to previous reports (Varghese et al., 2009). The mean (SD) error rate for any aminoacid mismatch was 0.14% (0.19%), but the mean (SD) error rate for actual drug resistance mutations was 0.03% (0.07%). The 99th percentile of mismatches would establish the threshold for nucleotide errors in 0.61% and the limit for identifying true drug resistance mutations in 0.20%.

3.2. Phylogenetic analysis

Unique overlapping sequences obtained with QDS were used to build a protein Multiple Sequence Alignment (MSA) using Musclev3.7 (Edgar, 2004). Sequence indeterminations were substituted for gaps and were subsequently removed. In addition, a DNA MSA was built concatenating triplets of bases according to the protein MSA. The protein alignment was used to identify the best fit molecular evolutionary model using PROTTEST v2.2 (Abascal et al., 2005). The evolutionary model obtained was used to build a maximum likelihood phylogenetic tree with PHYMLv3.0 (Guindon and Gascuel, 2003). MEGA v4.1 (Kumar et al., 2004) was used to build the tree topology based on a Neighbor-Joining approach, using a pairwise deletion, with the best evolutionary model found by PROTTEST and implemented in MEGA as a distance model. A Simodaira Hasegawa test was used to assess the most likely tree topology to explain the sequence evolution (Shimodaira and Hasegawa, 1999).

To further investigate the origin of Q148R and N155H mutants detected at the time of VF using an independent phylogenetic

Table 2
Linkage analysis of major and accessory integrase inhibitor resistance mutations at virological failure by quantitative deep sequencing.

Major mutation	Accessory mutations in integrase codons					#Clones	% Relative to clones with the major mutation	% Relative to total clones at virological failure
	138	140	151	163	Other[a]			
Consensus B	E	G	V	G	N/A			
Q148R	K					895	53.56	26.45
		S				357	21.36	10.55
		S		R		143	8.56	4.23
						109	6.52	3.22
	K			R		93	5.57	2.75
					X	74	4.43	2.19
N155H				R		1353	85.47	39.98
						111	7.01	3.28
	K			R		41	2.59	1.21
					X	78	4.93	2.31
Q148R + N155H	K			R		31	53.43	0.92
				R		9	15.53	0.27
		S		R		9	15.53	0.27
	K					7	12.07	0.21
						1	1.73	0.03
		S				1	1.73	0.03
Y143H + Q148R	K					1	33.33	0.03
	K					1	33.33	0.03
		S		R		1	33.33	0.03
Y143C + N155H				R		3	100	0.09
Y143H + N155H				R		8	100	0.24

N/A, not applicable.
[a] Only clones representing > 1% of the total sequences obtained by quantitative deep sequencing at virological failure are shown for single Q148R and N155H major mutants; all clones are shown for dual major mutants. "Other" includes the sum of all clones being detected in less than 1% of the total sequences at virological failure that show mutation combinations different from the ones presented in the table; other combinations are represented by "X".

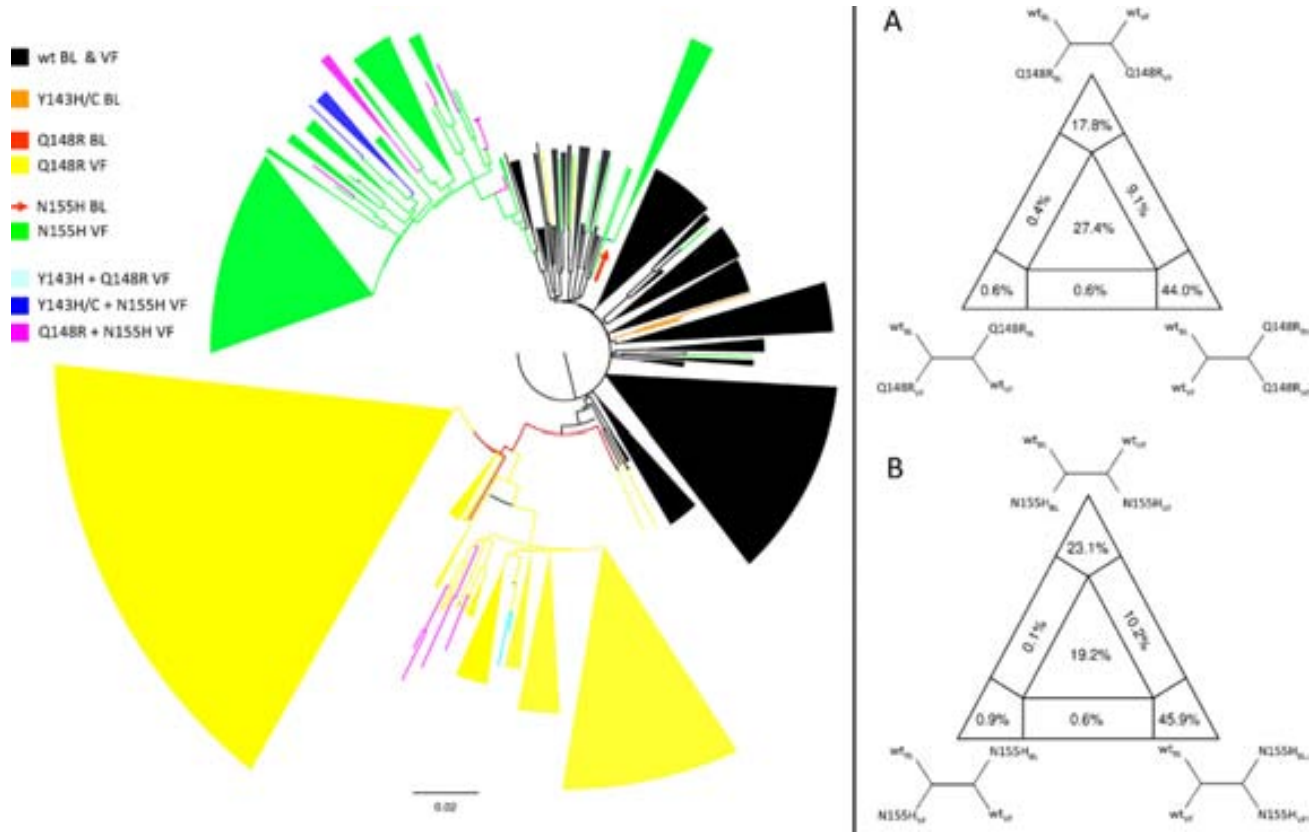

Fig. 2. Origin of viruses escaping raltegravir pressure. Left panel: Evolution of integrase sequences obtained by quantitative deep sequencing. Neighbor Joining Tree with branch lengths computed according to a heterogeneous JTT + Γ model of protein evolution. This was the most likely tree to explain sequence evolution according to a Shimodaira–Hasegawa test (Shimodaira and Hasegawa, 1999). For clarity, monophyletic groups of sequences containing the same major integrase resistance mutation or combination of mutations were collapsed into a cartoon with colours indicating the explored mutation and the size of the cartoon being proportional to the number of sequences included. Right panels: Quartet likelihood mapping analysis of the origin of Q148R and N155H raltegravir-resistant viruses detected at virological failure. Four clusters of sequences containing, respectively, mutants at baseline (BL), mutants at virological failure (VF), wildtype (wt) viruses at BL; and wt viruses at VF were created. All possible quartets of sequences containing one sequence from each cluster were generated. A distance phylogenetic tree was then calculated for each sequence quartet and was compared with the phylogeny of each of our three hypotheses, shown in the triangle vertices. Numbers in the triangle show the proportion of quartet phylogenetic trees matching each hypothesis. The percentage of solved phylogenies is shown in the triangle vertices; unsolved phylogenies are represented in intermediate regions of the triangle. Separate analyses were performed for single Q148R (panel A) and single N155H (panel B) mutants at virological failure. Wildtype was defined as absence of major integrase inhibitor-resistant mutations at positions 143, 148 and 155.

method, we used the four-clustering likelihood mapping technique implemented in TREEPUZZLE v5.2 (Schmidt et al., 2002). In brief, we constructed 4 clusters of sequences containing, respectively, mutants detected at baseline, mutants present at virological failure, wildtype (wt) viruses found at baseline; and wt viruses observed at virological failure. Wildtype was defined as absence of major integrase inhibitor-resistant mutations at positions 143, 148 and 155. Then, we tested the hypotheses that mutant viruses at virological failure derived from baseline mutants, baseline wt, or wt at virological failure. These analyses were performed separately for Q148R and N155H mutants, excluding sequences with other major integrase resistance mutations than the one being tested (Table 2).

Genetic linkage between major and accessory mutations was investigated using in-house algorithms.

4. Results

Pre-treatment viruses were only susceptible to raltegravir and tenofovir (Fig. 1). Population sequencing detected the major raltegravir resistant mutations Q148R and N155H and the accessory G163R mutation at virological failure, mixed with the corresponding wild type. All other baseline mutations remained detectable at the time of virological failure.

Out of 3390 clonal sequences obtained with QDS before raltegravir initiation, nine (0.27%) had the Y143H/C mutation alone, four (0.12%) contained the Q148R mutation, one (0.03%) had the N155H mutation and none (0%) harbored two major mutations together. Of 3384 clonal sequences obtained with QDS at the time of virological failure, 1668 (49.29%) were single Q148R mutants, and 1575 (46.54%) had the N155H alone. Double Q148R + N155H mutants were found in 58 (1.71%) sequences at virological failure. Three baseline Q148R sequences were identical to 79/3384 (2.34%) sequences at virological failure, whereas the baseline N155H sequence was identical to 83/3384 (2.45%) sequences at virological failure.

The best evolutionary model obtained with PROTTESTv2.2 (HIVw + Γ with $\alpha = 2.921$) was used to perform the maximum likelihood tree; a Neighbor Joining distance tree was performed with the second best model detected by PROTTESTv2.2 (JTT + Γ with $\alpha = 3.204$), given that the best model is not implemented in MEGA4. A Shimodaira and Hasegawa test (Shimodaira and Hasegawa, 1999) considered the Neighbor Joining tree as the one most likely to explain the sequence evolution. The tree topology suggested that Q148R and the N155H mutants evolved in two separate clusters (Fig. 2). Most Q148R mutants found at VF originated from pre-existing Q148R mutants whereas N155H mutants found at VF could have originated from either the baseline N155H mutant or from baseline wildtype viruses. Double Q148R + N155H mutants were found interspersed at the edges of either Q148R or N155H cluster. Single Y143C/H mutants clustered together at baseline but were not

found at VF, suggesting that they were less fit, compared to Q148R and/or N155H, in the presence of raltegravir. A four-clustering likelihood mapping technique implemented in TREEPUZZLE v 5.2, independently supported the hypothesis that most Q148R and N155H mutants emerging at virological failure originated, respectively, from pre-existing Q148R and N155H mutants (Fig. 2).

No viruses with major raltegravir-resistant mutations had other mutations linked on the same genome before therapy initiation (not shown). Conversely, extensive associations between major and accessory mutations were observed at VF (Table 1). Only 6.5% and 7% of sequences, respectively, contained mutation Q148R and N155H alone at virological failure; all double Q148R + N155H mutants contained other accessory mutations.

5. Discussion

Our study shows that Q148R and N155H mutants developing during virological failure to raltegravir can originate from minority mutants generated spontaneously before treatment exposure. The spontaneous generation of mutants is predicted by extant models of viral replication in view of HIV-1's high turnover and the error-prone nature of its reverse transcriptase (Coffin, 1995; Najera et al., 1995). Here, mutants could not have been transmitted because integrase inhibitors had just been commercialized. The high antiviral potency of raltegravir (McColl and Chen, 2010) in a context of virtual dual therapy exerted potent selective pressure over pre-existing resistant viruses, as predicted from mathematical modeling of HIV resistance (Nowak et al., 1997).

Pre-existing mutants, however, were found below the error threshold of the technology; point errors at drug resistance sites converting a wildtype to a resistant mutation were 0.2% in our own controls and in previous studies (Shao et al., 2009; Wang et al., 2007). Nevertheless, two independent phylogenetic analyses indicated that pre-existing mutants were the most likely origin of Q148R and N155H mutants at virological failure; indeed, sequences identical to the baseline mutants were found in about 2% of viruses at virological failure. Using various technologies, other studies found pre-existing Q148R/H mutants at similar levels (Ceccherini-Silberstein et al., 2009; Charpentier et al., 2009).

Whereas baseline mutants did not incorporate other mutations in the genome region explored, more than 90% of viruses evolving during virological failure had accumulated accessory mutations in their genome. We cannot completely rule out that the presence of double Q148R + N155H mutants in 1.7% of viruses was due to PCR recombination (Shao et al., 2009), although it seems unlikely. The two mutations lie 6 codons apart and were found in similar proportions in two overlapping amplicons generated independently through separate triplicate PCRs. Interestingly, dual mutants often carried mutations E138K and G163R on the same genome. The ability of such accessory mutations to restore the impaired fitness of double Q148R + N155H mutants *in vivo* (Fransen et al., 2009) merits further investigation.

This case study provides further evidence that HIV-1 can escape from antiretroviral drug pressure through selection of pre-existing drug-resistant mutants. Our findings underscore the importance of prescribing fully active antiretroviral regimens to all HIV-1-infected subjects, as well as the need of developing more sensitive assays to detect transmitted as well as spontaneously generated drug-resistant minority variants.

Conflicts of interest

F. García has been a consultant on advisory boards, or has participated in speaker's bureaus, with Roche, Boehringer-Ingelheim, BMS, GSK, Gilead, Janssen, Merck and Pfizer. R. Delgado has received consulting fees and grant support from Abbott, BMS, Gilead and Roche. D. Dalmau has been a consultant on advisory boards, has participated in speaker's bureaus, or has conducted clinical trials with Roche, Boehringer-Ingelheim, Abbott, BMS, GSK, Gilead, Tibotec, Janssen, Merck and Pfizer. J. Martínez-Picado has received research funding, consultancy fees, or lecture sponsorships from GlaxoSmithKline, Merck and Roche. M. Álvarez-Tejado works for Roche Diagnostics S.L., Spain, which commercializes the 454 sequencing technology in Spain. B. Clotet has been a consultant on advisory boards, has participated in speakers' bureaus, or has conducted clinical trials with Roche, Boehringer-Ingelheim, Abbott, BMS, GSK, Gilead, Tibotec, Janssen, Merck, Pfizer, Siemens, Monogram Biosciences, and Panacos. R. Paredes has received consulting fees from Pfizer and grant support from Pfizer, Siemens, Merck and Boehringer Ingelheim. FM Codoñer, C. Pou, A. Thielen, MJ. Buzón, JR. Santos and L. Ruiz report no conflicts of interest relevant to this article. No other potential conflict of interest relevant to this article was reported.

Acknowledgements

This study was supported by the CDTI (Centro para el Desarrollo Tecnológico Industrial), Spanish Ministry of Science and Innovation (IDI-20080843); the Spanish AIDS network 'Red Temática Cooperativa de Investigación en SIDA' (RD06/0006), 'The European AIDS Treatment Network' (NEAT – European Commission FP6 Program, contract LSHP-CT-2006-037570) and 'CHAIN, Collaborative HIV and Anti-HIV Drug Resistance Network', Integrated Project no. 223131, funded by the European Commission Framework 7 Program. FMC was supported by the Marie Curie European Reintegration Grant number 238885, 'HIV Coevolution', also funded by the European Commission Framework 7 Program. This work was presented in part at the 8th European HIV Drug Resistance Workshop, 17–19 March 2010, Sorrento, Italy (Poster #51).

References

Abascal, F., Zardoya, R., Posada, D., 2005. ProtTest: selection of best-fit models of protein evolution. Bioinformatics 21, 2104–2105.

Buzon, M.J., Dalmau, J., Puertas, M.C., Puig, J., Clotet, B., Martinez-Picado, J., 2010. The HIV-1 integrase genotype strongly predicts raltegravir susceptibility but not viral fitness of primary virus isolates. Aids 24, 17–25.

Ceccherini-Silberstein, F., Armenia, D., D'Arrigo, R., Vandenbroucke, I., Van Baelen, K., Van Marck, H., Stuyver, L., Rizzardini, G., Antinori, A., Perno, C., 2009. Baseline variability of HIV-1 integrase in multi-experienced patients treated with raltegravir: a refined analysis by pyrosequencing. In: 16th Conference on Retroviruses and Opportunistic Infections, Montreal, Canada.

Charpentier, C., Piketty, C., Tisserand, P., Bélec, L., Laureillard, D., Karmochkine, M., Si-Mohamed, A., Weiss, L., 2009. Allele-specific real-time polymerase chain reaction of the presence of Q148H, Q148R, and N155H minority variants at baseline of a raltegravir-based regimen. In: 16th Conference on Retroviruses and Opportunistic Infections, Montreal, Canada.

Coffin, J.M., 1995. HIV population dynamics in vivo: implications for genetic variation, pathogenesis, and therapy. Science 267, 483–489.

Cooper, D.A., Steigbigel, R.T., Gatell, J.M., Rockstroh, J.K., Katlama, C., Yeni, P., Lazzarin, A., Clotet, B., Kumar, P.N., Eron, J.E., Schechter, M., Markowitz, M., Loutfy, M.R., Lennox, J.L., Zhao, J., Chen, J., Ryan, D.M., Rhodes, R.R., Killar, J.A., Gilde, L.R., Strohmaier, K.M., Meibohm, A.R., Miller, M.D., Hazuda, D.J., Nessly, M.L., DiNubile, M.J., Isaacs, R.D., Teppler, H., Nguyen, B.Y., 2008. Subgroup and resistance analyses of raltegravir for resistant HIV-1 infection. N. Engl. J. Med. 359, 355–365.

Edgar, R.C., 2004. MUSCLE: multiple sequence alignment with high accuracy and high throughput. Nucleic Acids Res. 32, 1792–1797.

Fransen, S., Gupta, S., Danovich, R., Hazuda, D., Miller, M., Witmer, M., Petropoulos, C.J., Huang, W., 2009. Loss of raltegravir susceptibility by human immunodeficiency virus type 1 is conferred via multiple nonoverlapping genetic pathways. J. Virol. 83, 11440–11446.

Guindon, S., Gascuel, O., 2003. A simple, fast, and accurate algorithm to estimate large phylogenies by maximum likelihood. Syst. Biol. 52, 696–704.

Kumar, S., Tamura, K., Nei, M., 2004. MEGA3: integrated software for molecular evolutionary genetics analysis and sequence alignment. Brief. Bioinform. 5, 150–163.

Liu, T.F., Shafer, R.W., 2006. Web resources for HIV type 1 genotypic-resistance test interpretation. Clin. Infect. Dis. 42, 1608–1618.

McColl, D.J., Chen, X., 2010. Strand transfer inhibitors of HIV-1 integrase: bringing in a new era of antiretroviral therapy. Antiviral Res. 85, 101–118.
Najera, I., Holguin, A., Quinones-Mateu, M.E., Munoz-Fernandez, M.A., Najera, R., Lopez-Galindez, C., Domingo, E., 1995. Pol gene quasispecies of human immunodeficiency virus: mutations associated with drug resistance in virus from patients undergoing no drug therapy. J. Virol. 69, 23–31.
Nowak, M.A., Bonhoeffer, S., Shaw, G.M., May, R.M., 1997. Anti-viral drug treatment: dynamics of resistance in free virus and infected cell populations. J. Theor. Biol. 184, 203–217.
Paredes, R., Clotet, B., 2010. Clinical management of HIV-1 resistance. Antiviral Res. 85, 245–265.
Rhee, S.Y., Gonzales, M.J., Kantor, R., Betts, B.J., Ravela, J., Shafer, R.W., 2003. Human immunodeficiency virus reverse transcriptase and protease sequence database. Nucleic Acids Res. 31, 298–303.
Schmidt, H.A., Strimmer, K., Vingron, M., von Haeseler, A., 2002. TREE-PUZZLE: maximum likelihood phylogenetic analysis using quartets and parallel computing. Bioinformatics 18, 502–504.
Shao, W., Boltz, V.F., Kearney, M., Maldarelli, F., Mellors, J.M., Stewart, C., Levitsky, A., Volfovsky, N., Stephens, R.M., Coffin, J.M., 2009. Characterization of HIV-1 sequence artifacts introduced by bulk PCR and detected by 454 sequencing. XVIII International HIV Drug Resistance Workshop: Basic Principles & Clinical Implications. Fort Myers, FL, USA, 9–13 June 2009 (Abstract 104). Antiviral Therapy 14 Suppl. 1, A123.
Shimodaira, H., Hasegawa, M., 1999. Multiple comparisons of log-likelihoods with applications to phylogenetic inference. Mol. Biol. Evol. 16, 1114–1116.
Steigbigel, R.T., Cooper, D.A., Kumar, P.N., Eron, J.E., Schechter, M., Markowitz, M., Loutfy, M.R., Lennox, J.L., Gatell, J.M., Rockstroh, J.K., Katlama, C., Yeni, P., Lazzarin, A., Clotet, B., Zhao, J., Chen, J., Ryan, D.M., Rhodes, R.R., Killar, J.A., Gilde, L.R., Strohmaier, K.M., Meibohm, A.R., Miller, M.D., Hazuda, D.J., Nessly, M.L., DiNubile, M.J., Isaacs, R.D., Nguyen, B.Y., Teppler, H., 2008. Raltegravir with optimized background therapy for resistant HIV-1 infection. N. Engl. J. Med. 359, 339–354.
Varghese, V., Shahriar, R., Rhee, S.Y., Liu, T., Simen, B.B., Egholm, M., Hanczaruk, B., Blake, L.A., Gharizadeh, B., Babrzadeh, F., Bachmann, M.H., Fessel, W.J., Shafer, R.W., 2009. Minority variants associated with transmitted and acquired HIV-1 nonnucleoside reverse transcriptase inhibitor resistance: implications for the use of second-generation nonnucleoside reverse transcriptase inhibitors. J. Acq. Immun. Def. Synd. 52, 309–315.
Wang, C., Mitsuya, Y., Gharizadeh, B., Ronaghi, M., Shafer, R.W., 2007. Characterization of mutation spectra with ultra-deep pyrosequencing: application to HIV-1 drug resistance. Genome Res. 17, 1195–1201.

Addendum IV

Other Publications by the Author

PUBMED INDEXED MANUSCRIPTS

1. RECall for automated genotypic tropism testing. **Pou C,** Bellido R, Casadellà M, Puig T, Clotet B, Harrigan R, Paredes R. J Clin Microbiol. 2013 Aug;51(8):2754-7.
2. HLA class I protective alleles in an HIV-1-infected subject homozygous for CCR5-Δ32/Δ32. Ballana E, Riveira-Munoz E, **Pou C,** Bach V, Parera M, Noguera M, Santos JR, Badia R, Casadellà M, Clotet B, Paredes R, Martínez MA, Brander C, Esté JA. Immunobiology. 2013 Apr;218(4):543-7.
3. In-depth characterization of viral isolates from plasma and cells compared with plasma circulating quasispecies in early HIV-1 infection. Dalmau J, Codoñer FM, Erkizia I, Pino M, **Pou C,** Paredes R, Clotet B, Martinez-Picado J, Prado JG. PLoS One. 2012;7(2):e32714.
4. Deep molecular characterization of HIV-1 dynamics under suppressive HAART. Buzón MJ, Codoñer FM, Frost SD, **Pou C,** Puertas MC, Massanella M, Dalmau J, Llibre JM, Stevenson M, Blanco J, Clotet B, Paredes R, Martinez-Picado J. PLoS Pathog. 2011 Oct;7(10):e1002314.
5. A non-infectious cell-based phenotypic assay for the assessment of HIV-1 susceptibility to protease inhibitors. Buzon MJ, Erkizia I, **Pou C,** Minuesa G, Puertas MC, Esteve A, Castello A, Santos JR, Prado JG, Izquierdo-Useros N, Pattery T, Van Houtte M, Carrasco L, Clotet B, Ruiz L, Martinez-Picado J. J Antimicrob Chemother. 2012 Jan;67(1):32-8.

6. A376S in the connection subdomain of HIV-1 reverse transcriptase confers increased risk of virological failure to nevirapine therapy. Paredes R, Puertas MC, Bannister W, Kisic M, Cozzi-Lepri A, **Pou C,** Bellido R, Betancor G, Bogner J, Gargalianos P, Bánhegyi D, Clotet B, Lundgren J, Menéndez-Arias L, Martinez-Picado J; EuroSIDA Study Group. J Infect Dis. 2011 Sep 1;204(5):741-52.

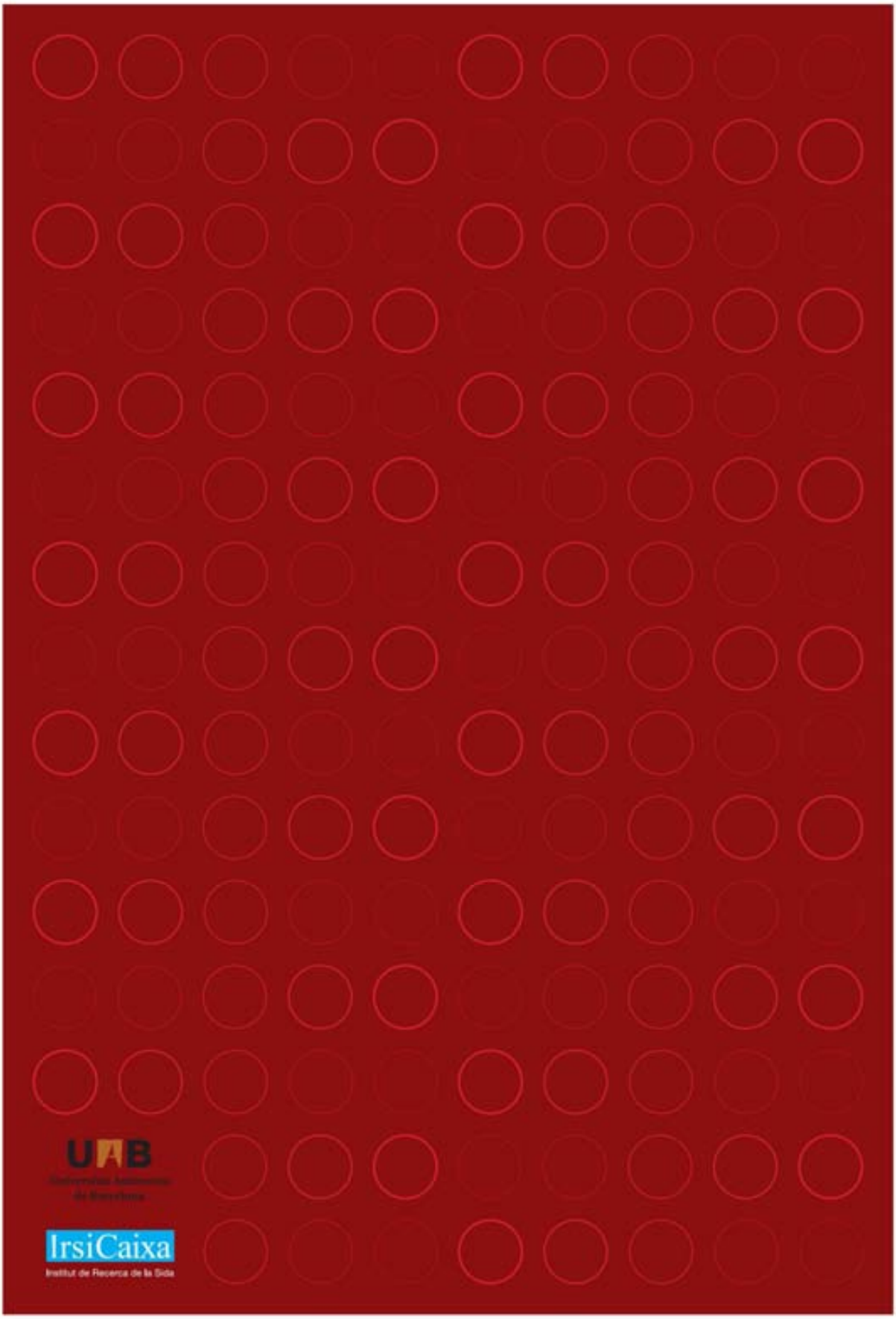
UAB
Universitat Autònoma de Barcelona
IrsiCaixa
Institut de Recerca de la Sida